Max Planck Institute of Molecular Plant Physiology
AG Stitt

Nitrate: Metabolism and Development

"Characterization of the glutamate dehydrogenase (*GDH*) family, an enzyme at the cross-roads of carbon-nitrogen interactions metabolites and Study of the regulation of flowering by nitrogen"

Dissertation

zur Erlangung des akademischen Grades
Doktor der Naturwissenschaften
(Dr. rer. nat.)

eingereicht an der
Mathematisch-Naturwissenschaftlichen Fakultät
der Universität Potsdam

INMACULADA CASTRO MARIN

Potsdam, October 2007

"It's the possibility of having a dream come true what makes life interesting"
(*The Alchemist*, Paulo Coelho)

TABLE OF CONTENTS

ABBREVIATIONS

%	Per cent
ºC	Degree Celsius
µE	Micro-mols of photons per meter squared per second
µl	Microliter
µM	Micromolar
aa	Amino acid
A_{***}	Absorbance at *** nm
Ala	Alanine
AMOZ	*Arabidopsis* Medium Ohne Zucker (german)
Amp	Ampiciline
APS	Ammonium persulphate
Arg	Arginine
AS	Asparragine synthetase
Asn	Asparragine
Asp	Aspartic acid
AspAT	Aspartate aminotransferase
A. thaliana	*Arabidopsis thaliana*
ATP	Adenosine 5'-triphosphate
bp	Base pair
BSA	Bovine serum albumin
C	Carbon
cDNA	Complementary deoxyribonucleic acid
Col	Columbia
CTAB	Cetyl-trimethihyl –ammonium bromide
d	Day
Da	Dalton
DNA	Deoxyribonucleic acid
DTT	Ditiothreitol
DTE	Dithioerythritol
DW	Dry weight
EDTA	Ethylene diamine tetraacetic acid

EGTA	Ethylene glycol tetraacetic acid
E. coli	*Escherichia coli*
FW	Fresh weight
g	Gram
g	Gravitational acceleration
gDNA	Genomic deoxyribonucleic acid
Gln	Glutamine
Glu	Glutamate
Gly	Glycine
GDH	Glutamate dehydrogenase
GOGAT	Glutamine oxoglutarate amino transferase
GS	Glutamine synthetase
GUS	β-glucuronidase
h	Hour
H^+	Proton
HAT	High affinity transport mechanism
HCl	Hydrochloric acid
Hepes	N-(2-hydroxyethyl)-piperazine-N'-(2-ethanesulfonic acid)
HPLC	High performance liquid chromatography
i.e.	That is
Kb	Kilobase
KDa; KD	Kilodalton
Km	Michaelis-Menten constant
KCl	Potassium chloride
KNO_3	Potassium nitrate
KOAc	Potassium acetate
KOH	Potassium hydroxide
l	Liter
LAT	Low affinity transport mechanism
LB	Left border
LB	Luria-Bertani broth medium
LD	Long day
LiCl	Lithium chloride
m	Meter, milli

M	Molar, molarity
MeOH	Methanol
MES	2-(*N*-morpholine) ethanesulfonic acid
mg	Milligram
min	Minute
ml	Milliliter
mM	Millimolar
mol	Mole
mRNA	Messenger ribonucleic acid
MS	Murashige-Skoog medium
MTT	C,N-diphenyl-N'-4,5-dimethyl thiazol-2-yl tetrazolium bromide
N	Nitrogen
N	Normal
NAD^+/NADH	Nicotinamide adenine dinucleotide (oxidized/reduced form)
NaOAc	Sodium acetate
NaOH	Sodim hydroxide
NCBI	National center for biotechnology information
NH_3	Ammonia
NH_4^+	Ammonium ion
NH_4Cl	Ammonium chloride
NIA	Transcript for nitrate reductase
NiR	Nitrite reductase
NR	Nitrate reductase
nm	Nanometer
No.	Number
OD	Optical density
o/n	Over night
oligo(dT)	Oligodeoxythymidylic acid
OPA	Ortho-phthaldialdehyde
PAGE	Polyacrylamide gel electrophoresis
PCR	Polymerase chain reaction
PES	Phenazine ethosulfate
PMS	Phenazine methosulfate
PMSF	Phenylmethylsulfonyl fluoride

PVPP	Polyvinylpolypirrolidone
PEPCase	Phosphoenolpyruvate carboxylase
PEPCK	Phosphoenolpyruvate carboxykinase
PIPES	Piperazine-1, 4-bis(ethanosulfonic acid)
PO_4	Phosphate
q RT-PCR	Quantitative real time PCR
RNA	Ribonucleic acid
RNAi	RNA interference
RNase	Ribonuclease
ROS	Reactive oxygen species
rpm	Revolutions per minute
RT	Reverse transcriptase
RT	Room temperature
RT-PCR	Reverse transcriptase polymerase chain reaction
RuBisCO	Ribulose 1,5-bisphosphate carboxylase/oxygenase
s	Second
SA	Salicylic acid
SAM	Shoot apical meristem
SD	Standard deviation
SD	Short day
SDS	Sodium dodecyl sulphate
TAIR	The Arabidopsis information resource
T*aq* polymerase	*Thermus aquaticus* polymerase
TBE	Tris borate-EDTA
TCA	Tricarboxylic acid cycle
T-DNA	Transferred DNA
TE	Tris-EDTA
TEMED	N,N,N',N'-Tetramethylethylenediamine
Tris	Tris(hydroxymethyl) aminoethane
Triton-X-100	Polyoxyethylene-p-isooctylphenol
Tween-20	Polyoxyethylene (20) sorbitan monolaurate
U	Unit of enzyme activity
UTR	Untranslated region
UV	Ultraviolet

V	Volt
v/v	Volume per volume
w/v	Weight per volume
wt; WT	Wild type

ACKNOWLEDGEMENTS

***I** would like to express my sincere gratitude to Prof. Mark Stitt for his direct supervision of this thesis. Thanks for giving me the opportunity to work in your group. I learned so much.*

***I** would like to thank to Prof. Lothar Willmitzer as being part of the additional PhD supervision, for his good comments and nice suggestions.*

***I** am very grateful to Prof. George Coupland (MPIZ, Cologne) for providing the collection of mutants and transgenic plants defective in flowering genes.*

***I** wish to thank Dr. Irene Loef for allowing me to continue her work. I never met you, but, thanks.*

***T**hanks to the gardeners team, especially Mr. Frank Hühn for the good care of the plants in the green house. Thanks to the media kitchen, especially to Ms. Renate Bathe for autoclaving my innumerable solutions and for her chats in German (I could learn a bit more!).*

***A**lso, I would like to thank Sven and Carsten (IT team), for my never ending troubles with computer staff. Danke schönn!!*

***M**y special thanks to Linda Bartetzko for the nice moments we spent together working under the clean bench and of course for showing me what an Arabidopsis plant is.*

***A**lso, to Diana Sunkel for making me laugh whenever we met in the corridors.*

***T**o my dear Tina for her good advices, her positive energy and for being such a good friend (more than a colleague). You also saved my life, remember? Thank you.*

***A**lso, thanks to Natalia Palacios for her support and helpful comments.*

***M**any thanks to Joanna Cross, besides that special girl there is a big person, thanks for your good suggestions, for the nice discussions and for showing me what an enzyme assay is.*

***T**o little Manuela for the technical support and nice company in the lab.*

***T**hanks a lot to Carles, although a little bit late, it was good to have two more hands and two more eyes for the stressing last work. Gracias.*

***T**hanks a lot to John Lunn and Maria Piques for their kindness. Also, many thanks to the rest of AG Stitt group, for the nice atmosphere in the lab and for allowing me to carry out the thesis. I learned a lot from all of you. Danke!!*

***T**hanks to my lovely Cami, you are the best friend that someone could have. Thanks for your friendship, your kindness, for your good feelings and for the "crying sections" we spent*

together. You helped me a lot. Eres una de las mejores cosas que me han pasado en Alemania, gracias por motivarme tanto y hacerme sentir bien en los malos momentos. Siempre te llevaré conmigo. Muito obrigada!!

***T**hanks to my Spanish friends at Max Planck Institute, to Jesús, Manuel, Maica, Ana, Rosa and Elena. It was soo nice to spend time with you speaking in Spanish; it didn't help to improve my English but helped me with soothing the stress. !!!Muchas gracias!!!*

***T**o my dear Silvia, for being always such a good friend, for her eternal support and for keeping me up dated with e-mails during my stay abroad. Also, thanks to Goyi for his encourage and for his friendship.*

***S**pecial thanks to my two Martas (Marta Godoy and Marta Campos). It was good to have such friends during the studies. Pero lo mejor de todo es conservar vuestra amistad (ésto también lo digo por ti, Silvia). !!Muchas gracias!!*

***I** wish to thank to my family in law, to Carmen y Paco, to Sofía, to Eleni and Piero for being always there, but specially for accepting me as another member in the family. Gracias por apoyarme siempre.*

***T**o my parents in law, for their affection and for considering me as another daughter. Gracias.*

***T**o Nuria, for her sweaty advices and for her sincerity.*

***S**pecial thanks to my brother, David. You have been always the best example to follow. Gracias por escucharme, apoyarme en los malos momentos, por confiar en mí y sobretodo por ser como eres. Te he echado mucho de menos. Te adoro, hermanito.*

***M**any, many, many thanks to my dear parents, Andrés and Marina, for giving me everything in the life. For their discipline, their education and their love. Gracias por cuidarme, enseñarme, guiarme y aconsejarme en cada momento. Espero que algún día perdonéis mi ausencia durante todo este tiempo. Siempre os llevo y os llevaré en el corazón. Gracias.*

***I** want to dedicate this thesis to my husband, Daniel. Gracias por estar ahí en los malos (y buenos) momentos, por tu gran paciencia, por tu sabiduría, por tus consejos y sobretodo por cuidarme y quererme. Eres lo mejor que me ha pasado en la vida. Te quiero.*

CHAPTER 1 INTRODUCTION

1. CHAPTER: INTRODUCTION

1.1 Importance of nitrogen metabolism in plants.

Nitrogen is the most important inorganic nutrient that plants have to capture from the soil solution because it is a major limiting factor for plant growth (Vitousek & Howarth, 1991) and it represents a major constituent of proteins, nucleic acids and cofactors. Also, it is an abundant component of chlorophylls and it is present in several plant hormones and secondary metabolites, like alkaloids and phenylpropanoids (Marschner, 1995).

Nitrate is a major source of nitrogen for plants and serves as a potent signal that affects plant metabolism as well as organ growth and development (Crawford & Forde, 2001; Forde, 2002; Stitt *et al.*, 2002; Foyer *et al*., 2003; Stitt, 1999). Nitrate signals rapid changes in the synthesis of nitrate transporters and the nitrate assimilatory enzymes (nitrate reductase (NR) and nitrite reductase (NiR)). It also induces genes encoding proteins to provide reducing equivalents (pentose phosphate pathway) and redirects carbon metabolism from starch, fructan and sugar synthesis to the production of organic acids to assimilate ammonium (Scheible *et al*., 1997a; Wang *et al*., 2000, 2003). The expression of enzymes involved in glycolisis, trehalose 6-phosphate metabolism and iron transport/metabolism is also affected by nitrate (Wang *et al.*, 2003; Scheible *et al*., 2004).

Nitrate is converted to nitrite and ammonium and is ultimately incorporated into amino acids. Thus, downstream metabolites of nitrate may play an important role in nitrate responses or, in fact may be the proximal signal. Because of that, many efforts have been focused to determine whether nitrate itself or closed related metabolites act as signal. For example, gene expression analyses in response to long-term nitrogen deprivation or short-term treatments with nitrate have revealed the substantial impact of nitrate response on plant metabolism (Wang *et al*., 2000, 2003; Scheible *et al*., 2004). In addition, the use of NR-deficient mutant has been of crucial importance to study nitrate metabolism and signalling (Wang *et al.,* 2004).

Nitrogen source is essential for plants and its withdrawal affects general plant growth and leads to changes in the expression of a wide range of genes involved in primary metabolism (Scheible *et al*., 2004). Nitrogen deficiency accelerates leaf yellowing and senescence caused by the coordinated repression of genes involved in photosynthesis, chlorophyll and plastid protein synthesis. In addition, nitrogen deprivation also affects secondary metabolism by inducing the synthesis of genes for phenylpropanoid and flavonoid metabolism (Scheible *et al*., 2004) visible by the redness in the whole rosette as a consequence of anthocyanin

accumulation (Diaz *et al*., 2006). Low nitrogen leads to modifications of plant growth rate promoting root growth and increased number of lateral roots (Scheible *et al*., 2004). Furthermore, the availability of nitrate regulates development accelerating the transition to flowering in plants when is under low concentrations in the sole source.

The present work has two separate topics. First, to investigate the GDH family, a small gene family at the interface between nitrogen and carbon metabolisms. For that approach, a combination of expression analyses and functional characterization of the genes by reverse genetic was carried out. Second, to investigate the mechanisms whereby nitrogen is regulating the transition to flowering time in *Arabidopsis thaliana*.

1.2 Nitrate uptake in plants.

Plants devote a significant portion of their carbon and energy reserves to nitrogen uptake and assimilation. Plants have evolved intricate mechanisms to detect nitrate and to integrate its assimilation with photosynthesis and the overall metabolism of nitrogen and carbon. These mechanisms allow plants to control growth rates, root architecture, carbon/nitrogen ratios, concentrations of reductants, and ionic and pH balances under diverse environmental conditions (Stitt, 1999; Stitt *et al*., 2002).

The assimilation of nitrate begins with its uptake into the cell. Ordinarily, nitrate is taken up from the soil solution by epidermal and cortical cells of the root. Primary uptake can also occur in leaves (important route for incorporation of foliar applications of fertilizer). Once within the symplasm, nitrate can be transported into the vacuole and stored at high concentrations. Nitrate can also be loaded into the xylem for long distance transport to the shoot (Forde & Clarkson, 1999).

Initial uptake across the plasma membrane is a regulated, active transport process driven by the H^+ gradient and catalyzed by a combination of high and low affinity transport mechanisms (HATS and LATS, respectively). Two classes of genes, *NRT1* and *NRT2* have been found to be potentially involved in both affinity transport systems. In many plants both *NRT1* and *NRT2* classes are represented by multigene families (Vedele *et al*., 1998; Orsel *et al*., 2001, Galván & Fernández, 2001). The *NRT1* family is more complex, including nitrate transporters with dual affinity (both low and high Km) or low affinity. The *NRT2* family encodes transporters that contribute to the inducible- high affinity uptake system. All *NRT2* genes are expressed at very low levels in roots in the absence of NO_3^- and are rapidly induced when NO_3^- is resupplied (Crawford *et al*., 2002; Forde, 2000; Scheible *et al*., 2004). The nitrate uptake system is also

feedback regulated according to the internal N status of the plant, for example by down-stream products formed during nitrate assimilation for example, ammonium and glutamine (Gojon *et al*., 1998). This regulation allows plants to coordinate the uptake rates with the plant's demand for nitrate (Forde, 1999; Forde, 2000; Imsande & Touraine, 1994**;** Glass *et al*., 2001).

1.2.1 Nitrate assimilation and its regulation in plants

Nitrate itself is not incorporated into organic compounds but is first reduced to ammonium in a two-step process. The first committed step in the nitrate assimilation pathway is the reduction of nitrate to nitrite catalyzed by the enzyme nitrate reductase (NR). NR and nitrate reduction are localized in the cytosol of cells throughout the vegetative organs of the plant. In most species, NR is found in shoots and roots, but its distribution depends on environmental conditions. However, some species (e.g., cranberry, white clover and young chicory) localize almost all their NR in roots, whereas others (e.g., cocklebur) express NR almost exclusively in leaves. Within a specific organ, NR shows cell-type specific localization. At low external concentrations of NO_3^- , NR is found primarily in epidermal and cortical cells close to the root surface. At higher external concentrations of NO_3^- , activity is also detected in cells of the cortex and vascular system.

The next step in the nitrate assimilation pathway is the reduction of nitrite to ammonia, which is catalyzed by the enzyme nitrite reductase (*NiR*). In C_3 plants, NiR is located in the chloroplast of leaves, and in C_4 plants it is found predominantly in the chloroplast of mesophyll cells. NiR of nonphotosynthetic tissues such as roots, it is localized in plastids.

The regulation of NR plays a key role in nitrate assimilation. Photosynthetic tissues have about 10-fold higher NiR activity than NR (Hoff *et al*., 1994), ensuring that nitrite, which is toxic, is converted through ammonia and therefore does not accumulate to toxic amounts. Thus, nitrate assimilation is subject to transcriptional, post-trancriptional and post-translational regulation at the step catalysed by NR (Hoff *et al*., 1994; Crawford, 1995; Nussaume *et al.*, 1995; Daniel-Vedele *et al*., 1998).

Plants use several mechanisms to adjust the concentration and activity of NR in response to such diverse signals as nitrate abundance, nitrogen metabolites (especially glutamine), CO_2, carbon metabolites (especially sucrose), cytokinins and light.

1.2.1.1 Transcriptional regulation

The *Nia* transcripts and NR protein are very low in nitrate-limited plants or in the presence of ammonium, and high in plants grown on high nitrate (Hoff *et al*., 1994; Scheible *et al*., 1997c).

These transcripts also show a marked diurnal rhythm. The *Nia* transcript is present at a high level towards the end of the night, stays high or rises slightly during the first 2 hours in the light, declines markedly during the remainder photoperiod and recovers gradually during the dark period (Galangau *et al*., 1988; Scheible *et al*., 1997c; Geiger *et al*., 1998b). The changes of NR protein occur in the same way than the *Nia* transcript but with a slight time delay as expected if the changes in the *Nia* transcript level contribute to the diurnal changes in NR protein. *Nia* transcription is induced by nitrate (Pouteau *et al.*, 1989; Cheng *et al*., 1992; Lin *et al*., 1994) and repressed by glutamine (Hoff *et al.*, 1994). These nitrogen metabolites probably play a major role in the regulation of *Nia* expression. The decrease of the *Nia* transcript during the photoperiod is correlated with a decrease of nitrate and an accumulation of glutamine (Scheible *et al.*, 1997c), and the gradual recovery during the night is correlated with a decrease of glutamine and a gradual increase of nitrate.

In addition to the primary signal, nitrate, *Nia* transcripts respond to other signals that link nitrate reduction to photosynthesis and carbon metabolism. Feeding experiments with sugars, suggest that *Nia* transcript and NR activity increase when high sugars are supplied exogenously (Vincentz *et al.*, 1993; Sivasankar, Rothstein & Oaks, 1997; Botrel & Kaiser, 1997). The observation that tobacco transformant plants with low Rubisco activity have low levels of sugars, low NR activity, low levels of aminoacids and accumulate large amount of nitrate (Stitt & Schulze, 1994) provides evidence that nitrate assimilation is inhibited when carbohydrates are low. Likewise, when tobacco plants are grown under short day conditions or exposed to an extended night, *Nia* transcripts and NR activity do not decrease until sugar levels are below about 3-4 μmol/g FW indicating that the sugar-mediated regulation only plays a major role in the regulation of *Nia* transcription when the sugar levels in leaves are very low (Matt *et al*., 1998; Stitt *et al*., 2002). However, the observation that sucrose and glutamine act antagonistically on the level of the *Nia* transcript (Morcuende *et al*., 1998) suggests that higher levels of sugars may be required in conditions where the plants are less depleted in amino acids.

1.2.1.2 Post-translational regulation

Post-translational mechanisms control NR protein concentrations and activity in response to certain physiological conditions. For example, NR proteins decrease when plants are deprived of nitrogen or light for several days while amounts of *Nia* transcripts remain high. A more rapid and reversible response that inhibits NR activity occurs when plants are exposed to darkness or low concentrations of CO_2. Under these conditions, NR is inactivated within

minutes in a two-step process that involves the phosphorylation on a serine residue by a calcium-dependent protein kinase, and the subsequent Mg^{2+} or Ca^{2+}-dependent binding of 14-3-3 proteins. This mechanism allows for rapid and reversible inhibition of NR activity when conditions do not favour nitrate assimilation (i.e., when light or carbon dioxide is limiting).

There are evidences about the effect of nitrogen signals on the post- translational regulation of NR. Scheible *et al*., (1997) showed that the dark inactivation of NR is partially or completely reversed in nitrate-limited wild type plants and in mutant or transformants with decreased expression of NR. This abolition of dark inactivation was correlated with a decreased level of glutamine and ammonium, and the activation of NR could decrease by feeding glutamine to detached leaves (Scheible *et al*., 1997; Morcuende *et al*., 1998).

Sugars are also implicated in the post-translational regulation of NR. Dark inactivation is reversed if sugars are supplied to leaves in the dark (Kaiser & Brendle-Behnish, 1991; Kaiser & Huber, 1994a), and light-activation does not occur if carbon fixation is prevented by water stress or low CO_2 concentrations (Kaiser & Föster, 1989; Kaiser & Brendle-Behnish, 1991).

1.2.1.3 Post-transcriptional regulation

There is evidence for mechanisms that modulate either the translation of the *Nia* transcripts and/or the rate of the degradation of NR protein. For example, NR protein still decreases in the second half of the photoperiod in transformants with constitutive expression of *Nia* (Vincentz and Caboche, 1991; Ferrario *et al.*, 1995). The decline of NR protein is absent in the second part of the photoperiod in mutants with lower number of functional *Nia* transcripts, even thought the *Nia* transcript level declines in the same way as in wild type plants (Scheible *et al.*, 1997c).

Protein phosphorylation not only allows reversible inactivation of NR but also initiates NR degradation. There is a correlation between the phosphorylation state or the activation state of NR and the rate at which NR protein decreases (Kaiser and Huber, 1997; Scheible *et al*., 1997c; Geiger *et al.*, 1998b).

The regulation of both NR transcription and activity allows plants for fine-tune the amount of nitrate reduction in order to prevent accumulation of toxic concentrations of down stream nitrate-related products like nitrite and ammonium.

1.2.2 Nitrite reduction

After the nitrate reduction, the next step in the nitrate assimilation pathway is the reduction of nitrite to ammonia, which is catalyzed by the chloroplastic nitrite reductase (NiR). NiR is

regulated transcriptionally, usually in coordination with NR. Because nitrite is toxic, cells must contain enough NiR to reduce all the nitrite produced by NR. Thus, plants maintain an excess of NiR activity whenever NR is present by inducing NiR gene expression in response to light and nitrate. If NiR concentrations are diminished, either by mutation or antisense expression, plants accumulate nitrite and display chlorosis (Wray, J.L, 1993). In wild type plants, the regulatory mechanisms that control NiR activity are thought to assist in preventing nitrite accumulation.

1.2.3 Ammonium uptake and assimilation by the GS/GOGAT cycle.

Plant cells have the capacity for active transport of ammonium ion (NH_4^+). Physiological studies have revealed multiphasic saturation kinetics implying low and high affinity components (Ullrich *et al*., 1984; Wang *et al*., 1993).

In vascular higher plants, ammonium can be produced by photorespiration, nitrate assimilation, N_2 fixation in nodules, the phenylpropanoid pathway, and nitrogen release for transport or breakdown of nitrogenous compounds (Ireland & Lea, 1999; Hirel & Lea, 2001). Ammonium is potentially toxic to plant function and so it must be rapidly assimilated into organic molecules for nitrogen cycling. This is achieved by the GS/GOGAT cycle that is comprised of the two enzymes, glutamine synthetase (GS, EC 6.1.1.3) and glutamate synthase (ferredoxin Fd-GOGAT, EC 1.4.7.1; NADH-GOGAT, EC 1.4.1.14) (Ireland & Lea, 1999). First, ammonium is added to glutamate by GS, whose isoforms GS1 and GS2 are located in the cytosol of roots and in the chloroplasts of leaves, respectively. An amide group is then transferred to 2-oxoglutarate by GOGAT, whose ferredoxin- and NAD(P)H- dependent isoenzymes are detected in the chloroplasts of leaves and in plastids of roots (Coschigano *et al*., 1998).

This pathway is of crucial importance since the glutamate and the glutamine produced are donors for the biosynthesis of major N-containing compounds, including amino acids, nucleotides, chlorophylls, polyamines, and alkaloids (Lea & Ireland, 1999).

1.2.3.1 Glutamine synthetase

Two classes of glutamine synthetase (GS: EC. 6.3.1.2) isoenzymes that are located in the cytosol (GS1) or chloroplast (GS2) have been identified by ion-exchange chromatography. The distinct physiological roles of GS2 and GS1 have been implicated by their organ-specific localizations. For instance, because GS2 is the predominant isoenzyme in leaves, it has been proposed to function in primary assimilation of ammonia and/or in the reassimilation of the

respiratory ammonia (Miflin & Lea, 1980). In contrast, cytosolic GS1 is predominant in roots, thus, it has been proposed to function in root nitrogen assimilation, although root plastid GS2 has also been implicated in this process (Miflin BJ, 1974). The specific localization of GS1 in phloem further supports the notion that cytosolic GS probably synthesizes glutamine for long-distance nitrogen transport (Carvalho *et al*., 1992; Kamachi *et al*., 1992). The GS isoenzymes are encoded by a gene family in all plants species and has been showed that each species appear to possess a single nuclear gene for chloroplastic GS2 and multiple genes for cytosolic GS1.

Studies performed in different species, demonstrated that GS2 gene expression is tightly regulated by light, and in several cases, this has been shown to be mediated at least in part by phytochrome activation (Miflin BJ, 1974). GS2 gene expression can also be regulated in response to carbohydrate and amino acid supplementation in tobacco and *Arabidopsis* (Faure *et al*., 1994; Oliveira IC & Coruzzi GM, 1999). In addition, GS2 mRNA accumulation has been reported to increase in leaves of plants grown under photorespiratory conditions (Edwards & Coruzzi GM, 1989; Miflin BJ, 1974), in agreement with one of the proposed roles of GS2, the reassimilation of the photorespiratory ammonia (Miflin BJ, 1974).

1.2.3.2 Glutamate synthase

In higher plants, there are two distinct forms of glutamate synthase (GOGAT) that use NADH or ferredoxin as the electron carrier (Lea *et al*., 1990; Sechley *et al.*, 1992; Stewart, *et al*., 1980; Suzuki *et al*., 1984). NADH-GOGAT is located primarily in plastids of nonphotosynthetic tissues such as roots where it has been hypothesized to function in primary assimilation or reassimilation of ammonia released during amino acid catabolism (Miflin & Lea, 1980). In contrast, Fd-GOGAT is located primarily in the leaf chloroplast where light leads to an increase in Fd-GOGAT protein and activity (Lea *et al*., 1990; Sechley *et al*., 1992). These findings suggested that the physiological role(s) of Fd-GOGAT is related to light-inducible processes in leaves such as photosynthesis and photorespiration. Fd-GOGAT may also play a smaller role in nonphotosynthetic tissues, since some Fd-GOGAT activity is associated with roots (Suzuki *et al*., 1982). A single gene has been identified in different plant species except *Arabidopsis* which has been shown to contain two expressed genes (*GLU1* and *GLU2)*, each encoding a distinct form or Fd-GOGAT.

1.3 Downstream metabolism of glutamine and glutamate

Glutamine and glutamate serve as nitrogen-transport compounds and nitrogen donors in the biosynthesis of an enormous number of compounds (Lea *et al*., 1989), including essentially all amino acids, nucleic acids and other nitrogen-containing compounds such as chlorophylls. Nitrogen may be subsequently channelled from glutamine and glutamate to aspartate by the action of aspartate aminotransferase (AspAT; E.C 2.6.1.1) or to asparagine by the enzyme asparagine synthetase (AS; E.C. 6.3.5.4). The four nitrogen-transport amino acids generated by this pathway (glutamine, glutamate, asparagine and aspartate) are the predominant amino acids found in higher plants.

1.3.1 Aspartate aminotransferase

AspAT, also known as glutamate-oxaloacetate aminotransferase (GOT), plays a central role in nitrogen assimilation in plants due to the ability of regenerate carbon skeletons (in form of α-Ketoglutarate) required for further nitrogen assimilation by transferring an amino group from glutamate to oxaloacetate.

AAT is encoded by a small gene family in *Arabidopsis* consisting of five genes, *ASP1* through *5* (for *ASP1-4*, see Schultz & Coruzzi, 1995; for *ASP5*, see Wilkie *et al*, 1995) predicted to encode isoenzymes targeted to different subcellular compartments such as the cytosol (*ASP2,* At5g19550, EC.2.6.1.1. and *ASP4*, At1g62800, EC.2.6.1.1.), mitochondria (*ASP1* At2g30970, EC.2.6.1.1.), chloroplast (*ASP3*, At5g11520, EC.2.6.1.1. and ASP5, At4g31990, EC.2.6.1.1.) or peroxisomes (*ASP3*, At5g11520, EC.2.6.1.1.), suggesting their distinct roles in transamination reactions in each of these compartiments (Miesak & Coruzzi, 2002).

1.3.2 Asparagine synthetase

In an ATP-dependent reaction, AS catalyses the transfer of the amide group from glutamine to aspartate, generating glutamate and asparagine. Asparagine, an inert amino acid with high nitrogen:carbon, serves as a major nitrogen transport and storage compound in many higher plants (Lea & Miflin, 1980).

Although glutamine is the preferred substrate for nearly all of the AS enzymes in higher plants, some evidences indicates that ammonium is also a possible substrate for AS, particularly in the case of maize roots (Oaks & Ross, 1984). Studies of AS cDNA clones isolated from *Arabidopsis* and asparagus have shown that the polypeptides contain a PurF-type glutamine-binding domain supporting the notion that glutamine is the preferred substrate for AS (Richards & Schuster, 1992). Moreover, studies of these cDNA clones, together with

biochemical data, have suggested that asparagine metabolism is regulated by the carbon/nitrogen status of the plant (Lam *et al*., 1994). The levels of asparagine and AS activities are also controlled by environmental and metabolic signals. The asparagine content of phloem exudates and the amount of AS activity are negatively regulated by light or by sucrose in numerous plant species, including *Arabidopsis* and Asparagus. Asparagine accumulation and AS activity are induced when light-grown plants are dark adapted (Lam *et al*., 1994).

Three cDNA clones encoding AS (*ASN1, ASN2* and *ASN3*) are present in *Arabidopsis*. *ASN1* (At3g47340, E.C. 6.3.5.4.) gene is negatively regulated by light (Tsai & Coruzzi, 1990, 1991; Lam *et al*., 1994). This light repression of *ASN1* expression is at least partially mediated through the photoreceptor phytochrome (Tsai & Coruzzi, 1990; Lam *et al*., 1994). Besides acting as a direct signal, light can also exert its effect on *ASN1* expression indirectly by changing the metabolic state of the plant, for instance, providing the energy source for photosynthetic processes which lead to the accumulation of carbon skeletons. Sucrose represses the dark induction of *ASN1,* and this effect is relieved by addition of a nitrogen source as glutamine, glutamate or asparagine (Lam *et al*., 1994). These observations support a model in which, when the carbon pool is low relative to the nitrogen pool, the *ASN1* gene product functions to redirect the flow of nitrogen into asparagine, which then acts as a shunt for nitrogen storage and/or long-distance nitrogen transport (Lam *et al*., 1994). The *ASN2* (At5g65010, E.C. 6.3.5.4) and *ASN3* (At5g10240, E.C. 6.3.5.4.) genes are distinct in sequence and in gene regulation. Levels of *ASN2* mRNA are low in dark-adapted plants and induced by the supplementation of sucrose. *ASN1* and *ASN2* are also reciprocally regulated by amino acids treatment, the sucrose induction of ASN2 mRNA is at least partially repressed by the addition of the nitrogen-transport amino acids (Lam *et al*., 1998).

1.4 Carbon metabolism in plants

1.4.1 Importance of carbohydrate metabolism in plants

Almost all plants convert simple nutrients such as carbon dioxide, water and inorganic ions into all the intermediated required for the biosynthesis of nucleic acids, proteins, lipids and polysaccharides as well as coenzymes and numerous secondary metabolites. Thus, in addition to fulfilling the energy requirements of the cell, plant carbohydrate metabolism must feed numerous anabolic pathways.

Photosynthesis is the process of converting light energy to chemical energy by using carbon dioxide from the atmosphere to synthesize reduced carbon compounds which are stored as

carbohydrates to provide energy and biomass to the plant. Sucrose is a major product of photosynthesis in green leaves, accounting for much of the carbon dioxide fixed during photosynthesis. It also serves as the principal long-distance transport compound in most plants and as a storage compound in some (including sugar beet, sugars cane and carrot) (Kruger, 1997). Starch, a polymer of glucose, is synthesized and stored in plastids during the light period. Together sucrose and starch provide the major substrates for respiration in most cells and therefore maybe considered to dominate the carbohydrate metabolism in higher plants. The synthesis of sucrose and starch are competing reactions. In *Arabidopsis thaliana* leaves, the Calvin cycle can feed carbon into the starch synthesis pathway when the rate of sucrose synthesis exceeds the rate of sucrose export from the cells (Stitt, 1984). The excess fixed carbon is finally stored in the chloroplast as starch.

Leaf starch acts as a transient store which is degraded during the night to provide substrates for sucrose synthesis to allow continued export to non photosynthetic parts of the plant, and to provide carbon skeleton, energy and reductant within the leaf cell (Geiger & Servaites, 1994). Therefore, the leaf presents an elegant mechanism for controlling the flow of carbon into sucrose to reflect the supply of photosynthate from the chloroplast.

1.5 The GDH- shunt

1.5.1 Reaction catalyzed by GDH.

The glutamate dehydrogenase (GDH) shunt present in plants could serve as a link between carbon and nitrogen metabolism, as it is capable to catalyze a reversible reaction where is able to transfer the ammonium to an organic molecule α-Ketoglutarate to form glutamate and NAD^+, or in the reverse reaction, to recycle α-Ketoglutarate from glutamate releasing ammonia and reducing groups (NADH).

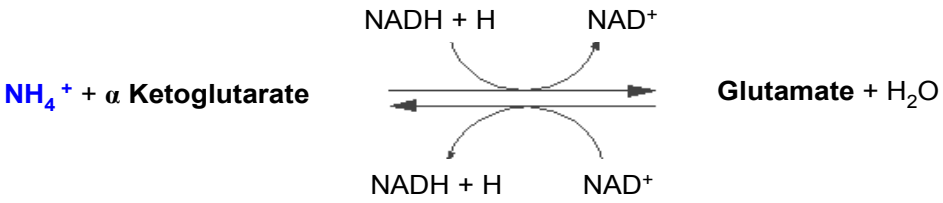

Figure 1. Reaction catalysed by GDH.

Two major forms of glutamate dehydrogenase (GDH) have been reported: an NADH-dependent form (NAD(H)-GDH; E.C 1.4.1.2) found in the mitochondria (Day *et al*., 1988;

Loulakakis CA & Roubelakis-Angelakis KA,1990) and an NADPH-requiring form (NADPH-GDH; E.C.1.4.1.4) localized to the chloroplast (Lea & Thurman, 1972).

1.5.2 Physiological role(s) of GDH

Although GDH enzyme activity exists in plant tissues at high levels, there is an ongoing debate about its physiological role in higher plants. Originally, GDH was proposed to be the primary route for the assimilation of ammonium and glutamate biosynthesis in plants. However, this biosynthetic role of GDH has been challenged by the discovery of the alternative pathway for ammonium assimilation via the GS/GOGAT cycle (Miflin & Lea, 1980). Several lines of data argue against GDH playing a major role in ammonium assimilation in higher plants. The relatively low affinity of GDH isoenzymes for ammonium (K_m values of 0.3 to 1.2 mM) when compared to that of GS (K_m values in the range of 10 to 150 μM) argues against a role in primary nitrogen assimilation (Stewart *et al*., 1980). Furthermore, all the ^{15}N labelling experiments performed in plants or using intact mitochondria have demonstrated that GDH operates in the direction of glutamate deamination (Aubert *et al*., 2001; Fox, *et al*., 1995; Robinson *et al*., 1992; Stewart, *et al.*, 1995). Additionally, treatment of plants with the GS inhibitor MSO (methionine sulfoximine) prevents the incorporation of ammonium into glutamate and glutamine, even though both GDH activity and ammonium levels remain high (Lea *et al*., 1990).

The high K_m of GDH for ammonium and its mitochondrial localization led to the suggestion that this enzyme might be involved in reassimilating the large amount of photorespiratory ammonium released in mitochondria instead. However, the isolation of photorespiratory mutants defective in chloroplastic GS2 (in barley) (Wallsgrove *et al*., 1987) or Fd-GOGAT (barley and *Arabidopsis*) (Avila *et al.*, 1993; Kendall *et al*., 1986; Somerville & Ogren, 1980) suggests that the GOGAT pathway and not GDH is responsible for ammonium re-assimilation in photorespiration (Wallsgrove *et al*., 1987). Together, these results may be used to argue against a biosynthetic role for GDH. Instead, the NAD-requiring form of the GDH enzyme was suggested to participate in carbon rather than in nitrogen metabolism (Robinson *et al*., 1992). Among the biochemical lines of evidence supporting the catabolic role for GDH, is the fact that GDH activity is induced under carbon limiting conditions (for example, darkness) (Robinson *et al*., 1991, 1992), presumably to deaminate glutamate and provide carbon skeletons both for the TCA cycle and energy production during carbon or energy deficit. This is supported by molecular analyses that demonstrated the accumulation of GDH mRNA specifically in response to low carbon availability (darkness or carbon-starvation conditions)

(Melo-Oliveira *et al.*, 1996). Likewise, gene regulation data revealed the induction of GDH mRNA in light grown plants in response to the addition of ammonia leading to the notion that GDH could play a role in the assimilation of nitrogen under such growth conditions (Melo-Oliveira *et al.*, 1996). This idea was supported by the growth phenotype of the *gdh1-1* mutant identified in *Arabidopsis*. The mutant defective in *GDH1* gene displayed exaggerated retarded growth on media containing high inorganic nitrogen specially under suboptimal conditions (without vitamins) compared to wild type what led to suggest the important role of GDH in response to high inorganic nitrogen specially under conditions of plant stress (Melo-Oliveira *et al.*, 1996).

An alternative role has been proposed in which GDH functions in ammonia detoxification, because its activity is increased in plants exposed to high levels of ammonium. More precisely, GDH has been assigned the role of reassimilating excess ammonium (due to the limitation of the GS/GOGAT cycle) during specific stages of development (Loulakakis *et al*., 1994), such as during germination, seed set (Srivastava & Singh, 1987; Yamaya & Oaks, 1987) and leaf senescence (Cammaerts & Jacobs, 1985) conditions where the rates of amino acid catabolism are high. Since the GS/GOGAT enzymes decrease rapidly during senescence (Kar & Feierabend, 1984) the activity of GDH may serve as an adaptation of leaves to detoxify the ammonium generated during senescence. The addition of a GDH shunt to the glutamate synthase cycle would provide a mechanism that could respond to the different needs of the cells for carbon and nitrogen compounds. However, GDH may be of particular importance in those situations leading to C/N imbalance (carbon limitation or ammonium excess) where GDH is most likely to act in the catabolism of Glu as a shunt to insure that N metabolism does not deplete the mitochondria and the cell of the organic acid 2-oxoglutarate (Lea & Miflin, 2003; Figure 2). It would also provide a means for regulating the internal glutamate concentration shown to remain remarkably constant in leaves (Stitt *et al*., 2002) and across a wide range of physiological situations (Fritz *et al*., 2006).

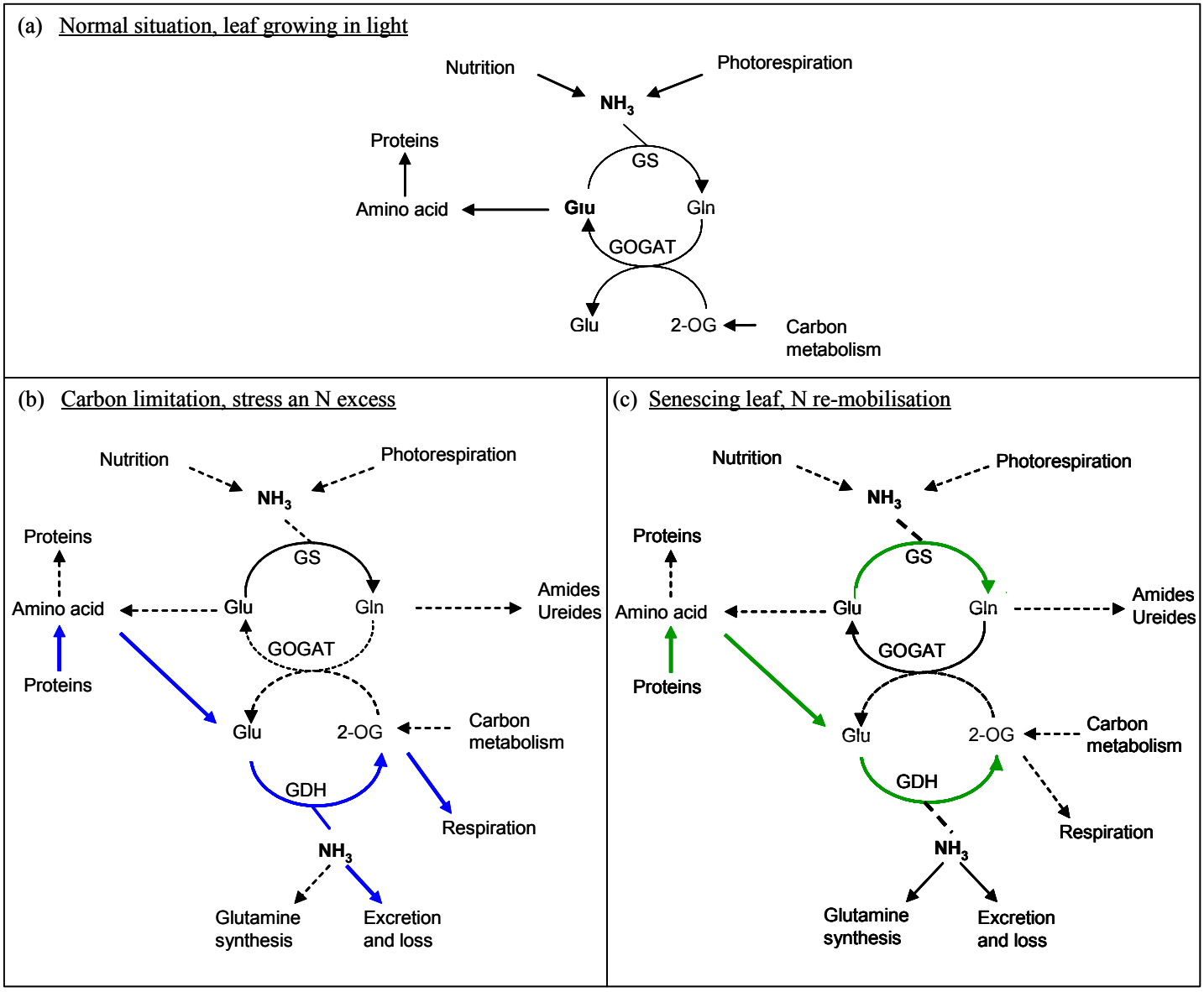

Figure 2. The role of GDH and GS/GOGAT cycle in carbon and nitrogen metabolism under different metabolic situations. (a) Normal situation, leaf growing in light; (b) Situation of carbon limitation, stress or excess of nitrogen.; (c) Situation of senescing leaf or nitrogen re-mobilisation. (Adapted from Lea & Miflin, 2003).

Clearly, there are still apparent contradictions in the literature and several unknown factors, such as the intracellular localization and/or temporal regulation, which may control the switch between glutamate metabolism and catabolism.

1.5.3 GDH family in *Arabidopsis thaliana.*

Screening of the *Arabidopsis thaliana* genome database for the presence of sequences homologous to *N. plumbaginifolia* GDH cDNAs allowed the identification of four putative GDH sequences (Restivo, 2004). The coding sequences from two of the clones shared 100% homology with two distinct cDNA clones previously identified and sequenced in *Arabidopsis thaliana* (Melo-Oliveira *et al.,* 1996; Turano *et al*., 1997) designated as *GDH1* (At5g18170)

and *GDH2* (At5g07440). The coding sequence of the third clone corresponded to a putative GDH (At3g03910) with high sequence homology to *GDH1* (Restivo, 2004). The fourth clone revealed the existence of a putative GDH (At1g51720) with low similarity to either of the NAD(H)-GDH genes of *Arabidopsis* and predicted to encode a protein of 624 amino acids compared with 411 AA for all known NAD(H)-GDH proteins. Furthermore, a protein database search indicated that At1g51720 is most similar to an NADP(H)-GDH (Purnell *et al*., 2005). Since NADPH + H^+ is almost exclusively used in the chloroplast (reviewed in James D. Mauseth, 2003; Maarten J. Chrispeels & David E. Sadava, 2003), the putative GDH has been associated to the chloroplast, to make sugars from carbon dioxide and water.

The GDH protein is a hexamer comprised of two subunit polypeptides that differ slightly in mass and charge. By convention the largest 43.0 KDa subunit is termed α and the 42.5 KDa subunit named β (Loulakakis & Roubelakis-Angelakis, 1991, 1996; Loulakakis *et al*., 1994). The association of α and β subunit in the hexameric holoenzyme yields seven possible GDH isoenzymes (Cammaerts & Jacobs, 1983; Loulakakis & Roubelakis-Angelakis, 1990b; Magalhaes *et al*., 1990). Phylogenetic analysis of higher plant GDH genes revealed that *GDH1* grouped with genes encoding for β subunits while the *GDH2* gene co-segregated with genes encoding for α subunit (Purnell *et al*., 2005).

The seven isoenzymes can be distinguished using native polyacrylamide gel electrophoresis followed by in-gel NAD-dependent activity (Turano *et al*., 1996). In *Arabidopsis*, the slowest-migrating isoenzyme in a native gel, GDH1, is a homohexamer composed of β subunits, and the fastest migrating isoenzyme, GDH7, is a homohexamer composed by α subunits. GDH isoenzymes 2 through 6 are heterohexamer composed of different ratios of α and β subunits (Turano *et al*., 1996; see Figure 3).

The identification of single GDH mutants in *Arabidopsis* (Melo-Oliveira *et al.*, 1996; Fontaine *et al.*, 2006), in *Zea mays* (Pryor, 1990; Magalhaes *et al*., 1990) and in *Nicotiana plumbaginifolia* (Fontaine *et al.*, 2006) show that no mutant is null for GDH activity because they possess normal amount of the other homohexamer.

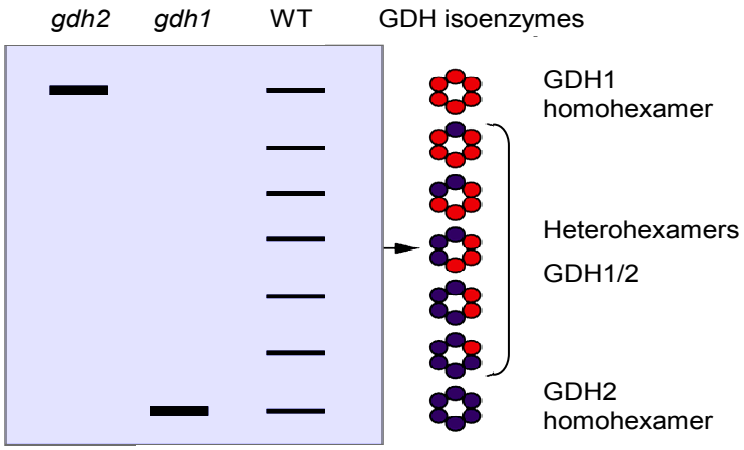

Figure 3. The seven isoenzymes of GDH in *Arabidopsis* are derived from the products of two genes, *GDH1* and *GDH2*. *gdh1* or *gdh2* mutants contain only one GDH isoenzyme, a homohexamer of *GDH2* or *GDH1* protein. WT, wild type (from Buchanan, Gruissem & Jones, 2000).

1.6. Light and metabolic control of nitrate assimilation and amino acid biosynthesis.

The incorporation of inorganic nitrogen into amino acids is considered a dynamic process regulated by external factors as light and by internal stores of carbon and nitrogen metabolites. The expression of genes controlling the assimilation of inorganic nitrogen into amino acids is subject to control by light and metabolic factors. For example, carbon skeletons produced by photosynthesis and sugar catabolism (as sucrose or glucose) affect the expression of genes involved in nitrogen metabolism, including genes encoding nitrate transporters (Lejay *et al*., 1999) and nitrate reductase (Cheng *et al*., 1992; Hoff *et al*., 1994). This is accompanied by a coordinated stimulation of organic acid synthesis. Sugar feeding leads to increase the levels of transcripts for important enzymes involved in the synthesis of organic acids (Koch, 1996; reviewed in Morcuende *et al.*, (1998)), including PEPCase, the cytosolic pyruvate kinase (Krapp *et a*l., 1993) and the NADP-dependent isocitrate dehydrogenase (NADP-ICDH) (Fieuw *et al*., 1995). Similarly, light and sucrose or glucose modulates the expression of genes involved in the assimilation of ammonium into glutamine like GS2 (Edwards & Coruzzi, 1989; Cock *et al*., 1991; Peterman & Goodman., 1991; Sakakibara *et al*., 1992; Oliveira & Coruzzi, 1999) and Fd-GOGAT (Coschigano *et al*., 1998). By contrast, light or the addition of sucrose has been shown to repress the expression of genes for asparagine synthetase in a number of species (Tsai & Coruzzi, 1990; Lam *et al*., 1994, 1998). In the light, when photosynthesis occurs and carbon skeletons are abundant, nitrogen is assimilated and transported as glutamine, a substrate in numerous anabolic reactions. In contrast, AS expression is induced when darkness prevents photosynthetic carbon reduction or when concentrations of organic nitrogen are high relative to those of carbon. Thus, under those conditions of low carbon availability or high organic nitrogen, plant direct the flow of nitrogen into asparagine, which has a higher N:C

ratio than glutamine and therefore acts as a shunt for storage and/or long- distance transport of nitrogen (Lam *et al.*, 2003; Figure 4).

GDH expression is regulated by light and/or carbon metabolites. GDH expression and activity accumulates specifically in dark adapted or carbon starved plants suggesting that under those conditions GDH could catalyze the deamination of glutamate releasing ammonium and carbon skeletons in form of α-ketoglutarate to support the tricarboxylic acid cycle (Oliveira *et al.*, 1996).

Conversely, sugars effects on plant parameters such as plant morphology and growth, storage reserve mobilization and photosynthesis are largely dependent on nitrate availability (Martin *et al.*, 2002). Martin and co-workers have shown in young *Arabidopsis* seedlings that carbohydrates to nitrogen ratios rather than the presence of one metabolite play a central role in regulating the processes underpinning seedling establishment. Moreover, recently, the combination of quantitative models showing gene expression changes in response to the C and N inputs and qualitative network model of known plant cell gene responses allowed understanding how C and N metabolites interact to regulate gene expression at multiple levels (Gutiérrez *et al.*, 2007). Moreover, Gutiérrez and co-workers suggested CN sensing as a mechanism that coordinates the global regulation of specific sets of molecular machines in the plant cell.

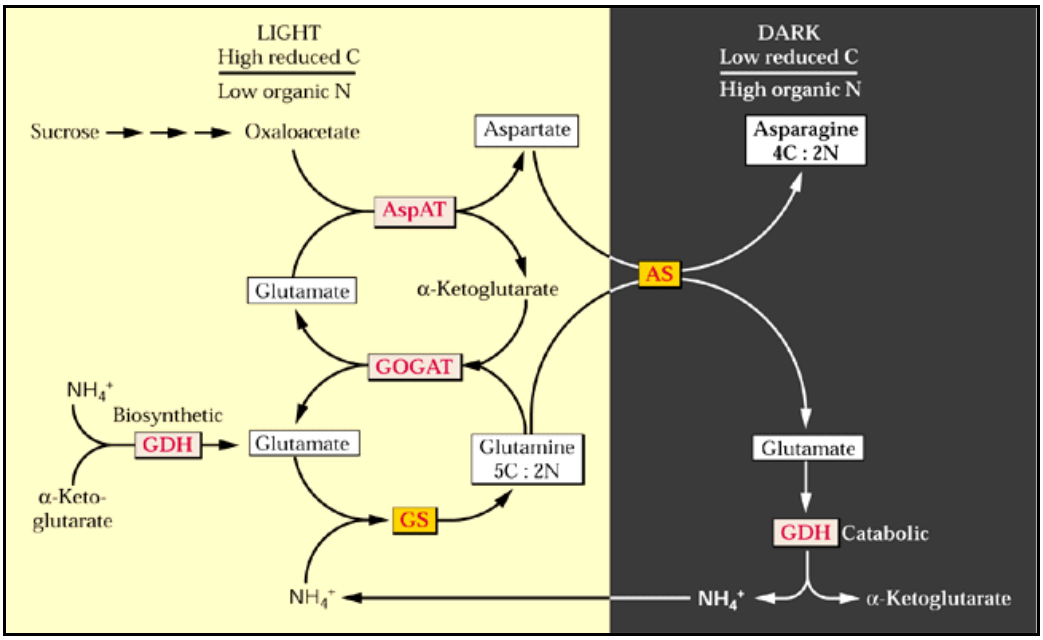

Figure 4. Major pathways of amino acid metabolism in *Arabidopsis*. The synthesis of glutamine and asparagine is sensitive to light and to the availability of reduced carbon. Under light conditions (high C:N ratio), glutamine and glutamate generated from the GS/GOGAT cycle are used as the major nitrogen donors or are metabolized into other nitrogen carriers, such as aspartate and asparagine. Under dark conditions (low C:N ratio), ASN1 functions to redirect the flow of nitrogen to asparagine with higher N:C ratio than glutamine and can transport and store nitrogen more efficiently when carbon skeletons are limiting. In dark, GDH may act in the catabolism of glutamate or in light to recapture the ammonium lost during photorespiration (from Buchanan, Gruissem & Jones, 2000).

1.7 Nitrate and its influence in plant development: analysis of the transition from vegetative state to the reproductive state, flowering.

Nitrate is emerging as a metabolite that triggers widespread and coordinated changes in plant metabolism and development (Stitt, 1999). Signals derived from nitrate and nitrogen metabolism interact with other fundamental processes in the regulation of plant gene expression, plant hormones and plant development.

Nutrient availability has a dramatic effect on flowering time, with a marked delay of flowering when nitrate is supplied (Stitt, 1999; Corbusier *et al*., 2001). Nitrate fertilization leads to increased growth (Marschner, 1995; Crawford, 1995), to changes in phytohormone levels (Marschner, 1995; Crawford, 1995), and to changes in the allocation and phenology including a decreased root:shoot ratio (Scheible *et al*., 1997a), altered root architecture (Marschner, 1995; Scheible *et al*., 1997a; Stitt & Feil, 1999) tuber initiation and senescence (Marschner, 1995; Crawford, 1995). Further changes induced by nitrogen fertilization include a delay in flowering (Bernier *et al*., 1993) and a stimulation of germination (Hilhorst & Karssen, 1989). Several studies in gene expression, metabolism, plant allocation and root architecture in mutants with decreased NIA expression show that nitrate (rather than metabolites further downstream in nitrogen metabolism) is the parameter sensed by the plant (summarised in Stitt, 1999; Scheible *et al*., 1997; Zhang & Forde, 1998; Zhang *et al.*, 1999).

An analysis of the regulation of flowering by nitrate will extend the understanding of the network that controls the flowering response and also open a rout to separate nitrate sensing and signalling.

1.8 Regulation of the transition to flowering.

Flowering is a major development event in the life cycle of plants since it represents the transition from vegetative growth to reproduction. The timing of flowering is determined by complex interactions between environmental cues and an internal genetic program in order to favour pollination success, seed production and survival of the progeny (Koornneef *et al*., 1998; Mouradov *et al*., 2002; Simpson *et al*., 1999). In most species, the timing of flowering is primarily influenced by environmental factors, which serve to communicate the time of the year and/or growth conditions favourable for sexual reproduction and seed maturation. These factors include photoperiod (i.e., day length), light quality, light quantity (photon flux density) and vernalization (exposure to a long period of cold). Other species are less sensitive to environmental variables and appear to flower in response to internal cues such as plant size or developmental stage.

In addition, plants can surpass the seasonal regulation and show precocious flowering under various stresses including biotic (e.g., pathogens) and abiotic stress (e.g., nutrient deficiency, drought, overcrowding or increasing growth temperature) to enable the plant to produce seeds, which are much more likely to survive the stress (Korves *et al.*, 2003; Martinez, C. *et al*., 2004; Balasubramanian *et al.*, 2006). But in contrast to vernalization and light, little is known about the pathways that mediate the responses to other environmental stresses and the mechanism of stress action is not clearly understood.

1.8.1 Physiological control of flowering time.

Over the years, physiological studies have led to three models for the control of flowering time (reviewed in Bernier, 1988, 1993, 2005; Thomas & Vince-Prue, 1997; Suárez-López, P., 2005 and references therein). The florigen concept (reviewed in Lang, 1952; Evans, 1971) was based on the transmissibility of substances or signals across grafts between reproductive "donor" shoots and vegetative "recipients". It was proposed that florigen, a flower-promoting hormone, was produced in leaves under favourable photoperiods and transported in the phloem to the shoot apex to initiate flowering. The identification of a graft-transmissible floral inhibitor also led to the concept of a competing "antiflorigen".

The inability to separate the hypothetical flowering hormones from assimilates led to a second model, the nutrient diversion hypothesis. This model proposed that inductive treatments result in an increase in the amount of assimilates moving to the apical meristem, which in turn induce flowering (reviewed in Sachs & Hackett, 1983; Bernier, 1988). The view that assimilates are the important component in promoting the transition to flowering was superseded by the multifactorial control model, which proposed that a number of promoters and inhibitors, including hormones and assimilates, are involved in controlling the transition to the flowering state (Bernier, 1988). According to this model, flowering can occur only when the limiting factors are present at the apex in the appropriate concentrations and at the right times. Genetic analysis of flowering time in some plants species supports the hypothesis that the transition to flowering is under multifactorial control (reviewed in Snape *et al*., 1996; Weller *et al*., 1997; Koornneef *et al*., 1998b) where some genes act to promote flowering and others to repress it; some of the genes interact with environmental signals and others appear to respond autonomously.

1.8.2 Genetic control of the transition to flowering.

The transition to flowering is controlled by complex genetic networks in *Arabidopsis*. The genetic and molecular analyses of *Arabidopsis* have revealed several interdependent genetic pathways for flowering, which enable plants to monitor both environmental and endogenous signals (reviewed in Mouradov *et al*., 2002; Simpson & Dean, 2002).

The photoperiod and vernalization pathways respond to environmental signals such as light and temperature, whereas the autonomous and gibberellic acid (GA)-dependent pathways monitor the endogenous developmental state of the plant.

1.8.2.1 Light dependent pathway.

Day length provides an environmental cue that allows plants to flower in response to the changing season. Molecular-genetic approaches have identified genes required for the day length response, and some of these are specifically involved in the regulation of flowering, while others encode components of light signal transduction pathways or are involved in circadian clock function.

In *Arabidopsis*, CONSTANS (*CO*) plays a central role in the induction of flowering by long days and encodes a nuclear protein containing zinc fingers (Puterill, J. *et al*., 1995; Robson, F. *et al*., 2001). *CO* mRNA abundance is regulated by the circadian clock and oscillates diurnally reaching a peak about 12h after the initiation of light (Suarez-López *et al*., 2001). Under short day conditions the *CO* mRNA peak occurs in the dark, and CO protein, which is only stable in the light, is unable to accumulate (Valverde *et al*., 2004). Under long day conditions, CO mRNA peak coincides with the exposure of plants to light and the translated protein reaches a significant level since nuclear CO protein is stabilized in the light (Valverde *et al*., 2004) and then CO protein is able to activate its target genes. *CO* is expressed mainly in leaves where activates the expression of Flowering Locus T (*FT)* gene, the major target of CO protein (Wigge *et al*., 2005). *FT* encodes a small globular protein with homology to RAF-Kinase-inhibitor like protein that promotes floral initiation (Kobayashi, *et al*., 1999**;** Kardailsky *et al.,* 1999; Suarez-Lopez, *et al*., 2001; Samach, *et al*., 2000). Because flowers form at a distant site, the shoot apex, some authors have suggested that the activation of *FT* RNA expression in leaves represents a long distance signal that primarily controls the timing of flowering (Abe *et al*., 2005; Wigge *et al*., 2005; Huang *et al*., 2005). It has recently been shown that *FT* action requires the presence of *FD,* a bZip transcription factor expressed on the flanks of the shoot apical meristem, where flower primordia are initiated (Abe *et al*., 2005; Wigge *et al*., 2005). Nevertheless, the demonstration that FT mRNA is transcribed in the leaves yet acts at the shoot

apex raises the question of whether the FT transcript can travel to the shoot apex. Huang *et al*., (2005) showed that FT detected in tissues dissected from the apex suggesting that FT transcript can move from leaves to shoot apex and it is sufficient to trigger flowering. Indeed, long distance movement of RNAs has been well documented in plants (Yoo *et al*., 2004; Kim *et al*., 2001; Xoconostle-Cazarés *et al.,* 1999; Ding, *et al*., 2003; Ueki *et al*., 2001) however, it remains to be determined if specific proteins are involved in the transport of FT transcripts through the phloem or whether FT protein moves to the apex as well. FT and FD promote floral transition through transcriptional activation of floral meristem genes such as *APETALA 1* (*AP1*), at the shoot apex (see section 1.8.2.5). Figure 5.

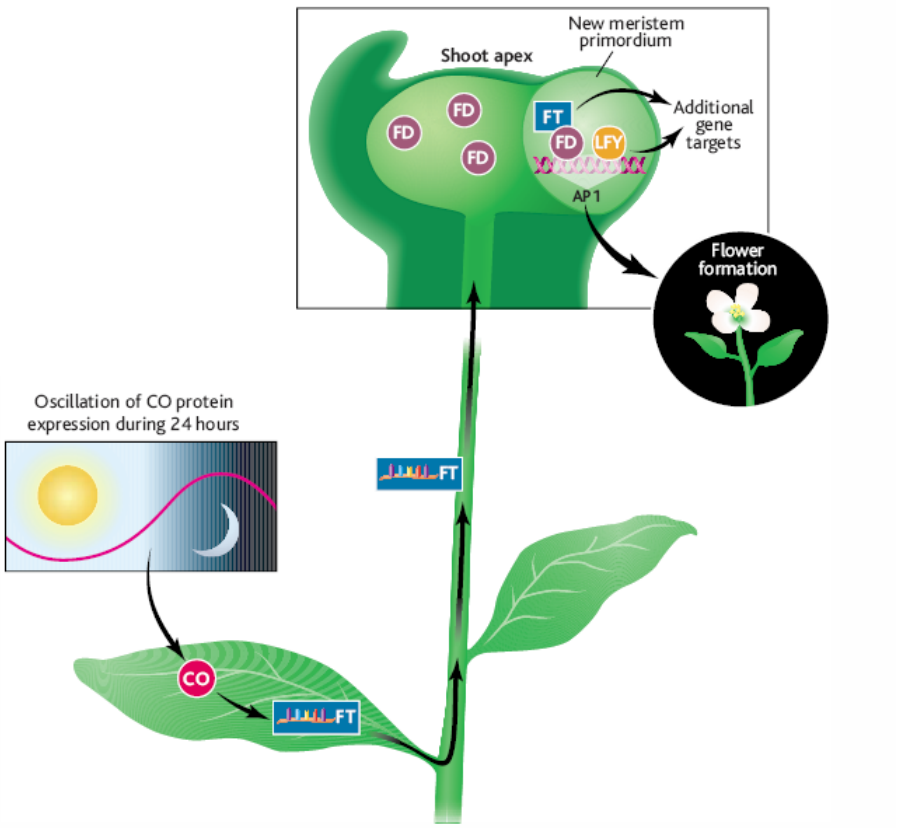

Figure 5. Integration of signals to generate a flower. Appropriate day length allows the accumulation of CO transcript that controls the expression of *FT* in the leaf. FT transcript moves through the phloem to the shoot apex where FT protein is produced and interacts with the transcription factor *FD*. The complex then activates key genes such as *AP1* to start flower development. LEAFY (*LFY*) is a transcription factor required for *AP1* expression in wild type plants. (Blázquez, 2005).

The finding that FT and FD act together to activate reproductive development in plants fills a gap in the understanding of how temporal information and spatial constraints are integrated, but it is intriguing how *AP1* expression is established in the floral primordia, given that *FD* is more widely expressed in the shoot apex. Abe *et al*., 2005 proposed that other proteins must restrict *AP1* expression to the correct location as is the case of TERMINAL FLOWER 1 (*TFL1)*, a protein with strong similarity to *FT*. *TFL1* has opposite roles to *FT* in the plant

acting as a potent regulator of *AP1* expression that prevents *AP1* from invading the central part of the shoot apex (Ratcliffe *et al.,* 1999). (See figure 6).

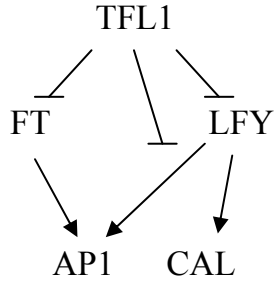

Figure 6. *TFL1* modulates *AP1* expression. *TFL1* prevents *LFY* expression from entering the shoot apex. Constitutive expression of *TFL1* makes LFY less efficient at inducing *AP1* and the *FT*-dependent *AP1* induction also does not occur. (F.Parcy, 2005).

Other target of *CO* is SUPPRESSOR OF OVEREXPRESSION OF CONSTANS 1 (*SOC1* or *AGL20*). *SOC1* encodes a MADS-box transcription factor that integrates signalling from the photoperiod, vernalization and autonomous flowering pathways in *Arabidopsis*. Additionally *SOC1* is positively activated by the gibberellic acid pathway, a major flowering signalling pathway under short days (Moon *et al*., 2003). *SOC1* is expressed in vegetative tissues and shows a gradual increase during vegetative growth. A similar pattern of age-dependent regulation has been reported for both *FT* and *LFY* (Blázquez *et al*., 1997; Kardailsky *et al*., 1999; Kobayashi *et al*., 1999).

1.8.2.2 Vernalization pathway.

Many temperate species only flower until they have experienced a prolonged period of cold, a process known as vernalization, which aligns flowering with the favourable conditions of spring. The vernalization requirement is conferred by a pair of epistatic loci, FRIGIDA (*FRI*) and FLOWERING LOCUS C (*FLC*), with *FLC* acting downstream of *FRI.*

FLC encodes a MADS box transcription factor (Michaels & Amasino,1999b; Sheldon *et al*., 1999) and plays a central role in the vernalization process inhibiting genes required to switch the meristem from vegetative to floral development. The expression of the floral repressor *FLC* is regulated by several independent pathways. A key regulator of *FLC* expression is *FRI* that encodes a novel protein with coil-coiled domains. *FRI* represses flowering by up regulating *FLC* RNA levels (Michaels & Amasino, 1999b; Sheldon *et al*., 2000). An increasing number of *FLC* activators have been identified by the analysis of early-flowering mutants. Two FRIGIDA-LIKE (*FRL*) genes, *FRL1 and FRL2*, are required for the up regulation of *FLC* expression by *FRI* (Michaels *et al*., 2004).

FLC mRNA levels are down regulated by vernalization. For annual plants, the vernalization response is saturated after several weeks of cold and, once established, the vernalized state is

stable though subsequent growth at ambient temperatures, although it is reset after meiosis. Similarly, repression of *FLC* levels is achieved after several weeks of cold and then is maintained at low levels throughout subsequent development, whilst being reset in the next generation (Sheldon *et al*., 2000). The maintenance of *FLC* repression following vernalization indicates that this gene is epigenetically silenced. Epigenetic silencing of genes is mediated by numerous covalent modifications of both DNA and histones. Vernalization increases histone H3 deacetylation and methylation, modifications associated with gene repression (Sung & Amasino, 2004).

Genetic screens for mutants have identified trans-factors that mediate repression of *FLC* in response to cold (Chandler *et al.*, 1996; Sung & Amasino, 2004). The earliest acting gene is VERNALIZATION INSENSITIVE3 (*VIN3*), which encodes a protein with a plant homeodomain (PHD) and fibronectin type III repeats. A second class of gene involved in the vernalization response is represented by the genes VERNALIZATION1 (*VNR1*) and VERNALIZATION2 (*VRN2*). *VRN2* is thought to be a component of a Polycomb repressor complex that mediates H3-K27 methylation of *FLC* chromatin, which probably leads to H3-K9 methylation (Sung & Amasino, 2004; Bastow *et al*., 2004). *VRN1*, a B3-domain-containig DNA-binding protein (Levy *et al*., 2002)

1.8.2.3 Autonomous pathway

Plants require not only external (environmental) factors but also internal (developmental) factors to promote flowering. The autonomous pathway acts in parallel to vernalization to repress *FLC* expression (Koornneef *et al*., 1991; Simpson & Dean, 2002). Although all members of this pathway act to limit *FLC* expression, genetic analysis has revealed that they have distinct functions. Genes in the autonomous pathway include *LD*, *FCA*, *FY*, *FPA*, *FVE*, *FLD* and *FLK*. *FPA* encodes a plant-specific, nuclear RNA binding protein (Macknight *et al*., 1997) with a C-terminal WW protein domain thought to be involved in protein-protein interactions (Macknight *et al*., 1997). *FCA* is able to regulate its own expression by promoting cleavage and polyadenylation of its own third intron; this auto-regulation is under developmental control and requires the WW domain (Quesada *et al*., 2003). Like *FCA*, *FPA* and *FLK* also contain a RNA recognition motif and are required for the regulation of *FLC*. *FLD* encodes a protein that is a homologue of a protein found in mammalian histone deacetylase complexes (He *et al*., 2003), emphasising the importance of histone modification in *FLC* regulation. *FVE* the nuclear WD-repeat protein, MSI4 typically found in complexes

involved in chromatin assembly and histone modification. *FLD* and *FVE* are likely to act together in a HDAC complex to repress *FLC* expression (Ausin, *et al*., 2004; He *et al*., 2003).
LD (LUMINIDEPENDENS) encodes a nuclear protein similar to transcriptional regulators. It is involved in the regulation of the meristem identity gene LEAFY *(LFY)* (Aukerman *et al*., 1999).
Therefore genes assigned to the autonomous pathway seem to represent protein complexes involved in RNA processing or histone modification and *FLC* expression seems to be particularly sensitive to disruption of these processes.

1.8.2.4 Gibberellic acid pathway.

Gibberellins (GAs) are one class of tetracyclic dirterpenoid phytohormone affecting many aspects of plant growth and development, including seed germination, root growth, stem elongation, leaf expansion, floral induction, and flower development (Langridge, J., 1957; Ross *et al.*, 1993). The effect of GA on the induction of flowering has been studied by applications of exogenous GA and using mutations that disrupt either GA biosynthesis or signalling (Wilson *et al*., 1992). The *Arabidopsis* mutant *ga1-3* contains a deletion in KAURENE SYNTHASE, which is believed to catalyse the first committed step of GA biosynthesis, and thus, the ga1-3 mutation produces a strong block to GA production (Sun *et al*., 1992). Under inductive long day conditions, *ga1-3* exhibits only a slight delay in flowering, however, in short-day (SD) conditions, the mutant remains vegetative until senescence without flowering (Wilson *et al.*, 1992). Furthermore, the block in flowering cannot be overcome by vernalization, indicating that under SD in the mutant *ga1-3,* GA must be required for vernalization.
The control of flowering has been also suggested by studying genes involved in GA signalling. GA regulates flowering by suppressing a group of DELLA protein nuclear repressors such as GIBBERELLIC ACID INSENSITIVE (*GAI*), REPRESSOR OF GA1-3 (*RGA*) and RGA-LIKE1 (*RGL1*). *GAI* and *RGA* are negative of GA responses in the control of stem elongation, flowering time, and root growth. *RGL2* is a major repressor of seed germination, because *rgl2* null mutations can significantly promote the germination of *ga1-3* seeds, which require GA for normal germination (Lee *et al.,* 2002).
The gene FLOWERING PROMOTER FACTOR1 (*FPF1*) is expressed in the apical meristem immediately after the photoperiodic induction of flowering by long day. Treatments with GA and paclobutrazol, a GA biosynthesis inhibitor, indicates that *FPF1* is involved in a GA-

dependent signalling pathway and modulates a GA response in apical meristems during the transition to flowering.

Genetic analysis suggests that the GA pathway acts in parallel to the long-day pathway because there is redundancy between mutations affecting both pathways. The effect of mutations that impair GA pathway is strongest under short days and double mutants affecting both pathways often did not flower under long days. In SDs, where the long-day is not active, GA is the major flowering pathway and loss of function of this pathway can prevent flowering. Also, the expression of the flowering time gene *SOC1* is promoted by GA and the long-day pathway.

1.8.2.5 Integration of *Arabidopsis* Flowering Pathways.

The four genetic pathways controlling the floral transition are integrated at the transcriptional regulation of the Floral Pathway Integrators, *FT*, *SOC1/AGL20* and *LFY* (reviewed by Araki 2001; Simpson & Dean, 2002; Boss *et al*., 2004) (see Figure 7). *FT* and *SOC1* are not only the immediate targets of the transcription factor *CO* (the central regulator in the photoperiod or long-day pathway), but also are negatively regulated by *FLC* which integrates vernalization and the autonomous pathways (see 1.8.2.2 and 1.8.2.3) (Lee *et al*., 2000; Onouchi *et al*., 2000; Samach *et al*., 2000). Therefore, *FT* and *SOC1* integrate long day and autonomous/vernalization pathways. In addition, *SOC1* is also regulated by the GA pathway whereas *FT* expression is not, suggesting that *SOC1* and *FT* act differentially in the integration of floral pathways. The other integrator, *LFY*, is regulated by both the long day and GA pathways trough separate *cis*-elements on the *LFY* promoter (Blázquez & Weigel, 2000). *LFY* can be considered both as a flowering time gene and a meristem identity gene. In contrast to *FT* and *SOC1*, *LFY* is not an immediate target of *CO*, suggesting the existence of mediators between the two genes (Samach *et al*., 2000). It has been reported that *FT* functions in parallel to *LFY* for floral initiation and is necessary for *LFY* function (Ruiz-García *et al*., 1997; Nilsson *et al*., 1998; Kardailsky *et al*., 1999; Kobayashi *et al*., 1999). However, the relationships among the three integrators are largely unknown.

The flowering signals ultimately lead to the induction of a set of genes called Floral Meristem Identity (FMI) genes responsible for the fate change of the meristems emerging on the flanks of the shoot apex (reviewed in Parcy, 2005). This group of genes includes LEAFY (*LFY*), APETALA (*AP1*) and CAULIFLOWER (*CAL*). They act early to control the initiation of flowers and are expressed throughout the incipient floral primordium (Lohmann & Weigel, 2002).

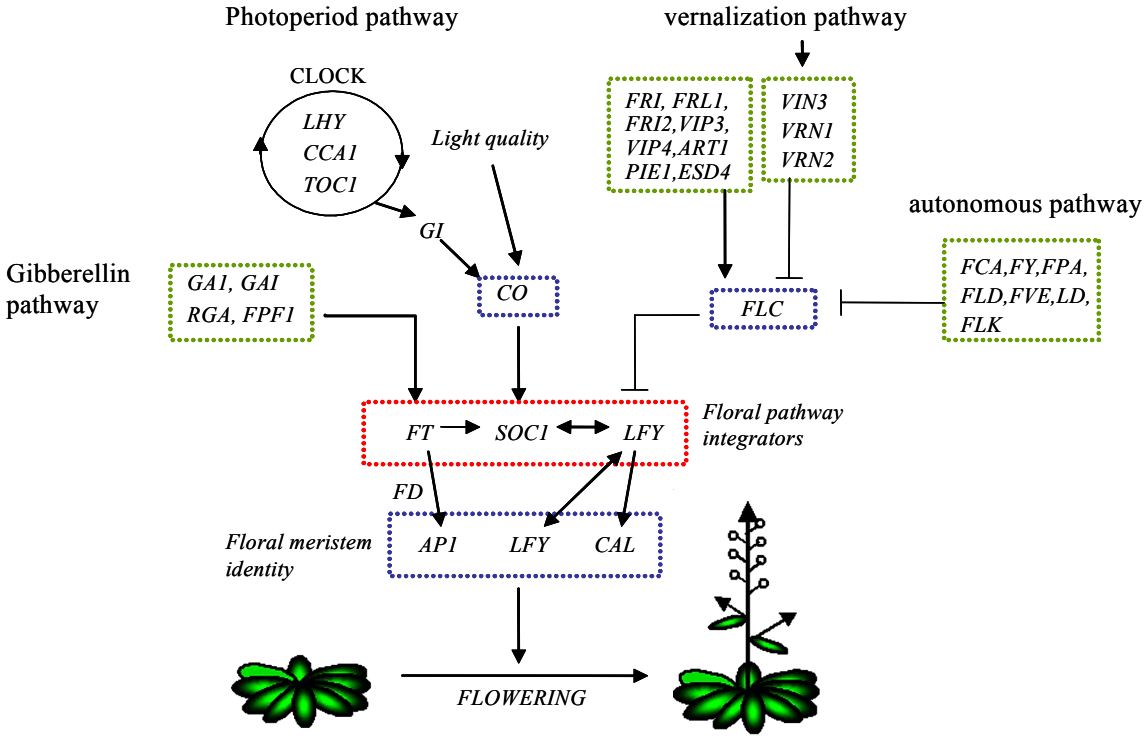

Figure 7. Pathways controlling flowering-time in *Arabidosis thaliana*. The photoperiod pathway promotes flowering under long days. The autonomous pathway negatively regulates the floral repressor *FLC* as well as the vernalization pathway. Gibberellin promotes flowering especially under short days. All four pathways converge on the transcriptional regulation of the floral integrator genes *FT* and *SOC1* which promote the expression of *LFY* and *AP1* required to confer floral identity to the floral primordia. (Adapted from Corbesier & Coupland, 2005).

LFY is necessary and sufficient to convert indeterminate shoots into flowers in *Arabidopsis*. In *lfy* mutants, shoots that would normally develop as flowers are converted into indeterminate shoots, and all the secondary shoots have emerged in the positions in which flowers would develop on a wild type inflorescence (Weigel *et al.,* 1992). Conversely, the ectopic expression of *LFY* promotes early flowering and the conversion of shoots to flowers (Blazquez *et al*., 1997; Weigel & Nilsson, 1995) (See figure 8). Thus, *LFY* gene functions in affecting the time to flowering and in defining floral meristem identity.

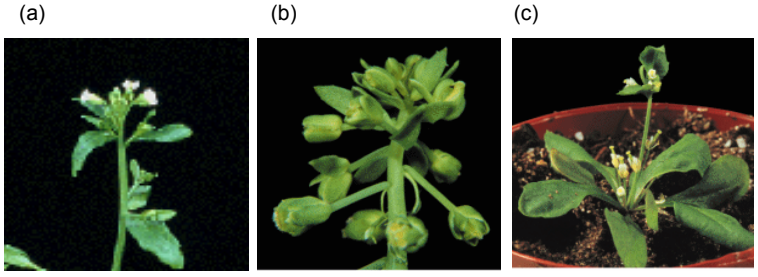

Figure 8. (a) Wild type flower of an *Arabidopsis thaliana* plant. (b) In *lfy* mutants, shoots that would normally develop as flowers are converted to indeterminate shoots. (c) In a *35S::LFY* plant expressing *LFY* constitutively, secondary shoots are converted into flowers and the primary shoot terminates early in a flower (from Buchanan, Gruissem & Jones, 2000).

LFY expression persists throughout young floral meristems where contributes to the specification of the floral bud by inducing the expression of *AP1* and CAULIFLOWER (*CAL*) (Parcy *et al*., 1998; Wagner *et al*., 2004). Although *cal* mutants have no visible phenotype, *cal ap1* double mutant floral meristems give rise to an indeterminate spiral of lateral meristems developing as a mass of apical meristems with no differentiated organs resulting in cauliflower-like inflorescences. The sequences and expression patterns of the proteins encoded by *AP1* and *CAL* are very similar, suggesting that their functions may be largely redundant (Kempin *et al*., 1995). Mutant phenotypic analysis and expression studies indicate that an important function of *LFY*, *AP1* and *CAL* is to up-regulate each other in the flower primordium (reviewed in Pidkowich *et al*., 1999).

Another gene that much affects the determinacy of *Arabidopsis* meristems is TERMINAL FLOWER 1 (*TFL1*) which influences *LFY* capacity to induce *AP1* expression (see 1.8.2.1, figure 6). *TFL1* has symmetrically opposite roles in the plant, acting as a potent inhibitor of flowering when over expressed and, conversely, causing premature terminal flowers to form when mutated (Bradley *et al*., 1997; Shannon & Meeks-Wagner, 1991). The opposite phenotypes of *lfy* and *tfl1* suggest that their gene products may act antagonistically.

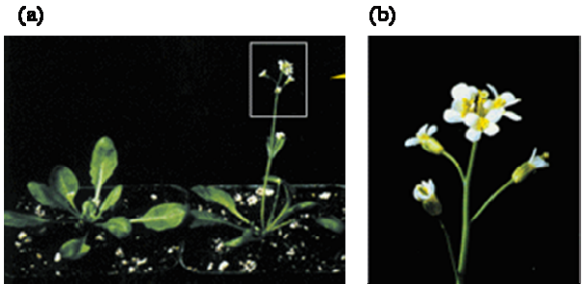

Figure 9. *TFL1* regulates flowering and indeterminacy. (a) *tfl1* inflorescence phenotype (right and enlargement) compared to wild type (left). Mutant plants terminate early in a terminal flower or a cluster of flowers (from Buchanan, Gruissem & Jones, 2000).

1.8.3 The ABC model of floral patterning

The formation of a flower requires a cascade of sequential gene activity that gradually converts a mass of undifferentiated cells (the apical meristem) into the parts of a flower. The homeotic genes encode transcription factors that act as master switches, turning on/off downstream genes that ultimately make each part of the flower in its appropriate location. The flower of dicots is organized into four concentric rings of organs termed whorls. The outer two whorls are occupied with the sterile organs (petals and sepals) and the inner two whorls are devoted to reproduction (stamen and carpel), the central purpose of flower formation.

Genetic analyses of mutants led to the proposal of the ABC model (Bowman *et al*., 1991; Coen & Meyerowitz, 1991). The model states that the development of four types of floral organs is governed by the overlapping activities of three classes of regulatory genes. Termed A, B and C, each class of genes is active in two adjacent whorls. Cells in which only "A genes" are expressed develop into sepals. This group of genes include *AP1* and *AP2*. Cells in which A and B genes are expressed develop into petals. *APETALA3* (*AP3*) and PISTILLATA (*PI*) belong to the "B group". Expression of B and C genes turns on the developmental program to form stamens. Expression of C genes alone turns on the development of carpels. AGAMOUS (*AG*) genes are included in the "C group".

A central question in understanding the floral patterning is how the pattern of ABC gene expression is set up. One of the candidates for upstream regulators of flower specific ABC genes is the floral integrator *LFY*, although it has been difficult to determine the interaction between *LFY* and ABC genes because *LFY* affects the identity of the floral meristem itself, an event that precedes the activation of the ABC genes. In addition, the expression of ABC genes in the abnormal flowers of lfy mutants indicate that *LFY* is not absolutely required for their activation and that ABC genes are redundantly regulated (Parcy *et al*., 1998).

1.19 Aims of the thesis.

The major aim of this thesis was to study the effect of nitrate on primary metabolism and in development of the model plant *Arabidopsis thaliana*.

The overall aims of this work are presented below:

1.To gain more insights into the regulation of primary metabolism by the functional characterization of the glutamate dehydrogenase (*GDH*) family, an enzyme putatively involved in the metabolism of amino acids and thus suggested to play different and essential roles in carbon and nitrogen metabolism in plants.

In order to better understand the role of GDH genes in *A. thaliana*, knock out mutants and transgenic plants carrying RNA interference construct were generated and characterized. The effect of silencing GDH on carbon and nitrogen metabolisms was investigated, especially the level of carbohydrates and the amino acid pool were further analysed. It has been shown that GDH expression is regulated by light and/or sugar status (see 1.7), therefore, phenotypic and metabolic analysis were developed in plants grown at different points of the diurnal rhythm and in response to an extended night period (it mimics a condition of sugar deprivation).

2. To study the influence of nitrate in the transition from vegetative growth to flowering time and to contribute to the pool of knowledge on the complex network that controls the reproductive state in *Arabidopsis thaliana.* Previous studies showed that there is a marked delay in flowering time in conditions of high nitrate suggesting the importance of nitrate as a putative signal molecule involved in the transition to flowering (Stitt, 1999). Moreover, analyses done by Dr. Irene Loef showed an influence of nitrate in the photoperiod and autonomous flowering promoting pathways and that the impact of nitrate in flowering time was due to nitrate itself or to a closed metabolite. A large focus of this work therefore was to better understand the regulation of flowering time by nutrients, especially nitrate, and to elucidate about the putative signalling pathway promoted by nitrate that controls the transition to flowering in *Arabidopsis thaliana*.

The use of different mutants and transgenic plants impaired in flowering signalling pathways was crucial to evaluate the impact of different nitrate concentrations on flowering time and to better understand the interaction of nitrate-dependent signals with other main flowering signalling pathways (see 1.8.2). Analyses of flowering time were performed in plants grown in response to various concentrations of nitrate under neutral day length photoperiod.

Global analyses of gene expression of two independent flowering systems, a light impaired mutant (*co2*tt4) and a constitutive over-expresser of the potent repressor of flowering (35S::*FLC*), were to be investigated under two different concentrations of nitrate in order to identify candidate genes that may be involved in the regulation of flowering time by nitrate.

CHAPTER 2 MATERIALS & METHODS

2. CHAPTER: MATERIAL AND METHODS

2.1 MATERIALS

2.1.1 Enzymes, chemicals and reaction kits

Enzymes

Tap polymerase	QIAGEN, Hilden, Germany
KOD HiFi DNA polymerase	Novagen**,**
Restriction enzymes	Fermentas, St Leon-Rot, Germany; Roche, Manheim, Germany
DNase I	Roche, Manheim, Germany
RNase I	Roche, Manheim, Germany
Reverse Transcriptase	Promega, Madison, USA
T4 DNA ligase	Promega, Manheim, Germany
GATEWAY™ BP clonase	Invitrogen Karlsruhe, Germany
GATEWAY™ LR clonase	Invitrogen Karlsruhe, Germany

Chemicals

Agarose (SeaKem-Le)	Cambrex, Rockland, ME, USA
Bromophenol Blue	Sigma, Deisenhofen, Germany
DNA Smart Ladder	Eurogentec, Liege
Phenol	Merck, Darmstadt, Germany
Chloroform	Merck, Darmstadt, Germany
Lithium Chloride	Sigma, Deisenhofen, Germany
NaOH	Merck, Darmstadt, Germany
Ethanol	Merck, Darmstadt, Germany
NADH	Roche, Mannheim, Germany
NAD^+	Roche, Mannheim, Germany
EDTA	Merck, Darmstadt, Germany
MTT	Sigma, Deisenhofen, Germany
PMS	Serva, Heidelberg, Germany
HEPES	Carl Roth GmbH & Co, Germany
Tris	Carl Roth GmbH & Co, Germany
Tricine	Sigma, Deisenhofen, Germany
Gibberellin	Sigma, München

Triton X-100	Serva, Heidelberg, Germany
Tween 20	Serva, Heidelberg, Germany
Trizol reagent	Invitrogen, Karlsruhe, Germany
X-glucuronidase	Duchefa, Haarlem, the Netherlands
X-gal	Duchefa, Haarlem, the Netherlands
Silwet L-77	Helena Chemical, Fresno, USA

Reaction kits

QIAquick PCR purification kit	Qiagen, Hilden, Germany
QIAquick Gel Extraction Kit	Qiagen, Hilden, Germany
QIAGEN Plasmid mini Kit	Qiagen, Hilden, Germany
pGEM®-T Easy vector ligation system	Promega, Manheim, Germany
pENTR_SD/D_TOPO® Cloning kit	Invitrogen, Karlsruhe, Germany
GATEWAY™ directional Cloning system	Invitrogen, Karlsruhe, Germany
Reverse Transcription Kit	Promega, Madison, USA
SYBR Green Master Mix	Applied Biosystems, Darmstadt, Germany
Random labelling primer system	Amersham, Freiburg, Germany

2.1.2 Oligonucleotides

Sequences are depicted in all cases from 5´to 3´. Primer synthesis was performed by *Invitrogen* (Paislay, Scotland).

Table 2.1 Primers used for T-DNA insertion lines analysis

Primer	Sequence	Description
LBb1	GCGTGGACCGCTTGCTGCAACT	Left Border, T-DNA specific
SALK 542736 F	GACATTACCGGAGCAATCAAGA	Forward genomic primer, SALK 542736 line
SALK 542736 R	GATATCACAATCCTCAACCAGTA	Reverse genomic primer, SALK 542736 line
SALK 602709 F	GTATCGACATCAACGCTCTCA	Forward genomic primer, SALK 602709 line

SALK 602709 R	AACTTTGCCTTCACATCTCCAG	Reverse genomic primer, SALK 602709 line
SALK 537861 F	GGGCAGCGAAGTTGATAAGTGA	Forward genomic primer, SALK 537861 line
SALK 537861 R	CGAATCAGGATCGATTGAATCA	Reverse genomic primer, SALK 537861 line

Table 2.2 Primers used for real time RT PCR analysis

Primer	Sequence	Description
GDH1 F	TATCCCGGCCTTGCTCAAGCATAC	Forward, *GDH1*
GDH1 R	CCCTGTTGATGACACCACCAAGTG	Reverse, *GDH1*
GDH2 F	TTGCCACCGAAGCTCTTCTTGCTG	Forward, *GDH2*
GDH2 R	CGCTTACTGCAACCACTTTACCGC	Reverse, *GDH2*
GDH3 F	ACCATATCTGGACAGCGATTCGCC	Forward, *GDH3*
GDH3 R	TTGCTCCTGTGACATCACTCACCG	Reverse, *GDH3*
Actin F	TCCCTCAGCACATTCCAGCAGAT	Forward, actin
Actin R	AACGATTCCTGGACGTGCCTCATC	Reverse, actin

Table 2.3 Primers used to check genomic DNA contaminations of RNA samples

Primer	Sequence	Description
Actin F	ACT TTCATCAGCCGT TTTGA	Forward, actin
Actin R	ACGATTGGTTGAATATCATCAG	Reverse, actin

(The actin gene product is 190 bp in length on cDNA template, and 631 bp in length on genomic DNA template)

Table 2.4 Primers for RNAi construction

Primer	Sequence	Description
GDH1 F	attB1 CTTTCACACTCGGTGTTAATCGT	Forward, *GDH1* cDNA
GDH1 R	attB2 GCTCATTAACTATTAGAGTCCA	Reverse, *GDH1* cDNA

GDH2 F	attB1 TGTGCCATACTCATTCTTGCAA	Forward, *GDH2* cDNA
GDH2 R	attB2 GGAAAGCTCAATGATTTTCAGT	Reverse, *GDH2* cDNA
GDH3 F	attB1 GGGAGCTAAAGACCTACATGACT	Forward, *GDH3* cDNA
GDH3 R	attB2 AGGTTAAACTGCAATTAGCAC	Reverse, *GDH3* cDNA

attB recombination sites sequences

attB1: GGGGACAAGTTTGTACAAAAAAGCAGGCTCC

attB2: GGGGACCACTTTGTACAAGAAAGCTGGGT

Table 2.5 Primers for gene promoter-GUS fusion analysis

Primer	Sequence	Description
GDH3 F	CACCGAGGGAATGGCCTTTTATATTTGTT	Forward, *GDH3*-GUS
GDH3 R	GGCTTTCTTCTCTCTTCTTTATTT	Reverse, *GDH3*-GUS

CACC: sequence to enable directional cloning

2.1.3 Plasmids

pGEM® T Easy Vector	Promega, Manheim, Germany
pSPECTRE	Scientific and Industrial Research Organization, Canberra, Australia
pJAWOHL 8	Max Plank Institute for Plant Breeding Research, Cologne, Germany
pENTR/SD/D_TOPO	Invitrogen, Gmbh
pKGWFS7	Karimi et al., 2002

2.1.4 Bacterial strains

Escherichia coli DH5α (GIBCO-BRL, Gaithersburg, USA).

Escherichia coli Top 10 (Gateway, Invitrogen, GmbH, Germany).

Agrobacterium tumefaciens pGV3101-pMP90RK

2.1.5 Antibiotics

For the selection of transformants antibiotics with final concentrations were used as follows:

ampicillin (Amp)…… 100mg/l

kanamycin (Kan)……. 50mg/l

spectinomycin (Spec)….. 100mg/l

carbenicillin (Car)…… 50mg/l

gentamycin (Gent) ……... 25mg/l

DL- phosphinotricin (PPT)… 20mg/l

rifampicin (Rif) ……... 50mg/l

2.1.6 Plant material and transformation

2.1.6.1 Plant material

Arabidopsis thaliana (L.) Heynh., ecotype Columbia (wild type, Col-0).

Arabidopsis thaliana (L.) Heynh., ecotype Lansdberg erecta (wild type, Laer).

T-DNA insertion mutants

Seeds of *Arabidopsis thaliana* (Col-0 ecotype) T-DNA insertion mutants for the genes At5g18170 (*GDH1*) (SALK_542736), At5g07440 (SALK_602709) and At3g03910 (SALK_537861) were provided from Nottingham Arabidopsis Stock Centre (Nottingham, UK).

Flowering mutants

Different flowering-time mutants and transgenic plants with modified expression in flowering time genes were recovered in the Landsberg erecta or Columbia ecotypes of *Arabidopsis thaliana.*

The mutant lines were obtained from the Nottingham Arabidopsis Stock Centre (Nottingham, UK). The transgenic lines were provided by George Coupland´s group, (Max Plank Institute for Plant Breeding Research, Cologne, Germany).

2.1.6.2 Plant transformation

A colony of transformed *A. tumefaciens* was inoculated and a pre-culture of 10ml YEB, pH 7.0 (Bacto-tryptone (5g/l), Bacto-yeast-extract (1g/l), Bacto-peptone (1g/l), sucrose (5g/l) in 1l H_2O) supplied with rifampicin (50mg/l), carbenicillin (50mg/l) and the specific selection for the vector was prepared. The mixture was incubated at 28° C for two days. The pre-culture was further inoculated in 400ml YEB selective medium and incubated at 28°C overnight. The bacterial cells were harvested by centrifugation at 8000 rpm for 10 min., at 4°C and resuspended in 200 ml infiltration medium (sucrose (50g/l), MS-Medium (2.2 g/l), MES (0,05 g/l), 10µl BAP (benzamine-aminopurine) in H_20, pH 5.7. The bacterial solution (200ml) was added to 1ml Silwet L-77. The plants inflorescences were dipped for 10 sec. In this solution and dried overnight (Clough and Bent, 1998).

2.1.7 Growth conditions

2.1.7.1 Plant growth on soil

Arabidopsis thaliana plants were grown in environmental chambers under standard conditions (60 % relative humidity, 20° C, 120 μEs^{-1} m^{-2} light), or in the greenhouse (50% relative

humidity day/ 80% night, 20°C day/ 18°C night, 16h light photoperiod at 250µmol m-2 s-1 light).

2.1.7.2 Plant growth on plates

- Seed surface sterilization

Seeds were surface sterilized in bleach solution containing 1/4 NaHClO (12%) and 3/4 sterile distilled water plus 0.005% (w/v) Tween 20 for 15 min. After washing 3 times with sterile distilled water, the seeds are resuspended in 0.15% sterile select agar solution being ready for the sowing on sterile agar plates.

- Plant growth media

Sterile AMOZ medium corresponding to sugar free 0.5X MS medium (2.45 g/l, MES (0.6 g/l), Select agar (7g/l) for 1 l distilled H_2O adjusted to pH 5.7 was used. Sucrose in a final concentration of 0.5%, was added to the medium after autoclaving. In the case of sugar starvation medium, the sugar addition was omitted during preparation. For selection of transformed plants, the medium was supplemented with 0.5% sucrose and the appropriate antibiotic.

Antibiotic selection was carried out for 5-6 days, unless indicated otherwise. Depending on the purpose, seedlings were subsequently analysed or transferred onto soil or onto different plates for sugar/nitrate treatments. Durations of sugar/nitrate treatments are indicated in the Results chapter.

For the nitrate treatments (flowering mutants), sterile seeds were germinated on horizontal agar plates containing different concentrations of nitrate, indicated in Table 2.6. Phosphate starvation treatment was similar to the 3mM nitrate medium with a final KH_2PO_4 concentration of 200µM.

After seeding, plates were sealed with Leucopore tape (Beiersdorf, Hamburg, Germany) and kept horizontally at 4°C for 3-5 days for vernalization. Then, transferred to sterile growth chambers, with 20°C day/night and 120µmol m-2 s-1 light. The photoperiod used was different depending of the seeds to analyse, SD (short day, 8h light/16h dark), neutral (12h light/12h dark) or LD (long day, 16h light/8h dark) conditions.

Root experiments were carried out vertically during 10-14 days in rectangular grey boxes keeping the root growing under no-light conditions. The medium used is indicated in each experiment.

Table 2.6 Agar medium with different nitrate concentration

1000 ml	0,150mM NO3	0,5mM NO3	1mM NO3	3mM NO3	10mM NO3	35mM NO3
10x KNO3	0.150mM	0.5mM	1mM	3mM	10mM	35mM
1M Mg (NO3)2						4mM
100x Mg SO4	1mM	1mM	1mM	1mM	0.5mM	0.5mM
1M Mg Cl2					4mM	
1M KCl	1.5mM	2.5mM	5mM			
100x KH2 PO4 (pH 5,66)	3mM	3mM	3mM	3mM	3mM	3mM
100x Ca Cl2	2mM	2mM	2mM	2mM	2mM	2mM
Select agar	8g	8g	8g	8g	8g	8g
Oligoelements	0.5ml/l	0.5ml/l	0.5ml/l	0.5ml/l	0.5ml/l	0.5ml/l
0,9 M MES	3mM	3mM	3mM	3mM	3mM	3mM
Na Fe EDTA	32mg/l	32mg/l	32mg/l	32mg/l	32mg/l	32mg/l
distilled H2O	full until 900ml	full until 900ml	full until 900ml	full until 900ml	full until 900ml	full until 900ml
After autoclave						
0,2M Glutamine		4mM	4mM	4mM	4mM	4mM
Sucrose	0.5%	0.5%	0.5%	0.5%	0.5%	0.5%

Table 2.7 Composition of the Oligoelements solution

100ml	final concentration
H3BO3	15mM
MnSO4	3.5mM
ZnSO4	0.25mM
CuSO4	0.150mM
NiCl2	1mM
Na2MoO4	0.075mM
CoCl2	0.005mM

All standard chemicals and media were purchased from *Merck* (Darmstadt, Germany), *Sigma* (Deisenhofen, Germany), *Fluka* (Seelze, Germany) or *DUCHEFA* (Brussels, Belgium).

2.2 METHODS

2.2.1 General molecular biology techniques

Standard molecular biology techniques such as cloning, plasmid extraction, digestion of plasmid with restriction enzymes or DNA extraction from plants were performed as described in Sambrook *et al*. (2001).

2.2.1.1 Extraction of genomic DNA from *Arabidopsis thaliana*

a) CTAB-method (Lukowitz *et al*., 2000)

The method yields relatively clean, high molecular weight DNA. Plant material (rosette-leaves) from T-DNA insertion lines were ground in liquid nitrogen using a ball mill (*Retsch*, Haan, Germany), and 300 µl of 2x CTAB- Buffer (1.4 M NaCl, 2% (w/v) cetyl-trimethihyl-ammonium bromide, 100 mM Tris-HCl, 20 mM EDTA; pH 8.0) were added. The solution was vortexed vigorously and incubated for 10 min at 65°C with occasional shaking. The mixture was allowed to cool to RT and 300µl of chloroform were added. The mixture was vortexed and then centrifuged at 10,000 rpm for 5 min to separate the phases. The upper aqueous phase was transferred to a fresh 1.5 ml microcentrifuge tube. The DNA was precipitated by adding 300 µl of 2-propanol to the aqueous phase. The precipitate was pelleted by centrifugation at 10,000 rpm for 5 min at RT. Then, the supernatant was discarded and the pelleted DNA was washed twice by suspension in 70% (v/v) ethanol and re-centrifugation. Ethanol was removed and the pellet allowed air-drying. The DNA was dissolved in 100 µl 1x TE buffer (10 mM Tris HCl, pH 8.0, 1 mM EDTA).

b) Alkaline lysis DNA preparation (Klimyuk *et al*., 1993)

Alkaline lysis method is quick and yields a roughly clean DNA. Part of a young rosette leaf or a small inflorescence (about 3 buds) was mashed with a polyethylene stirring rod in 50 µl 0.25 N NaOH and incubated for 30 sec at 96°C. Then 50 µl 0.25 M HCl and 25 µl 0.5 M Tris-HCl pH 8.0 / 0.25 % (v/v) IGEPAL CA-630 were added and the mixture was incubated for 2 min at 96°C.

2.2.1.2 DNA purification

QIAquick Gel Extraction Kit was used for DNA-elution from agarose gels and the QIAquick PCR purification Kit was used for cleaning of PCR products. DNA molecules bind to silica columns. Unreacted primers, polymerases and nucleotides pass the silica column without sticking to it and are therefore separated from the DNA. The DNA binds to the silica column under high-salt concentrations while the contaminations are passing through the membrane. Under low-salt concentrations with Tris-buffer the DNA was eluted from the column afterwards. The protocols were used according to the manufacturer's instruction.

2.2.1.3 Plasmid DNA isolation from *E. coli* and *Agrobacterium tumefaciens* cells

a) Plasmid DNA isolation from *E. coli*

DNA plasmid was isolated using QIAGEN Plasmid mini Kit. Single bacterial colonies were picked to inoculate 3.2 ml LB medium (20 g/l Bacto Tryptone, 5 g/l Bacto Yeast Extract, 5 g/l NaCl, pH adjusted to 7.2-7.5 with NaOH; autoclaved) plus selective antibiotic. Cultures were incubated at 37°C, 200 rpm overnight. The cells were harvested by short centrifugation and resuspended in 250 µl solution A1 (50 mM Tris-HCl, 10 mM EDTA, pH 8.0, 100 µg/ml RNAse). The EDTA in the resuspension buffer forms complexes with bivalent cations such as Mg^{2+} or Ca^{2+}, which are necessary for bacterial cell wall stability, therefore, the cell walls are destabilized. Cells were lyzed by the addition of 250 µl of solution A2 (200 mM NaOH, 1 %SDS) followed by gentle mixing and incubation at RT for 5 min. Then A3 buffer (3M KOAc, pH 5.5) was added to precipitate chromosomal DNA and protein. After centrifugation at 12.000 rpm for 10 min, the supernatant containing the plasmid DNA was loaded onto a provided column and centrifuged briefly. The flow was discarded and the column washed with A4 buffer (containing ethanol 40%). Plasmid DNA was eluted from the column by adding TE buffer and centrifuging at 12.000 rpm for 1 min. DNA concentration was measured spectrophotometrically.

b) Plasmid DNA isolation from *A. tumefaciens*

Single bacterial colonies were picked to inoculate 4 ml selective YEB medium. Cultures were incubated at 28°C, 200 rpm for two days. Cells were harvested by centrifugation at 14.000 rpm 1 min and washed two times with 1ml 1 M NaCl. The bacterial pellet was resuspended in 200 µl of solution Biddo I (25 mM Tris-HCl, 10 mM EDTA, 50 mM glucose; pH 8.0; 50 mg/ml lysozyme, 50 µg/ml RNAse) and incubated at 37° C gently shaking for 30 min. Then, the same protocol than the isolation from *E. coli* using QIAGEN Plasmid mini Kit was followed but using double amount of volumes.

2.2.1.4 Spectrophotometric determination of DNA or RNA concentration

DNA concentrations were either determined by absorption measurements or quantitatively in an agarose gel. The latter comprises comparing the intensity of the fluorescence emitted by an ethidium bromide-stained DNA sample relative to the known concentration of the bands of the applied size standard.

Absorbance measurement was performed using a spectral biophotometer (Eppendorf) under UV light in specific UV light-permeable cuvettes. The spectrophotometric measurement is

based on DNA's maximum absorption at the wavelength of 260 nm. The aromatic rings of the bases are responsible for the absorption. The absorption maximum for proteins is at 280nm due to the aromatic amino acid residues. By calculating the ratio of absorption at 260 nm to 280 nm the protein contaminations in the DNA/RNA solution can be determined and allows an estimation of nucleic acid purity. Pure DNA or RNA preparations have OD_{260}/OD_{280} ratios of 1.8 and 2.0 respectively (Sambrook *et al*., 1989)

2.2.1.5 DNA-agarose gel electrophoresis

The agarose gel electrophoresis is used to separate and visualize the size of certain DNA fragments. Due to the negative charge of the phosphate groups, which form part of the backbone of nucleic acids, DNA and RNA are moved by an electrical field and migrate towards the anode through a molecular sieve (agarose, a polysaccharide of D-galactose and 3,6-anhydro - L- galactose).

The agarose was dissolved in running buffer (1x TBE buffer: 0.1 M Tris-base, 0.1 M boric acid, 2 mM EDTA; pH ~8.3) and melted by boiling. DNA fragments of 800 bp to 8 Kbp were separated by electrophoresis in 0.8 % (v/v) agarose gels containing 0.5 µg/l ethidium bromide. Smaller fragments (< 800 bp) were separated in 1 % (v/v) agarose gels. Ethidium bromide was added as a dye for nucleic acid detection. The dye intercalates into double strands of nucleic acids and fluoresces after UV- light excitation (254 nm). The electrophoresis was performed in horizontally positioned gel chambers (RunOne Electrophoresis System: *EmbiTec*, Zandhoven, Belgium). Nucleic acid samples for gel separation were mixed with 0.1 volumes of 6x loading buffer (0.25 % (w/v) Bromophenol Blue, 40 % (w/v) sucrose). For size determination of the separated fragments, 5 µl of a size standard (Smart Ladder, *Eurogentec*) were added to each gel. The voltage applied was normally 50 V. Detection of the ethidium bromide stained bands was performed using the ChemiDoc system (*Bio-Rad*) according to the manufacturer's protocol.

2.2.1.6 DNA sequencing

All DNA sequencing reactions, either isolated plasmids DNA, or PCR products, were performed by *AGOWA* GmbH (Berlin, Germany).

2.2.1.7 Restriction digestion of nucleic acids

Restriction enzymes are bacterial enzymes that bind and cleave specifically hydrolytic phosphodiesterified bonds of both strands of a DNA molecule. Various kinds of endonucleases

differ in their recognition site, cleavage site and organism of origin. The biological function of these enzymes is recognition and degradation of invading alien-DNA. The organism's own DNA is protected from degradation by specific modifications, mostly methylations preventing the endonucleases from recognizing and cleaving the sequence. Some restriction enzymes cut in the middle of their recognition site, creating blunt-ended DNA fragments. However, the majority of enzymes make cuts staggered on each strand, resulting in a few base pairs of single-stranded DNA at each end of the fragment, known as "sticky"ends. The sticky-ended fragments can be easily ligated to other sticky-ended fragments with compatible single-stranded overhangs, resulting in efficient cloning.

The DNA to analyse is incubated under defined buffer conditions with the appropriate restriction enzyme under defined temperature and incubation time. The optimal temperature for most restriction enzymes is 37°C. The restriction buffer usually contains Tris-buffer, $MgCl_2$, NaCl or KCl and a sulfhydryl reagent (DTT, DTE or β-mercaptoetanol). An optimal pH value of 7.5-8 and a bivalent cation (commonly $Mg^{2+)}$ are essential for enzyme activity.

Composition of restriction digests are as follows:

- Restriction digestion of genomic DNA for Southern blotting

genomic DNA	15 µg
enzyme buffer (10x)	5 µl
enzyme (5 U/µg DNA)	75 U
ddH_2O	ad 50 µl

The mixture is incubated for 4 h at 37°C

- Standard plasmid restriction digest

plasmid DNA	2 µl
enzyme buffer (10x)	2 µl
enzyme	1-2 U
ddH_2O	ad 20 µl

The mixture is incubated 1 h at 37°C

2.2.1.8 Southern blotting

Southern blotting is a technique that allows analysis of specific DNA sequences. The method includes transfer of digested DNA fragments separated by agarose gel electrophoresis to a

nylon membrane. On this membrane, specific fragments can be detected by their hybridization to specific radiolabelled probes.

DNA was isolated from plants according to 2.2.1.1. Approximately 15 µg of whole plant genomic DNA was digested with an appropriate restriction endonuclease in a 50 µl reaction with 75 U of the enzyme for 4 h. After complete digestion the DNA was separated according to size by agarose gel electrophoresis. Afterwards, the agarose gel was submerged in depurination solution (0.125 M HCl) for 10 to 15 min until the bromophenol bands get yellow indicating that the gel has been completely saturated with the acid. The depurination takes the purines out, cutting the DNA into smaller fragments to allow proper transfer to the membrane. Afterwards, the gel was soaked in denaturation solution (1.5 M NaCl, 0.5 M NaOH) for 30 min, which separates double-stranded DNA into single stranded DNA, given that only single-stranded DNA can be transferred. After denaturation, the gel was blotted onto a nylon membrane (Hybond N^+, *Amersham Biosciences*) by capillary transfer using Whatman 3MM filter paper (*Whatman International Ltd*., Maidstone, UK) and Denaturation buffer. After the transfer overnight at RT, the membrane was briefly washed with 2x SSC solution (20x SSC: 3 M NaCl, 0.3 M sodium citrate; pH 7.0) to remove salt residues and then fixed to a membrane using an UV Stratalinker 1800 (*Stratagene*).

2.2.1.9 Total RNA isolation from *Arabidopsis thaliana*

Total RNA was isolated using Trizol reagent (*Invitrogen,* Karlsruhe, Germany). Trizol is an extraction reagent consisting of guanidine isothiocyanate and phenol. As guanidine isothiocyanate is a strong detergent, it denatures cellular RNases, membranes and proteins. Phenol decreases the pH value and thus leads to a separation of proteins and DNA fragments from RNA. 1ml Trizol reagent was added Per 100 mg of frozen ground material. Samples were shaken until the material was melted. Afterwards, 200 µl of chloroform were added, vortexed and incubated 5 min at RT. This step facilitates the separation of other organic compounds, proteins and DNA from the aqueous phase in which the RNA was solved. The two phases were separated by spinning for 10 min. at 13000 rpm, at 4°C. The resulted aqueous phase is transferred into a fresh, sterile tube (around 500-600 µl), mixed well with 500 µl isopropanol and left overnight at -20°C for RNA precipitation. The RNA was pelleted by centrifugation at 13000 rpm for 10 min. The pellet obtained was washed with 1 ml 70 % ethanol and then centrifuged again at 13000 rpm for 5 min. This removes co-precipitated salts and replaces the isopropanol with the more volatile ethanol, making the RNA easier to redissolve. The pellet appears clear and almost gelatinous. After few minutes of air-drying, 40-50 µl sterile water

were added to dissolve the pellet. A DNA digestion step was necessary, given that a small DNA amount was also present in the pellet.
The integrity of the RNA was checked by agarose gel electrophoresis.
RNA isolation for Affymetrix purposes was slightly different and is described below.

RNA isolation for Affymetrix Gene Chip hybridisations.

500 mg of frozen ground material were completely dissolved in 5 ml of Trizol reagent and incubated for 10 min on ice homogenizing the mix in between. The insoluble compounds, as starch and cell wall, were discarded by centrifugation at 4000g for 20 min at 4°C. The supernatant was transferred to a new screw-cap tube and mixed with 3ml of chloroform. After incubation for 5 min at RT, the two phases were separated by centrifugation at 4000g for 20 min at 4°C. The aqueous phase (around 1 ml) was transferred into a new screw-cap centrifuge tube and mixed with isopropanol and 0.8 M sodium citrate / 1.2 M NaCl, ½ volume of the aqueous phase each. The RNA was precipitating overnight at 4°C. The precipitation and wash steps were similar to the ones used for real time RT PCR purposes (see 2.2.1.9).
High quality RNA was sent to the German Resource Center for Genomic Research (RZPD, Berlin, Germany) for probe preparation and Arabidopsis GeneChip hybridisation.

Analyses of expression data and statistical analysis

The raw Affymetrix signals (CEL files) were processed using the software package RMAExpress (log-scale Robust Multi-array Analysis) to normalize and estimate signal intensities (Irizarri *et al.,* 2003). This data reduced from ~ 22K genes to 12 probe sets per gene. Each probe set consist of a perfect match (PM) complementary to the target sequence and a mismatch probe (MM) to give information on non-specific hybridisation. The detention call assigns a "present" (P) or "absent" (A) to each probe set and serves to determine if the 12 PM probes are significantly higher that the MM probes.
Standard operations, including regression plots and correlation coefficients were performed in Microsoft Excel. Tables for assigning Affymetrix probe set identifiers to Arabidopsis Genome Initiative codes were obtained from the Arabidopsis Information Resource (http://www.arabidopsis.org). Table associations were done with Microsoft Access.

2.2.1.10 DNA-ase treatment of isolated RNA

To avoid DNA contaminations in the isolated RNA and further interferences in certain sensitive RNA applications (as q RT-PCR), a DNA digestion was performed. To 30 µl of total

RNA (around 30 µg RNA), 1 µl of DNase (*Roche,* 10 u / µl) was added and incubated at 37°C for 30 min. The sample was heated at 65°C for 10 min to denature both the DNase I and RNA hairpins. Sterile water was added to the sample up to 200 µl and an additional 200 µl of 4 M LiCl were used to precipitate RNA overnight at 4°C. RNA was collected after a centrifugation step at 13.000 rpm for 10 min at 4°C. Then, the pellet was washed in 200 µl 70 % ethanol and allowed to air-dry. The RNA was dissolved in 30-50 µl sterile water.
DNA contamination was checked after DNase treatment by performing a PCR reaction using the RNA as template and a pair of primers which amplifies a specific product on genomic DNA (actin gene, see Table 2.3).

2.2.1.11 First strand cDNA synthesis

The cDNA synthesis was performed according to Promega's description. For 2 µg of total RNA the following components were added:

$MgCl_2$, 25 mM …….. 4 µl
Reverse transcription Buffer (10 X) ……. 2 µl
dNTP mix , 10 mM ……. 2 µl
Recombinant RNasin® Ribonuclease Inhibitor……..... 0.5 µl
AMV Reverse Transcriptase (High Conc.)…….15 u / µg
Oligo $(dT)_{15}$ Primer …….. 0.5 µg
Total RNA……... 2 µg
Nuclease free water …… add 20 µl

The components were well mixed by pipeting and incubated at 42°C for 45 min. The reaction was inactivated at 95°C for 5 min. The resulted cDNA was used as a template for PCR amplification.

2.2.1.12. Real time RT-PCR analyses

Polymerase chain reactions were performed in an optical 96-well plate with an ABI PRISM® 7900 HT Sequence Detection System (Applied Biosystem; Foster City, CA, USA) using SYBR® Green to monitor double strand (ds) DNA synthesis. The reactions were set in 10 µl volume, containing 5 µl 2x SYBR® Green Master Mix Reagent (Applied Biosystem), 1 µl of diluted cDNA (1/10) and 4 µl of a mix of the primer pair (0.5 µM forward and reverse). A standard thermal profile reaction programme was used for amplification: 50°C for 2 min, 95°C for 10 min, followed by 40 cycles of 15 sec at 95°C and 1min at 60°C. The resulting data were

analysed using the SDS 2.0 software (Applied Biosystem). All amplification plots were analysed with a threshold of 2.0 to obtain Ct (threshold cycle) values. The Ct values corresponded to the cycle number at which SYBR® Green Fluorescence reached an arbitrary threshold value (0.2) during the exponential phase of cDNA amplification. The Ct values were first normalised to the Ct values of actin 2 (At3g18780) housekeeping gene, in order to compare the results from different PCR runs or cDNA samples. The Relative Transcript Level (RTL) was calculated as follows: ΔCt (target gene) = Ct (target gene) – Ct (housekeeping control gene). RTL = $2^{-\Delta Ct}$.

2.2.2 DNA cloning methods

2.2.2.1. Amplification of DNA fragments via polymerase chain reaction (PCR)

The polymerase chain reaction is an in vitro procedure for specific DNA-sequence amplification. PCR makes use of thermo-stable DNA-polymerases, which are capable of synthesizing the opposite strand of a DNA matrix in 3' direction, starting for short DNA molecules (oligonucleotide primers) which can hybridize to a single-stranded DNA matrix. By selecting a second oligonucleotide primer oriented in the opposite direction, the specific sequence between the two primers was amplified. The main principle is the cycle repetition of single amplification steps leading to an exponential amplification of the desired part of the matrix.

A PCR cycle starts by thermal denaturation at 90-95°C of the double strand DNA. The DNA melts and two single-stranded DNA molecules originate. The next step is the hybridization of primers to the single-stranded DNA at temperatures a bit lower than the melting point (T_M) of the primers used. Then the single strand is synthesised at a reaction temperature appropriate for the DNA-polymerase used.

For analysis, the QIAGEN *Taq* DNA polymerase, a thermostable DNA polymerase isolated from *Thermus aquaticus*, was used. For cloning purposes, KOD Hifi DNA polymerase, a DNA polymerase with 3´-5´exonuclease activity (proofreading) was used.

A standard PCR mixture (25 µl or 50 µl volume) was comprised of 1 x PCR Buffer, 0.2 mM dNTPs (mixture of dATP, dCTP, dGTP, dCTP), 0.4 µM of each primer (forward and reverse), 1mM $MgCl_2$ (if not present in the PCR Buffer), 10-100 ng DNA templeta and ddH_2O up to 25 or 50 µl. Then, one unit of KOD- or *Taq* DNA polymerase was added and incubated in the Mastercycler® Gradient (*Eppendorf*). The annealing temperature varied from 54–64°C depending of the template used for the amplifications.

The basic program utilized with most reactions is shown in table 2.8.

Table 2.8 Standard program for PCR reaction

Cycle	Conditions
Initial denaturation	95°C, 2 min
Denaturation	95°C, 15 -30 sec
Annealing	54-64°C, 30 sec
Primer extension	72°C, 1 min per Kb
Back to step 1 for 30-40 x	
Final extension	72°C, 2 min

2.2.2.2. Ligation

Ligation consists in the introduction of DNA fragments in a desired cloning vector. The pGEM®- T Easy Vector System (*Promega*) was used for the cloning of A-tailed PCR products generated by certain polymerases, e.g. *Taq*- polymerases. These polymerases often add a single deoxyadenosine to the 3' ends of the amplified fragments. The pGEM®- T Easy Cloning Vector contains a linear deoxythimidine overhang at each end, making possible the hibridization with the PCR products with high specificity. A standard ligation reaction (10 µl) comprises: 50 ng pGEM®- T Easy Vector , 5 µl of 5x Rapid Ligation Buffer, ~ 150 ng PCR product and 3 units (U) of T4 DNA Ligase. The ligation is incubated 1 h at RT.

2.2.2.3. Transformation methods

a) Preparation of heat-shock competent *E. coli DH5α* cells

E. coli DH5 α competent cells were prepared as described by Inoue *et al*., (1990). Bacterial cells are cultivated on LB-agar plates at 37°C overnight. 10-12 colonies are picked-up and inoculated in 250 ml LB medium in 1l flask, growing at 19°C with vigorous shaking (200 rpm) to an optical density of 0.5-0.6 measured at 600 nm. The culture was cooled down on ice and centrifuged at 4°C for 10 min at 3.000 g (5000 rpm). The pellet was resuspended in 80 ml ice-cold transformation buffer (10 mM Pipes- Na^+, 15 mM $CaCl_2$, 250 mM KCl, 55 mM $MnCl_2$; pH 6.7, adjusted with KOH). After 10 min on ice the solution was centrifuged again and resuspended in 20 ml of ice-cold transformation buffer. 1.5 ml of Dimethylsulphoxide (DMSO) was added to the cells while gently mixing and they were incubated for another 10 min on ice. Then the solution was quickly separated in 200 µl aliquots per reaction tube, immediately shock-frosted in liquid nitrogen and stored for later usage at – 80°C.

b) Heat-shock transformation of *E. coli DH5α* cells.

Transformation of *E. coli* was performed as described by Hanahan *et al*., (1983). 100 µl of *DH5α* competent cells were defrosted on ice and the ligation product (1-10 µl) was added in a 1.5 ml sterile tube and placed on ice for 30 min. Then the sample was heat-shocked at 42°C for 45 sec. Afterwards, immediately 400 µl of sterile SOC or LB medium with no antibiotic selection was added to the transformed cells and incubated at 37°C for 45 min with gently shaking. The cells were plated out on LB selective agar plates containing the appropriate antibiotic and incubated overnight at 37°C.

c) Electro transformation of *Agrobacterium tumefaciens* GV 3101 pM90 RK cells

Agrobacterium tumefaciens cells can be transformed with the *E. coli* vector and permit the shuttling of the vector-constructs into plant cells where they are integrated into the plant genome. *Agrobacterium tumefaciens* GV 3101 cells with a pM90 RK- virulence plasmid in 50 µl aliquots were defrosted on ice. About 150 ng of vector DNA were added to the cells on ice and the mixture transferred to a cold cuvette for the following incorporation of the DNA into the cells by electroporation. The electroporation was carried out in a 2 mm cuvette, under the following conditions: capacitance 25 µF, voltage: 1.8 KV, resistance: 200 Ohm, and pulse length: 5 msec in the electroporation apparatus (*Bio-Rad*). After electroporation, 800 µl of YEB medium without antibiotic selection was added to the cells and they were allowed to regenerate at 28°C for 2-3 h. Then 50 and 100 µl of the cells were plated on a YEB plus Rif / Carb / Kan selective plate and incubated for 2 days at 28°C.

2.2.2.4 GATEWAY® cloning technology

GATEWAY® cloning technology is a novel universal system for cloning and subcloning DNA sequences, facilitating gene functional analysis and protein expression. This technology employs in vitro site-directed recombination instead of restriction and ligation to insert a DNA fragment of interest into a Donor vector to obtain an Entry vector containing the DNA fragment with its orientation and reading frame maintained. The DNA fragment can subsequently be subcloned into various Destination Vectors to obtain Expression Vectors ready to be used in the appropriate host. The GATEWAY® technology is based on the well-characterized lambda phage site-specific recombination system.

For the PCR reactions, the primer pair used contained at their 5´ ends two recombination sites, *att*B1 and *att*B2 added to the forward and reverse primer, respectively. These 25 bp-long *att* sites contain the binding sites for the proteins that mediate the recombination. The PCR

fragment obtained was then cloned by a so-called BP reaction into a Donor Vector. The Donor Vector plasmid contained a selectable marker (e.g. resistance to Kanamycin) and a gateway cassette with chloramphenicol resistance gene and a gene for negative selection, *ccdB*. The products of a BP reaction were the Entry Vector containing two new created sites flanking the integrated PCR fragment, *att*L1 and *att*L2, with no loss of DNA sequence. The Entry Vector was used to subclone the PCR fragment into a variety of Destination Vectors by a so-called LR reaction. These plasmids contain two recombination sites (*att*R1 and *att*R2) that flank a gene for a negative selection, *ccdB* and an antibiotic resistance gene which are replaced by the gene of interest. When integration occurs, two new sites are created in the Expression Vectors, *att*B1 and *att*B2, flanking the PCR fragment, with no loss of DNA sequence. The recombination sites confer directionality and specificity for recombination, so that only *att*L1 will react with *att*R1 to form *att*B1, and *att*L2 with *att*R2 to form *att*B2. The product of these two recombination events is the Expression Vector containing the PCR fragment.

2.2.2.5 *GDH*s RNA interference

Fragments of 315, 258 and 331 bp in the 3' UTR were chosen to create an RNA interference construct for each *GDH* gene. The primers were designed in the untranslated region of each gene in order to have specific RNAi effect (see Table 2.4). The fragments were amplified from cDNA. PCR products were cloned into the vector pSPECTRE (a modified pDONOR with resistance against spectinomycin) and subcloned into the pJAWOHL8 vector. This vector contains the promoter and terminator of the cauliflower Mosaic Virus. In this vector, the intron number 1 of a WRKY gene in *A.thaliana* is in between one inverted repeat of the gateway cassette. Consequently, the PCR fragments are inserted twice in the vector in opposite orientation. The correct cloning and the lack of mutations were verified by sequencing (*AGOWA,* GmbH, Germany). Selection was carried out in *E. coli* and *A. tumefaciens* with spectinomycin and Kanamycin, respectively and with phosphinotricin in plants. As a control empty vector, the pJAWOHL3 vector was used (kindly provided by Dr. Stéphanie Arrivault, Max Planck Institute for Molecular Plant Physiology, Golm, Germany). This vector is similar to pJAWOHL8, but does not contain gateway cassettes.

2.2.2.6 *GDH3*-GUS promoter fusion

A 1782 bp sequence of *GDH3* promoter was amplified by PCR using the primer combination indicated in Table 2.5. The product was cloned into the Entry vector pENTR/SD/D-TOPO® (pENTR Directional TOPO® Cloning Kit, Invitrogen) and then subcloned into the destination

vector pKGWFS7 (Karimi *et al*., 2002) containing the GUS reporter gene cloned in frame. Selection was carried out with kanamycin. Seeds from T3 generation were used in the analysis.

2.2.3 Protein analysis

2.2.3.1 Crude Protein extraction and native gel electrophoresis

Proteins were extracted from 20 mg of frozen ground material as described by Turano *et al*., 1996. Proteins were extracted in 40 µl of extraction buffer (40 mM Tris-HCl, pH 7.2, 1 mM EDTA, 5 % (v/v) glycerol, 0.01mg/ml Bromophenol Blue and 0.05 % (v/v) Triton X-100) using a stir-bar and vortex. The samples were incubated on ice for 30 min. Debris was removed from the sample by centrifugation at 12000 rpm, for 10 min at 4°C. 10-15 µl of the supernatant was used for the gel electrophoresis.

Proteins were separated by native-PAGE gel electrophoresis that allows the separation of proteins according to their size and protein's charge in native nondenaturing conditions. To identify different GDH isoenzymes, proteins were separated in a 5 % polyacrylamide gel using a Mini-Protean II system (*Bio-Rad*). Gels were stained for NADH-GDH activity using the following developing mix: 100 mM Tris-HCl, pH 9.3, 50 mM Glutamic acid, 0.5 mM NAD^+, 0.25 mM nitroblue tetrazolium and 0.1 mM PMS (phenazine methosulfate). All incubations were yielded protecting from light.

2.2.4 Biochemical methods

2.2.4.1 GDH enzymatic reaction

a) Enzyme extraction

Around 20 mg of frozen ground material was extracted with an extraction buffer for soluble enzymes (50 mM Hepes/KOH pH 7.5, 10 mM $MgCl_2$, 1 mM EDTA, 1 mM EGTA, 1 mM benzamidine, 1 mM ε-aminoacapronic acid, 0.25% (w/v) Bovine Serum Albumine (BSA), 10% (v/v) glycerol, 4 µM Leupeptin, 0.1% (v/v) Triton X-100, and 1 mM phenylmethylsulfonyl fluoride (PMSF)). 0.8 ml of extraction buffer and 0.01 mg/ml PVPP were used, leading to an initial dilution of ~40-fold (w/v) dilution. Samples were incubated on ice for 2 min and centrifuged at 12000 rpm for 2 min at 4°C.

b) GDH aminating reaction

GDH catalyses a reversible reaction. In the aminating reaction is able to transfer the ammonium to an organic molecule α-Ketoglutarate to form glutamate and NAD^+, and in the

reversed reaction, recycles α-Ketoglutarate from glutamate releasing ammonia and redactor power NADH.

GDH was assayed in the aminating direction by measuring the production of NAD^+ by GDH. Standards were prepared in the same extraction buffer ranging from 0 to 1 nmol of NAD^+. GDH activity was determined using 5 µl of the extracted samples in the presence of 100 mM Tricine, pH 8.0, 1 mM ADP, 100 µM NADH (preheated for 10 min at 95°C to remove contamination with NAD^+), 10 mM of α-Ketoglutarate and 5 µl of 0.5 M ammonium acetate as substrate. After letting the reaction occur for 10 min at RT, the reaction was stopped with 20 µl of 0.5 M HCl and centrifuged at 2000 rpm for 1 min. Afterwards, samples were heated at 95°C for 10 min and allowed to cool down. Then, the reaction was neutralized with 20 µl of buffer containing 0.5 M NaOH plus 0.1 M Tricine pH 9.0. After, the reaction was developed with 100 µl of the following mix: 8 mM EDTA, 0.3 M Tricine pH 9.0, 1 mM thiazolium blue (MTT), 0.1 mM phenazine ethosulfate, 0.0625 µl alcohol dehydrogenase (88000 U/ml Sigma), distilled water up to 90 µl and 10 µl of 10% ethanol. The assay is a cyclic reaction since NAD^+ is reduced by alcohol dehydrogenase to NADH which is then oxidized by PES (an electron coupling reagent) which in turn is reoxidized by MTT (a redox dye) yielding a colour change reaction. The measurement was performed at 570 nm.

2.2.4.2. Determination of metabolites

a) Ethanolic extraction

Frozen plant material (~20 mg) was extracted with 80% ethanol, mixed and incubated for 20 min at 80°C. After centrifugation at max speed for 5 min, the supernatant was transferred to a new eppendorf tube and the pellet was re-extracted in two subsequent steps with 50% ethanol. The supernatants were combined and used for immediately assay. The pellet of the ethanolic extraction was used for protein and starch analysis.

b) Determination of soluble sugars (glucose, fructose and sucrose) and starch

Ethanol extracts were used to measure glucose, fructose and sucrose enzymatically using a microplate spectrophotometer. The assay contained in a final volume of 200 µl 100 mM HEPES-KOH (pH 7.0), 3 mM $MgCl_2$, 5 µl of NADP (36 mg/ml), 5 µl of ATP (60 mg/ml), 0.5 U glucose 6-phosphate dehydrogenase and 50 µl of ethanolic extraction. The reactions were started by successive addition of 1 U Hexoquinase, 1 U phosphoglucoisomerase and 20 U Invertase and determined spectrophotometrically at 340 nm.

The pellets of the ethanol extracts were used to measure starch after enzymatic digestion to glucose. Pellets were suspended in 80 µl of 0.5 M HCl and 0.1 M acetate/NaOH, pH 4.9. Aliquots of 40 µl were taken and starch was digested by the addition of a degradation mix and incubated overnight at 37°C. The digestion mix consisted of 25 ml 50 mM acetate buffer, 500 µl amyloglucosidase and 5 µl α- amylase. After the incubation, the samples were centrifuged and used for glucose measurements (kinetic at 340 nm).

c) Determination of proteins and total amino acids

Total proteins were measured with the Bradford assay method. Pellets of ethanol extracts were re-suspended in 400 µl of 0.1 M NaOH, heated at 95°C for 30 min and allowed to cool at RT. After a centrifugation at max speed for 5 min, 3 µl of the supernatant were gently mixed with 180 µl of 1:5 diluted dye reagent and measured at 595 nm absorbance.

Total aminoacids were quantified by the Fluorescamine method. To 2 µl of sample, 15 µl of 0.1 M sodium borate buffer, 90 µl fluorescamine and 100 µl distilled water were added. After incubation for 5 min at RT, total amino acids were quantified by fluorescence at 405 nm excitation and 485 nm emissions.

2.2.4.3. Determination of free amino acids by HPLC.

Amino acids were measured by high-performance liquid chromatography (HPLC). HPLC is a liquid chromatographic separation technique in which the separation is based on the different retention times of substances within two phases (liquid and solid). The separation takes place on a column filled with silica particles providing a uniform polar stationary phase upon which long chained carbon hybrids are fixed via covalent bonds. These carbon hybrids are non-volatile polar compounds (mobile phases). As a result of this arrangement, a stronger retardation of the polar compounds happens, since these are bound relatively firmly to the stationary phase. The pores size of the column plays an important role for the separation, the smaller the molecules, the better the crossing of the stationary phase.

The HPLC system used consisted of an automated sample injector (Autosampler 460), a spectral fluorescence detector (Fluorometer SFM 25, Kontron instruments, München) and a pump system with integrated gradient mixer. Stock A buffer consisted of 0.4 M $Na_2 HPO_4$, pH 6.8 (adjusted with H_3PO_4). Buffer A consisted of a 20 ml of stock A and 4 ml tetrahydrofourane add 1 l distilled water. Buffer B consited of 25 ml stack A buffer, 225 ml distilled water, 150 ml methanol and 105 ml acetonitrile. Both buffers were first filtered (cellulose acetate filter, 0.45 µm of pore size; *Sartorius*, Goettingen, Germany) and then

degassed by ultrasonification. The OPA solution (derivatising agent) consisted of 25 mg o-phthalacid-aldehyd (*Sigma,* Germany) in 500 µl methanol, 4.5 ml 0.8 M borate-KOH buffer (pH 10.4) and 50 µl mercaptopropionic acid. 35 µl of ethanol extract was derivatised with 35 µl OPA solution in special vials (closed with SnapCaps to prevent evaporation). After 1.5 min the mixture was injected into the HPLC. The gradient program (with a flow of 0.8 ml/min) was as follows:

Gradient program		
0 min	95%	Buffer A
4.3 min	95%	Buffer A
16.25 min	85%	Buffer A
26.3 min	50%	Buffer A
38.3 min	40%	Buffer A
43 min	30%	Buffer A
47 min	0%	Buffer A
52 min	0%	Buffer A
53.5 min	95%	Buffer A
62 min	100%	Buffer A

Short program for major Aa		
0 min	100%	Buffer A
16 min	87%	Buffer A
17.25 min	85%	Buffer A
19.5 min	0%	Buffer A
25.5 min	0%	Buffer A
27 min	100%	Buffer A
35 min	100%	Buffer A

Detection was performed by fluorescence (excitation at 330 nm and detection at 450 nm). A hypersil ODS column was used for the separation of the aminoacids. The aminoacids were identified by elution time and peak form of corresponding standards. The standards consisted of 10-20 µM of the aminoacids, respectively. The Chromeleon 6.3 chromatography data software (Dionex) controlled the whole HPLC system and was used for data evaluation. The amount of amino acids was calculated via software from the peak area by using a calibration factor obtained from standard runs.

2.2.4.4. Determination of α Ketoglutarate.

a) Perchloric acid extraction

A perchloric acid extraction was used for the determination of α ketoglutarate. Frozen ground material (~100 mg) was extracted with 400 µl of 1.5 M $HClO_4$/ 5 mM EGTA, well mixed and incubated on ice for 30 min. After centrifugation at 14000 rpm, the supernatant was transferred to a new eppendorf tube, and the pellet was resuspended two times with 100 µl distilled water. Supernatants were combined into the same tube. Afterwards, the pH was neutralized with 125 µl-130 µl with 5 M KOH/1 M TEA. The supernatant was collected after centrifugation at max speed for 5 min and the white pellet was washed two times with 50 µl distilled water. Then, the sample

was colourless with a bit of charcoal and transferred to a new tube after centrifugation at max speed for 5 min. Samples were immediately measured or properly stored at - 80 °.

b) Determination of α Ketoglutarate.

Perchloric extracts were used to measure the organic acid α ketoglutarate using a Sigma Kontron spectrophotometer with an amplification of 50 and a voltage of 1000. The assay contained in 600 µl was carried out in 1ml plastic cuvettes as follows: 565 µl of analysis buffer (100 mM Hepes/KOH, pH. 7.5 and 20 mM NH_4Cl), 10 µl NADH (2 mg/ml) and 25 µl of perchloric extract. Both channels (A and B) had to be adjusted to 1.000 ± 10 and once the baseline was straight, 2 µl of the enzyme GDH (glutamate dehydrogenase, *Sigma*) were quickly added in order to start the reaction. The assay consisted in the reduction of α ketoglutarate into glutamate by GDH and the production of NAD^+. NAD^+ was then quantified spectrophotometrically at 334 nm-405 nm.

2.2.4.5 GUS activity assay

Transgenic plants carrying gene promoter – GUS fusion constructs were checked for the GUS activity using X-Gluc (5-bromo-4 chloro-3-indolyl β-D-glucuronic acid, *DUCHEFA*) as described in Jefferson *et al*., 1987. Seedlings or plants were immersed in fresh prepared GUS staining solution containing 0.5 mg/ml X Gluc, 50 mM sodium phosphate buffer (0.6 M Na_2HPO_4 and 0.4 M NaH_2PO_4, pH 7.0), 10 mM EDTA, 0,33mg/ml K-Hexacyanoferrat III, 0.1% (v/v) Triton X-100 and 0.1% (v/v) Tween 20. Samples were infiltrated under vaccum twice for 15 sec and stained at 37°C overnight. Removal of chlorophylls was performed by successive washes in 80% ethanol for a better GUS staining analysis. Pictures were taken under confocal and binocular microscopes (Olympus, Leica, Germany).

CHAPTER 3 RESULTS
GDH CHARACTERIZATION

3. CHAPTER: RESULTS ON *GDH* CHARACTERIZATION

3.1. GDH gene family in *Arabidopsis thaliana.*

3.1.1. Alignment of protein sequences of GDH family in *Arabidopsis thaliana*.

The sequence of the *Arabidopsis thaliana* genome (Arabidopsis Genome initiative, 2000) revealed that it contains four genes encoding proteins with glutamate dehydrogenase activity, named GDH1, GDH2, GDH3 and plastidial GDH. An alignment of the amino acid sequences pointed out that three of them contain some conserved domains (Figure 10). Three of the polypeptides appear to contain a putative mitochondrial target sequence rich in positive amino acids and located in the N terminal region of the protein. Other conserved sequences among the proteins include an α- ketoglutarate-binding domain, and a putative NAD(H)-binding domain from Phe-209 to Asp-237, which contains the nucleotide binding domain motif GXGXXG(A) (Britton *et al*., 1992). The amino acid residues Lys-90, Thr-169 and Ser-344, are involved in Glu binding according to Britton *et al.,* 1992. Only the gene product for GDH2 contains a region with similarity to an EF-hand loop motif associated with Ca^{2+} binding.

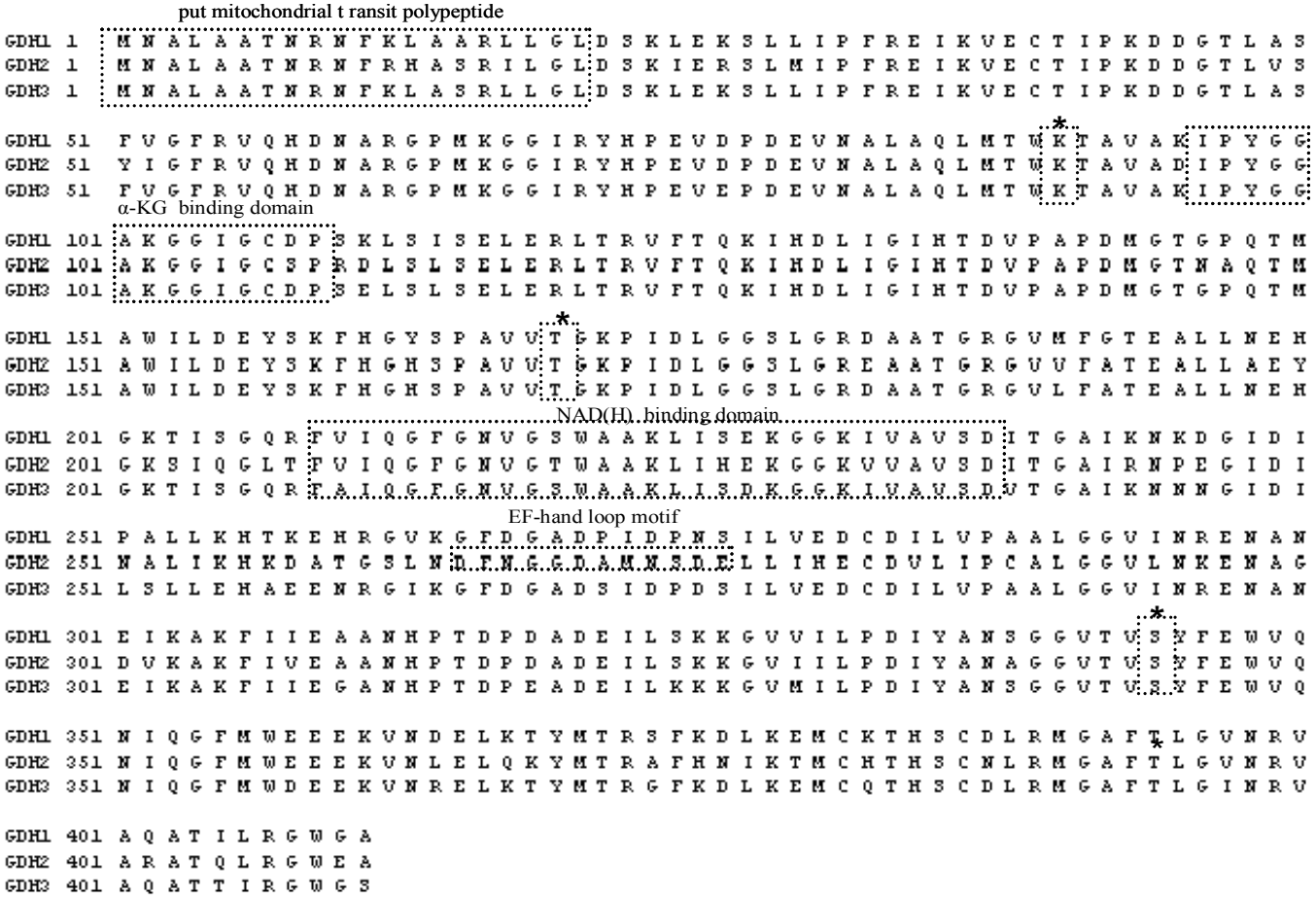

Figure 10. Alignment of the deduced amino acid sequences of *Arabidopsis* GDH1, GDH2 and GDH3. The GDH protein sequences were retrieved in TAIR database (The Arabidopsis Information Resource). The alignment was performed using DNASTAR (MegAlign) program. The mitochondrial transit sequence, α-ketoglutarate-binding domain, the NAD(H) binding domain and the EF-hand motif are labelled and boxed. Amino acid residues associated with Glu binding domain are indicated with an asteric.

The protein percentage identity between GDH1 and GDH2 is 80, 5 % and 92, 0 % with GDH3. The sequence distance between GDH2 and GDH3 is around 78, 6 %.

The plastidial GDH protein sequence appears to be more distant compared to the others GDHs with a protein percentage identity around 5, 6 %.

3.1.2 Phylogenetic tree of NAD(H) GDHs

Glutamate dehydrogenases peptides from *Arabidopsis* were aligned with the deduced amino acid sequences of other plant species in order to visualize the evolutionary interrelationships between the plant species (figure 11). These studies suggest that GDH1 and GDH3 from *Arabidopsis thaliana* are closer between them and grouped with sequences from tobacco and tomato. In contrast, GDH2 it is similar in sequence to the GDH from *Brassica napus*.

GDHs homologs can be found in several species. Comparative analyses of GDHs sequences from plants are very distant from GDH sequences found in other organisms such as bacteria, fungi or animals (figure 12).

In general, from the analyses, we can conclude that GDH1 and GDH3 are more similar between them compared to GDH2. In contrast, the plastidial GDH is very different in sequence compared to all the GDHs sequences found in plants, being similar to the GDH found in other organisms like bacteria, yeast or fungi.

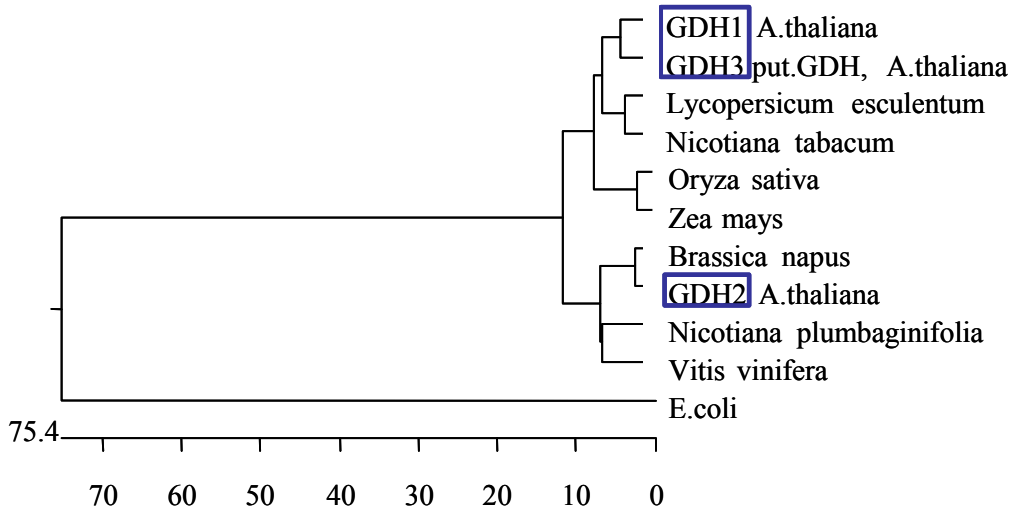

Figure 11. Phylogenetic tree of GDHs in plant species. The cladogram was made after a multiple comparison of nucleotidic sequences using the Clustal method (Lasergene, DNASTAR program). Blue boxes indicate GDHs from *Arabidopsis thaliana*.

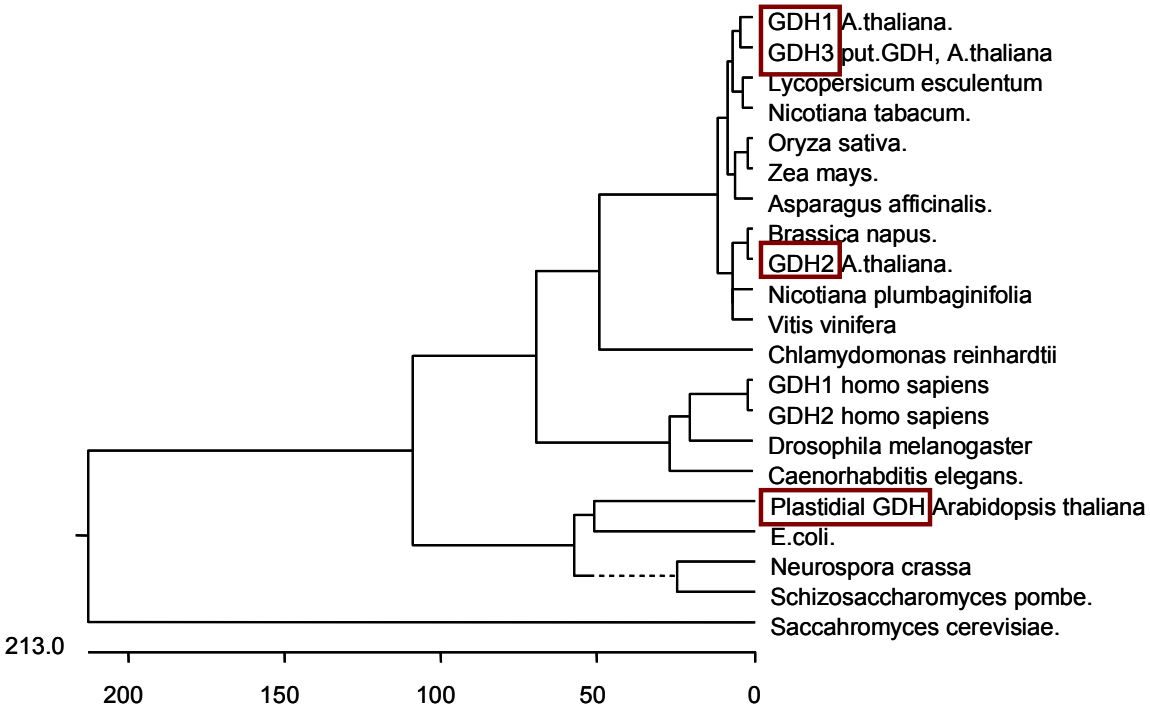

Figure 12. Phylogenetic tree of GDHs in several species. The cladogram was made after a multiple comparison of nucleotidic sequences using the Clustal method (Lasergene, DNASTAR program). Red boxes indicate GDHs from *Arabidopsis thaliana*.

3.2. Analysis of GDH gene expression in *Arabidopsis thaliana.*

3.2.1 *In silico* analysis

Several databases regroup data sets from different tissues and different developmental stages in wild type plants of *Arabidopsis thaliana*.

For this study, the *Genevestigator Database* (http://genevestigator.ethz.ch) was used. The experimental data and annotations are provided by the Gruissem Laboratory (ETH Zurich; http://www.fgcz.ethz.cg/), the Functional Genomics Center Zurich (FGCZ; http://www.fgcz.ch/), by the Arabidopsis Functional Genomics Network consortium (AtGenExpress; http:// web.uni-frankfurt.de/fb15/botanik/mcb/AFGN/atgenex.htm), as well as by public repositories such as Nottingham Arabidopsis Stock Centre Transcriptomics Service (NASCarrays, http://ssbdjc2.nottingham.ac.uk/narrays/experimetnbrowse.pl), the European Bioinformatics Institute (ArrayExpress; http://www.ebi.ac.uk/arrayexpress/) and the Gene Expression Omnibus at NCBI (GEO; http://www.ncbi.nih.gov/geo/).

The Gene Atlas function of the *Genevestigator Database* was used because it queries the database with respect to plant organ specificity (Figure 13).

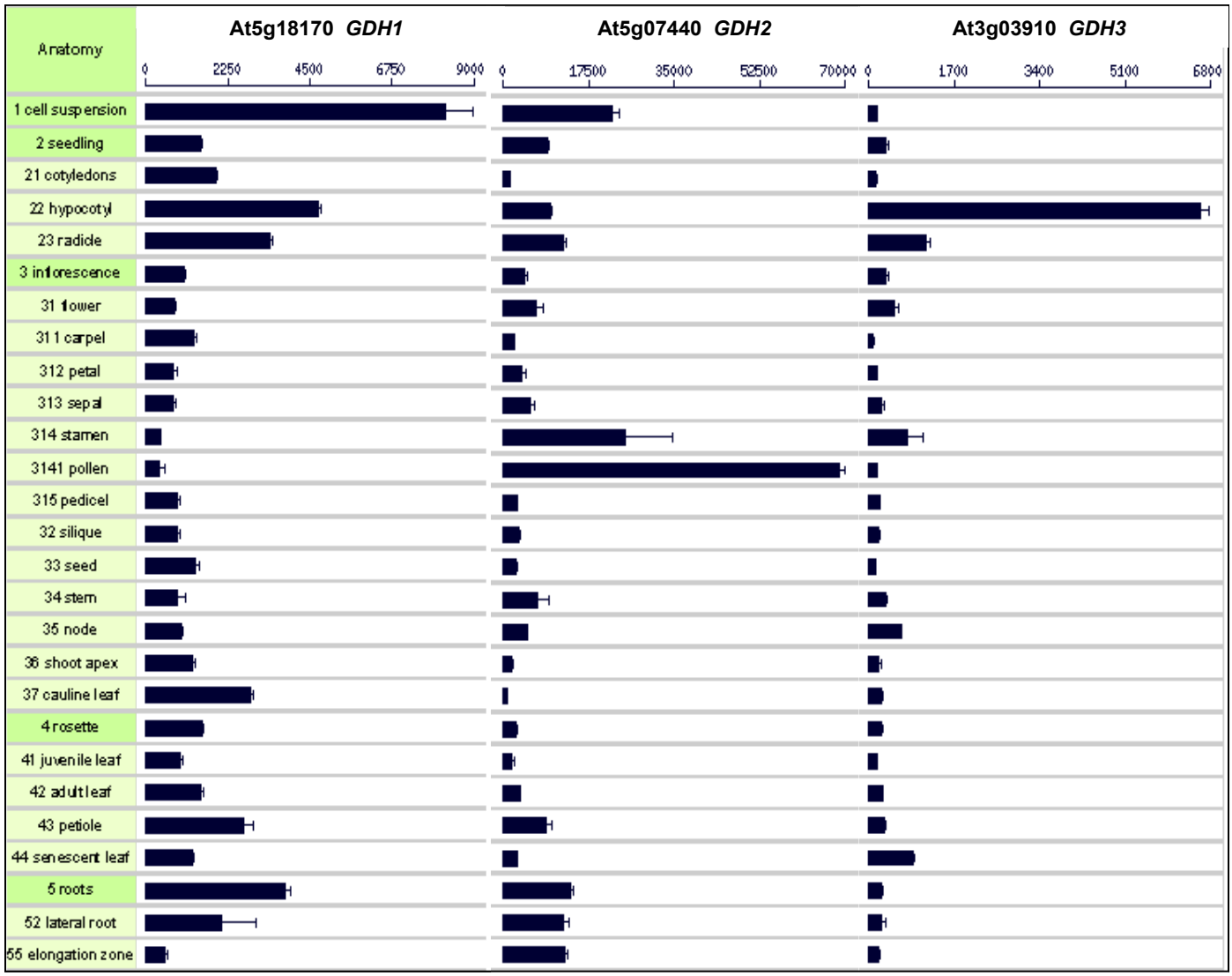

Figure 13. Expression pattern of *GDH1, GDH2 and GDH3* determined by the *GeneAtlas* function in the *Genevestigator Database*. *GeneAtlas* results. Results are given as the average and the standard error of each category.

Analysis revealed that *GDH1* was expressed ubiquitously in *A. thaliana*. *GDH1* was expressed in young seedlings, particularly in hypocotyls and radicle. It appeared to be poorly expressed in all flower tissues with the exception of cauline leaf. *GDH1* was also expressed in green tissues, especially in the petiole and in lateral roots.

The gene *GDH2* was the highest expressed ubiquitously in *A. thaliana* compared to the others GDHs. It was present in young seedlings, especially in hypocotyls and radicle. *GDH2* did not appear to be expressed in all flower tissues but only in stamen and pollen. It was expressed in green tissue, mainly in petiole, and roots.

The putative *GDH3* appear to be highly expressed in seedlings, particularly in hypocotyls and radicle. *GDH3* was poorly present in inflorescence, green tissue and roots compared to *GDH1* and *GDH2*.

To confirm these results, analysis of the transcript levels in different *A. thaliana* organs was performed. The use of real-time RT-PCR was an alternative technology suitable to quantify the level of expression in different organs of *A. thaliana*.

3.2.2. *GDH* transcript abundance in *A. thaliana* using Quantitative real-time RT-PCR

Real time RT-PCR analysis was used to investigate expression patterns of *GDH*s in different parts of *A. thaliana* plant. RNAs were extracted from different organs of *A. thaliana* wild type Col-0 plants grown on soil. To obtain equal amounts of starting cDNA for each organ, equal amounts of RNA were reverse transcribed and further used as template for the real time RT-PCR analysis (see material and methods, Section. 2.2.1.11). RT-PCR primers designed from the sequences of each GDH were used to check the expression level of the corresponding genes.

The Ct value corresponded to the cycle number in a real-time RT-PCR, at which the fluorescence intensity of SYBR ® Green reached an arbitrary value (set at 0.2) during the exponential phase of cDNA amplification (see section 2.2.1.12). An adequate constitutive gene should have a mean Ct of a maximum of ±1 in an analysis of different organs when identical amounts of starting cDNA are used in each reaction.

Using actin 2 gene (At3g18780) as a constitutively expressed control gene, real-time RT-PCR was performed on cDNA from vernalized seedlings, etiolated seedlings, root, siliques, inflorescence, stem and leaves (cauline and old leaves) of *A. thaliana* wild type plants grown on soil (figure 14).

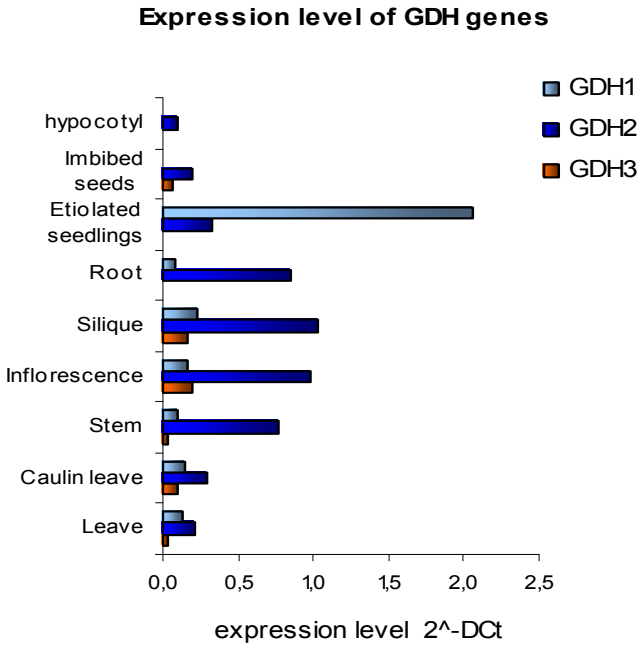

Figure 14. Expression analysis of *GDH*s in *A. thaliana*. Transcripts levels were assayed in hypocotyls from 2 weeks old plants, vernalized seedlings (imbibed seedlings at 4º for two days), etiolated seedlings (seedlings at 4º for two days and then complete darkness) and roots, siliques, inflorescences, stem and leaves (cauline and old leaves) from plants grown under normal greenhouse procedure. Values are means of relative transcript levels 2^-DCt calculated from one representative experiment. Those values were normalized according to the values of the housekeeping gene, actin (At3g18780).

According to these results, we can observe that *GDH1* was the highest expressed in etiolated seedlings compared to the rest of the tissues, being poorly expressed in silique, inflorescence, stem and leaves. Its expression is completely absent in hypocotyls, what clearly contrast with *Genevestigator* analysis that showed higher expression of *GDH1* in this tissue. *GDH2* appeared to be ubiquitously in all the tissues with higher expression in siliques, inflorescences, stem and root. In contrast, the putative *GDH3* was less present in all the tissues, being poorly expressed in siliques, inflorescence and cauline leaves. However, its expression in hypocotyls contrasts to *Genesvestigator* analysis that revealed higher expression in the hypocotyl. It was therefore interesting to determine the expression of *GDH3* in these organs (see 3.2.3).

3.2.3. Promoter GUS (β-glucuronidase) expression analysis of the putative *GDH3*.

The expression pattern of the putative *GDH3* is very low all over the tissues so, it was interesting to obtain more information about its spatial-temporal expression. For this purpose, the promoter of the *GDH3* gene was fused to a GUS reporter gene. The encoded β-glucuronidase enzyme from *E. coli* has been well documented to provide desirable characteristics as an expression marker in the transformed plants. The GUS reporter gene has many advantages including stable expression of the *E. coli* GUS enzyme, no interference with normal plant metabolism and low intrinsic GUS activity in higher plants.

A 1782 bp sequence of *GDH3* promoter was amplified by PCR using a combination of primers designed to introduce appropriate restriction sites to become suitable for cloning into the destination vector pKGWFS7 that contains the GUS reporter gene cloned in frame (see Material and Methods, table 2.5). The vector (12.7 kb size) contains a kanamycin resistance gene as selectable marker. The generated GUS construct was first cloned in *E. coli* competent cells. Afterwards, the plasmid was purified and partially sequenced to check that the promoter region was in correct fusion with the *GUS* gene. Then, the confirmed plasmid was introduced into *Agrobacterium tumefaciens pGV3101* cells by electroporation, and finally used to transform *Arabidopsis thaliana* Col-0 plants, using the floral dip infiltration method. Transformed plants were selected on kanamycin containing agar-medium plates and then transferred to soil. In order to check the expression pattern, the plants were immersed in GUS staining solution, containing X-Gluc (5-bromo-4 chloro-3-indolyl β-D-glucuronic acid) as a substrate for the β-glucuronidase enzymatic reaction, and subsequently analyzed for the presence of the blue GUS signal of the reaction product. Plants grown in soil under greenhouse conditions (16h light photoperiod; 20 ºC day/18 ºC night) were subjected to the assay, to determine the spatial-temporal expression pattern occurring during growth and development.

The *GDH3* promoter is active in rosette leaves (mainly in vascular tissue) and in the roots of plants before the flowering stage (figure 15, panels A, B, C and D); the staining of the root was restricted to the root primordia.

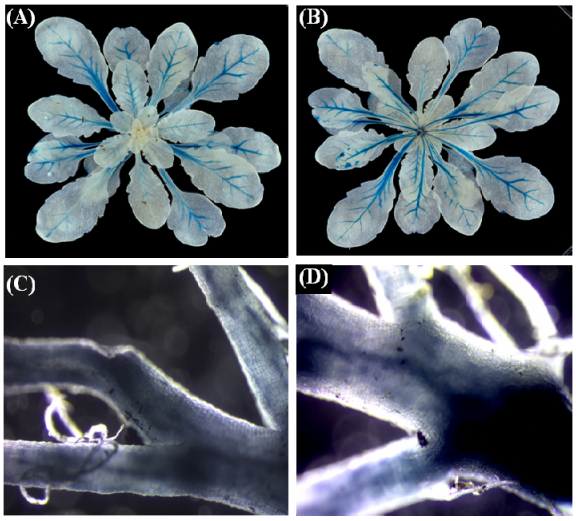

Figure 15. GUS expression signal in transgenic *Arabidopsis thaliana* Col-0 plants carrying a *GDH3* promoter-GUS fusion, before the flowering stage. (A), (B) The expression pattern in both sides of rosette leaves (upside and downside, respectively); (C), (D) The expression pattern in different parts of the root.

In the mature plants (around 8 weeks old, after the flowering stage), the expression signal is present in old flowers, siliques (at the dehiscence zone), petiole and vascular tissue of rosette leaves (Figure 16, panels A, B, C, D, E and F). The expression was absent in young inflorescences.

All these GUS-staining analysis suggest the possibility that the putative *GDH3* could play a general role in the remobilization of nitrogen compounds (by amino acids catabolism) in old tissues in order to transport them to the young part of the plant (sink) and therefore support the growth and development.

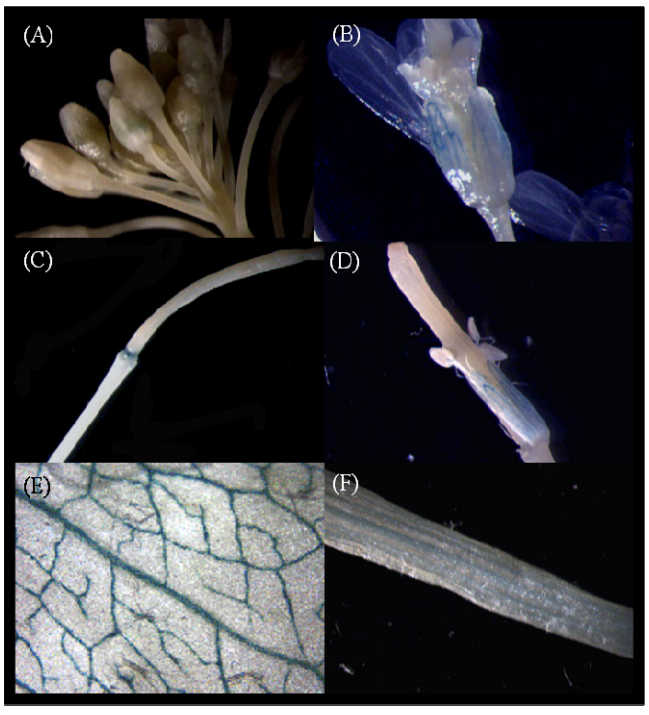

Figure 16. GUS expression signal in transgenic *Arabidopsis thaliana* Col-0 plants carrying a *GDH3* promoter-GUS fusion, in mature plants after the flowering stage. (A to F) Histochemical staining for GUS activity in tissues from 8 weeks old transgenic plants was performed overnight. (A) No signal was detected in young inflorescences. (B) Flowers; (C) green siliques (dehiscence zone); (D) old flowers; (E) rosette leaf; (F) leaf petiole.

3.2.4. Metabolic and Diurnal regulation of *GDH*s in *A. thaliana* using ATH1 arrays and promoter GUS expression analysis.

3.2.4.1 Metabolic regulation

The ability of metabolites to regulate metabolic and developmental processes in plants is well known. Both carbon and nitrogen metabolites have been shown to regulate growth/development and the expression of numerous genes in plants.

The AtGenExpress Database provides a collection of Affymetrix ATH1 array data from different environmental stresses in *A.thaliana* (http://arabidopsis.org/info/expression/ATGenExpress.jsp).

Additional ATH1 array data from Max Planck Institute of Molecular Plant Physiology includes data from different nutrients and diurnal responses in *A. thaliana*. The experiment consisted on plants grown in full nutrition media during one week followed by two days under nutrient (sucrose, nitrate or phosphate) starvation and then readdition (of the nutrient). Samples were taken 30 minutes and 3 hours after the readdition of the nutrient (Scheible *et al*., 2004).

The expression analyses of *GDH*s extracted from these data are given in figure 17. They revealed that *GDH1* and *GDH2* have a higher expression under carbohydrates starvation and that the addition of sugars resulted in repression of the genes. These results are supported by the work of Aubert *et al*., 2001 and by studies on GDH genes in *A. thaliana* (Melo-Oliveira *et al*., 1996) that show that the expression of one of the GDH genes, *GDH-1*, is highest in dark-adapted or sucrose-starved plants. Such conditions enhance the expression of the gene and the activity of the enzyme producing local C/N imbalances that require the operation of the GDH-shunt because in that situation the plant may need to give priority to carbon metabolism and keto-acid production over nitrogen metabolism. Also, *GDH2* was slightly increased upon phosphate starvation and down regulated after the addition of the nutrient (figure 17, panel C).

Less is known about the metabolic control of the putative *GDH3*. Transcripts appear to be unaltered by the effect of sugars (figure 17, panel B). Contrarily, its expression was highly increased upon nitrate starvation and markedly repressed by the addition of nitrate suggesting its possible role in the recycling of ammonium during amino acid catabolism.

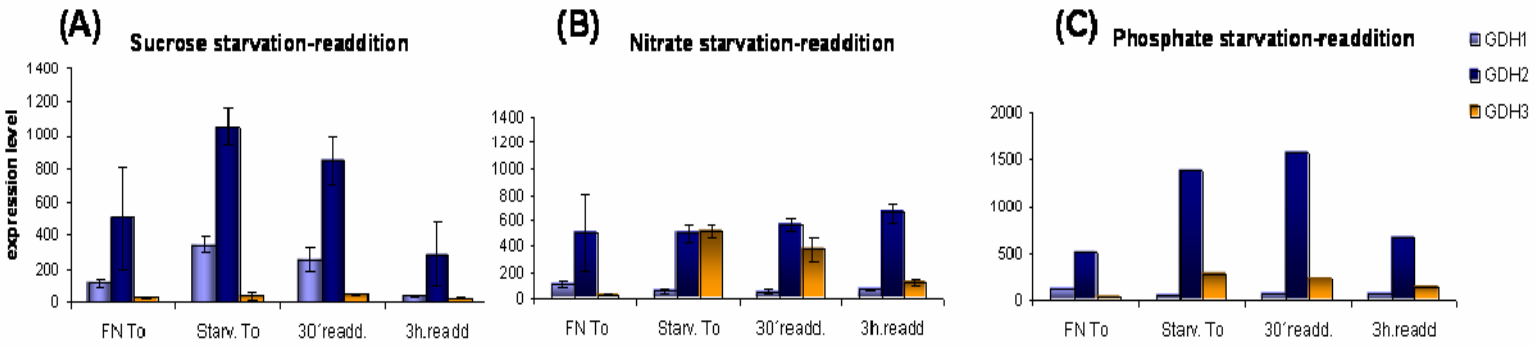

Figure 17. ATH1 gene chip expression profile of GDHs in nutrient starvation and re-addition experiments. Wild type Col-0 seedlings were grown as described in Scheible *et al*., 2004. (A) Sucrose, (B) nitrate and (C) phosphate experiments; Full nutrition (FN); Starvation (Starv. T0) and readdition (30min readd, 3h. readd.) experiments.

In order to confirm the expression pattern of *GDH3* in response to nitrate, promoter GUS-analysis were carried out under the same conditions as described in Scheible *et al*., 2004. The results indicated that seedlings grown during 9 days under full nutrition media showed no staining compared to those ones transferred to a medium deprived of nitrogen. The starved seedlings showed blue staining throughout the aerial part of the plant, mainly localized to the cotyledons (figure 18, panels B, H, J) indicating that these conditions resulted in the up regulation of *GDH3* expression in the transgenic lines. When grown on medium without the added nitrogen compounds, the roots of the transgenic seedlings exhibited blue staining localized to the specialization/root hair zone of the primary root (figure 18, panel B), and to the specialization zone of lateral roots (figure 18, panel D). GUS staining was also visible in root hairs and was not observed in root tips of primary or lateral roots. These results were in agreement with the ATH1 array data indicating that *GDH3* expression is higher under nitrogen limitation and decreases with the re addition of the nitrogen compounds to the same media (figure 18, panels A to J). In addition, the deprivation of nitrogen during two days led to senescence (especially the colyledons), to reduced chlorophylls and protein degradation, a typical phenology of nitrogen-limited plants (Scheible *et al.*, 2004).

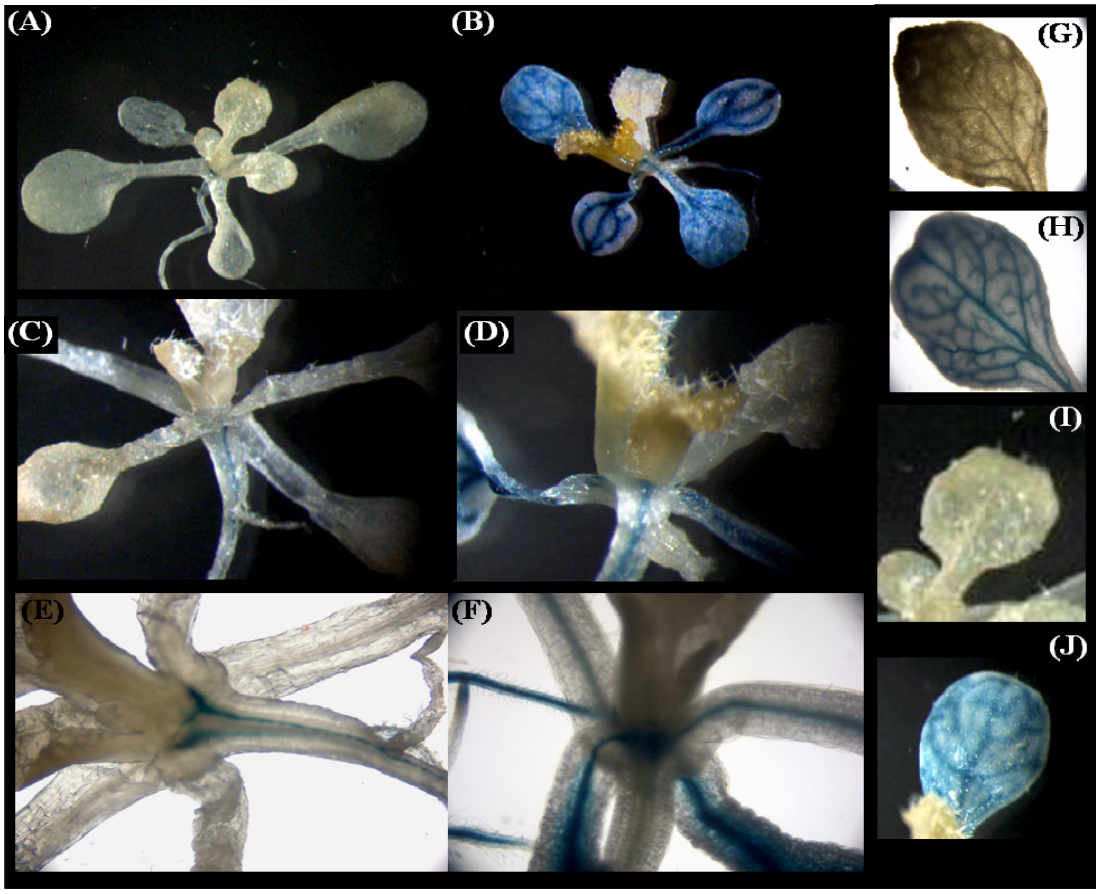

Figure 18. GUS expression signal in transgenic *Arabidopsis thaliana* Col-0 plants carrying a *GDH3* promoter-GUS fusion, in seedlings grown in liquid cultures as described by Scheible *et al.*, 2004. (A to J) Histochemical staining for GUS activity of 9 days old seedlings was performed overnight. (A), (C) and (E), seedlings grown in control medium (FN conditions). (B), (D), and (F) seedlings grown in conditions of nitrogen starvation. (G) and (I) individual cotyledon from seedlings grown in full nutrition; (H) and (J) cotyledons of seedlings grown under nitrogen deprivation.

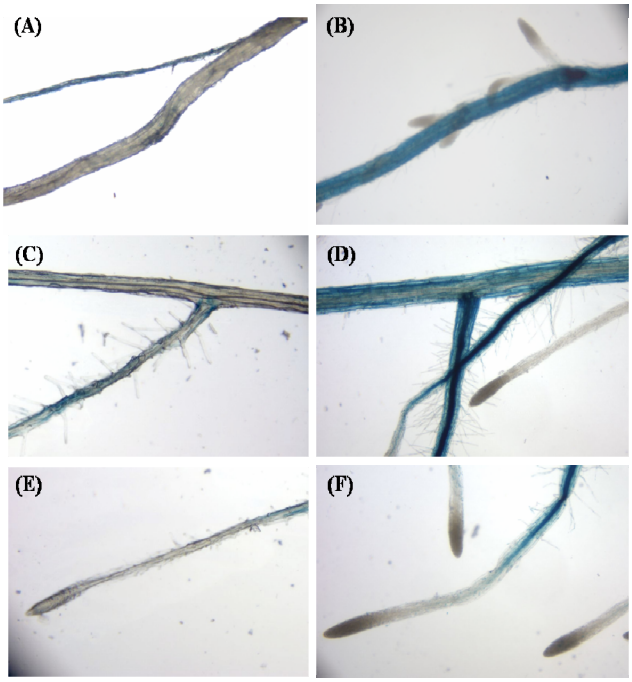

Figure 19. GUS expression signal in transgenic *Arabidopsis thaliana* Col-0 plants carrying a *GDH3* promoter-GUS fusion, in seedlings grown in liquid cultures as described by Scheible *et al.*, 2004. (A to F) Histochemical staining for GUS activity of 9 days old seedlings was performed overnight. (A), (C) and (E) represent parts of the root of seedlings grown on control medium. (B) Detail of the apical zone of a root grown on nitrogen starvation; (D) Detail of the specialization/root hair zone of a seedling grown on nitrogen starvation ; (F) Root tips of seedlings grown on media without the added nitrogen.

3.2.4.2. Diurnal regulation of GDHs genes

Regarding diurnal responses, analyses of expression by ATH1 gene chip hybridization in wild type *A. thaliana* plants, revealed that *GDH1* (and less marked in *GDH2*) seem to be diurnally regulated with the highest expression at the end of the night (Bläsing *et al*., 2005) (figures 20 and 21). Plants during the day convert the light energy to chemical energy to synthesize reduced carbon compounds which are stored as carbohydrates to provide energy and biomass to the plant. During the dark period, the plant becomes a net consumer of carbon so leaf starch is degraded providing carbon skeleton, energy and reductant within the leaf cell. *GDH1* expression is down regulated at the end of the day (conditions of high sugar levels), and arises towards the end of the night (when sugar levels are low). These changes are less marked for *GDH2* expression. The coincidence of the diurnal regulation of *GDH*s with the metabolic response to sugars, lead to the conclusion that *GDH1* and *GDH2* could be regulated by the level of carbohydrates within the cell. These results were confirmed by real time RT-PCR analyses (material kindly provided by Dr. O. Bläsing) (see figure 21).

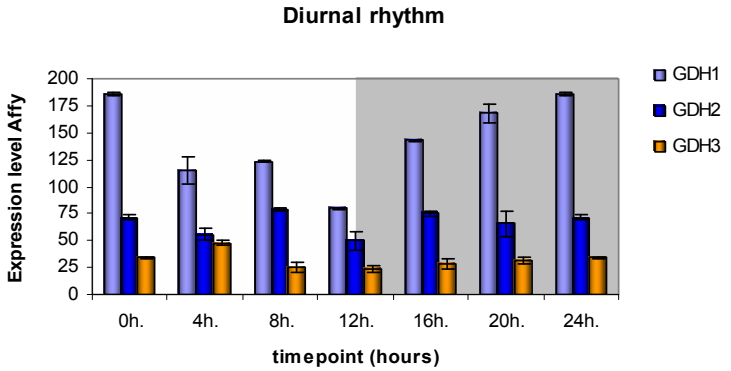

Figure 20. Diurnal regulation of *GDH*s in wild type *A. thaliana* plants by ATH1 gene chip expression profile. ATH1 gene chip expression profile of *GDH*s extracted from data of Dr O. Bläsing (Bläsing *et al*., 2005). *Arabidopsis thaliana* rosettes were harvested six times in a 12h light/12h dark light period. The results represent the average of two biological replicates. Standard deviation is represented on the graph.

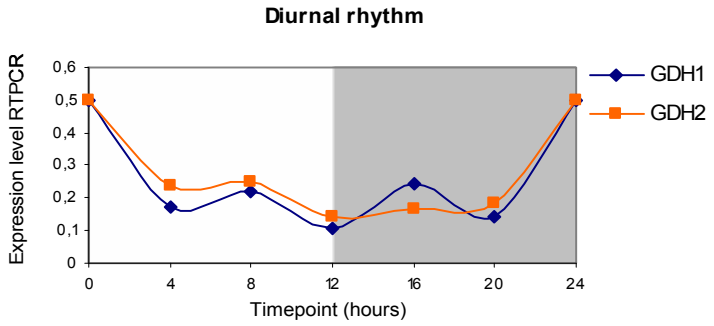

Figure 21. Diurnal regulation of *GDH*s in wild type *A. thaliana* plants measured by RTPCR. Transcript levels were measured by real time RT-PCR in rosette leaves from plants harvested six times in a 12h light/12h dark light period (material kindly provided by Dr. O.Bläsing). Values are means of relative transcript levels 2^-DCt calculated from one representative experiment. Those values were normalized according to the values of the housekeeping gene, actin (At3g18780). GDH3 expression was undectectable in leaf material used in the analysis.

Interestingly, the expression pattern of *GDH3* was not diurnally regulated suggesting once again, that it could play a different role compared to the others GDHs.

These results resemble the situation in the *pgm* mutant which lacks plastid phosphoglucomutase activity, an essential enzyme for photosynthetic starch synthesis (Caspar *et al*., 1985). The starchless *pgm* mutant accumulates high levels of sugars during the day whereas becomes sugars depleted during the night (Caspar *et al*., 1985; Gibon *et al*., 2004b). Thus, genes diurnally regulated by the levels of sugars should show accentuated responses in the *pgm* mutant. As shown in Gibon *et al*., 2004b, transcript levels for *GDH1* and *GDH2* underwent extreme diurnal changes in *pgm*, with a 20 fold induction towards the end of the night compared to wild type plants (see figure 22, panels a) and b)). GDH expression was dramatically increased after prolonged night period leading to an increase on GDH activity in the starchless mutant compared to wild type. These results indicate that the increase in GDH transcripts at the end of the night in the *pgm* mutant is a consequence of low sugar. A possible explanation could be that *GDH1* and *GDH2* maybe are involved in supplying carbon skeletons in form of α-ketoglutarate under depleted concentration of sugars.

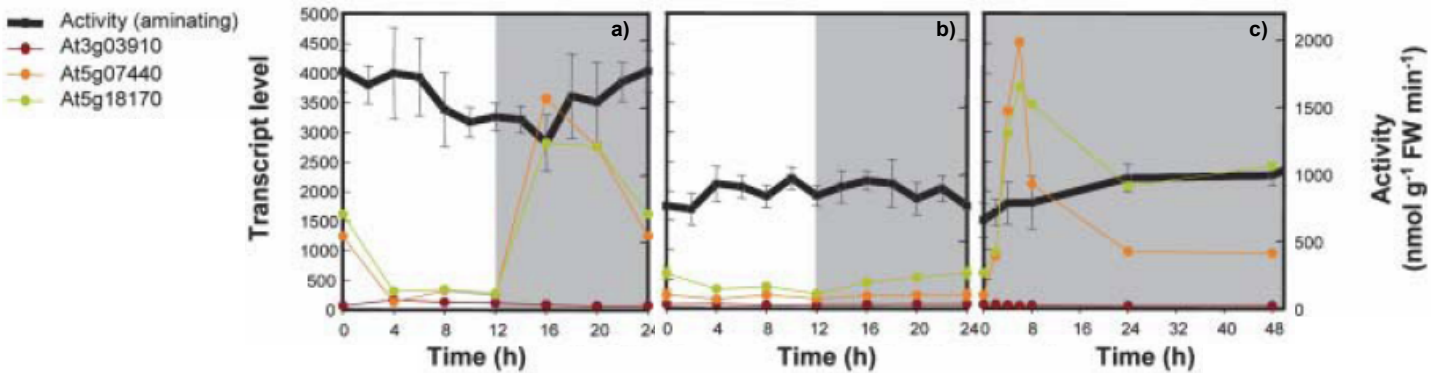

Figure 22. Changes of enzyme activity and transcript levels of GDH gene family throughout diurnal cycle and after transfer to continuous darkness. 5 weeks old *Arabidopsis* Col-0 wild type and *pgm* rosette leaves were grown as described in Gibon *et al*.,2004b. a) Diurnal cycle in the mutant *pgm*; b) diurnal cycle in wild type Col-0 and c) extended night in wild type Col-0. (Adapted from Gibon *et al*., 2004b).

Taken together, these results show that expression of *GDH1* and *GDH2* is modulated by the internal level of sugars in the plant which is consistent with the diurnal regulation and the dramatic increase in expression after prolonged night period (see figures 20 and 22, panel c). According to some authors, *GDH1* and *GDH2* could be involved in the supply of carbon skeletons (in form of α-ketoglutarate) in response to low sugars in order to support the metabolism. To test this hypothesis, the sugars composition and the amino acids pool should be investigated in plants with reduced expression of GDH. If GDH is involved in carbohydrates metabolism, a reduction of GDH should be reflected on a change in the internal

sugar levels. Moreover, since GDH is involved in glutamate metabolism, the flux of nitrogen from glutamate into the amino acids pool could give insights about the function of GDH.
Contrarily, the expression pattern of the putative *GDH3* resulted to be unaffected by the level of sugars, however, its response to the level of nitrate indicated that it must play a different role compared to the others GDHs. Thus, analyses of metabolites in plants with reduced *GDH3* expression was investigated in response to limited nitrogen conditions.

3.3 Functional characterization of *GDH* genes in *Arabidopsis thaliana.*

3.3.1. Generation of transgenic plants with decreased GDH expression.

3.3.1.1. Study of T-DNA insertion lines of GDH genes.

A technique for suppressing gene function is to insert a T-DNA (tumor-producing DNA) fragment into the coding sequence, resulting in a mutant called a mutant of insertion. This fragment may disturb or suppress the transcription of the targeted gene and this may result in arrested mRNA production or in production of non functional truncated version of the gene.
From the initial screen by Rosana Melo-Oliveira *et al*., (1995), only one deficient mutant allele *gdh1-1* was isolated in *Arabidopsis thaliana*. The mutant *gdh1-1* allele co segregates with the *GDH1* gene and behaves as a recessive mutation. No mutants were available for any of the other GDH. In order to investigate the consequences of knock-out mutations, T-DNA insertion lines available for *GDH1*, *GDH2* and *GDH3* were studied.
T-DNA insertion lines for each GDH were ordered from the Salk collection: Salk_042736, Salk_102709 and Salk_037861, all of them carrying the insertion in different exons (fig. 23).

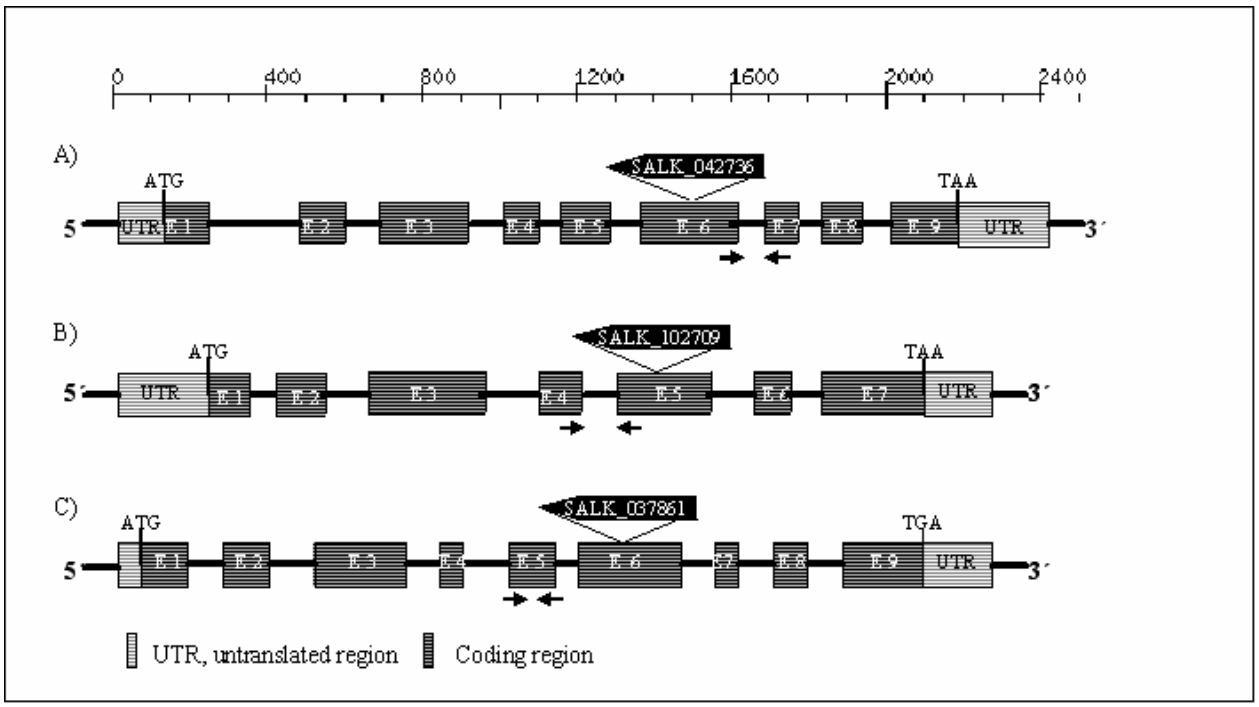

Figure 23. T-DNA insertion lines for GDH genes. (A to C) Gene structure including the T-DNA insertion in *GDH1* (At5g18170), *GDH2* (At5g07440) and *GDH3* (At3g03910), respectively. Exons are indicated as dark boxes, introns the segments between exons. The black arrow with the triangle indicates the insertion point and the direction of the T-DNA within the gene sequence. Small black arrows indicate the primers pairs used for real time RT-PCR analyses.

The three insertion lines were screened by PCR reaction. The isolated genomic DNA of each T-DNA insertion plant was tested using either a pair of primers amplifying the specific wild type product, or primers specific for the T-DNA insertion, in order to identify homozygous lines for the T-DNA insertion. The plants were also observed for any visible alteration of the phenotype. Homozygous insertion lines were found for the *GDH1* gene, but this showed no visible phenotypic change. No homozygous T-DNA insertion plants were identified from the screening of *GDH2* and *GDH3* plants. For *GDH2* T-DNA line, a total of 70 plants were used at the beginning from which around 20% showed heterozygote genotype in the T1 generation. However, from approximately 225 plants used in the next generation no homozygote lines were identified. Regarding the *GDH3* T-DNA line, 20% of plants showed heterozygote genotype in the T1 and from 450 plants checked in the next generation, no plants were identified as positive for the analysis.

Gene expression and protein stability of GDH1 were analyzed in the putative *gdh1*KO lines identified from the screening. The absent of *GDH1* transcripts is complete in the transgenic plants compared to the control WT (see figure 24). The enzymogram demonstrated that subunit α encoded by *GDH1* is necessary for the formation of the five GDH isoforms formed by combination of α and β subunits and therefore only a homohexamere composed by β subunits (encoded by *GDH2*) was functional in the T-DNA plants (figure 25).

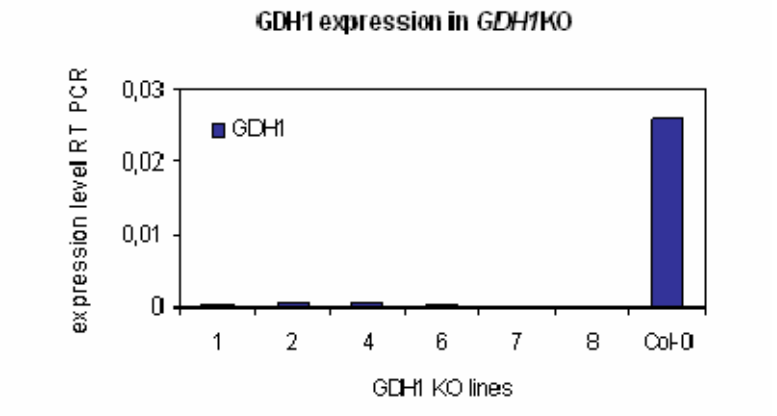

Figure 24. GDH1 expression in *gdh1*KO plants. Transcript levels were measured by real time RT-PCR in rosette leaves from GDH1 T-DNA plants selected from the screening (from 1 to 8) and compared to WT (Col-0). Values are means of relative transcript levels 2^-DCt calculated from one representative experiment. Those values were normalized according to the values of the housekeeping gene, actin (At3g18780).

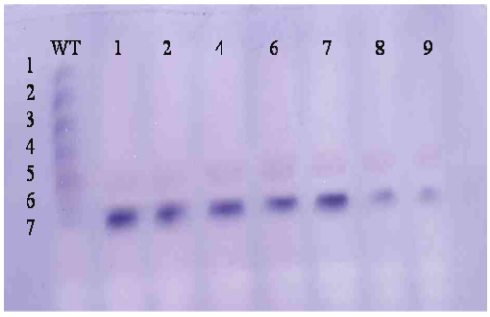

Figure 25. Native polyacrilamide protein gel in *gdh1*KO. WT (wild type) shows seven bands corresponding to the seven isoforms formed by the combination of GDH1 and GDH2 subunits. The transgenic lines are cited by numbers from 1 to 9. The lower bands correspond to the GDH isoform composed only by β subunits, the product of GDH2 gene. This confirmed the non functionality of GDH1 gene in the transgenic plants.

Southern blot was performed in some of the *gdh1*KO lines in order to confirm the right insertion of the T-DNA. The genomic DNA was digested with *Hind*III and hybridized with the p35S marker present in the T-DNA. As depicted in figure 26 hybridizing fragments of 1880 bp and 2094 bp were expected for the *Hind*III restriction with the 35S probe, however, several other larger hybridizing fragments were present indicating the putative presence of additional transgenic loci.

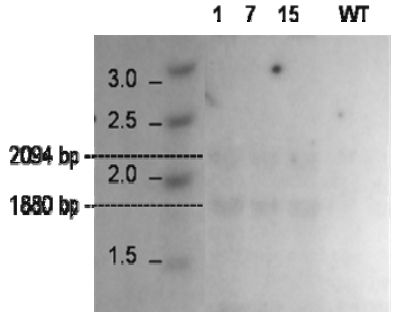

Figure 26. Southern blot analysis of *gdh1*KO lines. Autoradiograph of *Hind*III restricted gDNA from T4 plants of *gdh1*KO lines and WT control hybridized with probe for the p35S region of the T-DNA insert. The expecting sizes of the hybridizing fragments are indicated by the dashed lines. No visible signal was detected in the WT used as control.

Expression of the *GDH2* and *GDH3* genes was investigated in heterozygous lines identified from the PCR screening using real time RT-PCR (the primer pairs used for each GDH are shown in table 2.2 from Material and Methods). The expression values found were similar to wild type showing no differences in gene expression (data not shown). The inability to identify homozygote knock out lines indicated that the homozygote mutants for *GDH2* and *GDH3* might be lethal suggesting the essential role of the genes. The silique phenotype and seed segregation were therefore checked in the progeny of plants identified as heterozygous for the T-DNA insertion in the *GDH2* and *GDH3* genes when screened by PCR, to identify whether these genes led to embryo lethality. Mature green siliques were observed under the microscope and compared to wild type siliques. The results showed no apparent alteration in seed development (Figure 27). Another possible explanation is that these genes may be required for pollen function. Interestingly, *GDH2* transcript is very high in pollen. However, this result must be viewed with caution, because of problems in normalisation of signals from pollen.

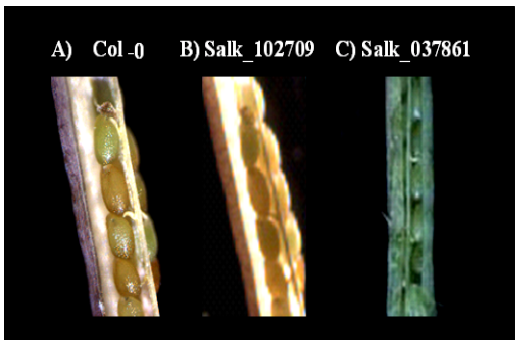

Figure 27. Mature green siliques from Salk lines identified as heterzygous compared to wild type. A) Wild type, Col-0; B) GDH2 T-DNA insertion plant; C) GDH3 T-DNA insertion plant. No alterations in seed development were visible in the heterozygous line compared to wild type.

Since none homozygous lines were identified for *GDH2* and *GDH3*, an RNA silencing strategy was carried out in order to provide further information about the role of the genes in *Arabidopsis thaliana*. In parallel, RNAi for *GDH1* was constructed to compare with the identified *gdh1* T-DNA insertion lines. Moreover, *gdh1* KO plants were transformed with the RNAi construct for *GDH2* with the goal to create the double transformant *gdh1*KO-*gdh2*RNAi.

3.3.1.2. Silencing of GDH by RNA interference (RNAi)

RNA induced gene silencing (alternatively also termed post transcriptional gene silencing or transgene silencing) is a useful tool to investigate gene function. The essence of RNA induced gene silencing is the entering of double-stranded RNA (dsRNA) into an organism or cell to induce a sequence specific RNA degradation mechanism that effectively silences a target gene. Gene silencing is achieved by transformation of plants with constructs expressing self complementary RNA (termed hairpin) containing homologous sequences to the target genes (Helliwell & Waterhouse, 2003).

The RNAi lines were generated by using a 315bp, 258 bp and 331 bp long fragments of *GDH1*, *GDH2* and *GDH3,* respectively (the primers used were specifically designed in the 3´UTR region of the gene of interest, see Material and Methods, table 2.4). The amplified fragments were then cloned into the gateway vector pSPECTRE using the gateway BP reaction. After, the gene-specific fragment was subcloned twice into the binary vector pJAWOHL8 using the LR reaction (one fragment in the sense orientation and the other in the antisense orientation). The two fragments were separated by an intron and placed under the control of the CaMV 35S promoter. The resulting plasmid was used for *Agrobacterium tumefaciens*-mediated transformation of wild type *Arabidopsis thaliana* plants. In the case of the double construction *gdh1*KO-*gdh2*RNAi, the transformation was made on *gdh1*KO plants using the same procedure than *Arabidopsis* wild type plants used for infiltration purposes.

Around thirty five BASTA-resistant plants were selected for *GDH1* and *GDH2*, seven of which were chosen for further analysis. The silencing effect was studied in rosette leaves harvested at the end of the night of T1 and T2 generation plants using real time RT PCR and native PAGE-protein gels. Transcript levels analysed by real time RT-PCR are shown in figure 28. The results demonstrated the effectiveness of the silencing with around 80% decrease in *GDH1* and 95.5% reduction in *GDH2* transcript level compared to wild type.

As we can observe in figure 28 the silencing effect is maintained in the F2 progeny, demonstrating the stability of the RNAi. Among the transgenic lines, some lines showed a substantial decrease in the expression while some others a partial decrease of mRNA accumulation. Two plants showed similar or higher transcripts compared to WT (Figure 28, panels A and D). According to these results, it was possible to select some lines for further analysis (lines 2 and 8 for *GDH1*RNAi and lines 39 and 46 for *GDH2*RNAi).

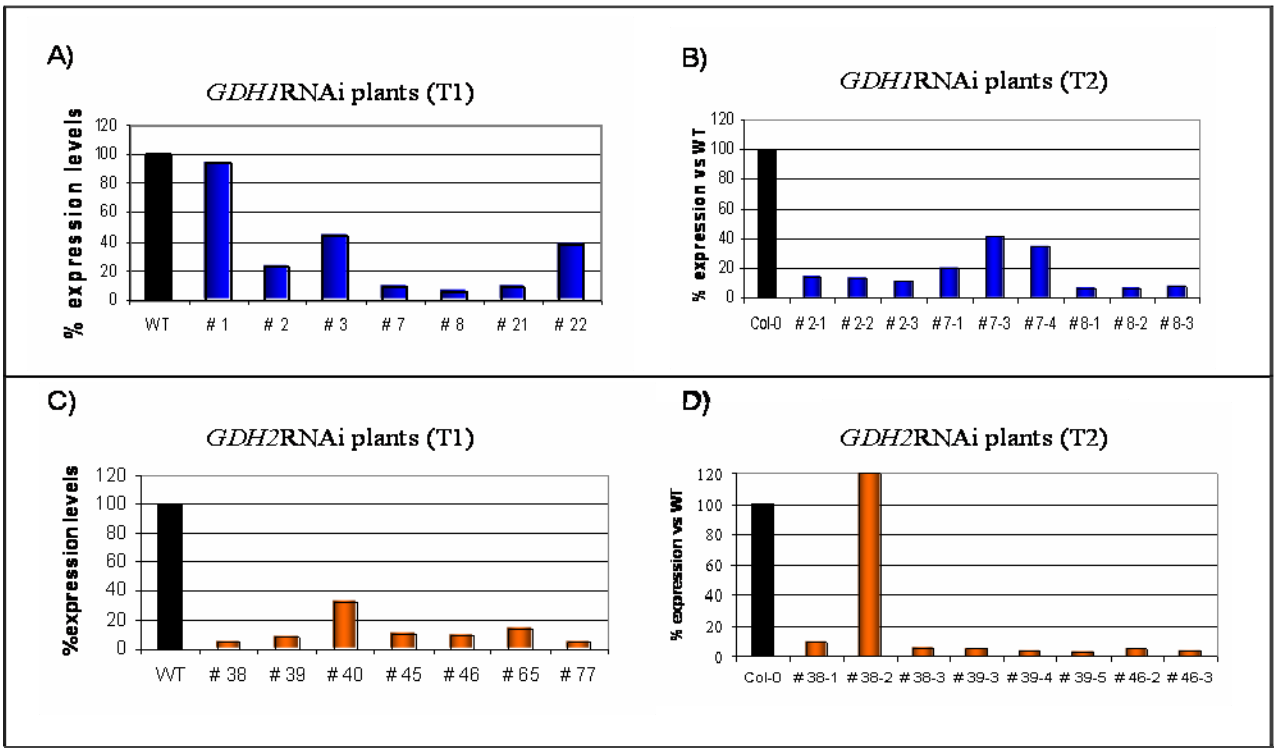

Figure 28. Expression values by real time RT PCR in *gdh1* RNAi and *gdh2* RNAi plants compared to wild type. Transcript levels were assayed in rosette leaves of plants (T1 and T2 generation) harvested at the end of the night, conditions where the transcript levels have been shown to be higher (see section 3.2.4.2). A) and B) *GDH1* transcript level in plants transformed with *GDH1*RNAi compared to WT in T1 and T2, respectively; B) and C) *GDH2* transcript level in plants transformed with *GDH2*RNAi compared to WT in T1 and T2,respectively. Values represent the percentage of mRNA accumulation in RNAi lines compared to wild type.

Regarding the putative *GDH3*, the analyses were inspected by real time RT-PCR analysis using flowers from the F1 progeny. The results showed no differences in the expression of the *GDH3* RNAi plants compared to the control wild type due to a very low expression of the gene

under normal conditions (data not shown). The analysis was continued in the transformed plants under conditions where GDH3 is induced (see section 3.2.4.1).

Double transformed plants *gdh1*KO-*gdh2*RNA were also analysed using rosette leaves material harvested at the end of the night. Among the transgenic lines analyzed there was a segregation of RNAi effect with some plants containing more expression of *GDH2* than WT. Transcript levels of GDH2 are presented in figure 29. From the results, some lines were chosen for further analysis. *GDH1* transcripts were completely absent due the T-DNA insertion plants in the gene (not shown).

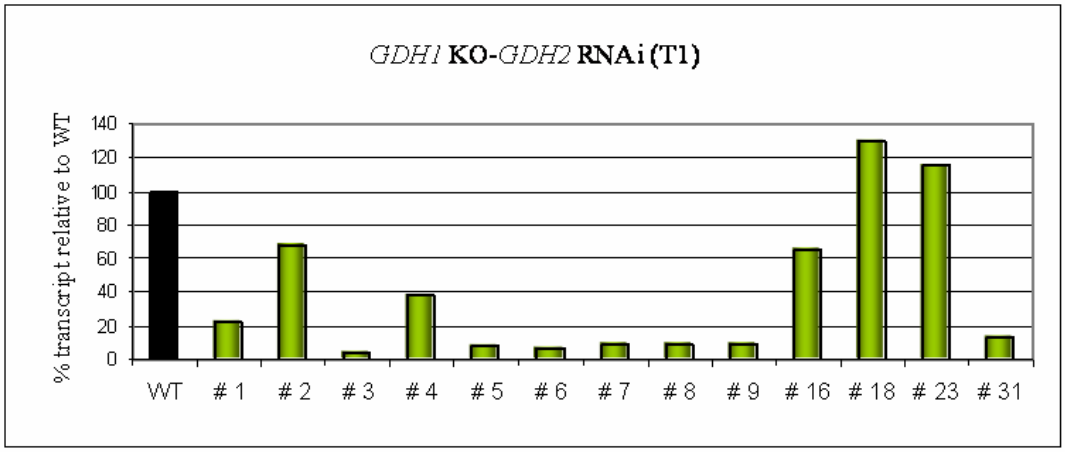

Figure 29. **Expression values of GDH2 by real time RT-PCR in double transformant *gdh1*KO-*gdh2*RNAi plants from T1.** The material was harvested at the end of the night Values represent the percentage of mRNA accumulation compared to WT. *GDH1* transcripts were completely absent due the T-DNA insertion plants in the gene (not shown).

3.4. Biochemical characterization of plants with decreased *GDH* expression

3.4.1. Analyses of GDH activity in *gdh1* K0 and *gdh2* RNAi lines.

Analyses of GDH activity were investigated in the *gdh1*KO and *gdh2*RNAi lines in order to see the effect of gene silencing on GDH activity in the plants. For reasons of convenience, the GDH activity was done using an assay in the direction of amination.

The *gdh1*KO mutant showed around 50% less activity and around 40% decrease in the RNAi line during the diurnal cycle and after an extended night compared to the wild type Col-0 (figure 30).

In the *gdh2* RNAi plants, the activity appeared to be around 48% decreased and the increase during the extended night was less marked in the transformant lines compared to the wild type (figure 31).

In general, a decrease in expression of *GDH1* and *GDH2* led to a change on GDH activity in the KO mutant and transgenic lines compared to wild type during a normal diurnal cycle.

Moreover, the activity did not increase after a prolonged night period as compared with the control wild type.

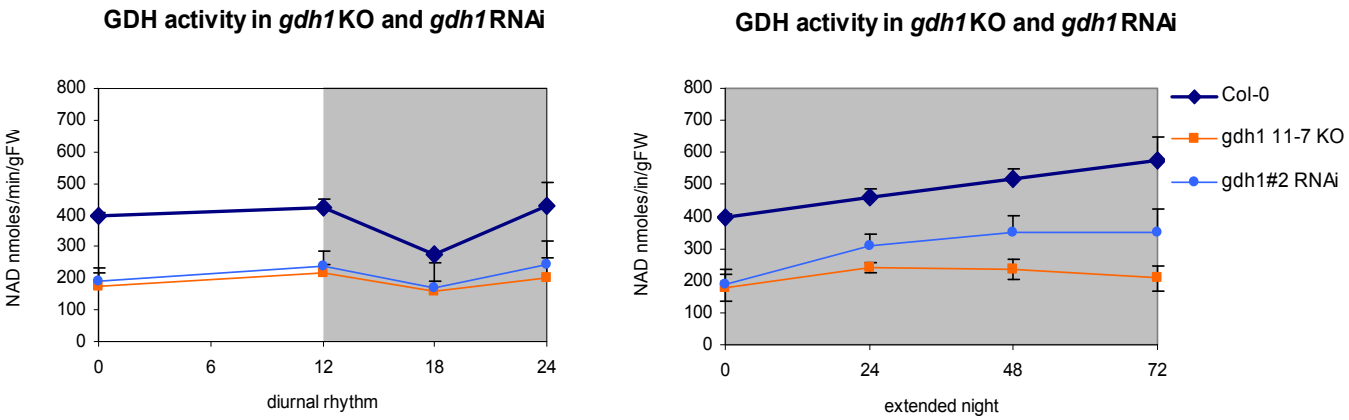

Figure 30. GDH aminating activity in *gdh1*KO and *gdh1*RNAi lines during the diurnal cycle and after transferred to an extended night. GDH activity was assayed in 20 mg of FW plant material. Activity is given in nmol_min_g FW of NAD+. Values are means ± SD (n=5).

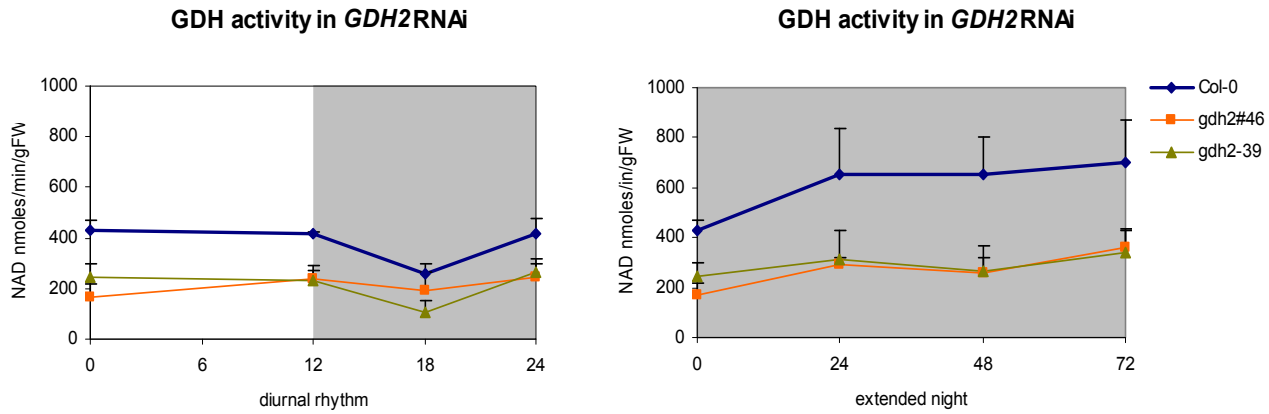

Figure 31. GDH aminating activity in *GDH2*RNAi lines during the diurnal cycle and after transferred to an extended night. GDH activity was assayed in 20 mg of FW plant material. Activity is given in nmol_min_g FW of NAD+. Values are means ± SD (n=5).

3.4.2. Analysis of metabolites in *gdh1* K0 and *gdh2* RNAi lines.

Arabidopsis thaliana plants with decreased expression of *GDH1* or *GDH2* did not exhibit obvious visual phenotypic alterations compared to the wild type (data not shown). Information about the metabolite composition could therefore give an idea about the possible function of GDH in plants.

The metabolite content including soluble sugars, starch and major amino acids were determined in the transgenic lines and compared to wild type. For that approach, plants were grown on soil and harvested at different points in a normal day/night conditions (diurnal rhythm) and at different times in a prolonged dark period (extended night experiments).

3.4.2.1. Sugar composition of *gdh1* K0 and *gdh2* RNAi lines.

Sugars belong to one of the most important factors that regulate plant metabolism and growth. Sugars levels undergo marked diurnal changes in leaves (Geiger & Servaites, 1994; Scheible *et al.*, 1997a, 1997b; Matt *et al.,* 2001a, 2001b) and non photosynthetic tissues. During the day, photosynthetic fixation of carbon in leaves leads to the synthesis and export of sucrose to the rest of the plant to support metabolism and growth. Plants during the night consume carbon and starch is remobilized to support sucrose synthesis and export. Even a few hours of carbon depletion lead to an inhibition of growth which is only slowly reversed when carbon becomes available again (Gibon *et al*., 2004a).

As shown in previous sections (3.2.4.2), GDH expression and activity are diurnally regulated and markedly affected by the presence of sugars. Therefore, to investigate if carbohydrates content was affected in the transgenic plants, rosette leaves of *gdh1*KO mutant and *gdh2* RNAi were harvested at different points in a 12h light /12h dark diurnal cycle. In parallel, some plants were transferred to complete darkness and harvested every 24h during 3 days.

The extended night experiment represents conditions where the plants are completely deprived of light (as during the night) and therefore simulates a situation of carbon starvation. The goal was to study the effect of GDH reduction in plants grown in those conditions where expression and activity are induced in wild type plants.

The sugar composition was assayed in the cited plants. The results showed no significant differences in sugar and starch content between the transgenic plants and the control wild type (see tables 1, 2, 3 and 4 from the Appendix).

3.4.2.2. Free amino acids in *gdh1* K0 and *gdh2* RNAi lines

The amino acid composition was studied in order to see whether the absence of *GDH1* or the absence of *GDH2* had any effect on the accumulation of glutamate or related amino acids linked to nitrogen assimilation.

Amino acids are the basic structural building units of proteins and enzymes. In addition to this role, they perform essential functions in primary and secondary metabolism and their synthesis control directly or indirectly various aspects of plant growth and development.

Plants are able to generate all the 20 amino acids necessary for protein synthesis by themselves. Some amino acids serve to assimilate nitrogen and transport it from sources to sinks, and some others serve as precursors to secondary products such as hormones and compounds involved in plant defence.

Glutamate is one of the main components of proteins and the amino acid generate first. Itself, can bind a further ammonium ion to form glutamine. Nitrogen assimilated into glutamate and

glutamine may be incorporated into aspartate and asparagine to be readily disseminated into the plant.

Amino acids were separated by high-performance liquid chromatography (HPLC) and detected by fluorescence measurements as ortho-phthaldehyde derivatives.

Special attention was set on the major amino acids including glutamate, glutamine, aspartate and asparagine due to their role in the assimilation of the inorganic nitrogen and its distribution into plant metabolism. Results are shown in tables 5, 6, 7 and 8 from the Appendix.

There were no significant changes in the transgenic plants compared to the WT.

The unexpected results showed that the reduction in GDH doesn't lead necessary to an alteration in the metabolism of sugars and amino acids among the transgenic lines in the conditions used for the analysis. It is possible that one gene is able to substitute the other and therefore to compensate its lack. The next thing to do was to analyse plants with decreased expression of both genes *GDH1* and *GDH2*. The measurement of metabolites in the transgenic plants could give indirect information about processes which lie downstream of GDH and help to understand its function in plants.

3.4.3. Analysis of GDH aminating activity in the double transformant *gdh1*KO-*gdh2*RNAi lines.

A double transformant mutant *gdh1*KO-*gdh2*RNAi was created as a result of the transformation of a *gdh1* T-DNA insertion mutant as genetic background with the RNAi construct of the other gene of interest, *GDH2*. Around 50 transgenic plants were identified in the T1 generation after a selection with BASTA and 17 plants were used for analyses of gene expression. Out of them, 7 plants revealed more than 50% reduction in *GDH2* expression, 4 plants presented a slightly reduction in *GDH2* expression and around 6 plants had similar *GDH2* expression when compared to wild type. *GDH1* expression was absent in all of the plants tested. Each plant was grown separately and seeds were collected individually. T2 seeds from 3 individual plants (*gdh1-2* #5, #6 and #9) were used for further analyses.

GDH activity in the selected plants was measured. *Arabidopsis* wild type transformed with the empty vector (WT ev, kindly provided by Dra. Stephanie Arrivault; Max Planck Institute, Golm) was included in the analysis for consistency. The results are shown in figure 32. In general, there was a trend to decrease total GDH activity in the transgenic plants compared to the control (Col-0 and WT-ev) and the reduction was marked towards the end of the extended night period.

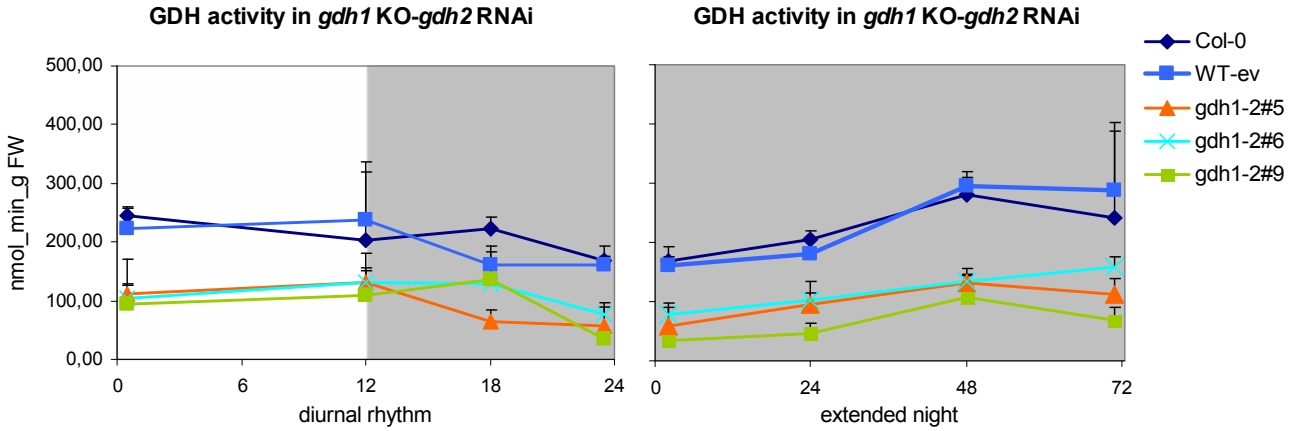

Figure 32. GDH aminating activity in double mutant lines and wild type plants in diurnal rhythm and extended night experiments. GDH activity was assayed in 20 mg of FW plant material. Activity is given in nmol_min_g FW of NAD+. Values are means ± SD (n=5).

3.4.4. Analysis of metabolites in the double transformant *gdh1*KO-*gdh2*RNAi lines.

3.4.4.1 Sugar composition in *gdh1*KO-*gdh2*RNAi lines.

Composition of soluble sugars and starch in three double mutant lines and wild type is presented in figure 33. The results showed no significant differences in sugar content between the transgenic plants and the control wild type during the diurnal cycle and extended night period suggesting that GDHs are not involved in sugars metabolism in response to the conditions used in the analysis.

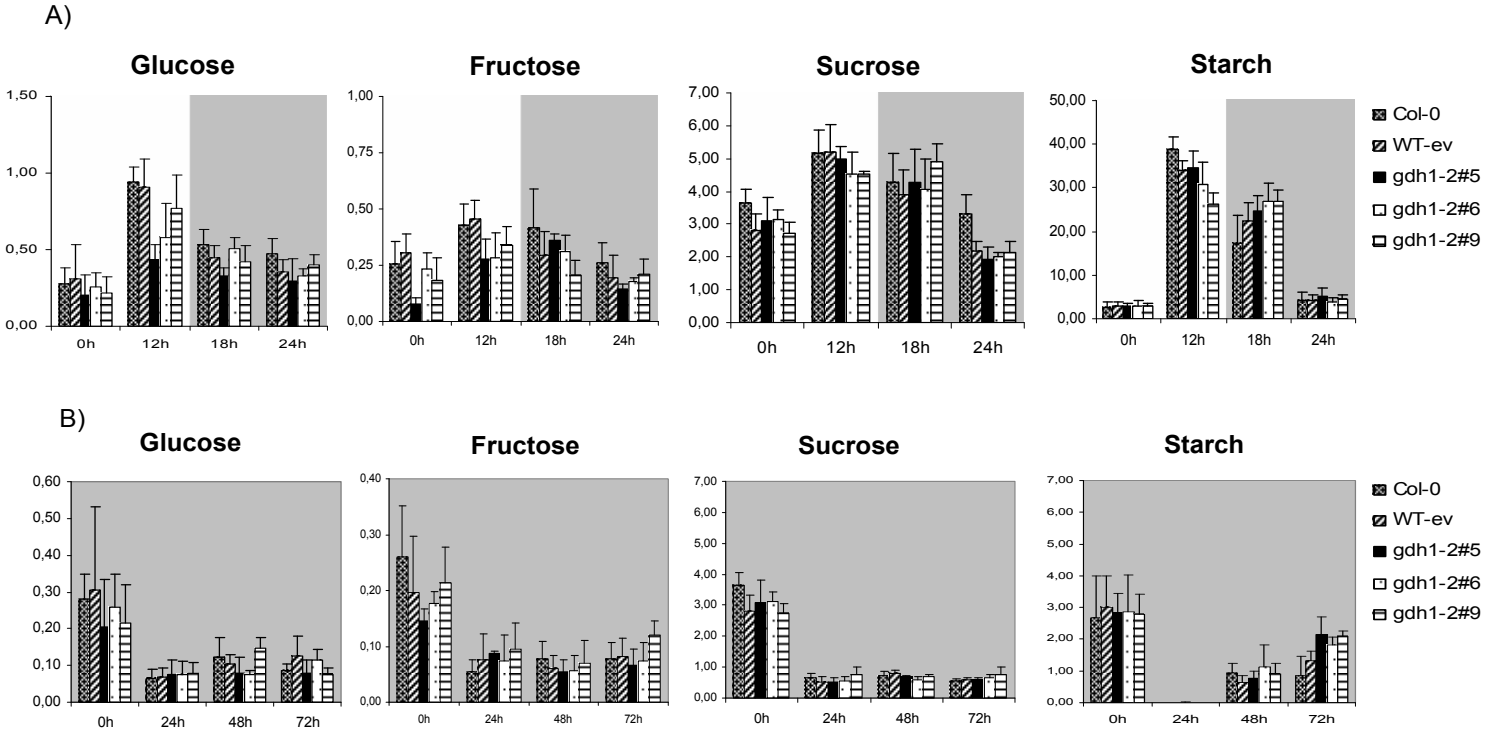

Figure 33. Sugar and starch content in *gdh1*KO-*gdh2*RNAi and WT. (A)Diurnal rhythm experiment. (B) Extended night experiment. Sugar and starch content were assayed in rosette leaves of 6 weeks old plants. Values given in µmol_ gFW and are means ± SD (n=5) in WT and ± SD (n=10-15) in transgenic lines.

Regarding the starch content, the starch breakdown was inhibited in *gdh1*KO-*gdh2*RNAi lines in the first 6 hours of the night and accelerated in the second half of the night compared to both wild types in which the consumption of starch during the night was linear through out the night. Additionally, starch content was higher after 72h of extended night *gdh1*KO-*gdh2*RNAi lines compared to both wild types.

3.4.4.2. Free amino acids in *gdh1*KO-*gdh2*RNAi plants.

The amino acid composition was analyzed in the three transgenic lines and WT. Contents of glutamate (substrate or product of GDH), glutamine, aspartic acid and asparagine were measured. Furthermore, amino acids such as serine and glycine were determined as products of photorespiratory processes. Aspartate is needed for the synthesis of asparagine, lysine and threonine that acts as precursor of isoleucine. Results of the selected amino acids are summarized in figures 34 and 35.

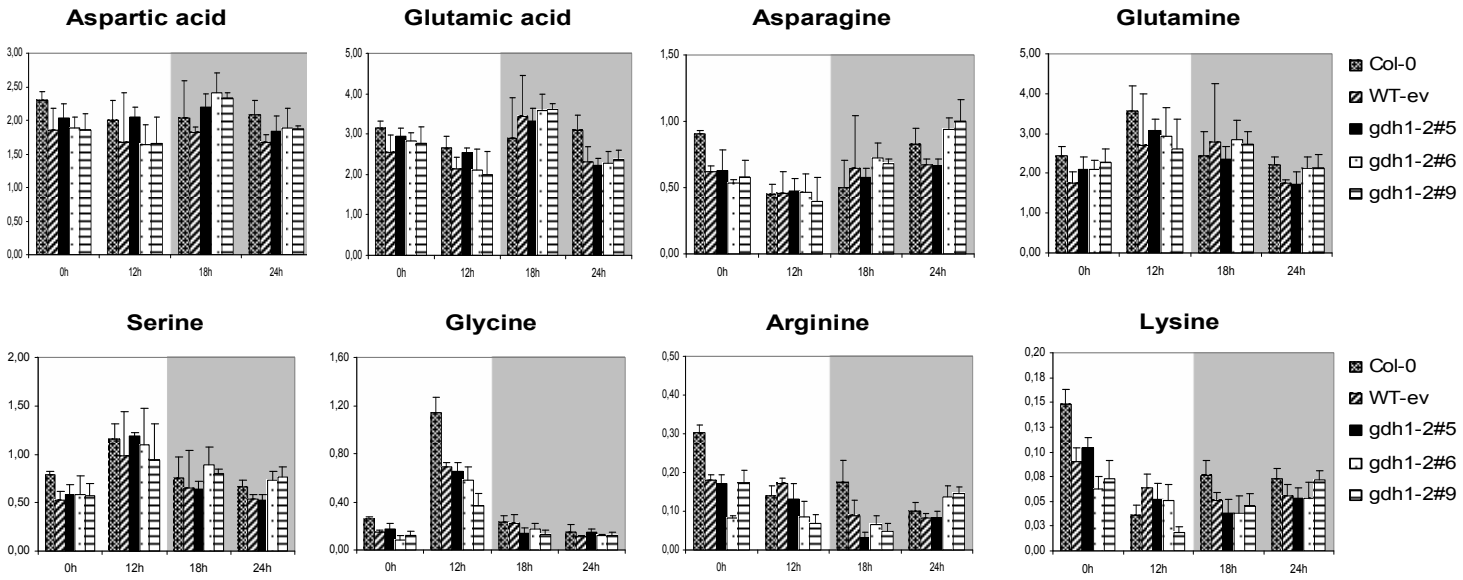

Figure 34. Individual amino acids in *gdh1*KO-*gdh2*RNAi and WT. Diurnal rhythm experiment. Individual amino acids were assayed in rosette leaves of 6 weeks old plants. Values are means ± SD (n=5) in WT and ± SD (n=10-15) in transgenic lines. Amino acid content is given in µmol_ gFW.

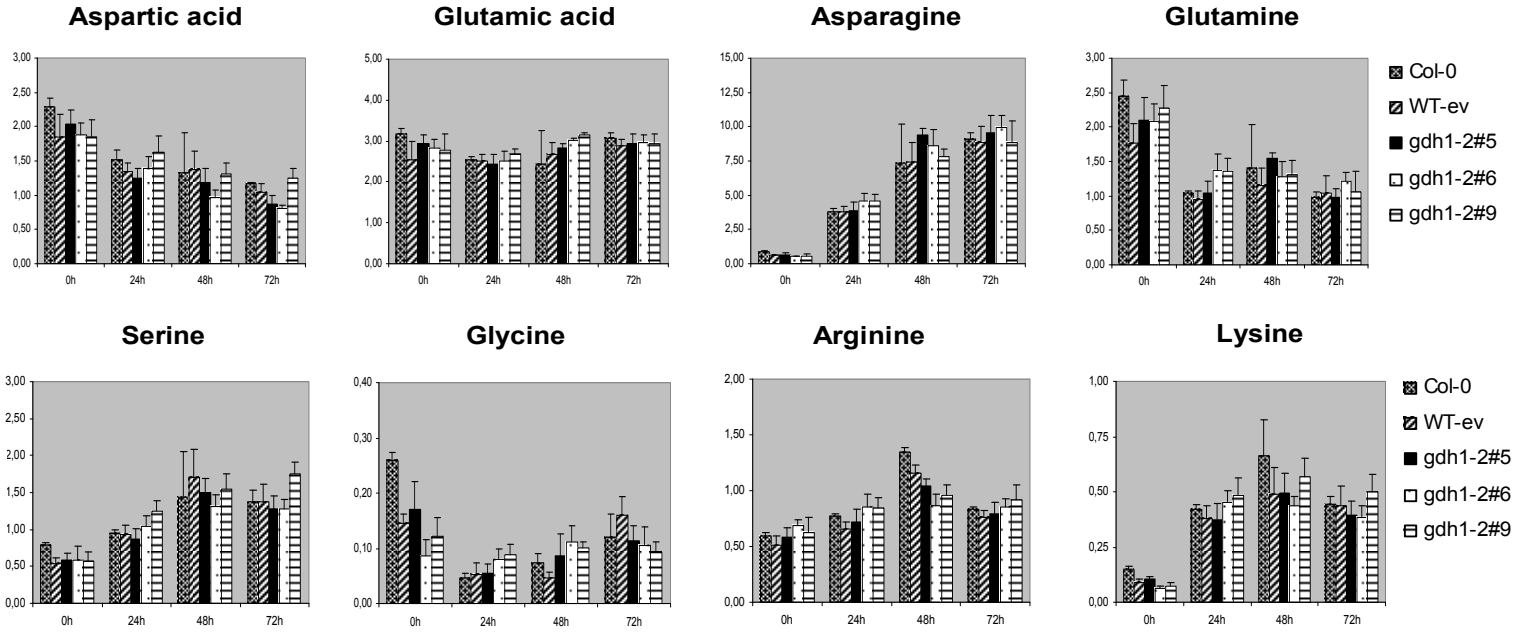

Figure 35. Free amino acids determined by HPLC in transgenic *gdh1*KO-*gdh2*RNAi and WT. Composition of the major amino acids of rosette leaves of plants harvested after transferring to continuous darkness. Free amino acids were assayed in rosette leaves of 6 weeks old plants. Values are means ± SD (n=5) in WT and ± SD (n=10-15) in transgenic lines. Values are given in µmol_g FW.

Surprisingly, no significant differences could be observed among the transgenic lines and the wild type suggesting the low importance of GDH in amino acid metabolism under those conditions.

Therefore, metabolite determination in plants with decreased GDH activity could not give any evidence about its role in plants under the conditions used for the analysis. Other analyses are needed to give any indication about the role of GDH in plants.

Another explanation is that even in the double mutant the decrease on GDH activity (2-3 fold) may not be enough to cause changes in the accumulation of sugars and/or nitrogen compounds.

3.5 Effect of Carbon Starvation in plants with decreased GDH.

Previous experiments revealed that the reduction of GDH activity on plants growing in soil under normal photoperiod had no effect on the central metabolites like carbohydrates or amino acids.

Nitrogen assimilation is not a simple process. A large repertoire of substrates and metabolites interact to influence gene expression and enzyme activities at multiple levels under different environmental conditions and in different tissue types. For example, in leaves under light conditions, the rate of photorespiration is likely to be a significant factor influencing the composition of amino acids exported from source leaves in C3 species (Madore & Grodzinski,

1984). Additionally, since we have postulated a role for GDH in glutamate deamination to 2-oxoglutarate in connection with amino acid catabolism, it is also possible that in leaves, the high activity of the photorespiratory pathway might in the dark allow an alternative route for ammonium release via glycine decarboxylase. In order to avoid such factor like photorespiration, root tissue was chosen for further analysis.

Leaves and roots of plants growing in medium without sucrose were analysed for the levels of metabolites like sugars and amino acids. To do this, four independent double mutant lines carrying a T-DNA insertion for *GDH1* and RNAi construct for *GDH2* were germinated and vertically grown on agar plates containing AMOZ medium without additional sugar. Col-0 and wild type with empty vector (WTev) grown under the same conditions served as controls. Root length and architecture were daily observed for phenotypes but no obvious visible differences among the genotypes could be seen.

3.5.1 Sugar levels in shoots and roots of plants under carbon starvation.

The sugar content of plants with decreased *GDH1* and *GDH2* expression was analysed in leaves and root tissues of plants grown vertically on agar plates containing AMOZ medium without sucrose and harvested after 11 days of sugars deficiency at the end of the day, the end of the night and after 24h of an extended night when the plants are C-starved. Figures 36, 37 and 38 depict the level of soluble sugars in roots and leaves of wild type plants in comparison to the four observed transgenic plants.

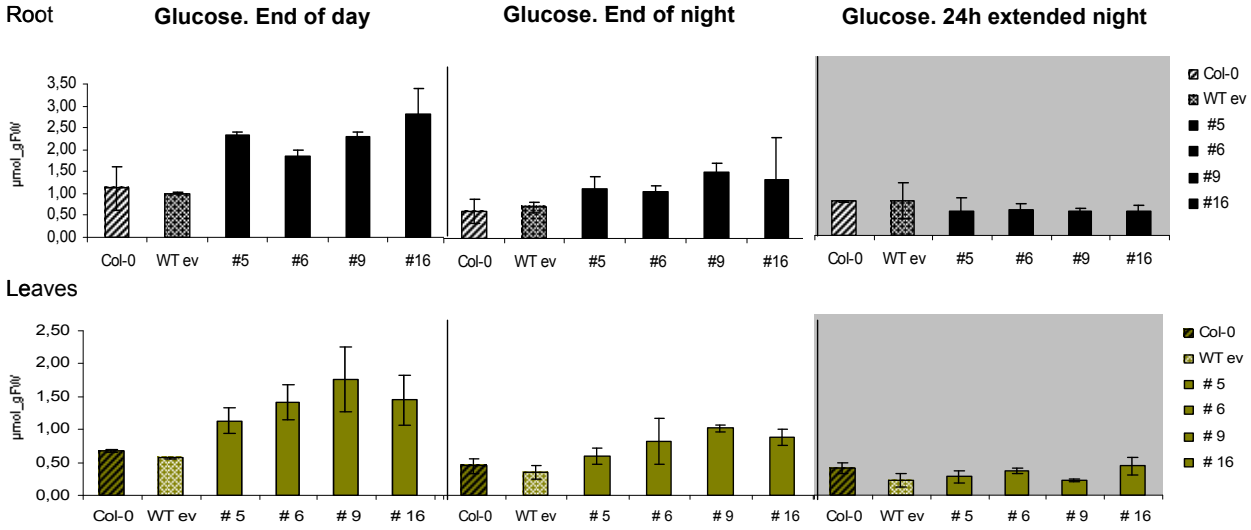

Figure 36. Glucose composition in transgenic plants and wild type under carbon starvation conditions. Sugars content from roots and leaves of 11 days old seedlings in wild type and four independent *gdh1*KO-*gdh2*RNAi transgenic plants harvested at the end of the day, end of the night and after 24h in darkness. Seedlings were grown on vertical agarose plates containing AMOZ medium without additional sucrose. Black colour indicates root material and green colour corresponds to shoot tissue. Each datapoint is the arithmetic mean of two independent biological replicates, each consisting of the leaves or roots pooled from 30-40 seedlings.

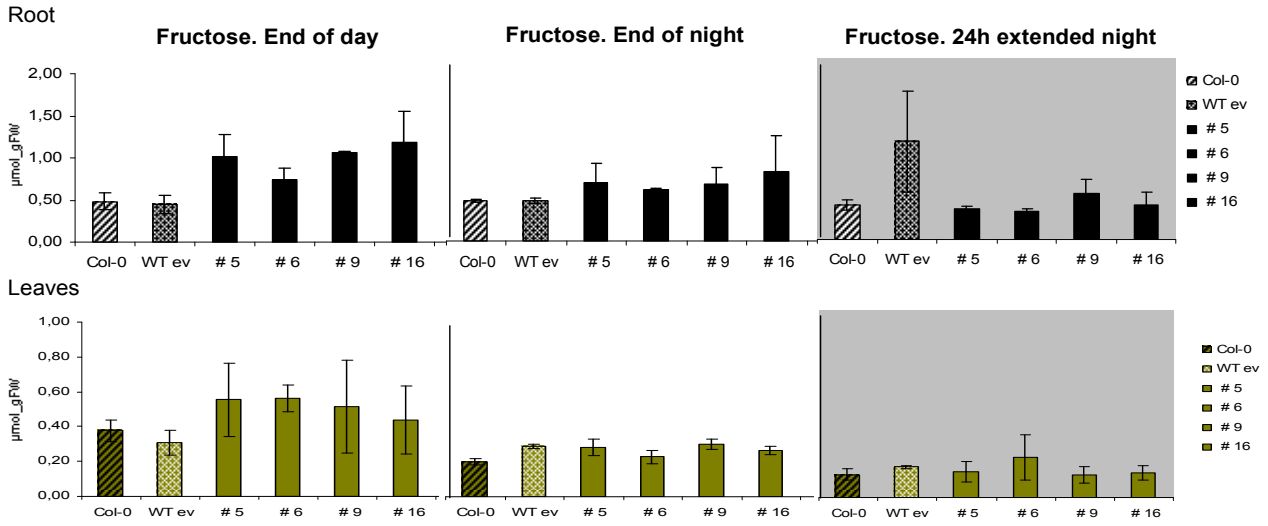

Figure 37. Fructose composition in roots and leaves of transgenic plants and wild type under carbon starvation conditions. Plants were harvested as described in figure 36.

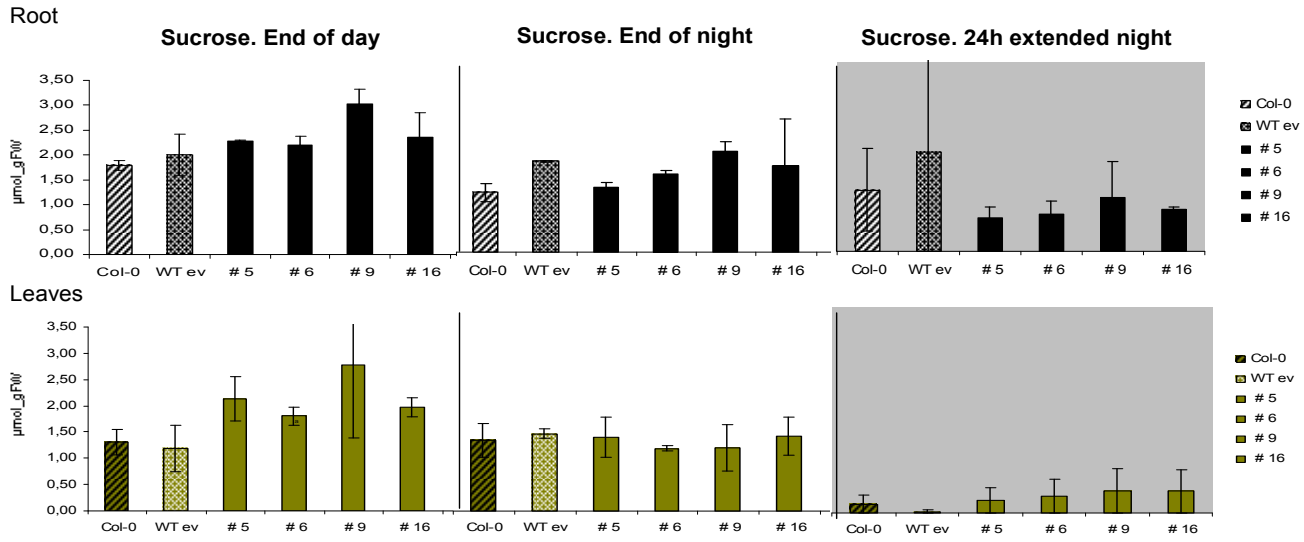

Figure 38. Fructose composition in roots and leaves of transgenic plants and wild type under carbon starvation conditions. Plants were harvested as described in figure 36.

Roots of wild type plants contained higher levels of soluble sugars (glucose, fructose and sucrose) than leaves. In general the level of sugars was higher in the transgenic plants at the end of the day when compared to both wild types. The accumulation of sugars was decreased towards the end of the night and during the extended night period in the observed plants and the differences between the mutants and the wild type was also less marked. Moreover, the level of starch was measured confirming the sugars accumulation stored in form of starch at the end of the day in leaves of the transgenic plants (see figure 39).

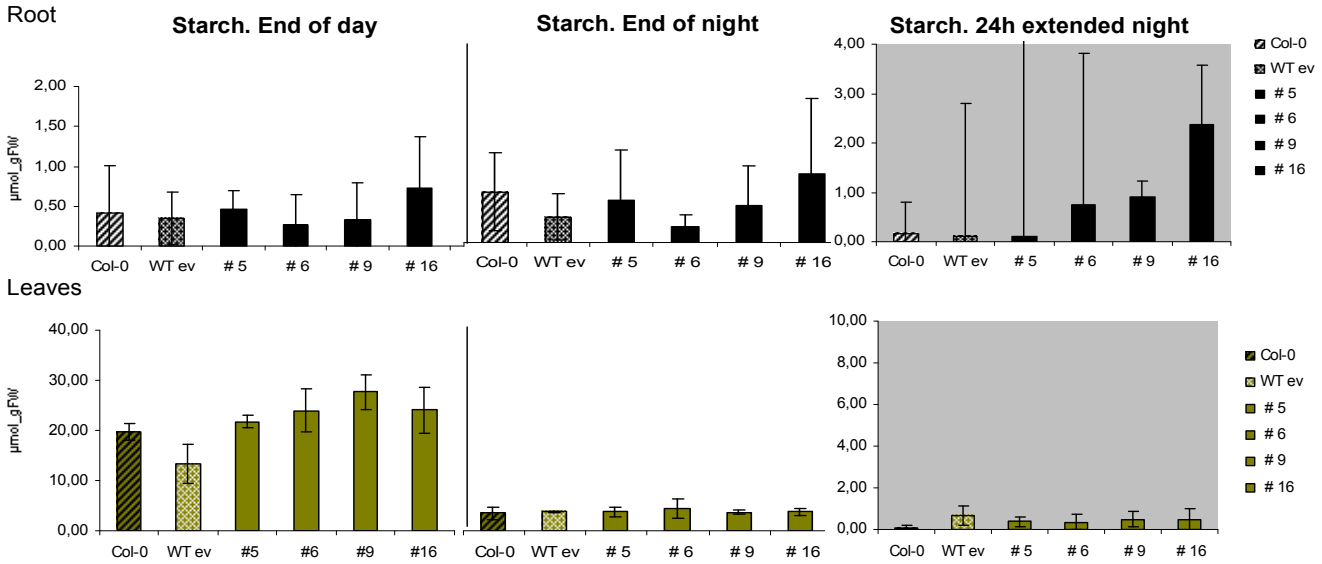

Figure 39. Starch content in roots and leaves of double transformant *gdh1*KO-*gdh2*RNAi. Starch content from roots and leaves of 11 days old seedlings in wild type and four independent *gdh1*KO-*gdh2*RNAi transgenic plants harvested at the end of the day, end of the night and after 24h in darkness. Seedlings were grown on vertical agarose plates containing AMOZ medium without additional sucrose. Each datapoint is the aritmetric mean of two independent biological replicates, each consisting of the leaves or roots pooled from 30-40 seedlings.

3.5.2 Amino acids composition in plants under carbon starvation.

The amino acid composition was analyzed in the four transgenic lines and WT. Results showed no significant differences between the transgenic plants and the wild type (Figure 1 from the Appendix).

3.5.3 α-ketoglutarate content in plants under carbon starvation.

The organic acid α-ketoglutarate was determined in shoots of the analysed plants. Measurements were not possible in root material due the low amount of plant material obtained. This makes the experiments in part inconclusive, as production of α-ketoglutarate is the direct postulated function of GDH during starvation. Results showed no differences among the transgenic plants and the wild type (see figure 40).

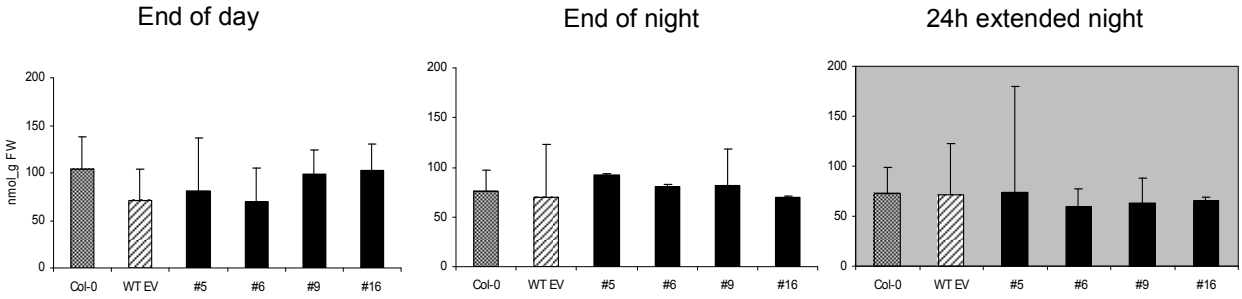

Figure 40. α-ketoglutarate content in shoots of double transformant *gdh1*KO-*gdh2*RNAi. Plants were grown and harvested as in Figure 36. Values are mean of two independent biological replicates, each consisting of the leaves pooled from 30-40 seedlings. Values are given in nmol_g FW.

3.6. Characterization of the putative *GDH3*

3.6.1. Promoter GUS expression analysis under different nitrate concentrations

Previous analyses have shown the metabolic regulation of *GDH3* by nitrogen indicating that the putative *GDH3* is highly expressed upon nitrate starvation and dramatically down regulated in response to the addition of nitrate (see section 3.2.4.1).

In order to investigate the metabolic regulation of *GDH3* more in depth, promoter GUS analyses were carried out in agar plates with different nitrate concentrations (0,150mM, 1mM, 3mM and 35mM, without additional glutamine). *GDH3*-GUS promoter lines were produced as described in section 2.2.2.6 from Material and Methods and the composition of the medium used is indicated in table 2.6 from Material and Methods.

The histochemical staining for GUS activity was performed in 14 days-old plants grown under different nitrate concentration. Results are shown in figure 41. Three independent lines with *GDH3* promoter-GUS fusion were analysed in the experiment.

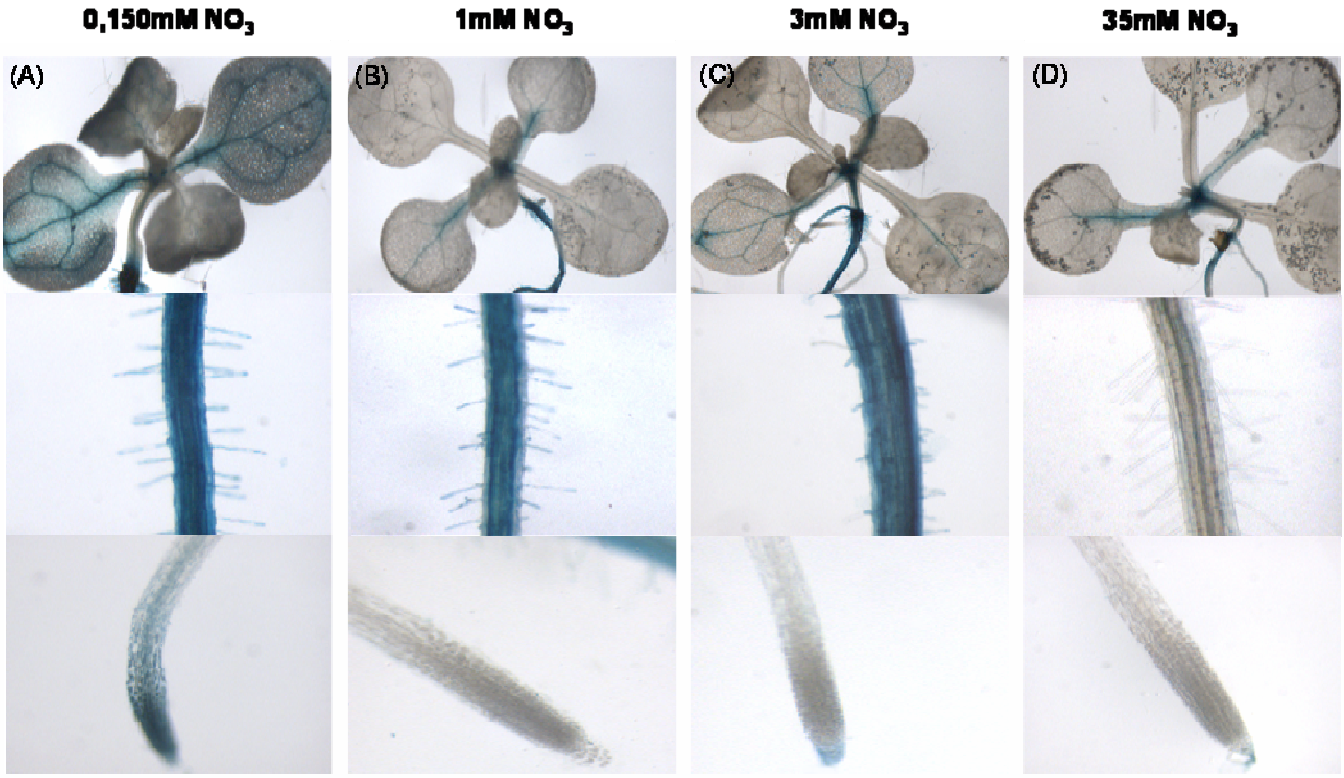

Figure 41. Localization and nitrate dependence of *GDH3* promoter activity in 14 days-old seedlings. (A-D) Histochemical staining for GUS activity in 14 days-old seedlings was performed overnight. Seedlings of transgenic lines transformed with *pGDH3::GUS* were grown on agarose plates containing different concentrations of nitrate without glutamine as additional nitrogen source (the different amount of nitrate used is indicated above the figures). (A) Different parts of a seedling grown under nitrate starvation 0,150mM NO_3; (B) Seedling grown in medium with low amount of nitrate, 1mM NO_3; (C) Parts of a seedling grown under normal medium with 3mM NO_3; (D) Parts of a seedling grown under high nitrate 35mM NO_3 . The figures show one from three independent lines with GDH3 promoter GUS fusion used in the experiment

According to what has been shown in section 3.2.4.1, *GDH3* expression is up regulated under nitrate starvation conditions. As we can observe in figure 41, panel A, *GDH3* expression is higher when the nitrate concentration is lower. The expression was gradually induced (depending on the nitrate concentration in the medium) and mainly located in vascular tissue, hypocotyl and upper-middle part of the main root. Therefore, these conditions (0,150mM, 1mM, 3mM and 35mM NO_3) were used to investigate the effect in metabolism of plants with decreased *GDH3* expression. Three independent lines with GDH3 promoter GUS fusion were used in the experiment.

3.6.2. Metabolites determination of plants with decreased *GDH3*

Results from GUS staining analyses indicated that the putative GDH is up regulated when plants are nitrogen limited. Three lines of plants transformed with a *GDH3*RNAi construct were further analysed and characterised. Moreover, plants with decreased expression of *GDH3* were visually observed for phenotypic alterations compared to wild type. Among other metabolites, sugars, protein content, total and individual amino acids were determined in those plants.

Metabolites analyses were assayed in transgenic plants grown on vertical agar plates in medium with different nitrate concentrations (0,150mM, 1mM, 3mM and 35mM).

3.6.2.1 Nitrate content

Nitrate content of the plants was first determined in order to confirm the conditions used in the experiment. Results showed that the amount of internal nitrate increased according to the concentration of nitrate in the medium. Also, the nitrate content was higher in shoot than in roots. (See figure 42).

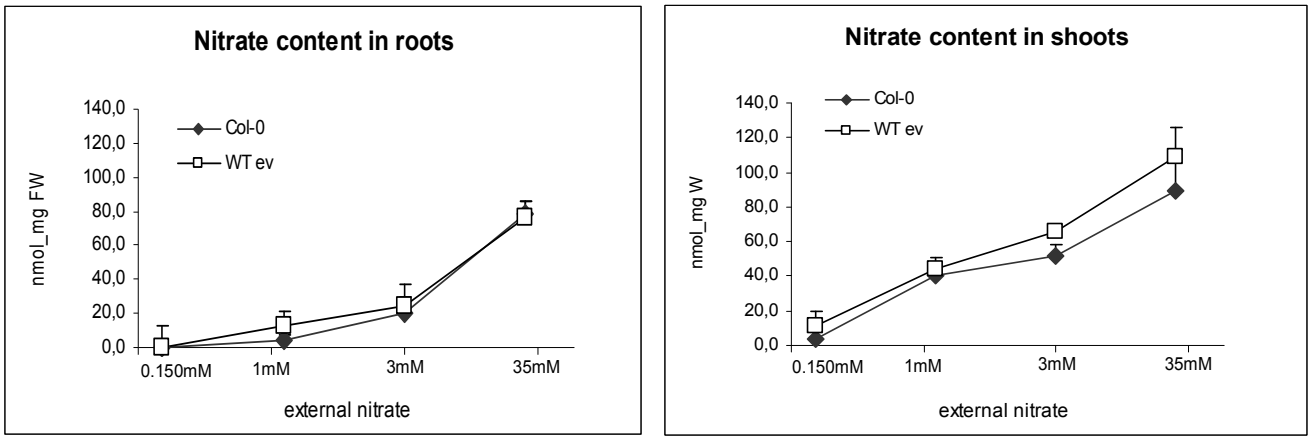

Figure 42. Nitrate content in wild type plants grown under different concentrations of nitrate. Internal nitrate was determined in roots and leaves of wild type plants at different nitrate concentrations, 0,150mM, 1mM, 3mM and 35mM. Plants were grown in vertical agar plates containing different concentrations of nitrate under normal 12h light/12h dark photoperiod. Shoots and roots were separated and harvested 14 days after the sowing

date. Values are mean of three independent biological replicates each consisting of the leaves or roots pooled from 30 seedlings. Values are given in nmol_mg FW.

3.6.2.2 RT-PCR expression analyses in *GDH3* RNAi plants

Real time RT-PCR expression analyses were carried out in the three *GDH3* RNAi plants selected in order to confirm the reduction in *GDH3* expression. Figure 43 depicts the expression of *GDH3* by real time-RT-PCR in roots and leaves of Col-0 plants and wild type with the empty vector (WT ev) under 3 different nitrate concentrations (0,150mM, 1mM and 35mM). Table 3.1 represents the percentage of *GDH3* transcripts in roots and leaves of the transformed plants compared to wild type and wild type with the empty vector. Expression of *GDH3* in both wild types is much higher in nitrate deficiency conditions (especially in roots) and decreases with the addition of nitrate in the medium. In general, transgenic lines showed a 2- to 4-fold decrease in *GDH3* transcript when compared to wild type with the empty vector (see table 3.1). However, line 8 showed an anomalous response in 0,150 mM nitrate, with higher levels than in wild type plants. This response was seen in roots and shoots. Overall, the decrease in transcripts is rather small, compared to the inhibition typically seen with RNAi.

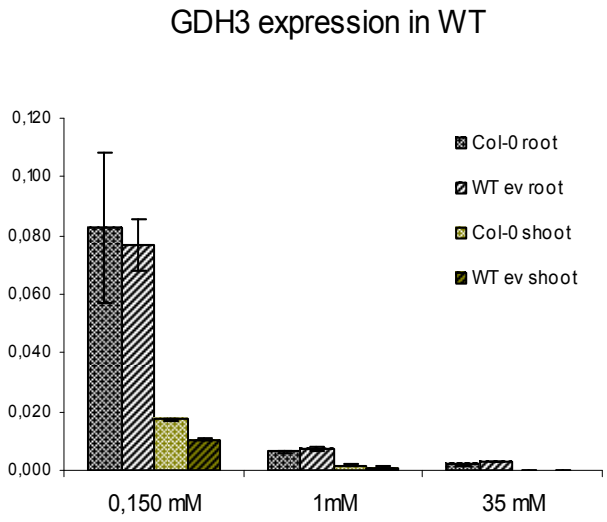

Figure 43. Expression pattern of *GDH3* in wild type under three different concentrations of nitrate. Plants were grown and harvested as in figure 42. Black colour indicates root material and green colour corresponds to shoot tissue. Error bars indicates the standard deviation from two technical replicates, each containing a combination of three independent replicates.

		Roots	Shoots
line	condition	% vs WT ev	% vs WT ev
Col-0	0,150 mM	107,3177519	164,205
Wtev	0,150 mM	100,00	100,00
#5	0,150 mM	42,98	71,53
#8	0,150 mM	152,56	119,66
#10	0,150 mM	51,01	36,05
Col-0	1mM	86,29	140,022
Wtev	1mM	100,00	100,00
#5	1mM	19,55	19,73
#8	1mM	39,47	111,02
#10	1mM	30,05	12,98
Col-0	35 mM	62,34	101,217
Wtev	35 mM	100,00	100,00
#5	35 mM	49,01	40,09
#8	35 mM	52,49	77,74
#10	35 mM	67,41	33,80

Table 3.1. *GDH3* transcript level by real time RT PCR. Values represent the percentage of mRNA accumulation in RNAi lines compared to WTev. Line #8 (0,150mM root and shoot) and #8 (1mM, shoot) gave strange result due the bad quality of the RNA sample (red colorured). In general there was a decrease in *GDH3* transcript in the transgenic lines compared to wild type with the empty vector.

3.6.2.3 Sugar determination in *GDH3*RNAi plants

Three transgenic plants with decreased *GDH3* expression were analysed and compared to wild type. In general, the sugar content in root tissue was higher than in leaves of the plants, except for starch that was not detected in root material. Increasing nitrogen in the growth medium led to a decrease in the endogenous sugar level of the plants. This may be because the assimilation of nitrate requires carbon skeletons in form of organic acids normally derived from the carbohydrates synthesis. Contrarily, seedlings grown under low nitrate (0,150mM KNO_3) growth conditions resulted in elevated sugar level suggesting a restricted use of carbon resources. Results from the sugar measurement in roots and leaves are presented in figure 2 from the Appendix. The sugars determination did not reveal significant differences among the mutants and the wild type.

Moreover, the organic acid α-ketoglutarate was measured in the plants in order to see if the decreased of *GDH3* expression had any effect in α-ketoglutarate content. The results showed no significant differences between the transgenic plants and the control wild type (see figure 2 from the Appendix).

3.6.2.4 Protein content

Protein content of the selected plants showed that the *GDH3*RNAi transgenic plants contained around 0.4 fold less amount of total proteins than wild type at 35mM nitrate condition in root

and shoot tissues, but no change in lower nitrate. Figure 44 depicts total protein content in roots and leaves tissues of the three transgenic plants and compared to wild type.

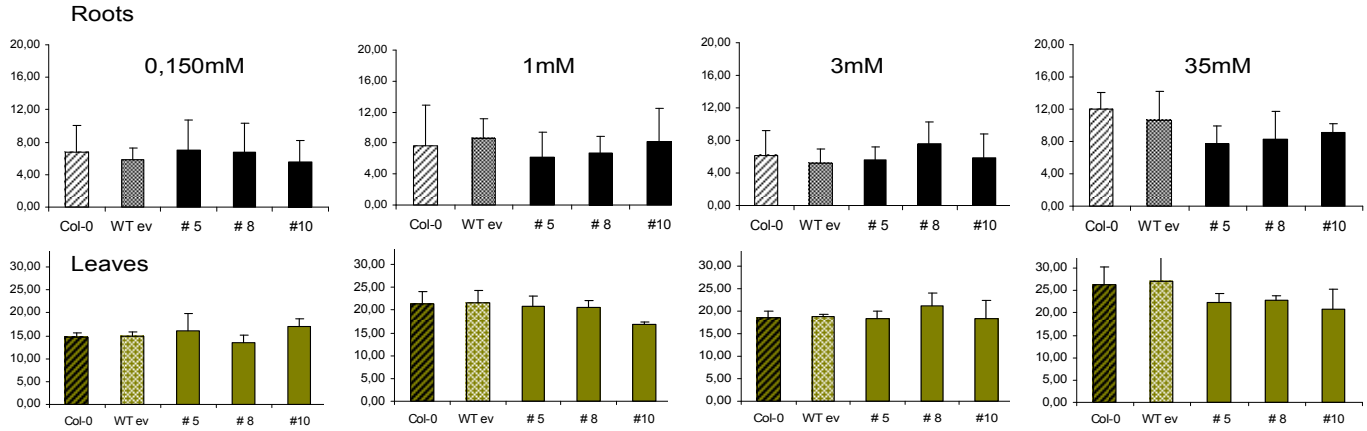

Figure 44. Protein content in roots and shoots of plants with decreased *GDH3* and compared to wild type (Col-0 and WT with the empty vector). Plants were grown and harvested as described in figure 42. Values are given in mg_g FW.

3.6.2.5 Total and individual amino acids

Total and individual amino acids were determined in the plants and compared to the control wild type. Results are depicted in Figures 45, 46 and 47.

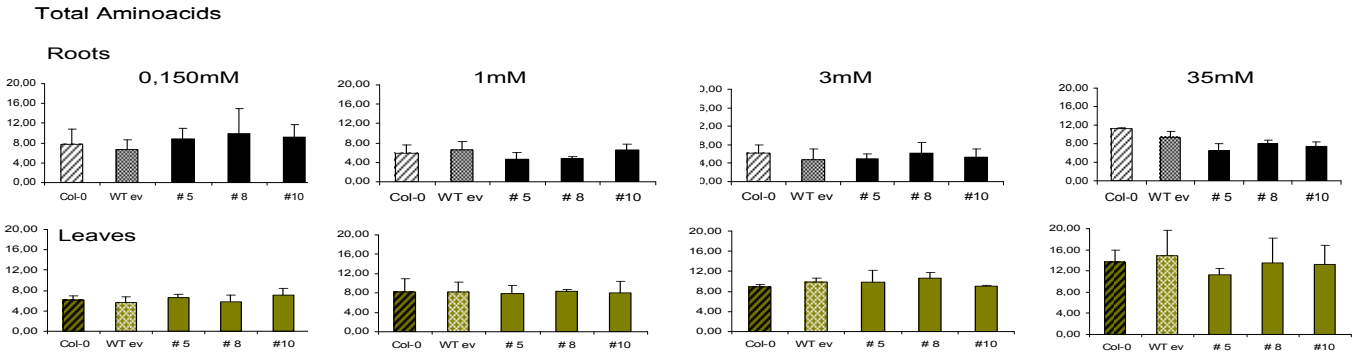

Figure 45. Total amino acids in roots and shoots of plants with decreased *GDH3* and compared to wild type (Col-0 and WT with the empty vector). Plants were grown and harvested as described in figure 42. Values are given in mg_g FW.

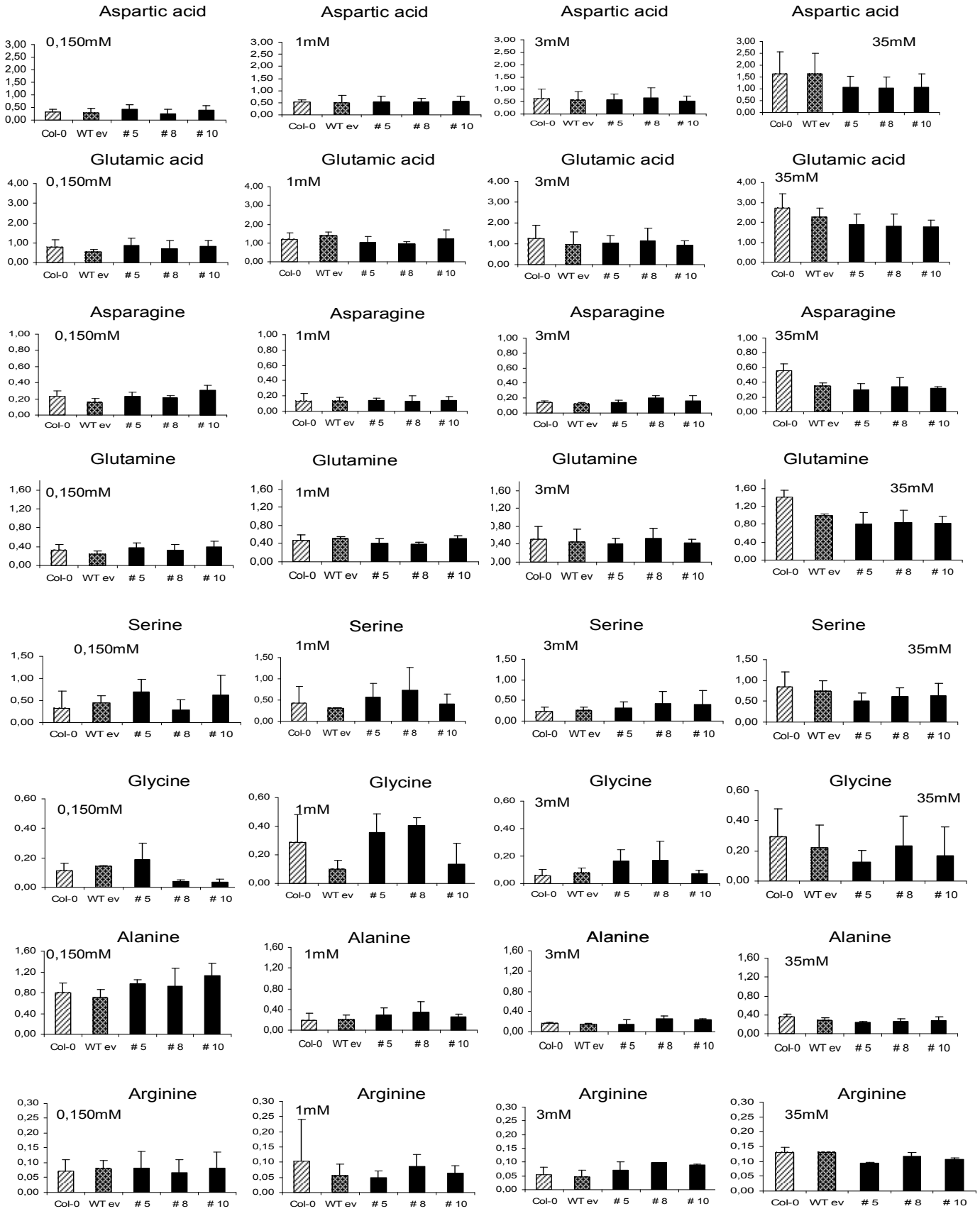

Figure 46. Individual amino acids in roots of plants with decreased *GDH3* and compared to wild type (Col-0 and WT with the empty vector). Plants were grown and harvested as in figure 42. Major amino acids (Asp, Glu, Asn, Gln, and Ser) and other interesting minor amino acids (Gly, Ala, Arg) were determined by HPLC in root tissue under different concentrations of nitrate.

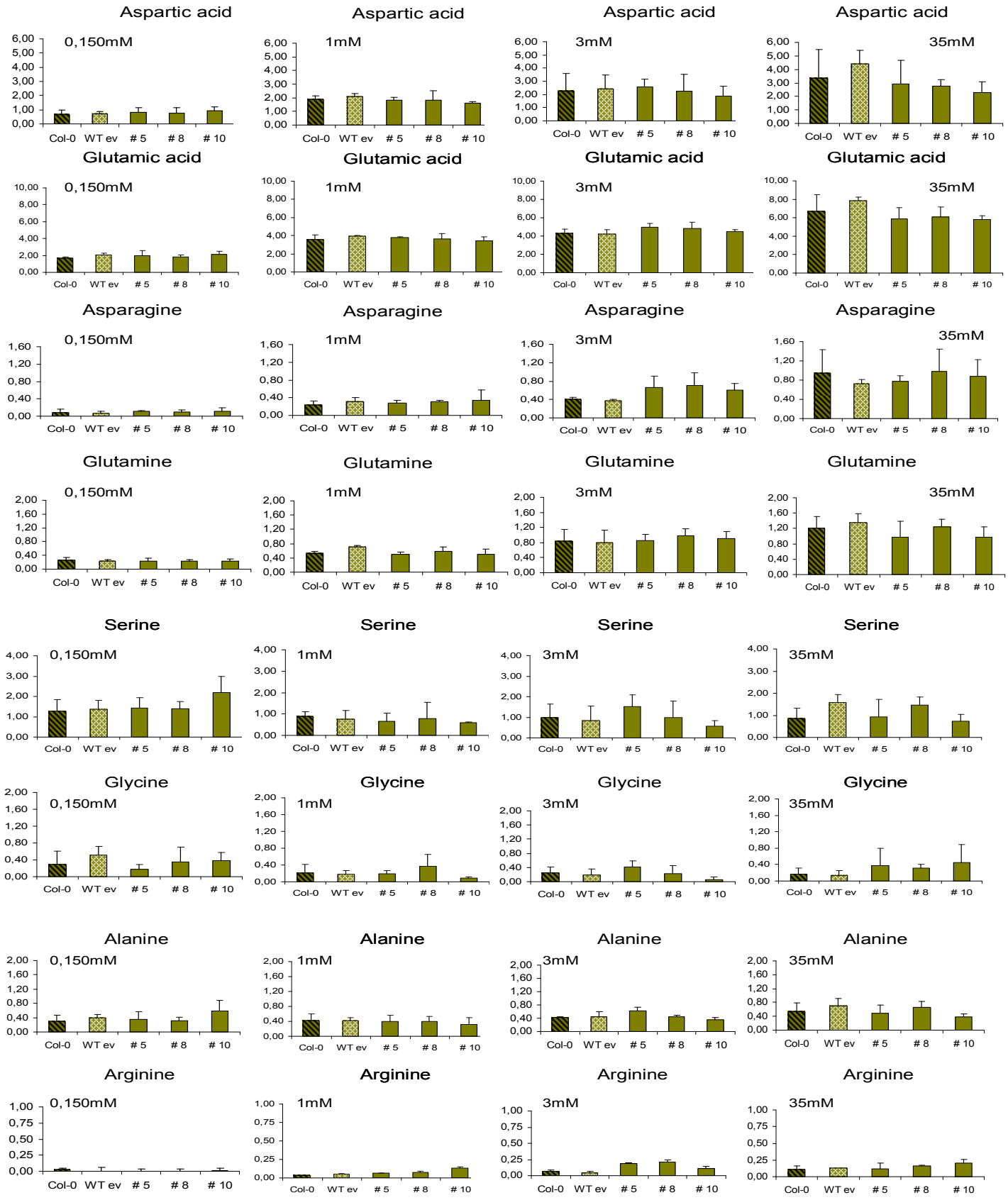

Figure 47. Individual amino acids in roots of plants with decreased *GDH3* and compared to wild type (Col-0 and WT with the empty vector). Plants were grown and harvested as in figure 42. Major amino acids (Asp, Glu, Asn, Gln, and Ser) and other interesting minor amino acids (Gly, Ala, Arg) were determined by HPLC in shoot tissue under different concentrations of nitrate.

The amino acids data revealed that the total content of amino acids was reduced in *GDH3*RNAi plants compared to wild type under conditions of high nitrate (35mM). This is in part due to the reduced amount of the major amino acids aspartic acid, glutamate, asparagine and glutamine, although results were more evident in root tissue (stronger *GDH3* expression). Looking at figure 44 (proteins) the protein level was reduced in the transgenic plants compared to wild type under 35mM nitrate conditions, confirming the amino acids data. There was a slight and non-significant trend to higher levels of several amino acids in the RNAi lines in 0,150mM, especially in lines 5 and 10, where *GDH3* transcript was decreased. All together these results were at least contradictory because the highest *GDH3* expression was found in root tissue under nitrate starvation, which would instead indicate that GDH3 plays a more important role in limiting nitrogen.

3.6.2.6. Phenotypic analyses of *GDH3* RNAi plants

The objective was to study the effect of nitrogen availability on growth and development of *GDH3* RNAi plants and compare to wild type *Arabidopsis* seedlings. Therefore, plants were observed under different concentrations of nitrate and compared to wild type (figure 48, panels A, B, C and D).

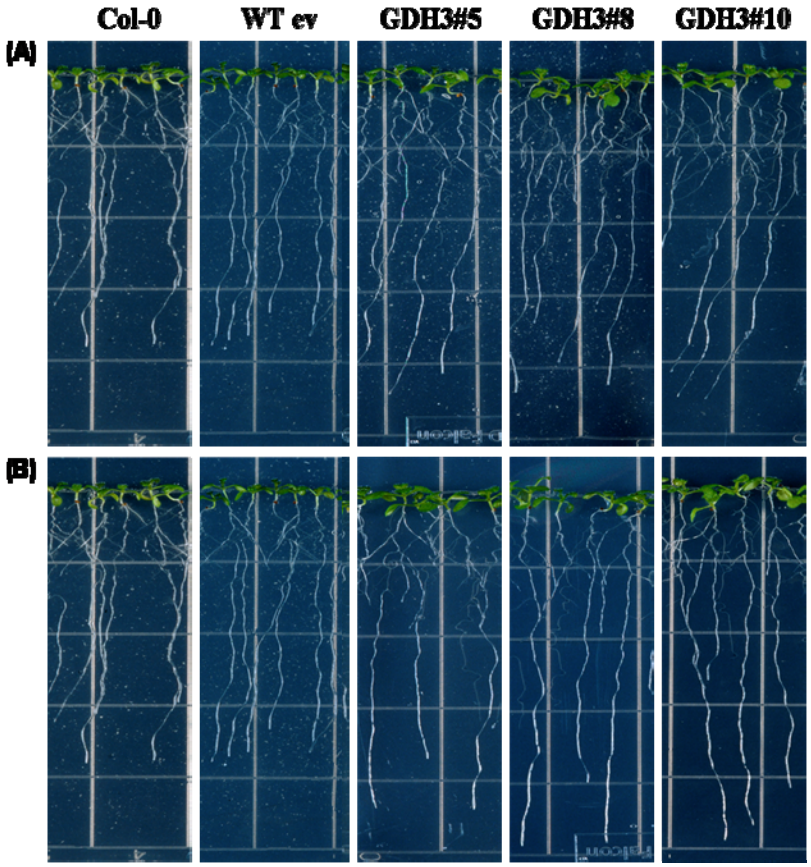

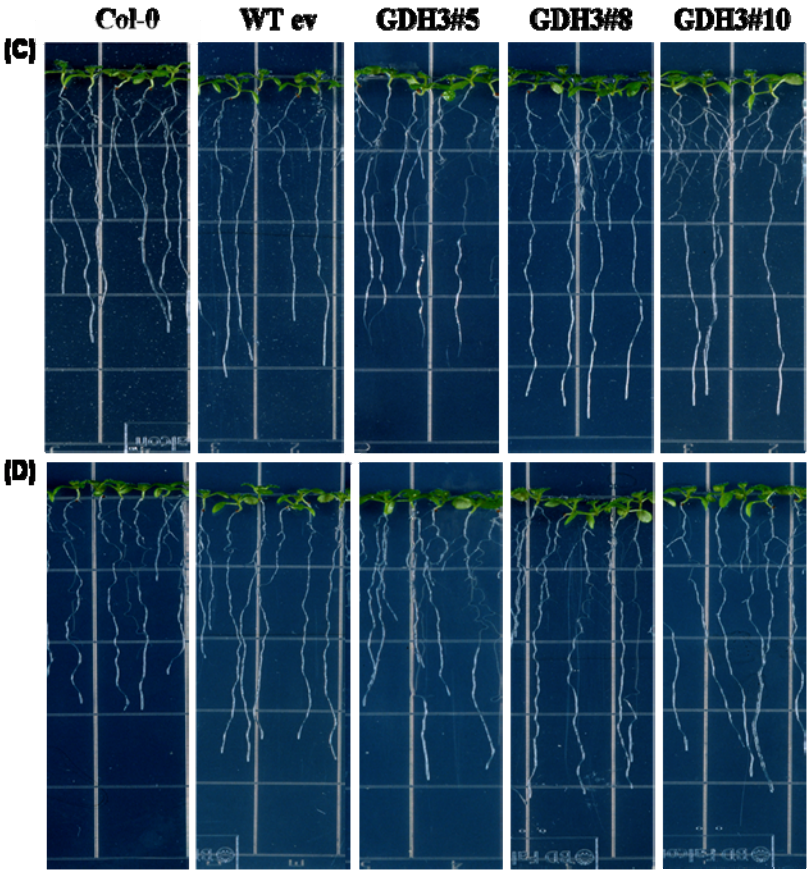

Figure 48. Phenotypes of *Arabidopsis* plants grown for 14 days on media containing different concentrations of nitrogen. Col-0 and wild type transformed with an empty vector (WT ev) were grown in vertical agar plates and compared to transgenic plants with decreased *GDH3* expression (lines #5, #8, #10). (A) 0,150mM, (B) 1mM, (C) 3mM and (D) 35mM, concentrations of KNO3 with 0.5% sucrose. The photoperiod used consisted on 12h day/night. Decreasing nitrate in the medium led to a reduction in cotyledon size and to an improved root growth with an increase in the number of lateral roots. Nitrogen replete seedlings (panel D) showed a reduced root/shoot ratio and decreased production of lateral roots in the different phenotypes. In general, transformed plants showed an improved root growth when compared to wild type in all the conditions tested.

A plant's ability to explore the medium and compete effectively for resources is critically dependent on the architecture of the root system and is believed to be important in determining the ability to compete for limiting resources. For example, withdrawal of nitrogen from the growing medium caused an increase in the root growth and a proliferation of lateral roots in order to forage for nitrogen containing compounds in the nitrogen deplete medium. On the other hand, well replete nitrogen plants showed a decreased root/shoot ratio (panel D) and decreased production of lateral roots usually associated with reduced allocation of resource to root growth. Surprisingly, generally the transformed plants with decreased *GDH3* expression displayed an improved root growth compared to both wild types, especially under limited nitrogen conditions (figure 48, panels A and B).

Decreasing nitrogen in the growth medium also influenced in the fresh weight of the seedlings (figure 49).

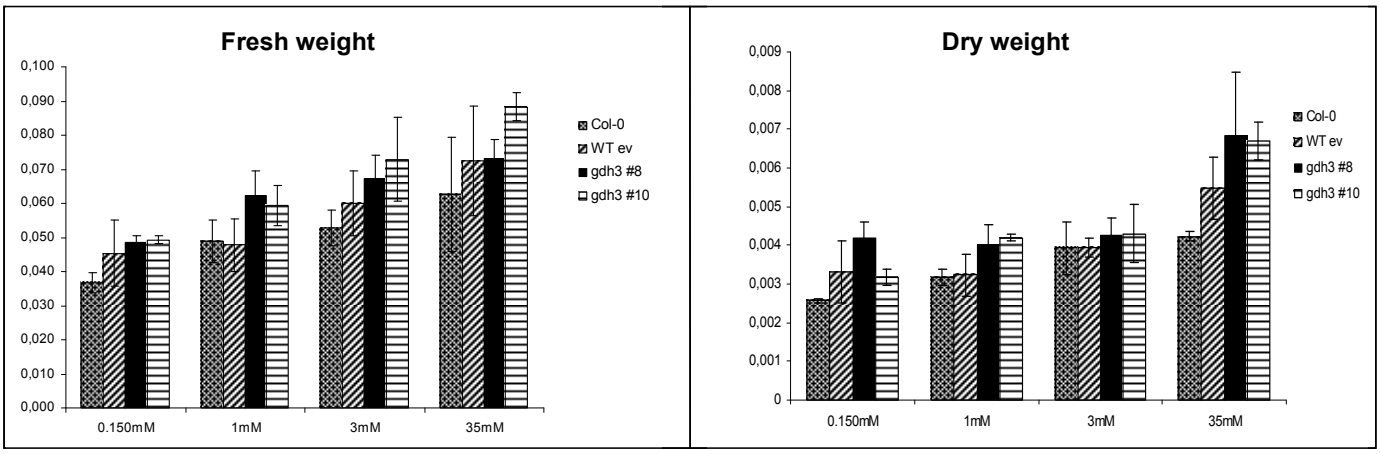

Figure 49. Fresh weight and dry weight of seedlings grown for 14 days in the presence of various nitrogen concentrations (0,150mM, 1mM 3mM and 35mM) and constant 0.5% sucrose. Dry weight was measured in plants dried after two days at 65º. Each bars represents the average fresh or dry weight of wild type and two transformed plants. The average fresh or dry weight was estimated in three independent experiments using batches of 10 seedlings in each experiment. Error bars show the SD of the average over the three independent experiments. Values are given in g_FW and g-DW.

As expected, fresh and dry weight increased in concordance with the increase of the nitrate amount in the growth medium. Moreover, transgenic plants with lower *GDH3* expression showed a slightly increase in weight confirming their improved growth compared to wild type. Taken together, reduction of *GDH3* expression in *Arabidopsis* plants led to a decrease of the amino acids level in roots and shoots and as a consequence to a decrease in the protein content, under replete nitrate conditions but did not alter the sugars and α-ketoglutarate pools. All this data indicate that *GDH3* could be involved in ammonia assimilation and amino acids synthesis rather than in catabolism especially under situations of high nitrate in the medium. Moreover, the transformed *GDH3*RNAi plants displayed significantly enhanced root growth and fresh weight compared to wild type. A causal link between the observed changes in nitrogen-related metabolites and the phenotypic alterations is not immediately evident. Other factors involved in plant development for example, hormones concentrations are needed to better understand the effect caused in root growth under nitrate starvation by the reduction of *GDH3* expression. However, since the decrease on transcripts is not large, the simple explanation is that the RNAi did not sufficiently decrease GDH activity and the effect on seedlings growth is an artefact caused by the RNAi.

CHAPTER 4 RESULTS FLOWERING PROJECT

4. CHAPTER: RESULTS FLOWERING PROJECT

4.1 Nitrate affects the transition to flowering time.

Nutrient availability has a strong influence on the promotion of flowering. Studies from Stitt (1999) showed that there is a marked delay in flowering time when nitrate is supplied to the medium growth. This suggests the importance of nitrate as a putative signal molecule regulating an essential process in plants suchlike the transition to flowering.

Previous analyses done by Dr. Irene Loef showed the influence of nitrate in the light dependent and autonomous pathways. Moreover, results from her work demonstrated that the impact of nitrate was due to the nitrogen concentration in the medium and not to changes in other metabolites.

Despite the possible role of nitrate in flowering time, it has not yet been subjected to molecular and genetic analyses. In the present work we will try to elucidate more about the influence of nitrate in the transition to flowering in *Arabidopsis thaliana*. The main tasks of this project were to investigate if the GA pathway is involved in the transition to flowering promoted by nitrate. Also, to study if nitrate interacts downstream with components of the light signalling pathway and to further investigate the interaction of nitrate with the floral repressor *FLC*. Additionally, the use of Affymetrix arrays was focused on the identification of any gene that could be involved in the induction of flowering promoted by the nitrate signal.

4.2. Previous analyses showed that high nitrate delays flowering in short days and low nitrate promotes flowering at an earlier physiological age (results from the work of Dr. Irene Loef).

4.2.1. High nitrate delays flowering in short days.

Arabidopsis thaliana cv *Columbia* plants were grown in horizontal agar plates under different nitrate concentrations (1mM KNO_3, 10mM KNO_3 and 35mM KNO_3) plus 4mM glutamine (see composition of growth medium in section 2.1.7.2) and under different regime of light: long day (16h light/8h dark), neutral day (12h light/12h dark) and short day conditions (8h light/16h dark). Glutamine was used as a constitutive nitrogen source to support the rapid growth and to avoid changes in the rate of plant growth. These results were obtained from the thesis of Dr. Irene Loef.

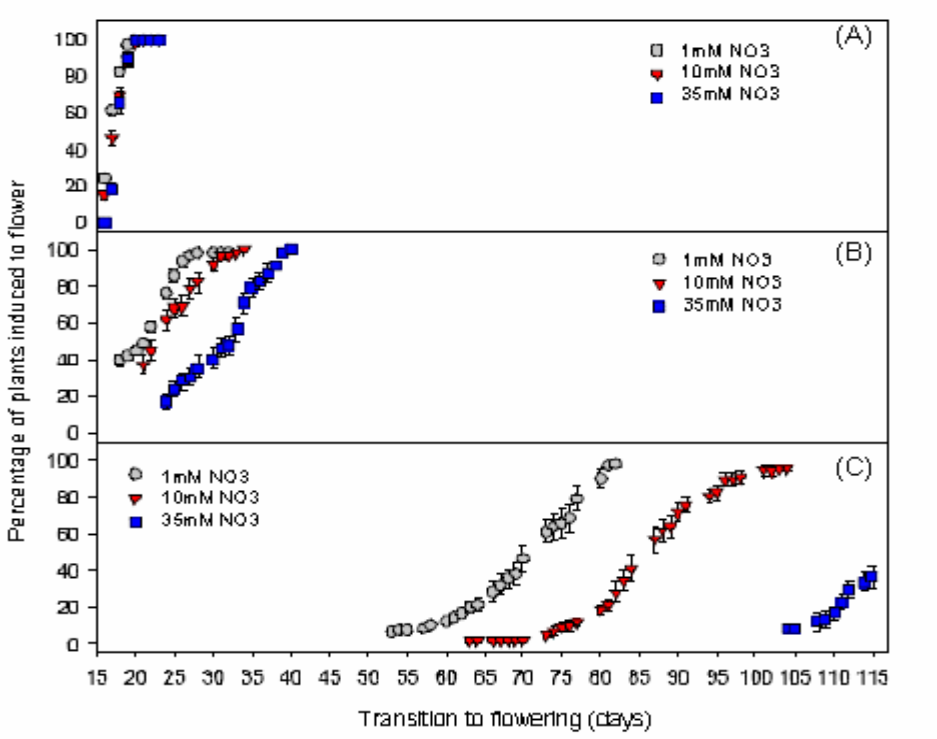

Figure 50. Transition to flowering in *Arabidopsis thaliana* cv Columbia under different nitrate concentrations and different photoperiods. (A) Long day conditions (16h light/8h dark), (B) normal day (12h light/12h dark) and (C) short day (8h light/16h dark). Temperature used was of 20º C day/night. Results obtained form the work of Dr. Irene Loef.

It is already known that *Arabidopsis thaliana* is a facultative long-day plant that is, it flowers vigorously under long day conditions.

As we can see in figure 50-A, under long day conditions, all the plants flowered at the same time showing no effect by the different nitrate concentration in the media. Under these conditions, plants are induced to flower due the up regulation of *CO* gene involved in the promotion of flowering under long day conditions (see introduction).

In a neutral day of 12h light, the transition to flowering is weakened and plants started to show differences in flowering time in response to the external nitrate concentration. Plants grown under high amount of nitrate displayed a slight delay in flowering compared to plants grown under 1mM and 10mM nitrate (figure 50-B). In short day conditions (8 h light), high nitrate led to a strong delay of flowering compared to those grown in low nitrate (figure 50-C).

4.2.2 Low nitrate promotes flowering at an earlier physiological age.

Plants were grown as explained in section 4.2.1. Leaf number and shoot/root ratio were determined at the time of the floral initiation (see figures 51 and 52).

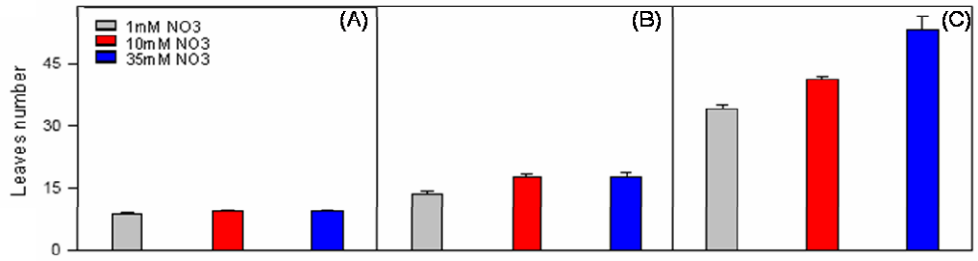

Figure 51. Leaf number of plants at the time of floral initiation in *Arabidopsis thaliana* cv Columbia. (A) Long day conditions (16h light/8h dark), (B) normal day (12h light/12h dark) and (C) short day (8h light/16h dark). Temperature used was of 20º C day/night. (A) All the plants flowered at 22 days. (B) Under 1mM nitrate plants flowered at 27 days, under 10mM at 33 days and under 35mM after 37 days. (C) Plants grown under 1mM nitrate flowered after 75 days old, under 10mM at 82 days and under 35mM flowered after 116 days. The light intensity was of 100 μEs^{-1} m^{-2} light. Vertical bars represent the average and standard deviation (n=10-15). Results obtained form the work of Dr. Irene Loef.

In long day conditions, all plants flowered with similar number of leaves in response to varied concentrations of nitrate (see figure 51-A). In a normal photoperiod, there was a slight difference between 1mM and 10mM but no difference between 10mM and 35mM (see figure 51-B). In short day conditions, plants grown in high nitrate showed an increase in leaf number at flowering (see figure 51-C). These results showed that in short days, high nitrate delays flowering in time that it is related to an increase in leaf number and to an increase in plant size (see figure 52). The increase in the leaf number and shoot/root ratio was a result of an enlarged vegetative phase and later physiological age of the plants caused by the nitrate concentration in the medium. Shoot/root ratio was determined in plants grown under different photoperiods and varied nitrate concentrations (see figure 52). Similar results were seen in *Arabidopsis thaliana* cv Landsberg (data not shown).

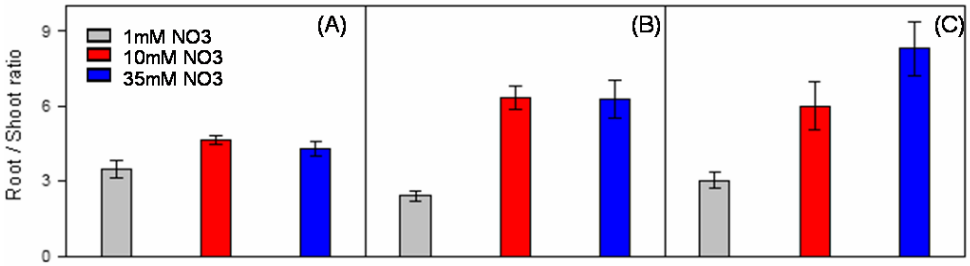

Figure 52. Shoot/Root ratio of plants at flowering time. Plants were grown under the same conditions as in figure 51.

4.2.3 Metabolites in plants growing under different nitrate concentrations.

Nitrate, total amino acids, soluble sugars, and starch content among others, were measured by Dr. Loef in 20mg fresh weight of roots and shoots of *Arabidopsis* plants grown under different photoperiods in response to different concentrations of nitrate in the medium (conditions described before). These measurements were carried out in order to check that the inclusion of glutamine in the medium indeed prevented nitrogen deficiency in those plants grown under low nitrogen conditions.

Higher external nitrate led to a higher nitrate content in the plants. In addition, the changes in nitrate content were independent from the daylength. Results are presented in figure 4 from the Appendix. By contrast, the level of total amino acids did not change with the external nitrate, but dropped with the shortening duration of light (see figure 4, section 7.13 from the Appendix).

The level of soluble sugars and starch decreased with the increase in nitrogen concentration, especially under long and neutral photoperiods (figure5 and 6, section 7.14 from the Appendix).

All together, the analysis of metabolites indicated that the effect of nitrate in flowering time was not related to changes in the level of key metabolites such as amino acids or sugars in the plant.

4.3 Characterization of flowering time mutants and transformed plants under different nitrate concentrations.

The transition to flowering time was analysed in different mutants and transgenic plants impaired in flowering signalling pathways. The objective was to study the influence of varied nitrate concentrations in the promotion of flowering in the cited plants compared to wild type. A collection of mutants and transgenic plants with altered expression in flowering time genes provided by Coupland's group (MPIZ, Cologne) is shown in table 4.1.

The photoperiod used was of 12h light/12h dark as a standard condition in order to avoid the prolonged time for flowering during the course of the experiment and because under these conditions there is still a detectable effect of nitrate. Moreover, in response to 12h light cycle it is possible to get flowering in mutants like the GA defective mutants (see section 1.8.2.4 of the introduction). In addition, the 12h light cycle was used to prevent dryness of the agar media in old plates (previously observed under short day conditions).

mutant	Description. Flowering signalling pathway affected
fca	Mutant in Autonomous pathway
fy	Mutant in Autonomous pathway
fve-1	Mutant in Autonomous pathway.
fd-1	Mutant in Photoperiod pathway
fwa	Mutant in Photoperiod pathway.
co2tt4	Mutant in CONSTANS, photoperiod pathway
35S::CO	Overexpression of CONSTANS, photoperiod pathway
gai	Mutant in Gibberellins pathway
ga1-3	Mutant in Gibberellins pathway
35S::FLC	Overexpression of the floral repressor FLOWERING LOCUS C
soc1-1	Mutant in a floral integrator gene.
ft-7	Mutant in a floral integrator gene.
soc1-1-ft-7	Double mutant.
fca-co2-ga1-3	Triple mutant. Impaired the three major flowering pathways
Laer	Wild type. Genotype background of the mutants.

Table 4.1. Collection of mutants and transgenic plants with impaired flowering signalling pathways. Flowering mutants were obtained from Nottingham Arabidopsis Stock Centre England or Ohio Stock Centre, (USA) and transgenic plants provided by Coupland's group (MPIZ, Cologne). L*aer* ecotype was used as genetic background of the mutants and transgenic plants.

Some of the mutants listed in the table above (table 4.1) were already characterized by Dr. Irene Loef. Plants were grown under different concentration of nitrate in a 12h light period and the time to flowering was scored.

Results from Irene's work showed that in *fwa-1* and *fd-1*, *fve-1* and *fy*, mutants affected in the photoperiod and autonomous pathways respectively, the response to nitrate was retained in all the mutants compared to wild type, that is, the flowering curves of the mutants displayed a delay in response to different nitrate conditions. Moreover, the lateness was prolonged in parallel to the increase of external nitrate in the growth medium (figure 53).

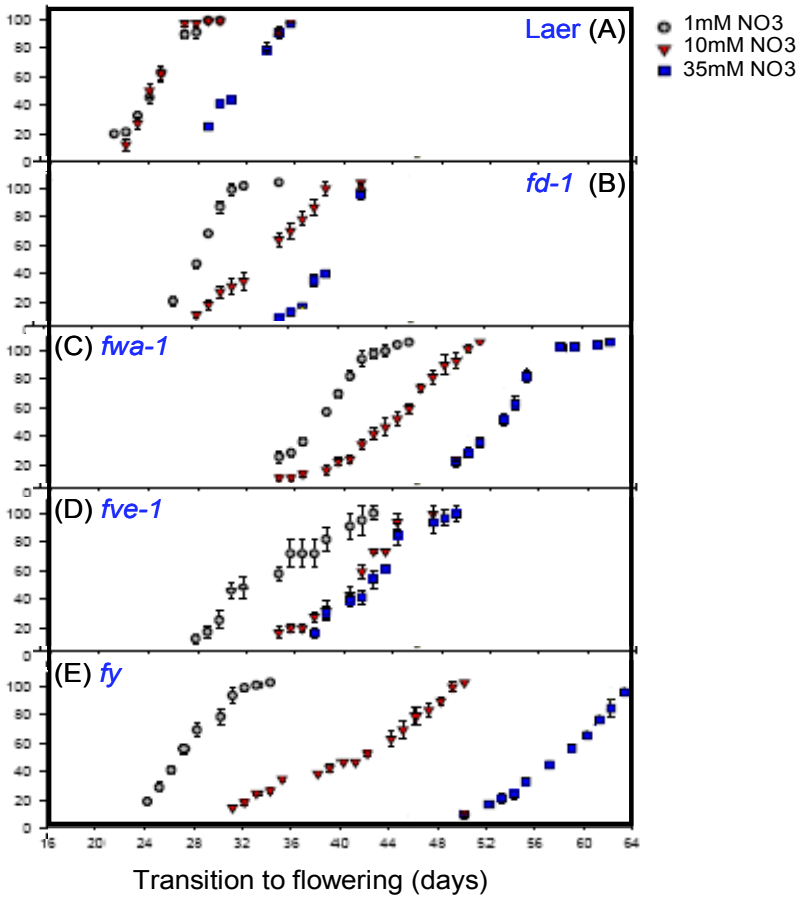

Figure 53. Percentage of plants induced to flower under different nitrate concentrations in different mutants impaired in flowering pathways. (A) L*aer*, wild type plant; (B) *fd-1*, mutant impaired in photoperiod pathway; (C) *fwa-1*, mutant impaired in photoperiod pathway; (D) *fve-1*, mutant impaired in the autonomous pathway; (E) *fy*, mutant impaired in the autonomous pathway. The temperature used was 20º C day/night and 12h of light period. Values represent the percentage of plants at the floral initiation point. L*aer* ecotype was the genetic background in all the mutants and transgenic plants.

As we can see in figure 53, the late flowering mutations in *FD, FWA, FVE* and *FY* did not prevent the early flowering under low nitrate as well as the delay caused by high nitrate. Indeed, in *fy* mutant, the impact of nitrate became more marked. The effect of nitrate was overridden in long days (as mentioned before).

Three important questions rose from this part:

a) Does nitrate interact further downstream than the mutants used by Dr. Loef in the photoperiod pathway?

b) Does nitrate interact downstream of the vernalization pathway?

c) Does nitrate interact via the gibberellin pathway?

In order to answer these questions, the flowering time of mutants impaired in photoperiod, vernalization and gibberellin pathways were studied in response to different concentrations of nitrate.

4.3.1. Light –dependent pathway (photoperiod pathway)

The photoperiod pathway promotes flowering in response to long days. *CO* gene promotes flowering under long day conditions (see section 1.8.2.1). Mutations in *CO* delay flowering under long and neutral day conditions and the over expression of *CO* promotes flowering independently of the day length. Mutant in *CO* gene (*co2tt4*) and plants with constitutive over expression of *CO* (35S::*CO*) were analysed under different nitrate conditions in a 12h light period. Figure 54 depicts the flowering curves corresponding to *co2tt4* and *CO* over expression lines compared to L*aer,* the genetic background in which all the mutants and transformant were created.

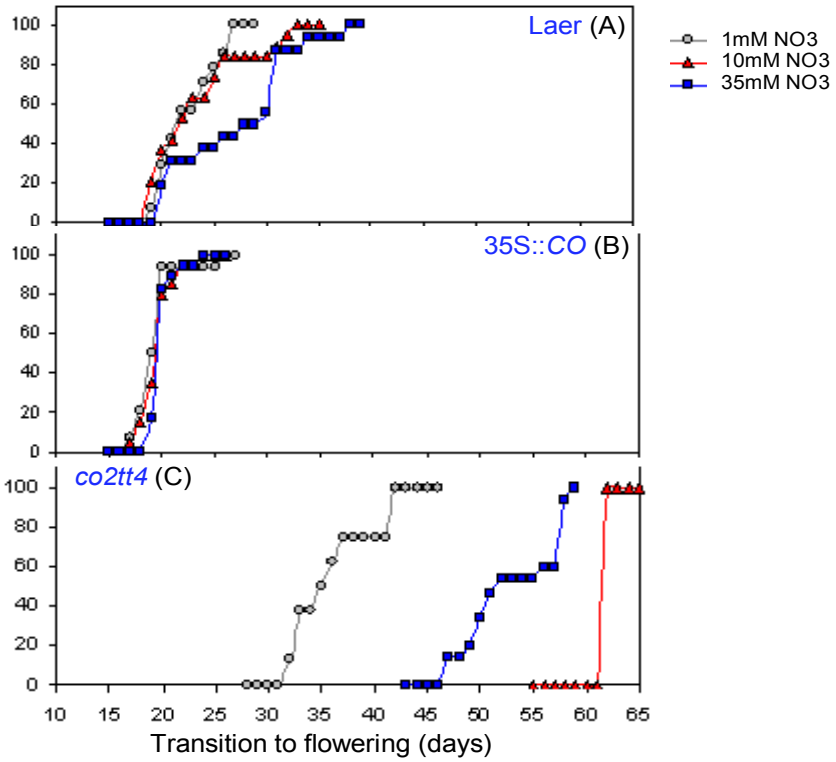

Figure 54. Flowering curves of *co2tt4* mutant and over expression of *CO* gene under different nitrate concentrations. (A) L*aer*, wild type plant (1mM, n= 14; 10mM, n= 14; 35mM, n=16); (B) 35S::*CO*, plants with constitutive over expression of *CO* (1mM, n= 14; 10mM, n= 20; 35mM, n=17); (C) *co2tt4*, mutant impaired in *CO* gene involved in photoperiod signalling pathway (1mM, n= 8; 10mM, n= 10; 35mM, n=8). L*aer* plants started to flower at 22 days after the sowing with a slight delay of around 5 days in plants grown in 35mM. All plants over expressing CO flowered at the same time, 19 days after the sowing date. 50 % of *co2tt4* plants under 1mM nitrate flowered 35 days after the sowing, around 15 days later than wild type and plants grown in 35mM nitrate flowered at 52 days and a bit later for 10mM nitrate treatment compared to wild type. The temperature used was 20º C day/night and 12h of light period. Values represent the percentage of plants at the floral initiation point. 50% of plants induced to flower were taken as reference for flowering time. L*aer* ecotype was the genetic background of the transgenic plants.

Plants over expressing *CO* displayed early flowering compared to wild type. All 35S::*CO* plants flowered around 19 days after the sowing independently of the nitrate concentration, whereas L*aer* showed a slight delay and a weak influenced by nitrate treatment (figure 54,

panels A and B). This resembles the response in long days. The over expression of *CO* overrode the nitrate response preventing the earlier flowering by low nitrate and a retardation in flowering time accounted by high nitrate. This effect was similar to that found in plants grown under long day conditions (see figure 54-A). On the other hand, the *co2tt4* mutant exhibited a dramatic delay compared to wild type (figure 54-C) and a total dependency from nitrate treatment. The response to nitrate was accentuated in the mutant in a similar manner to that seen in wild type plants grown under short day conditions (see figure 54-C). From these results we can conclude the nitrate signal acts downstream of the photoperiod-day length pathway.

4.3.2. Gibberellic acid signalling pathway.

Gibberellins are well known to regulate plant growth and promote flowering under non-inductive photoperiods (Michaels, SD & Amasino, RM, 1999). In order to see how mutants defective in the production and in the perception of GA responded to nitrate, the plants were grown under varied nitrate concentrations and the time to flower was investigated. Results are shown in figure 55.

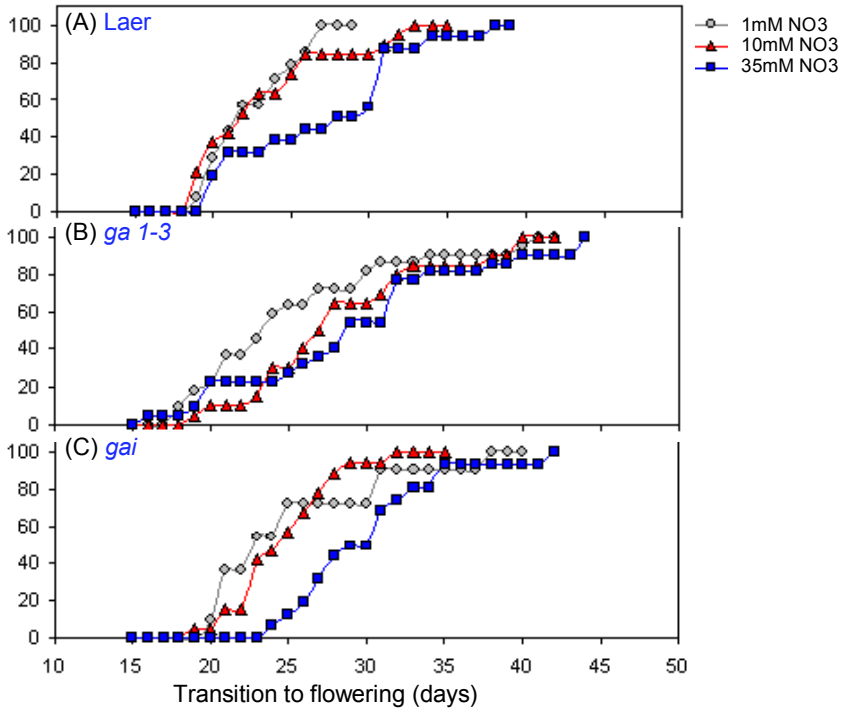

Figure 55. Flowering curves of a mutant defective in GA synthesis and mutant insensitive to GA under different nitrate concentrations. (A) L*aer,* wild type plant (1mM, n= 14; 10mM, n= 14; 35mM, n=16); (B) *ga1-3*, plants affected in the biosynthesis of GA (1mM, n= 11; 10mM, n= 19; 35mM, n=16); (C) *gai*, mutant insensitive to gibberellins (1mM, n= 11; 10mM, n= 20; 35mM, n=22) . Laer plants started to flower at 22 days after the sowing with a slight delay of around 5 days in plants grown in 35mM. Both mutants displayed delayed flowering compared to L*aer* and weak response to nitrate. The temperature used was 20º C day/night and 12h of

light period. Values represent the percentage of plants at the floral initiation point. 50% of plants induced to flower were taken as reference for flowering time.

The *Arabidopsis* mutant *ga1-3* contains a deletion in an enzyme that catalyzes an early step in the synthesis of gibberellic acid (Michaels, S.D. & Amasino, and R.M.1999a). It has been shown that *ga1-3* mutant plants cannot flower under 8-h short-day (SD) conditions, even after vernalization suggesting that it may be required for an alternate pathway that promotes flowering in non inductive photoperiods. In the 12/12h LD cycle used in these experiments, *ga1-3* displayed a slight delay in all the treatments compared to Laer. 1mM nitrate led to earlier flowering compared to 10mM and 35mM nitrate that flowered at 26 and 28 days respectively (figure 55-B).

The *gai* mutation affects GA reception or subsequent signal transduction conferring a reduction in gibberellin (GA) responsiveness. Genetic analysis indicates that *GAI* it is involved in a signalling pathway that regulates GA responses negatively (Peng, J., *et al*., 1997). The mutant, *gai*, displayed similar pattern of response than *ga 1-3* mutant, with a light shift in 35mM nitrate condition. There were no significant differences between 1mM and 10mM nitrate but plants grown in 35mM showed a slight displaced flowering curve (figure 55-C), which resembles the response in the wild type *Laer*.

From these results we can conclude that there is still a response to nitrate in the GA defective and insensitive GA mutants. Therefore nitrate signal must operate downstream of the GA signalling pathway.

4.3.3. Low nitrate still induces flowering in the triple mutant *fca co2 ga1-3*.

Three genetic pathways promote flowering of *Arabidopsis* under long photoperiods. These pathways are represented by the genes *CO*, *FCA*, and *GA1*, which act in the long-day, autonomous, and gibberellin pathways, respectively. The triple mutant *fca1co2ga1-3* was constructed and obtained from George Coupland´group (MPIZ, Cologne). These plants never flowered under long- or short-day conditions, indicating that the three pathways impaired by these mutations are absolutely required for flowering under these conditions (Reeves, RH & Coupland, G., 2001). The vegetative phenotype of the triple mutant could be overcome by vernalization, suggesting that a fourth pathway promoted flowering under these conditions. In order to see how the triple mutant responded to nitrate, the plants were grown under different nitrate concentrations and the flowering time was investigated. Results showed that low nitrate is able to induce flowering even when the major flowering pathways are blocked, whereas high

nitrate prevents it at least 90 days. The impact of nitrate was much stronger in the triple mutant than in the wild type L*aer*.

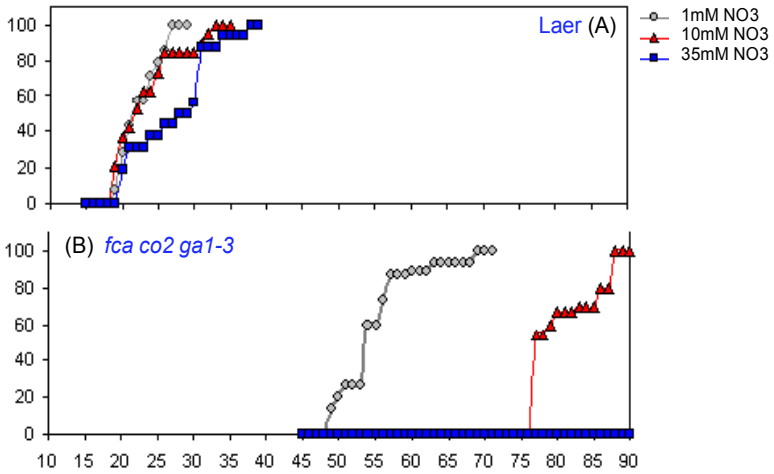

Figure 56. Flowering curves of the triple mutant mutant *fca co2 ga1-3* and Laer under different nitrate concentrations. (A) Laer, wild type plant (1mM, n= 14; 10mM, n= 14; 35mM, n=16); (B) *fca co2 ga1-3*, triple mutant impaired in the major flowering signalling pathways (1mM, n= 15; 10mM, n= 15; 35mM, n=12). The triple mutant *co-2 fca-1 ga1-3* never flowered under long- or short-day conditions, indicating that the three pathways impaired by these mutations are absolutely required for flowering under these conditions (Reeves, RH & Coupland, G. 2001). The triple mutant displayed a strong delay in flowering under 1mM and 10mM nitrate. No plants flowered under high nitrate concentration. The temperature used was 20º C day/night and 12h of light period. Values represent the percentage of plants at the floral initiation point. 50% of plants induced to flower were taken as reference for flowering time. The experiment was repeated three times obtaining similar results.

4.3.4. Over expression of *FLC*

Flowering locus C (*FLC*) encodes a MADS-Box transcription factor expressed predominantly in shoot and root apices and vascular tissue. It plays an important role in the transition to flowering because it inhibits genes required to switch the meristem from vegetative to floral development (see section 1.8.2.2). Thus, as to see the response to nitrate, plants constitutively over expressing the floral repressor were tested in different nitrate conditions and compared to Laer.

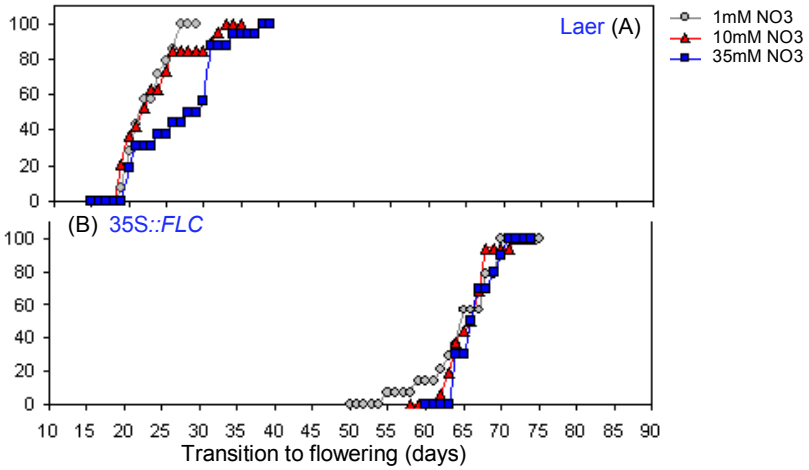

Figure 57. Transition to flowering in Laer and 35S::*FLC* under different nitrate concentrations. (A) Laer, wild type plant (1mM, n= 14; 10mM, n= 14; 35mM, n=16); (B) 35S*::FLC*, plants over expressing FLC (1mM, n= 14; 10mM, n= 16; 35mM, n=13). 35S::*FLC* plants showed a strong delay in flowering time due to the over expression of the floral repressor FLC. Compared to Laer there is a retardation of around 42-45 days for all the nitrate treatments. The temperature used was 20º C day/night and 12h of light period. Values represent the percentage of plants at the floral initiation point. 50% of plants induced to flower were taken as reference for flowering time. The experiment was repeated three times obtaining similar results.

Looking at figure 57 we can observe the strong delay in flowering time due the over expression of the floral repressor FLC. The flowering curves of the transformant are shifted around 42-45 days later compared to wild type. Strikingly, there were no differences between the nitrate concentrations. These results suggest that the constitutive over expression of *FLC* partly suppress the effect caused by nitrate, and hence nitrate signal must enter downstream of *FLC*.

4.3.5. Downstream of *CO* and *FLC*: floral integrators *FT* and *SOC1*.

SUPRESSOR OF OVER EXPRESSION OF CONSTANS 1 (*SOC1*) and FLOWERING LOCUS T (*FT*) are termed as "floral pathway integrators" because they integrate signals from the main pathways that control flowering. Both are controlled negatively by FLC but positively by CONSTANS and by signals from the GA pathway. They promote the transition to flowering by the activation of the "floral meristem identity genes" which convert the vegetative meristem to a floral fate. The response to nitrate was investigated in *soc1-1*, *ft-7* and double mutant *soc1 ft-7*.

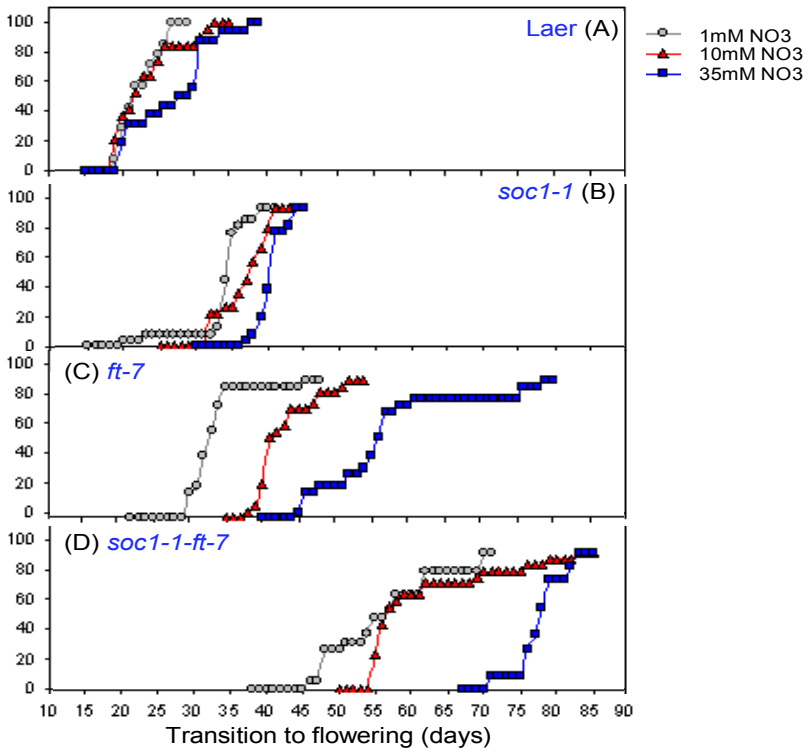

Figure 58. Transition to flowering in *soc1-1* and *ft-7* mutants under different nitrate concentrations. (A) Laer, wild type plant (1mM, n= 14; 10mM, n= 14; 35mM, n=16); (B) *soc1-1*, mutant plants in SOC1-1 (1mM, n= 23; 10mM, n= 12; 35mM, n=12). (C) *ft-7*, mutant plants in FT (1mM, n= 16; 10mM, n= 21; 35mM, n=22). (D) *soc1-1 ft-7*, double mutant in flowering pathway integrators (1mM, n= 17; 10mM, n= 15; 35mM, n=10). The three mutants displayed delayed flowering compared to Laer. *soc1-1* showed shifted flowering curves compared to Laer and weak differences among the different nitrate conditions. *ft-7* mutants displayed delayed flowering compared to Laer with marked differences between the nitrate concentrations, showing a strong delay in flowering time by high nitrate. The double mutant exhibited the most striking influences by nitrate showing earlier flowering in 1mM and 10mM and a delay due the high nitrate. The temperature used was 20º C day/night and 12h of light period. Values represent the percentage of plants at the floral initiation point. 50% of plants induced to flower were taken as reference for flowering time. The experiment was repeated three independent times obtaining similar results.

The transition to flowering was delayed in *soc1-1*, in *ft-7* and in the double mutant *soc1-1 ft-7* (see figure 58) and in general flowering was accelerated in exposure to low nitrate. The response to nitrate was more accentuated in *ft-7* mutant than in *soc1-1*. Results from this part concluded that the nitrate signal is entering downstream or independently of *SOC1* and *FT*, promoting flowering when plants are grown in low nitrate and delaying under high concentration of nitrate.

A general overview of flowering responses from all flowering mutants used during this work can be seen in figure 15 of the appendix.

4.4. Stress and flowering: does stress promote flowering?

An important question rose suggesting the possibility that flowering is promoted in the triple mutant *fcaco2ga1-3* as a response to a stress situation.

In order to gain more insights into the regulation of flowering by stress, wild type plants (Laer and Col-0) and the triple flowering mutant were subjected to various abiotic stresses and the transition of flowering time was analysed.

4.4.1. Phosphate Stress.

To study if the induction of flowering is promoted by nutritional stress, the transition to flowering time was analysed in the triple mutant *fcaco2ga1-3* under nitrate and phosphate starvation and compared to wild type. Plants were grown under 0,150mM nitrate (without supplemented glutamine) and 0.200mM phosphate in a 12h light period (for medium's composition see table 2.6 of Material and Methods). The time to flowering in the triple mutant compared to Laer is depicted in figure 59.

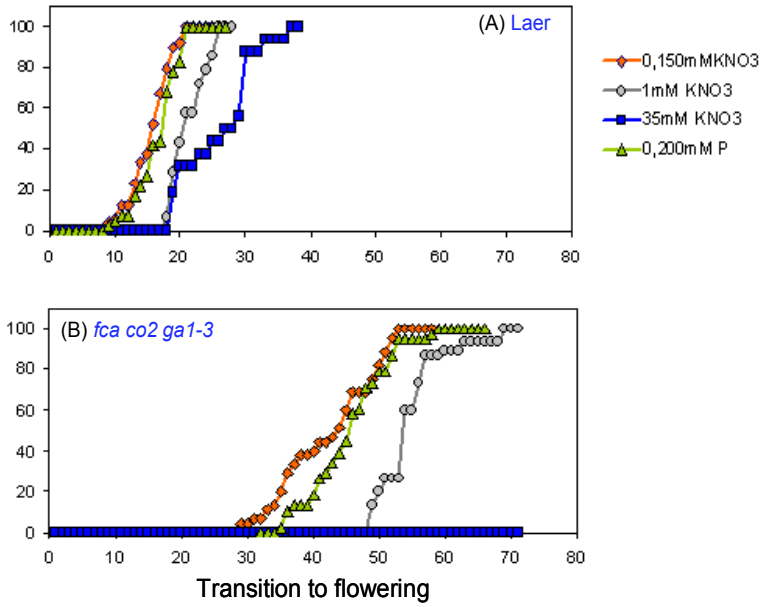

Figure 59. Flowering time of Laer and triple mutant *fca co2 ga1-3* under nitrate and phosphate starvation conditions. (A) Laer, wild type, 0.150mM KNO_3 (0.150mM KNO_3, 3mM KH_2PO_4, 0mM glutamine), n= 48; 1mM KNO_3 (1mM KNO_3, 3mM KH_2PO_4, 4mM glutamine), n= 14; 35mM KNO_3 (35mM KNO_3, 3mM KH_2PO_4, 4mM glutamine), n=22; 0.200mM KH_2PO_4 (3mM KNO_3, 0.200mM KH_2PO_4, 4mM glutamine), n= 41. (B) *fcaco2ga1-3*, triple mutant, 0.150mM KNO_3 (0.150mM KNO_3, 3mM KH_2PO_4, 0mM glutamine), n= 45; 1mM KNO_3 (1mM KNO_3, 3mM KH_2PO_4, 4mM glutamine), n= 15; 35mM KNO_3 (35mM KNO_3, 3mM KH_2PO_4, 4mM glutamine), n=14; 0.200mM KH_2PO_4 (3mM KNO_3, 0.200mM KH_2PO_4, 4mM glutamine), n= 48). All mediums were supplemented with 4mM glutamine except in the case of 0.150mM KNO_3. Results indicate that either nitrate or phosphate starvations were able to induce the transition to flowering in the triple mutant. Laer and the triple mutant showed earlier flowering in response to low nitrate or low phosphate. The triple mutant never flowered in high nitrate. The temperature used was 20º C day/night and 12h of light period. Values represent the percentage of plants at the floral initiation.

These results confirm our previous experiments in wild type Laer and in the triple mutant *fcaco2ga1-3*. As we can observe in figure 59, low nitrate led to early flowering in the wild type Laer and the effect was more marked in the triple mutant where flowering was totally suppressed in response to high nitrate. Low phosphate also induced earlier flowering in wild type Laer and in the triple mutant in a very similar manner to low nitrate. In this experiment, visual phenotypes were also documented (figure 60, panels, A-H).

In nitrate starvation medium, Laer plants were smaller and presented higher number of roots, caused by the deprivation of nitrogen in the medium (figure 60-A). Also, the triple mutant *fcaco2ga1-3* presented great root abundance in response to nitrogen deficiency (figure 60-B). Under phosphate starvation, the wild type flowered at similar time as in response to nitrogen starvation (see graph, figure 59-A) and displayed anthocyanine's accumulation in old leaves as a typical symptom of phosphate deficiency (figure 60-G). Moreover, phosphate limitation was able to promote flowering in the triple mutant. It has been suggested by some authors the cross talk between nitrate and phosphate responses. According to Wu *et al.,* (2003) Pi starvation led to coordinated changes in carbon and nitrogen metabolisms with the repression of photosynthetic genes and down regulation of primary ammonia assimilation upon phosphate starvation.

In general, the triple mutant displayed a general yellowing in older leaves compared to young leaves, indicating the beginning of senescence. Leaf senescence can be induced by developmental signals, aging or stress and its first visible symptom is chlorophyll degradation. During senescence, nutrients are mobilized and recycled from green leaves to developing seeds to prepare the next generation. Hence, from the pictures, it is evidence that plants were dramatically delayed at flowering time compared to the wild type.

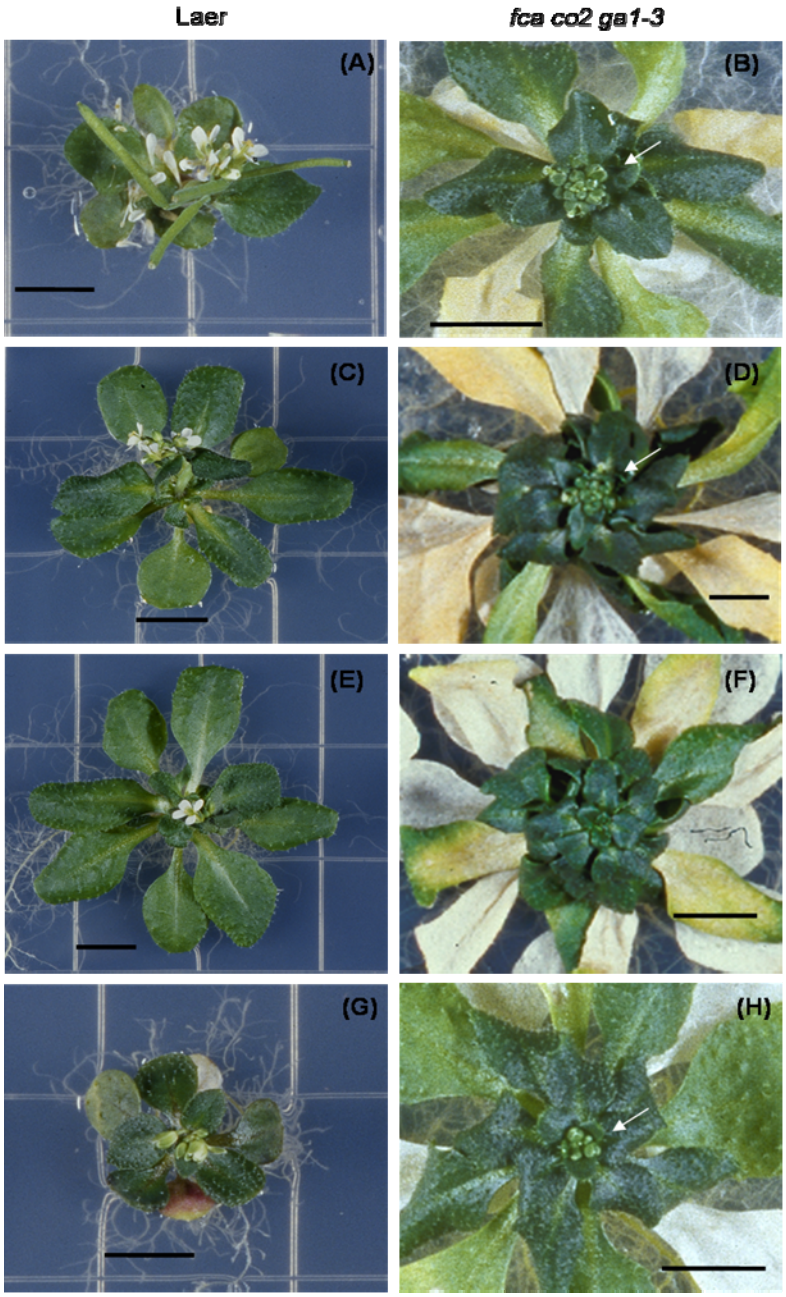

Figure 60. Pictures of La*er* and triple mutant *fcac2ga1-3* plants after flowering. La*er* is presented on the left side and the triple mutant on the right side of the figure. Plants were grown as described in figure 59. (A) to (B) La*er* and *fcaco2ga1-3* in nitrate starvation conditions (0.150mM of KNO3); (C) to (D) La*er* and *fcaco2ga1-3* under 1mM nitrate concentration; (E) to (F) represent La*er* and *fcaco2ga1-3* in high nitrate (35mM KNO_3); (G) to (H) represent La*er* and *fcaco2ga1-3* in conditions of phosphate starvation (0,200mM of KH_2PO_4). White arrow indicates the floral bud formed in the triple mutant. The temperature used was 20º C day/night and 12h of light period. Scale bars correspond to 5 mm. Photos were taken at 30 days after the sowing date in the wild type Laer and around 55 days after the sowing date in the mutant *fcaco2ga1-3*.

From this part we can conclude that not only low nitrate but also low phosphate are able to induce flowering in the triple mutant suggesting the close interaction between nitrate and phosphate metabolisms in response to a situation of nutritional stress. Phosphate and nitrogen have been proposed to share responses under starving conditions and therefore it was not

surprising the similar behaviour displayed by the triple mutant in both -N and -P limited conditions.

The transition to flowering in wild type *Arabidopsis* and in the triple mutant was therefore investigated in response to other further stresses.

4.4.2. Flowering transition in response to high light, photo-chilling, high temperature and continuous light.

Floral induction in Laer and *fcaco2ga1-3* plants was studied under different stress conditions such as high light, photo-chilling, high temperature and continuous light. Plants were sown and germinated in soil following a normal greenhouse protocol consisting on 2 weeks in cold night and high humidity to activate germination, and afterwards changed to short day conditions for a minimum of 7 days to promote post-germinative growth. After 2 weeks in short day conditions, various batches of plants were separated and transferred to different stresses for further analyses of flowering time. A batch of plants remained in short day (8h light/16h dark) or changed to neutral day (12h light/12h dark) conditions as controls.

4.4.2.1 High light stress.

Exposure of plants to irradiances far above the light saturation point of photosynthesis is known as high-light stress. This excess of light can damage the photosynthetic apparatus caused in part by reactive oxygen species (ROS) generated by electrons leaking from the photosynthetic electron transport system.

In order to investigate the flowering behaviour of *Arabidopsis* plants in response to high light stress, the plants after two weeks in short day conditions (180-200 μEs^{-1} m^{-2} light), were transferred to a growth environmental chamber with high light (800 μEs^{-1} m^{-2} light) while retaining the same 8h light photoperiod. Some plants were maintained in short day conditions in the standard low irradiance level as control. Figure 61 depicts the flowering curves of wild type and the triple mutant in response to high light.

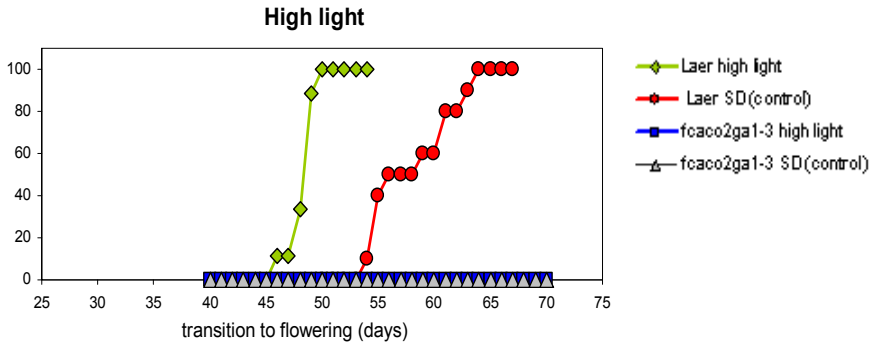

Figure 61. Flowering time in La*er* and triple mutant in response to high light (800 µEs^{-1} m^{-2} light) in a short day light cycle. As control, La*er* and triple mutant plants were grown in short day conditions and normal light intensity 180-200 µEs^{-1} m^{-2} light. Values represent the percentage of plants induced to flower. La*er* high light, n=16; La*er* SD (control), n=10; *fcaco2ga1-3* high light, n=16; *fcaco2ga1-3* SD (control), n=16.

High light treatment induced flowering in Laer (figure 61) compared to plants grown under normal light intensity. Similar results were obtained for Col-0 (not shown). The triple mutant did not flower either in response to high light or under normal light conditions. Phenotypes of the plants are presented in figure 62. Pictures show that Laer was able to produce normal flowers in response to the stress caused by high light. The triple mutant did not flower in stressful or under normal light conditions suggesting that the stress caused by high light was unable to promote flower in the triple mutant under that conditions.

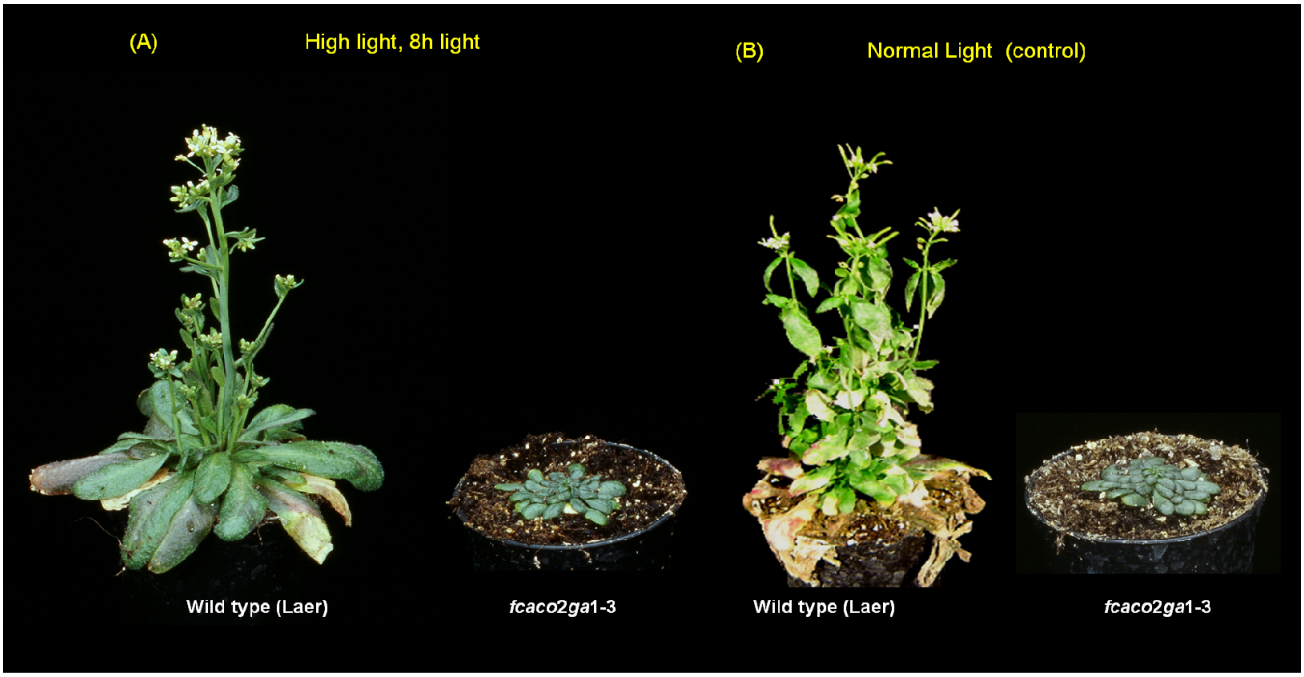

Figure 62. Phenotype of plants grown under high and normal light intensities. (A) Wild type Laer, (right) and triple mutant *fcaco2 ga1-3* (left) in conditions of high light (800 µEs^{-1} m^{-2} light) under 8h light photoperiod. (B) Wild type Laer, (right) and triple mutant *fcaco2 ga1-3* (left) in normal light (180-200 µEs^{-1} m^{-2}) under 8h light photoperiod.

4.4.2.2 High temperature.

A slight increase in temperature, even transiently, may affect physiological and biochemical processes of plants to a great degree (Singla, *et al*., 1997). High temperature induces protein denaturation, alters membrane fluidity, can disrupt the overall balance of metabolic processes, leads to oxidative stress (Dewey, 1989; Larkindale & knight, 2002) and affects the cytoskeleton as assessed by cytoplasmic streaming (Alexandrov, 1994).

Our aim was to study the effect in flowering time caused by the exposition of *Arabidopsis* plants to high temperatures and to see if the triple mutant is able to flower under these conditions. Therefore, plants were grown as described previously and transferred to a growth control chamber with 26º C day and 22º C during the night in a 12h light cycle. Some plants were transferred to 12h light day/night and 20º C day/night as control. Figure 63 depicts the transition to flowering in Laer and triple mutant under the cited conditions.

The transition to flowering time in Laer showed a slight acceleration of flowering at high temperature compared to control plants (figure 63). This is in agreement to the ability of plants to survive high temperatures by acclimatation or thermo tolerance mechanisms.

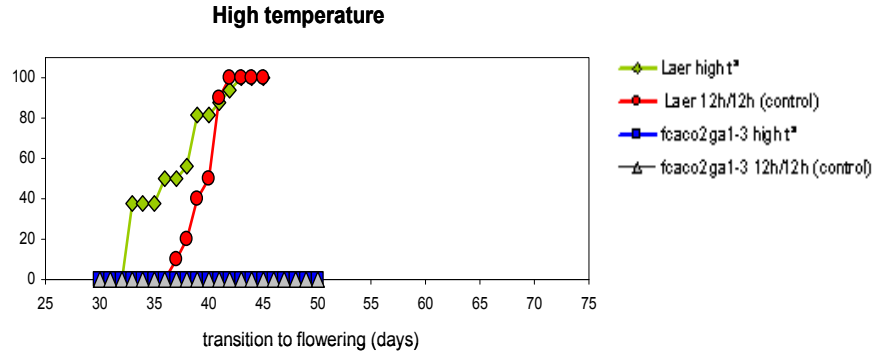

Figure 63. Flowering time in La*er* and triple mutant in response to high tº (26ºC day/22ª night) in a neutral day cycle (12h day/12h night, 20ºC). As control, La*er* and triple mutant plants were grown in neutral day of 12h light and constant tª of 20ºC. Values represent the percentage of plants induced to flower. La*er* high tª, n=16; La*er* 20ºC (control), n=10; *fcaco2ga1-3* high tª, n=16; *fcaco2ga1-3* 20ºC (control), n=16.

The triple mutant was unable to flower in response to high temperature. Also, they did not flower under control condition, suggesting that the stress caused by the increased tª had no effect in the induction of the triple mutant to the flowering stage. Phenotypes of the plants are shown in figure 64.

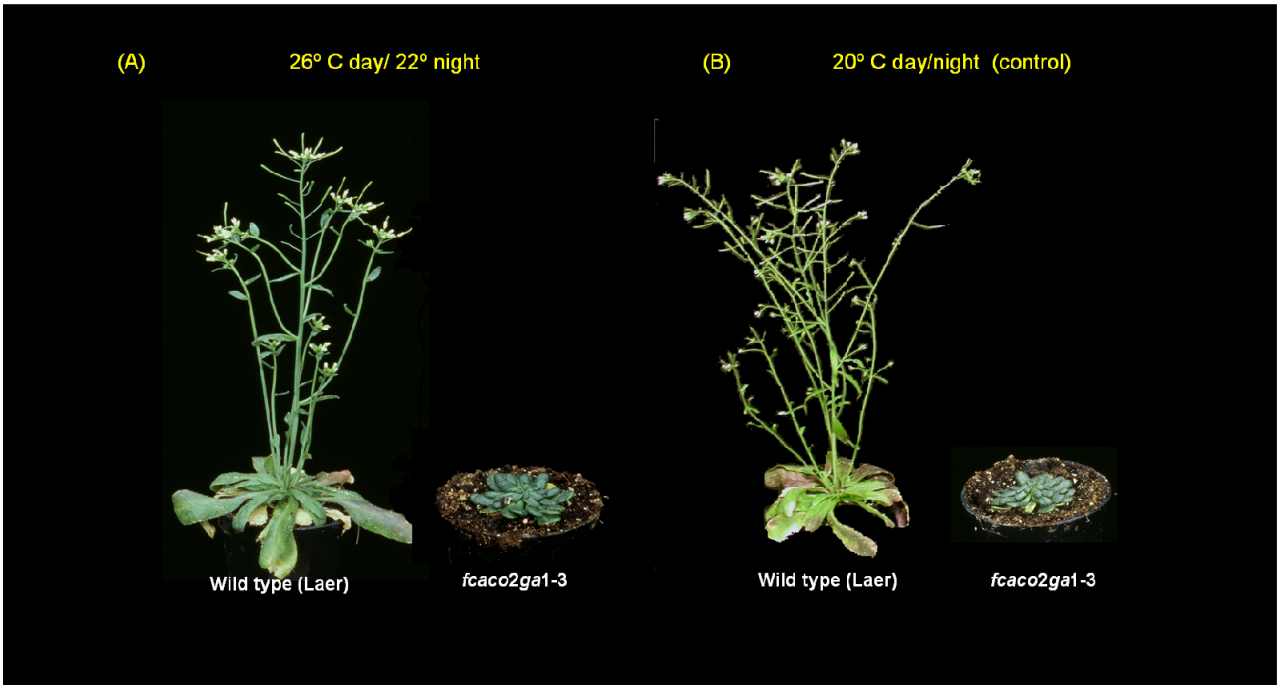

Figure 64. Phenotype of plants grown under high t[a] and normal photoperiod. (A) Wild type Laer, (right) and triple mutant *fcaco2ga1-3* (left) in conditions of high t[a] (26 ºC days/ 22 ºC nigh) in 12h light photoperiod. (B) Wild type Laer, (right) and triple mutant *fcaco2ga1-3* (left) under normal conditions 20ºC and 12h light photoperiod.

4.4.2.3 Photo-chilling stress

High light intensities and low temperatures produce a decrease of carbon fixation rate in the Calvin cycle leading to a photo-oxidative stress termed as photo-chilling. Low temperatures slow all metabolic reactions, particularly those involved in CO_2 carbon fixation and those involved in regulating stomata aperture leading to an inhibition of photosynthesis.

In order to investigate the effect of photo-chilling in the promotion of flowering, wild type and the triple mutant were analysed in response to photo chilling. Plants were grown under low temperatures (16 ºC day/night) and high light (800 µE $s^{-1}m^{-2}$ light) and compared to plants grown under normal light and 12h light photoperiod.

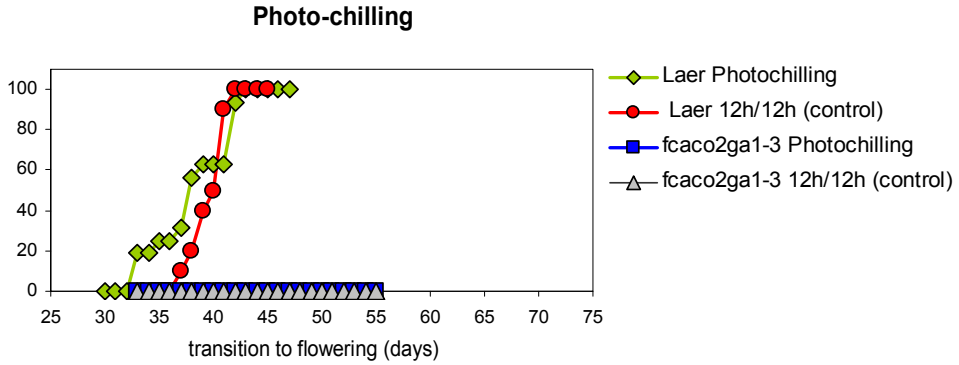

Figure 65. Flowering time in La*er* and triple mutant in response to photo-chilling in a neutral day cycle. As control, La*er* and triple mutant plants were grown in neutral day of 12h light and constant t[a] of 20ºC. Values

represent the percentage of plants induced to flower. La*er* photo-chilling, n=16; La*er* 12h day/12h night (control), n=10; *fcaco2ga1-3* photo-chilling, n=16; *fcaco2ga1-3* 12h day/12h night (control), n=16.

As we can see on figure 65, no significant differences in flowering time were visible in response to photo-chilling or in control conditions indicating that photo-chilling does not promote flowering in *Arabidopsis thaliana.* The triple mutant did not flower in response to high light and low temperature suggesting that photo-chilling is not promoting flowering in the triple mutant. Phenotype of the plants is shown in figure 66.

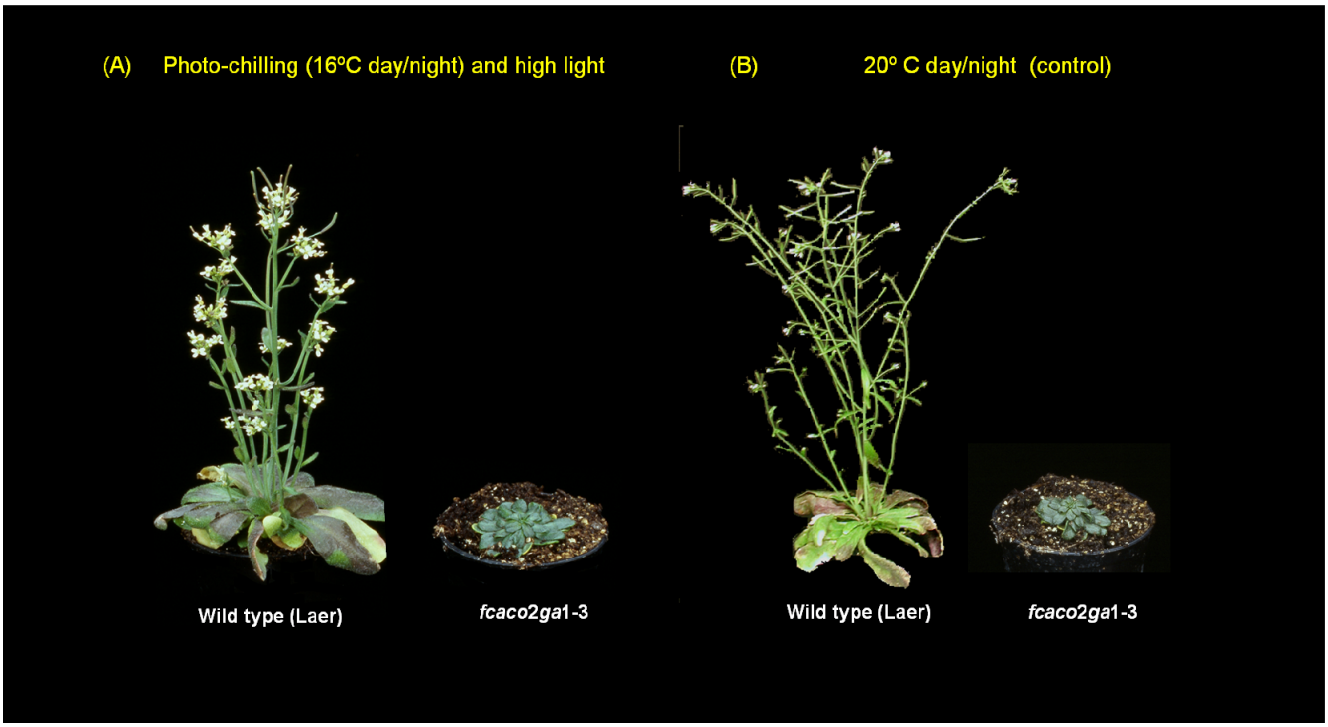

Figure 66. Phenotype of plants grown in response to photo-chilling and in normal conditions. (A) Wild type Laer, (right) and triple mutant *fcaco2 ga1-3* (left) in conditions of photo chilling (16 ºC days/nigh) in 12h light photoperiod. (B) Wild type Laer, (right) and triple mutant *fcaco2 ga1-3* (left) under normal conditions 20ºC and 12h light photoperiod.

4.4.2.4 Continuous light treatment.

In early-flowering ecotypes such as Landsberg *erecta* (La*er*), strong photoperiodic treatments can induce mature vegetative plants to initiate flowers (Hempel & Feldman 1994). Hence, it was interesting to study the effect on flowering time caused by an excess illumination in the triple mutant compared to wild type. Therefore, the triple mutant and wild type plants were transferred to continuous light and the transition to flowering time was studied. Results are shown in figure 67. The flowering curve of plants exposed to continuous light was earlier than those plants grown in short day conditions. This is explained by the regulation of flowering time in *Arabidopsis* by the day-length signalling pathway. By contrast, the triple mutant was

unable to flower in response to continuous light treatment indicating the total block in the major pathways involved in flowering time.

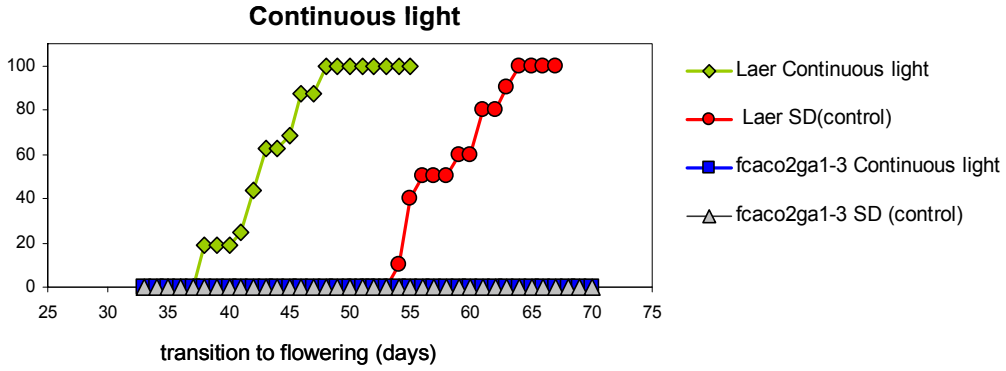

Figure 67. Flowering time in La*er* and triple mutant in response to 24h of light period. As control, L*aer* and triple mutant plants were grown in short day conditions (8h light/16h dark) and constant tª of 20ºC. Values represent the percentage of plants induced to flower. La*er* continuous light, n=16; La*er* 8h light/16h dark (control), n=10; *fcaco2ga1-3* continuous light, n=16; *fcaco2ga1-3* 8h light/16h dark (control), n=16.

Phenotypes of plants grown under continuous light are presented in picture 68. Wild type plants were promoted to flower in response to the excessive illumination whereas the triple mutant remained vegetative in all treatment.

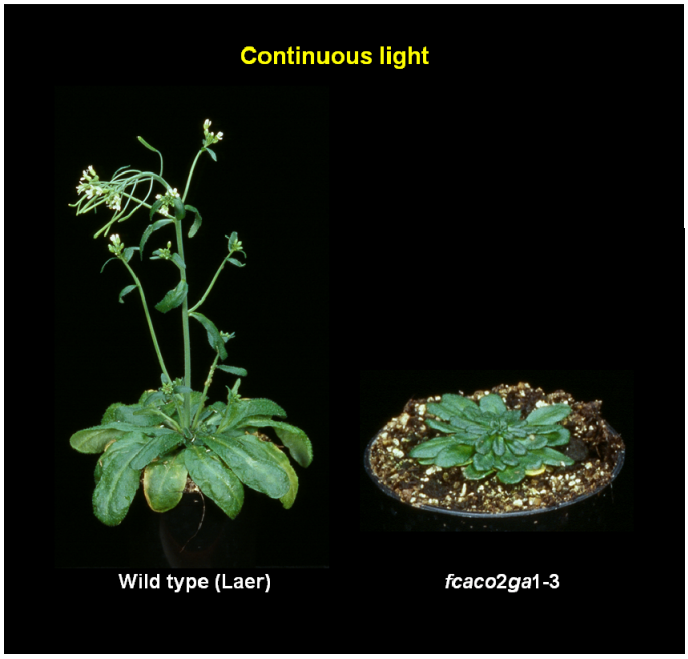

Figure 68. Phenotype of plants grown in response to continuous light. Wild type L*aer*, (right) and triple mutant *fcaco2ga1-3* (left) in conditions of continuous photoperiod. Wild type displayed earlier flowering phenotype and the triple mutant remained vegetative in response to 24h light photoperiod.

The conclusion from this part is that the transition to the floral stage in wild type *Arabidopsis* is promoted in response to a specific stress situation (for example, high light and high temperature). In contrast, the triple mutant was unable to flower in four of the abiotic stresses tested (high light, high temperature, photo-chilling and continuous light) and was induced to

flower only under the nutritional stress caused by phosphate or nitrate limitation. Also, the results show that under conditions of high nitrate, the triple mutant remains vegetative and dyes without producing flowers. These results allow us to suggest that flowering time in *Arabidopsis thaliana* is affected by nitrate and that the "nitrate-signal" must operate downstream or in parallel of the main known flowering signalling pathways. However, it is also possible that there may be an analogous signal related to low phosphate.

4.5. Affymetrix Gene Chip hybridizations analyses.

To monitor global changes in gene expression, we used Affymetrix Gene Chip hybridisations analyses. These array experiments were done for two main reasons:

a) To complete the phenotypic analyses previously characterised by Dr. Irene Loef in wild type plants in response to three different growth regimes (1mM KNO_3, 10mM KNO_3 and 35mM KNO_3).

b) To investigate at transcriptional level which genes may be involved in the regulation of flowering time by nitrate in *Arabidopsis thaliana*.

For the analyses, two different transgenic lines, *co2tt4* (named *co2* for abbreviation) and 35S::*FLC,* were grown under two distinct nitrate treatments (1mM KNO_3 and 35mM KNO_3) and sampled at different times along the transition to flowering (see figure 69).

During this work, it has been shown that the photoperiod pathway interferes clearly with the "nitrate-signalling pathway" (see section 4.3.1), so that the over-expression of *CO* gene prevents the earlier flowering caused by low nitrate and, in the other side, the down regulation of *CO* gene expression uncovers the effects caused by nitrate leading plants to flower at different time in response to distinct treatments of nitrate. Therefore, to avoid the photoperiod signal, *co2* transgenic plants were chosen for the expression profiling analyses.

In order to see a global response of plants to nitrate, low nitrate (1mM KNO_3) was used as inducing treatment, and high nitrate (35mM KNO_3) as repressive treatment. In low nitrate, batches of 15-20 plants were harvested (without roots) at certain points during the vegetative phase and prior to the floral initiation. Similar sampling was carried out in *co2* plants grown in high nitrate conditions (same harvesting times).

As control plants, transgenic plants over-expressing the floral repressor *FLC* were used under the same conditions as described for *co2* mutant. These plants are smaller and therefore they were sampled at later time to represent similar size when compared to those at 25 days in *co2tt4* mutant.

35S::*FLC* plants displayed a strong delay in flowering time (in response to both treatments) suggesting that the putative signals promoting flowering should be "postponed" in time, thus, 35S::*FLC* plants may serve as a good control for that changes that may occur in *co2* mutant during the transition to flowering. Analysis of flowering time is presented in figure 70.

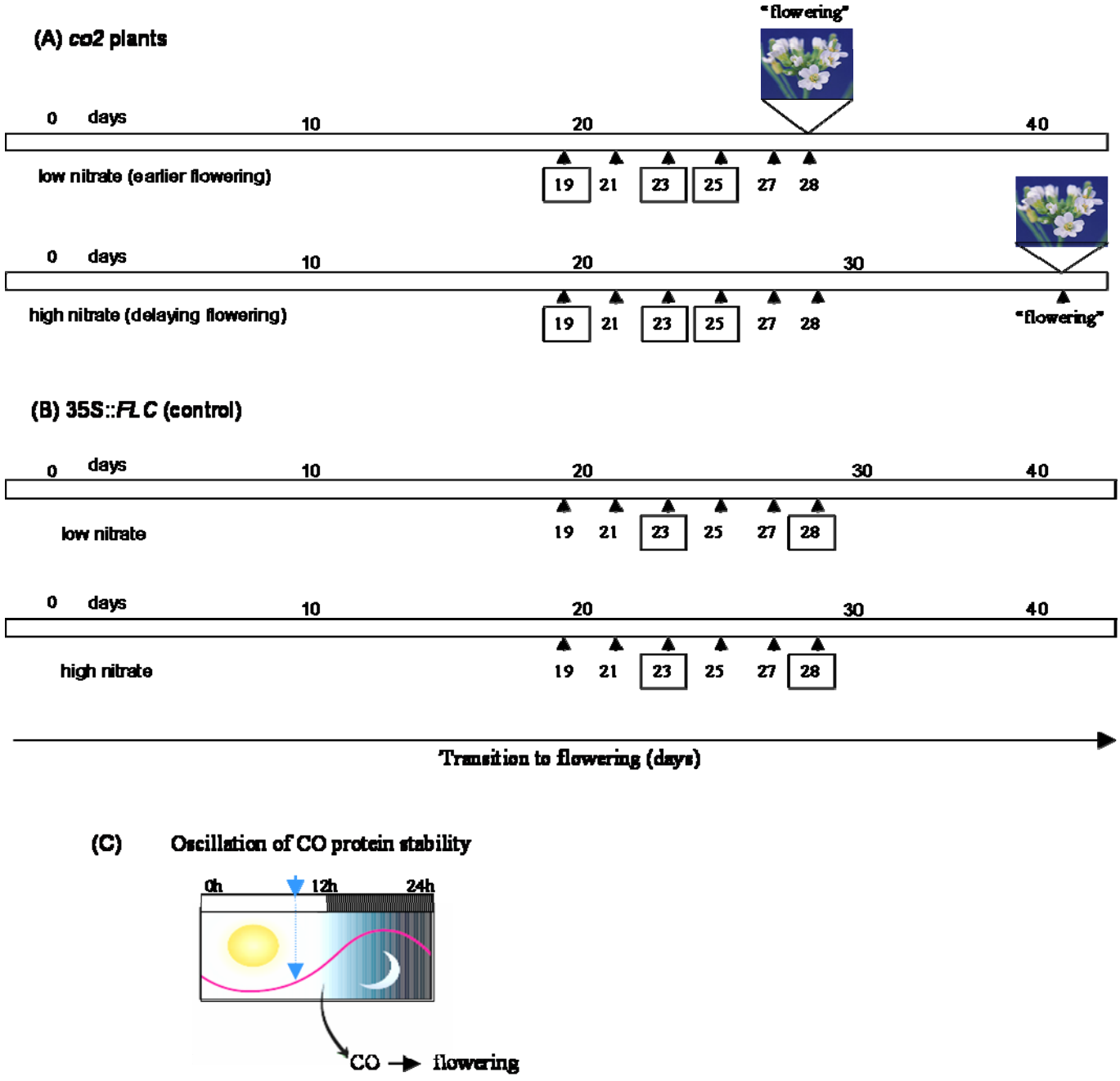

Figure 69. Sampling details of transgenic plants, *co2* and 35S::*FLC*, for Affymetrix Gene Chip hybridization analyses. (A) *co2* transgenic line grown under low nitrate (1mM KNO_3, above) and high nitrate (35mM KNO_3, below) during the transition to the floral stage. In low nitrate conditions 50% of *co2* plants flowered at around 28 days after the sowing date and 50% around 41 days under high nitrate treatment. Batches of 15 pooled plants (without roots) were harvested at different times along the vegetative phase before the floral initiation. Numbers inside squares indicate the day of the sampling. The estimated day for flowering is indicated in the figure. (B) 35S::*FLC* over-expressing line grown under low nitrate (1mM KNO_3, above) and high nitrate (35mM KNO_3, below) during the transition to flowering. 35S::*FLC* plants remained vegetative during the course of the experiment and were used as control for the expression changes in *co2* plants. Numbers inside squares

indicate the day of the sampling. (C) Diurnal oscillation of CO protein stability. Plants were grown in sterile growth chambers under neutral day length (12h light) and 20ºC day/night. Each harvesting was made two hours before the end of the light period to avoid high expression/stability of CO protein and to minimize changes promoted by photoperiod. Blue arrow indicates approximately the time of sampling.

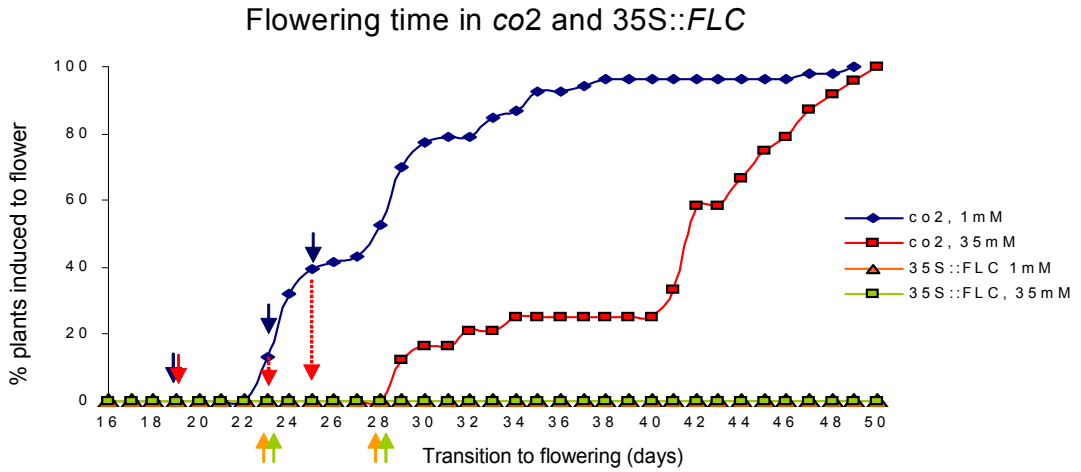

Figure 70. Flowering time of *co2* and 35S::*FLC* transgenic lines. Plants were grown under low nitrate (1mM KNO_3) and high nitrate (35mM KNO_3) in 12h light photoperiod and 20º C day/night. Around 50% of *co2* plants flowered 28 days after the sowing date in low nitrate conditions (1mM KNO_3) and 50% of the plants flowered around 41 days after the sowing in high nitrate treatment (35mM KNO_3). 35S::*FLC* over-expressing plants remained vegetative in response to both nitrate treatments. Dark blue and red arrows represent the time at which samples were taken for the *co2* mutant (1mM and 35mM, respectively) and orange and green arrows represent the time at which samples were taken for the 35S::*FLC* mutant (1mM and 35mM, respectively) in the Affymetrix arrays.

There are two possible and complementary filters to identify genes putatively involved in the flowering induction. First, those genes should be changing between 1mM nitrate and 35mM nitrate in the mutant *co2* but not in 35S::*FLC*. Second, those genes should change between *co2* and 35S::*FLC* in 1mM nitrate but not in 35mM nitrate.

It would be especially interesting if these genes show the same changes between low and high nitrate in the seedlings system. However, it is also possible that nitrate-dependent changes in genes that are closely related to floral induction may not occur at this developmental stage, and therefore this criteria is more indicative rather than stringent.

Genes showing selective changes in *co2* of the sort indicated above may be changing because they are involved in the early nitrate-dependent signalling, or because they are involved in downstream changes during flowering. To try to filter out the latter, the genes showing these changes should be compared with the genes that change during floral initiation promoted by other signal.

4.5.1 Comparison with array data on nitrate response.

As we are studying the regulation of flowering time by nitrate, we need to be sure that the experimental conditions used in the analyses are appropriate of plants grown in response to

low and high nitrate, respectively. A general comparison of our results with the ATH1 analyses of Scheible *et al.*, (2004) revealed that many genes showed similar responses. However, it cannot be comparable since a big percentage of genes showed opposite response due to different experimental systems. One of the main differences between both systems is that in Scheible *et al*., (2004), *Arabidopsis* seedlings are grown in sterile liquid cultures under continuous light, in contrast to the horizontal agar plates and a 12h light photoperiod used in this work. Secondly, in Scheible *et al*., (2004), after seven days growing in full nutrient medium they transferred plants to low nitrate without glutamine and two days later they re-supplied nitrate to the growing medium. This strongly contrasts to our system in which plants are maintained in the agar plates with a determined nitrate concentration that includes glutamine since the beginning of the experiment. Scatter plots between the two individual experiments are shown in figure 71.

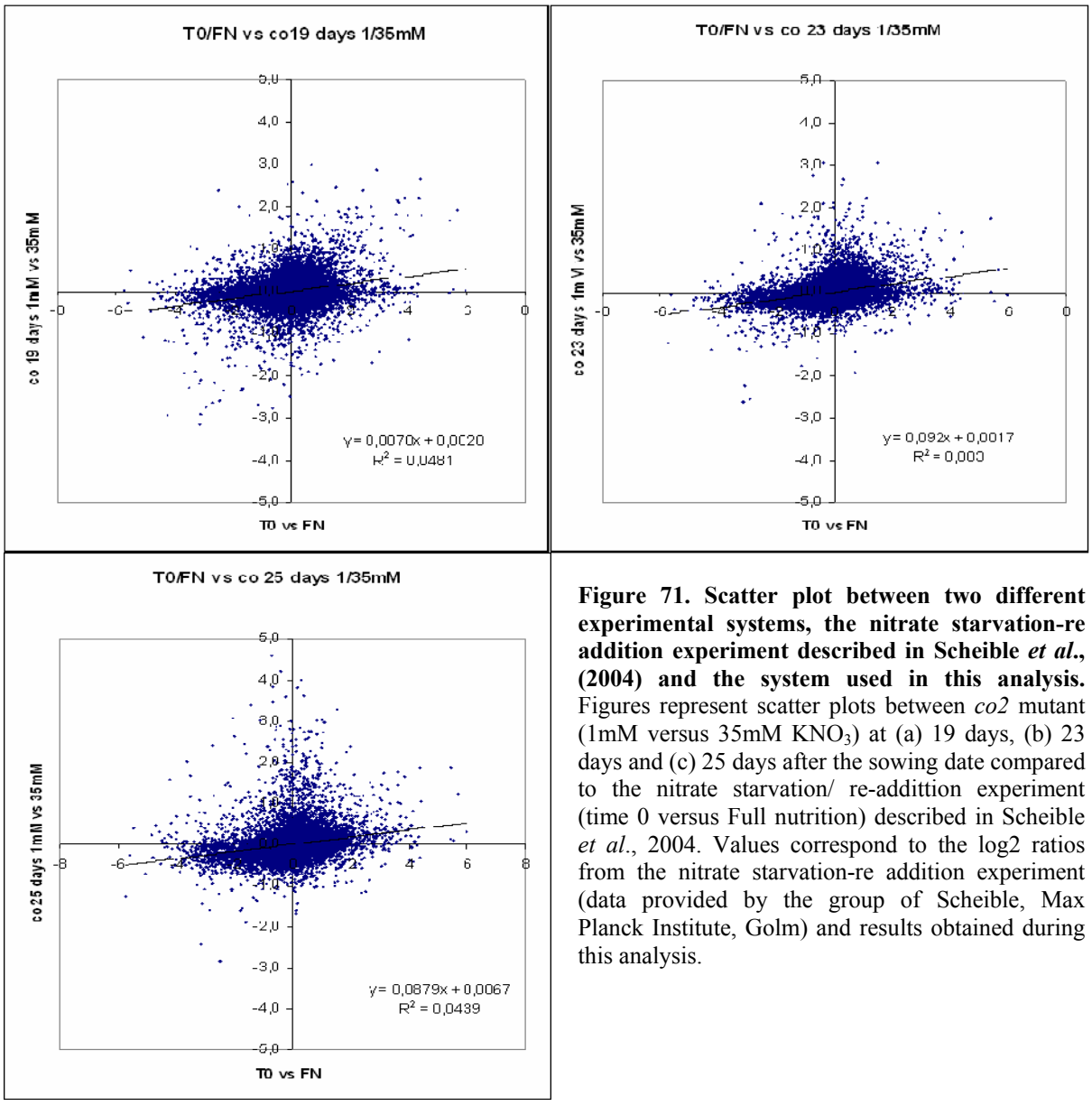

Figure 71. Scatter plot between two different experimental systems, the nitrate starvation-re addition experiment described in Scheible *et al*., (2004) and the system used in this analysis. Figures represent scatter plots between *co2* mutant (1mM versus 35mM KNO_3) at (a) 19 days, (b) 23 days and (c) 25 days after the sowing date compared to the nitrate starvation/ re-addittion experiment (time 0 versus Full nutrition) described in Scheible *et al*., 2004. Values correspond to the log2 ratios from the nitrate starvation-re addition experiment (data provided by the group of Scheible, Max Planck Institute, Golm) and results obtained during this analysis.

4.5.2 Functional gene categories.

The raw Affymetrix data was analysed as described previously in section 2.2.1.9. Genes with significance expression change were classified into functional gene categories (table 4.2).

	***co* 1mM vs 35mM**						**35S::*FLC* 1mM vs 35mM**			
	19 days		**23 days**		**25 days**		**23 days**		**28 days**	
	Up	**Down**	**Up**	**Down**	**Up**	**Down**	**Up**	**Down**	**Up**	**Down**
Total number	152	158	157	29	339	37	262	28	214	61
Transcription factors	12	20	29	1	68	2	12	6	11	3
Signalling	7	13	13	1	34	1	7	1	8	4
Hormone signalling	1	3	–	2	4	4	1	1	1	1
Defense	9	14	12	4	16	3	9	1	4	6
Stress	8	5	2	–	7	1	13	1	6	2
Light-mediated responses	1	–	1	–	–	–	–	–	–	–
Cell Wall	1	–	–	–	3	2	6	1	4	–
Carbohydrate metabolism	20	8	5	2	10	2	13	1	15	1
Lipid metabolism	3	1	1	–	1	1	6	–	3	–
Nitrogen Metabolism	1	1	1	2	2	–	3	–	4	–
Secondary metabolism	4	–	–	–	–	–	2	–	2	–
Photosynthesis/Respiration	3	1	5	–	4	2	9	–	8	5
Protein regulation/degradation	–	–	2	–	5	–	1	–	2	–
DNA	1	–	–	–	–	–	–	–	–	–
Miscellaneous	46	32	33	8	61	9	113	17	95	28
Unidentified	35	59	52	9	124	10	55	11	24	11

Table 4.2. Summary of up and down-regulated transcripts classified in functional categories. Up- regulated genes (≥ 2 fold changes) and down-regulated genes (≤ -2 fold changes) were included in the analysis (see table heading for each comparison). Up or down regulated genes are distinguished.

Looking at table 4.5, we can see that in *co2* mutant there is an increase in the total number of induced transcription factors upon the floral initiation while remained practically constant in the control 35S::*FLC*. Similarly, there is an increase in the number of induced genes involved in signalling.

4.5.3 Looking for candidate genes.

To find possible candidates genes involved in the regulation of flowering time by nitrate, each data set (see figure 69, sampling schedule) was analysed, compared and filtered following some criteria.

a) *Genes differentially expressed in low nitrate versus high nitrate upon the transition to flowering*.

To gain insights into whether there are genes differentially expressed under low nitrogen versus high nitrate in the *co2* mutant towards the floral initiation, we selected those transcripts

with significant gradual induction or repression (-1≥ log2 ≥ 1) upon flowering. Moreover, since we assume that *co2* mutant is induced to flower in response to low nitrate (the response is delayed under high nitrate), all these changes must be insignificant in those plants over-expressing the floral repressor *FLC*, used as control.

Approximately 380 transcripts were found to be changed (≥ 2 fold changes) in *co2* 1mM on each of the three days, around 170 genes were up- or down- regulated in two of the three days and 50 genes were significantly changed in one of the time-points used. All of these genes showed unchanged expression (1≥ log2 ≥ -1) in control 35S::*FLC* plants.

A general list of genes showing induction or down-regulation in *co2* 1mM/35mM between day 19 and day 25 are listed in tables 10 and 11 (sections 7.16 and 7.17) from the Appendix.

A list of main transcription factors showing up-or down-regulation are ranked in table 4.3. The expression of the genes in response to low nitrate (data from Scheible´s group) is also included in the table.

Gene code	*co* 1/35mM 19days	*co* 1/35mM 23days	*co* 1/35mM 25days	FLC oex 1/35mM 23days	FLC oex 1/35mM 28days	T0/3h	T0/FN	Descriptions
At1g80840	-0,910	3,060	4,213	-0,292	0,737	0,163	-0,398	transcription factor similar to WRKY transcription factor
At3g55980	-0,637	1,620	3,809	-0,227	0,361	-0,356	0,176	putative protein zinc finger transcription factor (PEI1)
At1g68840	0,018	1,488	3,613	0,517	0,782	0,393	-0,226	putative DNA-binding protein (RAV2-like)
At1g28370	-0,628	1,747	2,859	0,298	0,115	0,763	-0,567	ethylene-responsive element binding factor,
At2g38470	-0,317	1,566	2,775	-0,205	0,470	0,441	0,640	putative WRKY-type DNA binding protein
At4g37610	-2,300	0,585	2,438	0,046	-0,180	-2,830	-1,651	putative protein SPOP
At3g50060	-1,022	0,037	2,307	0,177	0,480	-0,211	-0,217	R2R3-MYB transcription factor
At5g27420	-0,345	1,428	2,271	-0,432	0,278	0,834	0,604	RING-H2 zinc finger protein-like
At4g25490	-0,334	1,249	2,262	0,129	-0,177	-0,228	-0,123	transcriptional activator CBF1 CRT CRE binding factor
At2g40140	-0,406	1,351	2,222	-0,672	0,574	-0,225	0,368	putative CCCH-type zinc finger protein also an ankyrin-repeat protein
At5g59450	0,123	1,310	2,009	0,196	0,355	0,793	1,473	scarecrow-like 11 - like
At5g67450	-1,116	0,823	2,003	-0,598	-0,159	0,720	0,502	Cys2/His2-type zinc finger protein 1
At1g18570	-0,195	1,387	1,989	-0,188	0,295	0,465	-0,512	myb factor
At5g04340	0,148	1,905	1,982	-0,603	0,626	0,902	0,986	putative c2h2 zinc finger transcription factor
At5g59820	-1,295	1,410	1,976	-0,659	0,746	-0,508	-0,246	zinc finger protein Zat12
At4g18880	-0,253	1,674	1,954	-0,218	0,114	0,028	0,929	heat shock transcription factor
At5g05410	-1,116	2,103	1,823	0,470	-0,028	0,060	-0,370	DREB2A
At5g47220	1,126	1,213	1,812	-0,028	0,277	1,327	-0,409	ethylene responsive element binding factor 2 (ATERF2)
At3g19580	-1,022	0,363	1,673	0,090	0,505	0,111	0,910	zinc finger protein
At1g42990	-0,289	1,093	1,597	0,299	0,381	-0,147	0,402	bZIP transcription factor
At1g22190	-1,107	0,790	1,596	-0,043	0,117	-0,529	-0,283	AP2 domain containing protein RAP2
At3g50260	0,037	1,075	1,444	0,732	0,305	1,458	0,685	putative protein EREBP-3 homolog
At2g46400	-1,001	1,139	1,443	0,289	-0,137	1,206	1,750	putative WRKY-type DNA binding protein
At3g44350	-1,477	0,500	1,437	0,048	-0,860	-0,072	0,064	NAC domain -like protein
At2g44840	-1,275	0,457	1,416	-0,390	0,229	0,325	-0,393	putative ethylene response element binding protein (EREBP)
At1g51700	-0,066	1,118	1,314	-0,667	0,093	0,553	0,224	dof zinc finger protein identical to dof zinc finger protein
At1g63840	0,213	1,239	1,292	0,542	0,526	1,071	1,304	putative RING zinc finger protein

At5g61600	-0,524	0,626	2,729	-0,876	0,677	-0,155	0,380	DNA binding protein - like DNA binding protein EREBP-4
At1g13260	0,438	0,463	2,168	-0,204	0,066	-0,279	-0,280	DNA-binding protein RAV1
At3g46600	-0,827	0,631	2,055	0,364	0,312	0,559	0,841	scarecrow-like protein
At3g16720	-0,301	0,833	1,720	-0,632	0,226	1,120	0,858	putative RING zinc finger protein similar to RING-H2 zinc finger protein
At4g17500	0,374	0,729	1,716	0,073	0,477	0,466	-0,412	ethylene responsive element binding factor 1
At2g17040	-0,945	0,482	1,710	-0,225	-0,548	1,917	2,083	NAM (no apical meristem)-like protein
At4g11370	0,333	0,793	1,682	0,054	-0,171	0,423	0,857	RING-H2 finger protein RHA1a
At4g37260	-0,636	-0,143	1,668	0,713	0,394	0,230	0,402	myb-related protein
At3g43430	-0,170	0,584	1,618	0,330	0,129	-0,659	-0,548	putative protein RING-H2 zinc finger protein ATL4
At1g25560	0,341	0,243	1,612	-0,363	-0,074	0,260	-0,177	DNA-binding protein RAV2
At3g05200	-0,303	0,601	1,561	0,182	0,338	-0,182	0,491	putative RING-H2 zinc finger
At3g49530	-0,806	0,905	1,527	0,191	0,308	0,793	0,526	NAC2-like protein NAC2
At1g08930	-0,651	0,602	1,365	0,577	0,255	0,532	0,242	zinc finger protein ATZF1
At4g17230	-0,920	0,610	1,289	0,534	0,240	0,644	0,653	scarecrow-like 13 (SCL13)
At1g06160	0,883	0,847	1,279	0,361	0,457	0,064	-0,636	ethylene response factor
At3g52800	-0,479	0,787	1,212	0,551	0,628	0,413	0,643	zinc finger
At5g24590	-0,601	0,506	1,194	0,604	0,315	0,324	0,417	NAC2-like protein
At4g25470	-0,166	0,590	1,178	-0,070	0,198	-0,119	-0,032	DRE CRT-binding protein DREB1C
At1g07520	-0,396	0,704	1,138	0,140	0,148	0,229	0,743	transcription factor scarecrow-like 14
At3g54810	-0,652	0,282	1,133	0,320	0,429	0,084	0,647	putative protein GATA transcription factor 3
At2g23320	-0,518	0,471	1,099	0,137	0,327	-0,065	0,337	putative WRKY-type DNA-binding protein
At4g31550	0,051	0,733	1,087	0,059	0,808	0,010	-0,180	putative DNA-binding protein WRKY3
At5g63790	1,330	1,003	0,749	-0,088	0,602	0,758	1,620	putative NAC-domain protein

Table 4.3. List of transcription factors significantly changed upon the floral onset in *co2* 1mM vs 35mM and compared to the control FLC.
Values represent the log 2 scaled ratio of each day in 1mM vs 35mM nitrate. The list includes genes with significant expression (≥ 2 fold changes) or unchanged expression (1≥ log2 ≥ -1). Expression data from Scheible´s group (starvation / re-addition experiment) was included for comparison with expression changes of *co2*.

Many genes showed up-regulation in *co2* plants under low nitrate towards the floral onset and no change in the control FLC over-expressing plants. Several transcription factors were induced. For example, fifteen genes encoding for AP2 DNA-binding containing domain proteins showed up regulation between day 19 and 25 in *co2* plants (At1g28370, At1g68840, At4g25490, At5g05410, At5g47220, At1g22190, At3g50260, At2g44840, At1g13260, At4g25470, At5g61600, At1g25560, At4g17500, At1g06160, At5g25190 and At4g01500). The AP2/EREBP transcription factor family is a large family of transcription factor unique to plants. They play variety of roles throughout the plant life being regulators of several developmental processes, like floral organ identity determination, control of leaf cell identity or response to abiotic and environmental stress (Riechmann, J & Meyerowitz, EM., 1998). Some transcription factors containing zinc finger regions and CCT motifs were also up-regulated, for example, At3g55980, At5g27420, At2g40140, At5g67450, At5g04340, At5g59820, At3g19580, At1g63840, At1g51700, A13g16720, At4g11370, At3g43430,

At3g05200, At1g08930 and At3g52800. Three members of the MYB family (At3g50060, At1g18570 and At4g03760) displayed increased induction upon flowering. It is known that MYB proteins play regulatory roles in developmental processes and defence responses in plants and also they have been supposed to be involved in some aspects of flowering plants (Yahui, *et al*., (2006). Three members belonging to WRKY superfamily of transcription factors (At1g80840, At2g38470, and At2g46400) were significantly changed towards flowering. The WRKY family members appear to be involved in the regulation of various physio-logical programs that are unique to plants, including pathogen defence, senescence and trichome development. Proteins involved in calcium-binding signalling showed also significant up-regulation upon flowering for example, At5g37770 and At2g41100, also termed touch responsive proteins. They have been shown to be induced in plants subjected to touch and darkness and they are expressed at sites of predicted mechanical stress like regions undergoing growth, vascular tissues and floral organs. Four NAC domain-like proteins, At3g44350, At2g17040, At3g49530 and At5g24590 belong to the NAM (no apical meristem) family of transcription factors that are involved in regulation of development. A putative NAC-domain transcription factor (At5g63790), among other genes, trended to fall down in expression during the transition to flowering.
Additionally, several unknown proteins showed significant changes. Similarly, a large number of regulatory proteins such as kinases, some calcium binding proteins and resistance proteins were significantly changing in *co2* plants under low nitrate towards the floral onset (see table 10, section 7.16 and table 11, section 7.17, from the Appendix)..

The expression of known central genes involved in the transition to flowering was investigated in *co2* induced plants and compared to control 35S::*FLC* (see table 12, section 7.18, from the Appendix). In general the expression of known flowering time genes was unchanged in any of the given time-points. A NAC domain protein NAM- like (At1g69490) was induced between day19 and 25 in *co2*. This gene is expressed in the floral primordia and it is involved in cell growth and flower development. Also, a flavin-binding kelch domain F box protein (FKF1/ADO3, At1g68050) showed slightly induction at 19d and tended to decrease thereafter. FKF is clock-controlled and it is involved in the regulation of the transition to flowering. The rest of central flowering time genes remained practically unchanged.

b) *Genes differentially expressed in plants induced to flower (co2) versus non-flowering control plants (35S::FLC).*

The goal was to select those transcripts that are differentially regulated in *co2* transgenic plants compared to 35S::*FLC* under the same nitrate condition. As mentioned before, *co2* transgenic plants showed earlier flowering in conditions of low nitrate (1mM) compared to high nitrate (35mM). Unlike, plants over-expressing the floral repressor FLC displayed strong delay, flowering around 30 days later than *co2* plants. In this case, a possible candidate gene, could trend to be up- or down-regulated in *co2* under low nitrate but then show no response or opposite behaviour in response to high nitrate. This expression pattern could therefore become the basis for identifying genes promoting flowering under low nitrate. Genes up- or down-regulated in low nitrate towards the floral initiation are listed in tables 4.4 and 4.5.

Gene code	co19d 1mM vs FLC 1mM	co23d 1mM vs FLC 1mM	co25d 1mM vs FLC 1mM	co19d 35mM vs FLC 35mM	co 23d 35mM vs FLC 35mM	co 25d 35mM vs FLC 35mM	Descriptions
At2g41640	-0,3271	1,6831	1,9080	0,9292	0,1885	-0,3328	unknown protein
At5g01600	1,9939	1,7501	1,8973	-0,5318	-0,8289	-0,0507	ferritin 1 precursor
At2g40300	1,6377	1,8969	1,8837	-0,1330	0,0340	0,1695	putative ferritin
At4g35480	1,3471	1,6647	1,8313	0,6434	0,6765	0,5888	RING-H2 finger protein RHA3b
At1g78410	0,6942	1,4123	1,6665	0,2072	-0,0338	-0,2798	hypothetical protein
At4g02410	0,5058	1,6300	1,6040	0,2005	0,2011	-0,1372	contains similarity to a protein kinase domain
At5g06510	1,0618	1,3698	1,4187	-0,0824	0,4086	0,8080	transcription factor-like protein CCAAT-binding factor
At3g49160	0,6499	1,2255	1,4077	-0,9507	-0,9311	-0,7515	pyruvate kinase
At3g19550	0,7941	1,2199	1,3984	0,0201	-0,1007	0,1808	hypothetical protein
At3g57540	0,6278	1,2041	1,3771	0,4872	0,9333	0,8678	putative protein putative DNA binding protein
At1g76360	0,7369	1,2400	1,3586	0,0942	0,5364	0,1755	putative protein kinase similar to protein kinase (APK1A)
At5g64410	0,6907	1,2865	1,2585	0,6958	0,5923	0,4542	Isp4-like protein
At3g45260	1,0056	1,1252	1,2419	0,4762	0,8280	0,8174	zinc finger protein ID1
At1g72830	0,6439	0,9869	1,1282	0,1413	0,4369	0,8524	CCAAT-binding factor B subunit homolog
At2g36885	1,0216	1,0749	1,1208	0,0886	0,5066	0,5126	Expressed protein
At1g52190	0,6947	1,0843	1,1034	0,5547	0,5911	0,6178	peptide transporter
At5g17170	1,0478	1,0677	1,0905	0,2698	0,3108	0,4646	unknown protein
At1g51700	0,0862	0,8671	1,0717	-0,1348	-0,5377	-0,5293	dof zinc finger protein
At5g53830	0,5300	1,0742	1,0510	0,6011	0,4082	0,5565	putative protein similar to unknown protein
At1g22440	-1,3655	-1,1172	-0,7264	-0,3573	-0,1953	-0,5763	alcohol dehydrogenase ADH
At5g58860	-1,2289	-1,0875	-0,7335	-0,5980	-0,4467	-0,7028	cytochrome P450 CYP86A1
At2g19590	-1,6584	-1,1301	-0,7477	-0,5251	-0,5220	-0,6076	1-aminocyclopropane-1-carboxylate oxidase
At4g38080	-1,7123	-1,4254	-0,7929	-0,7268	-0,7197	-0,7939	putative protein
At1g17620	-1,3948	-1,1746	-0,8142	-0,6797	-0,5655	-0,7031	unknown protein
At2g33850	-1,2870	-1,1179	-0,8316	-0,4579	-0,1042	-0,1341	unknown protein
At5g56980	-1,4854	-1,0516	-0,8403	-0,4765	-0,7427	-0,8339	putative protein non-consensus CG donor, GA donor
At4g10500	-1,8726	-1,0663	-0,8655	-3,2410	-3,1265	-2,7820	putative Fe(II)/ascorbate oxidase SRG1 protein
At1g27300	-1,0601	-1,0016	-0,8670	-0,2290	-0,2328	-0,2492	hypothetical protein
At1g31710	-1,1409	-1,0838	-0,9116	-0,7900	-0,5959	-0,5148	copper amine oxidase
At1g52820	-1,2148	-1,0141	-0,9185	-0,3707	-0,3819	-0,6927	putative oxidoreductase similar to gibberellin 20-oxidase
At1g14130	-1,0967	-1,0766	-0,9344	-0,8487	-0,7275	-0,4497	dioxygenase-like protein

At1g68670	-1,1992	-1,0770	-0,9440	-0,4331	-0,3434	-0,7905	hypothetical protein
At2g24100	-1,3009	-1,1861	-0,9478	-0,6566	-0,8662	-0,1410	unknown protein
At5g17330	-1,5695	-1,2647	-0,9490	-0,3033	-0,3258	-0,6303	glutamate decarboxylase 1 (GAD 1)
At3g10450	-1,2977	-1,0543	-0,9522	-0,4807	-0,3706	-0,1648	putative glucose acyltransferase
At4g14060	-1,3310	-1,3207	-0,9531	-0,5971	-0,5788	-0,6166	major latex protein like
At1g17750	-1,0704	-0,9943	-0,9569	-0,4766	-0,3723	-0,4339	receptor-like protein kinase
At1g14890	-1,4690	-1,1858	-0,9594	-0,9798	-0,9180	-0,6208	unknown protein similar to pectinesterase
At5g57910	-1,2848	-1,0617	-0,9846	-0,5412	-0,5341	-0,6693	putative protein similar to unknown protein
At4g15920	-1,3088	-1,0129	-0,9885	-0,8306	-0,5445	-0,6349	cytochrome oxidoreductase like protein
At3g16460	-1,3265	-1,3081	-0,9899	-0,0528	-0,1239	-0,2919	putative lectin contains
At1g44800	-1,3096	-0,9973	-0,9922	-0,8955	-0,9940	-0,5882	nodulin protein
At5g04020	-1,7056	-1,0035	-0,9983	-0,8471	-0,6643	-0,9111	putative protein fimbriae-associated protein Fap1
At3g16860	-1,6889	-1,0027	-0,9991	-0,5542	-0,8660	-0,8559	unknown protein
At4g31800	-2,0778	-1,0965	-1,0073	-0,9341	-0,3827	-0,8892	Expressed protein
At1g77500	-1,2062	-1,0431	-1,0159	-0,1873	-0,4960	-0,5784	unknown protein
At1g11670	-1,3595	-1,0838	-1,0211	-0,8375	-0,8858	-0,6770	unknown protein
At4g37410	-1,3546	-1,2562	-1,0216	-0,9739	-0,6455	-0,8826	cytochrome P450 monooxygenase
At4g26950	-1,2577	-1,2171	-1,0287	-0,8825	-0,9444	-0,8835	putative protein
At5g09440	-1,3931	-1,2090	-1,0294	-0,7693	-0,5437	-0,8073	putative protein phi-1
At5g09530	-2,1200	-1,2917	-1,0509	-0,7091	-0,6806	-0,8587	periaxin - like protein periaxin
At2g16890	-1,3662	-1,0668	-1,0695	-0,9041	-0,8681	-0,3105	putative glucosyltransferase
At4g15610	-1,3392	-1,0204	-1,0722	-0,5082	-0,2648	-0,5614	hypothetical protein
At5g11810	-1,3486	-1,2774	-1,0845	-0,9391	-0,9292	-0,8972	putative protein
At3g55310	-1,2275	-1,1485	-1,0904	-0,9690	-0,7416	-0,6398	beta-ketoacyl-ACP reductase
At3g56200	-1,2632	-1,1783	-1,1166	-0,9144	-0,7140	-0,7451	putative protein neuronal glutamine transporter
At4g21680	-1,5040	-1,2614	-1,1456	-0,3099	-0,0929	-0,3592	peptide transporter - like protein peptide transporter (ptr1)
At5g63970	-1,2759	-1,2282	-1,1501	-0,4849	-0,5120	-0,3419	putative protein
At2g23540	-1,8807	-1,5559	-1,1617	-0,8539	-0,6981	-0,7038	putative GDSL-motif lipase/hydrolase similar to APG proteins
At1g64660	-1,4410	-1,2430	-1,1629	-0,8580	-0,5732	-0,2665	methionine/cystathionine gamma lyase
At2g18140	-1,4105	-1,2898	-1,1630	-0,4918	-0,5768	-0,7888	putative peroxidase
At3g26470	-1,4808	-1,3237	-1,1797	-0,4974	-0,3877	-0,6302	unknown protein
At5g25770	-1,4075	-1,2958	-1,2000	-0,5357	-0,4693	-0,4791	putative protein
At1g52060	-1,3385	-1,3632	-1,2099	-0,1874	-0,2132	-0,3625	jasmonate inducible protein
At5g05440	-1,5420	-1,3584	-1,2320	-0,0485	-0,0954	-0,8350	putative protein
At3g29410	-1,6401	-1,5094	-1,2440	-0,3838	-0,5514	-0,7243	terpene synthase
At4g33070	-1,6469	-1,4073	-1,3631	-0,5360	-0,3203	-0,9337	pyruvate decarboxylase-1 (Pdc1)
At2g44790	-1,5581	-1,4947	-1,3793	-0,4062	-0,5324	-0,9177	phytocyanin identical to GB:U90428
At2g34930	-1,6439	-1,4320	-1,3981	-0,0925	-0,4106	-0,0194	putative disease resistance protein
At3g26460	-1,7392	-1,7041	-1,4014	-0,6049	-0,5216	-0,5480	major latex protein
At5g16340	-1,7983	-1,4682	-1,4215	-0,7307	-0,6127	-0,9935	AMP-binding protein
At1g70850	-2,7686	-2,1128	-1,5040	-0,8901	-1,0296	-0,8464	major latex protein (MLP149)
At5g24420	-2,3769	-1,7703	-1,5654	-0,8064	-0,8995	-0,8573	6-phosphogluconolactonase-like protein
At4g28085	-1,8565	-1,8200	-1,7610	-0,6103	-0,5233	-0,4725	Expressed protein
At1g62660	-2,3095	-2,0674	-2,0268	-0,9878	-0,6743	-0,6463	beta-fructosidase
At4g15660	-2,4416	-2,3527	-2,2310	-0,0937	-0,5486	-0,6088	glutaredoxin
At4g19690	-2,7734	-2,6017	-2,4455	-0,6263	-0,8195	-0,7213	Fe(II) transport protein

Table 4.4. Genes induced or dis-repressed between day 19 and 25 in *co2* 1mM versus the 35S:: *FLC* plants. 35mM treatment was included as control. For 35S::FLC, the average between 23d and 28d under 1mM and 35mM were used. Values represent the log 2 scaled ratio of each day in *co2* 1mM vs 35S::FLC 1mM nitrate. The list includes genes with significant expression (≥ 2 fold changes) or unchanged expression (1≥ log2 ≥ -1).

Several transcripts increased significantly their expression in *co* induced plants grown under low nitrate whereas remained practically unchanged in response to high nitrate. Two CAAT binding transcription factors were induced (At5g06510 and At1g72830) upon flowering. Interestingly, both of them contain potential target sites for different microRNAs (MIR13, MIR43, MIR47 and MIR 57 regulate At1g72830; MIR 40 and MIR47 regulate At5g06510). Micro RNA-guided degradation of specific mRNAs has recently shown to be important in plant development, including the regulation of flowering time and floral organ identity (Palatnik *et al.*, 2003; Aukerman & Sakai, 2003; Chen, 2004). This indicates that the genes could be involved in the promotion of flowering time under lo nitrate conditions. A dof-type zinc finger domain containing protein (At1g51700) displayed slight tendency to increase, and interestingly the gene was also induced in *co2* plants grown under low nitrate compared to 35mM (see preceding table 4.3). Dof 1 transcription factors have been related with an improved nitrogen assimilation and growth under low nitrogen conditions (Yanagisawa *et al*., 2004).

Gene code	co19d 1mM vs FLC 1mM	co23d 1mM vs FLC 1mM	co25d 1mM vs FLC 1mM	co19d 35mM vs FLC 35mM	co 23d 35mM vs FLC 35mM	co 25d 35mM vs FLC 35mM	Descriptions
At2g46100	1,1425	1,0386	0,9759	0,6829	0,8003	0,6433	unknown protein
At2g28720	1,4631	0,9827	0,9130	-0,0839	0,3591	0,7328	putative histone H2B
rpl16.chlor.	1,4600	1,2273	0,8878	0,0517	0,3750	0,1443	ribosomal protein L16
At3g30180	1,3360	1,1484	0,8532	0,1515	0,3930	1,3319	cytochrome P450 homolog
ycf5	1,1671	1,1514	0,8512	0,3054	0,5833	0,4594	hypothetical protein
At1g48330	2,1623	1,1922	0,8312	0,1891	0,0728	1,3198	hypothetical protein similar to hypothetical protein GI:9294146
At5g45820	1,5873	1,1995	0,6996	-0,0262	0,1150	0,1046	serine threonine protein kinase
psaI	1,2947	1,1902	0,6128	0,2385	0,6108	0,3589	PSI I protein
rps16	1,6234	1,2732	0,6049	0,3769	0,8645	0,5214	ribosomal protein S16
At4g29610	1,4412	1,1843	1,2732	0,6495	0,8267	0,7405	cytidine deaminase 6 (CDA6)
At5g51010	1,1724	1,1575	1,0627	0,5545	0,5477	0,6175	unknown protein
At5g54190	1,1371	1,1029	0,9953	0,6144	0,3218	0,4709	NADPH:protochlorophyllide oxidoreductase A
At5g34940	-0,9765	-1,0005	-1,0959	-0,6910	-0,4933	-0,4197	putative protein heparanase
At1g72680	-1,0563	-1,0955	-1,0964	-0,7527	-0,6430	-0,6262	putative cinnamyl-alcohol dehydrogenase
At2g26870	-0,9975	-1,0198	-1,1076	-0,1908	-0,1061	-0,2076	putative phospholipase C
At4g31910	-0,9785	-1,0846	-1,1194	0,3264	-0,1473	-0,2596	putative protein anthranilate N-hydroxycinnamoyl/benzoyltransferase
At2g22470	-0,9580	-1,0640	-1,1653	0,3468	0,1548	0,0584	unknown protein
At1g78680	-0,9226	-1,2279	-1,2293	-0,9048	-0,5493	-0,5051	gamma glutamyl hydrolase
At5g38530	-0,9819	-1,1999	-1,2473	-0,9362	-0,8162	-0,4219	tryptophan synthase beta chain
At4g16740	-1,1801	-1,2238	-1,2501	-0,1760	-0,2187	-0,5296	limonene cyclase like protein
At1g76470	-0,9979	-1,2631	-1,3358	-0,6269	-0,6343	-0,9243	putative cinnamoyl-CoA reductase
At2g35730	-1,2013	-1,2195	-1,3793	-0,4804	-0,3450	-0,4258	Expressed protein
At3g50770	-1,4175	-1,5040	-1,5968	-0,9180	-0,9417	-1,3079	calmodulin-like protein flagellar calmodulin
At1g69920	-1,4774	-1,5117	-1,6163	-0,6253	-0,6831	-0,7690	putative glutathione transferase
At1g19610	-1,4588	-1,4982	-1,6256	0,0322	-0,0570	-0,7886	defensin AMP1
At3g46660	-1,4277	-1,5813	-1,6303	-0,0995	0,2010	-0,0834	glucosyltransferase-like protein UDP-glucose glucosyltransferase
At3g44860	-1,0394	-1,5603	-1,6391	-0,7616	-0,7556	-0,7127	AtPP -like protein AtPP protein

At2g02990	-1,1948	-1,4197	-1,6978	-0,0587	-0,0842	-0,4376	ribonuclease, RNS1
At5g05250	-1,4816	-1,8677	-1,8356	-0,0932	0,6090	0,3224	unknown protein
At3g53480	-1,5884	-1,6749	-1,8369	-0,2029	-0,3133	-0,3802	ABC transporter - like protein PDR5-like ABC transporter
At5g56080	-1,5370	-1,5722	-1,8619	-0,6364	-0,6650	-1,0390	nicotianamine synthase
At4g18440	-1,2361	-1,6100	-1,8643	-0,9720	-0,9250	-0,7417	adenylosuccinate lyase
At3g21670	-1,5753	-1,8541	-1,9788	-0,4733	-0,2643	0,0099	nitrate transporter
At3g44970	-1,7920	-2,0821	-2,0668	-0,5131	-0,3305	-0,6353	cytochrome P450
At1g52070	-1,9773	-2,0998	-2,1032	-0,0972	-0,3171	-0,2570	jasmonate inducible protein
At1g17020	-1,9681	-1,9428	-2,1731	-0,7009	-1,0803	-0,8085	SRG1-like protein, a new member of the Fe(II)/ascorbate oxidase superfamily
At4g12470	-1,3218	-2,1433	-2,1983	-0,6448	-0,0476	-0,8365	pEARLI 1-like protein Arabidopsis thaliana
At2g43820	-1,8584	-2,0240	-2,2158	-0,2374	-0,2095	-0,8680	putative glucosyltransferase
At1g10585	-1,9381	-2,0626	-2,2458	-0,1126	0,0864	-0,0432	Expressed protein
At4g22470	-1,5848	-1,5944	-2,2649	-0,5184	0,0279	-0,3381	extensin - like protein hybrid proline-rich protei
At3g56980	-1,5016	-2,0945	-2,3143	0,3536	0,2958	-0,0469	putative protein
At1g17180	-3,8725	-4,0656	-4,2000	-0,4428	-0,3866	-0,6846	putative glutathione transferase

Table 4.5. Genes with gradual repression between day 19 and day 25 in *co2* 1mM versus the 35S:: *FLC* plants.. 35mM treatment was included as control. For 35S::FLC, the average between 23d and 28d under 1mM and 35mM were used. Values represent the log 2 scaled ratio of each day in *co2* 1mM vs 35S::FLC 1mM nitrate. The list includes genes with significant expression (≥ 2 fold changes) or unchanged expression (1≥ log2 ≥ -1).

The expression of known central genes involved in the transition to flowering was investigated in *co2* induced plants versus the control 35S::*FLC* in response to both conditions of nitrate (see table 12, section 7.18 from the Appendix).

Most of the genes involved in flowering time, presented non-significant changed expression between all the comparisons. Among the positive regulators of flowering, only *CO*, *SOC1/AGL20* and a putative bZip transcription factor (FD) showed significant up-regulation, whereas a NAC domain protein and the transcription factor *SPL3* were down-regulated in any given time point. Regarding the negative regulators of flowering, *SVP* (short vegetative phase), a putative AP2 domain protein and *ELF3* showed slight induction in any of the conditions whereas *VIP3* and the floral repressor *FLC* showed strong down regulation.

Results from this part concluded that there must be changes at transcript level upon the floral transition that are responding to nitrate as signal molecule, however, their identification remains unknown. Flowering is a very complex regulated by multiple factors, and thus, it is very difficult to distinguish among signals coming from nitrate itself or other known signalling pathways involved in flowering.

CHAPTER 5 DISCUSSION

5. CHAPTER: DISCUSSION

The overall objective of this study was to investigate the physiological importance of carbon/nitrogen interaction as a vital process controlling plant growth and development. For this purpose, two different approaches were considered:

1.- A major effort to understand the function of GDH through a forward genetic approach yielding GDH transgenic plants with reduced GDH activity.

2.- The analysis of the influence of nitrogen, and in particular nitrate, in one of the most important aspects of plant development the transition from vegetative to reproductive stage.

5.1. Physiological significance of GDHs

For many years it was thought that bacteria and higher plants assimilate ammonia into glutamate via the GDH pathway, as in certain fungi and yeasts. In 1970, it became clear that in bacteria an alternative pathway of ammonia assimilation (involving glutamine synthetase (GS) and NADPH-dependent glutamine 2-oxoglutarate amidotransferase (GOGAT) or glutamate synthase) should be operating in response to low ammonia concentrations in the growth medium (Tempest *et al*., 1970). *Escherichia coli* is known to have two primary pathways for glutamate synthesis, one, the GS-GOGAT pathway, essential for glutamate synthesis and maintaining of the glutamine pool under low ammonium concentrations and in those conditions when the cell is not under energy limitation since the reaction involves the participation of ATP (Helling, 1994; 1998). The second pathway for glutamate synthesis is the GDH pathway, which is able to operate as the only pathway provided the media contains high concentrations of ammonium and in energy supplying limitations (Helling, 1994; 1998). In the cyanobacteria *Synechocystis* sp. strain PCC 6803, the presence of GDH appears to offer a selective advantage under non exponential growth conditions, while GS-GOGAT is the primary pathway of ammonia assimilation (Chavez *et al.,* 1999).

The yeast *Saccharomyces cerevisiae* synthesizes glutamate through the action of either NADP(H)-glutamate dehydrogenase encoded by *GDH1* (under conditions of ammonia excess) or through the combined action of GS and GOGAT encoded by *GLN1* and *GLT1* (under ammonia limitation conditions) (Avendano *et al*., 1997). A third pathway for glutamate biosynthesis has been also suggested since a double mutant of *S. cerevisiae* lacking NADP(H)-GDH and GOGAT activities was able to grow on ammonium as the sole nitrogen source (Avendano *et al*., 1997).

GDH was thought to be the main route for ammonia assimilation and glutamate biosynthesis in higher plants prior the discovery of GS-GOGAT cycle by Miflin & Lea (1980).

Since most organisms possess the two pathways to produce glutamate, GS/GOGAT and GDH, it is important to elucidate whether this redundancy in the primary incorporation of ammonium has a biological significance. Glutamine synthetase seems to be the unique enzyme involved in the biosynthesis of glutamine, an essential amino acid playing a central role in nitrogen metabolism in all organisms. On the other hand, the necessity for NAD(P)H-GDH participation has been matter of discussion due to the concomitant involvement of GOGAT in glutamate formation.

In vascular plants the in vivo direction(s) of the GDH reaction and hence the physiological roles of the enzyme remain obscure. Current opinion is divided as to whether GDH plays (1) a role in ammonia assimilation, under high ammonium concentrations, (2) a role in glutamate catabolism or (3) a redundant and dispensable role in nitrogen assimilation. According to Melo-Oliveira *et al*., (1996) GDH plays a minor role, if any, in the re-assimilation of photorespiratory ammonia, but could be involved in ammonia detoxification since its activity was increased in plants exposed to high levels of ammonia. However, the isolation of photorespiratory mutants defective in GS (Wallsgrove *et al.,* 1987) or GOGAT (Kendall *et al*., 1986; Somerville & Ogren, 1980) together with analyses of plants treated with MSO (methionine sulfoximine, an inhibitor of GS) suggested that GDH should not be important in photorespiration, arguing against its biosynthetic role. Other studies have proposed a role for GDH in the assimilation of ammonia into glutamate under particular physiological conditions for example in old source leaves when nitrogen remobilisation is maximal (Srivastava & Singh, 1987; Masclaux *et al*., 2000; Masclaux *et al*., 2006) leading to the proposal that the physiological role of the enzyme could be to synthesize glutamate for transport in senescing leaves (Miflin & Habash, 2002) consistent with the higher activity of GDH in response to a natural senescence (Masclaux *et al*., 2000; Masclaux-Daubresse *et al*., 2002), but all ^{15}N labelling experiments performed in vivo on a variety of plants have demonstrated that GDH should operate in the direction of Glu deamination (Robinson *et al*., 1992; Fox *et al*., 1995; Stewart *et a*l., 1995; Aubert *et al*., 2001).

It has been also suggested that GDH is involved in the supply of 2-oxoglutarate rather than in assimilation of ammonium (Robinson *et al*., 1992; Aubert *et al*., 2001; Miflin & Habash, 2002)

or in recycling nitrogen from amino acids into asparagine when carbon becomes limiting (Melo-Oliveira *et al*., 1996; Lam *et al*., 1998; Thimm *et al*., 2004; Price *et al*., 2004; Osuna *et al*., 2007). The recent finding that GDH is mostly located in vascular tissue, led some authors to propose that the enzyme could also play a sensing role in C and N metabolite through the phloem stream during plant growth and development (Tercé-Laforgue *et al*., 2004).

All these controversial suggestions about the main role of GDH are still matter of discussion and lead to affirm that the presence of the enzyme in plants suggests that it has a role but not what that role is (Miflin & Habash, 2002).

A major effort to understand the physiological significance of GDH in *Arabidopsis thaliana*, was the identification of KO mutants and RNAi with altered expression of each individual GDH. If GDH plays a role in ammonia assimilation or ammonia release, plants with altered GDH expression should reveal changes on nitrogen metabolism and/or on sugar status in the plants.

5.2 Preliminary characterization of *GDH* mutants refutes the assimilatory role of GDH

Studies of mutants lacking GDH activity (Magalhaes *et al*., 1990; Melo-Oliveira *et al*., 1996) begun to shed some light on the role of GDH in plants. The *GDH1* null mutant of *Zea mays* exhibited 40-50% lower rate of $^{15}NH_4$ assimilation into total reduced N and a lower shoot:root ratio than the wild type, suggesting a role of the enzyme in ammonium assimilation (Magalhaes *et al*., 1990). Similarly in *Arabidopsis thaliana*, a *GDH* null mutant displayed a growth effect specifically in the presence of exogenously supplied inorganic N, supporting the notion that GDH could play a role distinct from that of GS in ammonia assimilation (Melo-Oliveira *et al*., 1996). However, no labelling or inhibitor evidence supported the assimilatory function of GDH. Based on our studies with mutants and transgenic plants lacking *GDH1* gene or with reduced *GDH2* expression, it is difficult to assess a possible function of the enzyme in the assimilation of ammonium especially since loss of function did not show a revealing phenotype when compared to the wild type. This is in agreement with the fact that GS is present and able to function, so there should not be a clear reason why assimilation of NH_3 should affect growth. Moreover, the reduction of GDH activity in the double mutant *GDH1*KO-*GDH2*RNAi, did not have an influence in the level of nitrogen-containing metabolites such as amino acids or protein content, suggesting that GDH may not be involved in the assimilation of ammonia at least in the conditions used in the analysis.

5.3 Carbon starvation induces GDH expression and activity in wild type plants and leads to accumulation of sugars in transgenic plants with reduced GDH activity.

The effect of carbon supply on GDH activity has been much studied in plants and there is agreement in the fact that sugars exert a regulatory effect on the enzyme (Robinson *et al*., 1991). Previous studies in carrot cells (Robinson *et al.,* 1991) showed an increase of GDH activity under conditions of carbon limitation, leading them to suggest a role for GDH in the oxidation of glutamate in order to provide carbon skeletons for effective functioning of the TCA cycle. Similar results were shown in *Arabidopsis*, where GDH mRNA accumulated to high levels in dark-adapted or sucrose-starved plants, supporting the catabolic role of GDH under carbon-limiting conditions (Melo-Oliveira *et al*., 1996). Moreover, GDH expression was specifically repressed by light or by the addition of exogenous carbon (Melo-Oliveira *et al*., 1996) consistent with previous results that showed the repression of GDH activity caused by the addition of various sugars (Oaks *et al.,* 1980; Sahulka *et al.,* 1980). Accordingly, the age-related induction of GDH in a range of plant tissues could be explained in part by a depletion of carbohydrates usually observed during senescence (Srivastava & Singh, 1987; Masclaux *et al*., 2000). However, conclusive results came from ^{15}N and ^{13}C labelling experiments that clearly demonstrated that GDH is only able to supply 2-oxoglutarate to tissues when carbon is limited (Aubert *et al*., 2001; Robinson *et al*., 1992).

During work presented in this thesis, the expression of GDHs in wild type plants was studied in response to sugar starvation. Carbon starvation induced the expression of *GDH1* and *GDH2* whereas re-addition of the sugar resulted in the down-regulation of both genes. Moreover, the observation that *GDH2* expression is also induced in response to phosphate starvation was previously shown by Wu *et al*., 2003 supporting a catabolic role for GDH in order to provide NH_4^+ for the cycle of Gln to Glu. The induction of GDH upon phosphate starvation is consistent with the fact that phosphate depletion leads to repression of photosynthesis resulting in carbon starvation which indeed could trigger the catabolism of proteins and amino acids and release of NH_4^+.

The expression of *GDH1* and *GDH2* showed diurnal regulation, peaking towards the end of the night and dropping to lowest levels at the end of the light period of a normal day cycle. Transcripts for *GDH1* and *GDH2* rise dramatically when plants are exposed to a prolonged night period, indicating the depletion of carbon in the plant (Thimm *et al*., 2004; Gibon *et al.,* 2004b). In addition, Gibon and co workers demonstrated that the increase in *GDH* transcripts

after a prolonged night led to an increase in GDH activity after a considerable time lag (Gibon *et al.,* 2004b). The induction of GDH under carbon depletion (sugar limitation or dark adaptation of plants) led to propose some hypothesis about its possible function(s) in plants.

The first hypothesis suggests GDH as a key step in amino acids catabolism in order to supply carbon skeletons, in terms of 2-oxoglutarate, to the TCA cycle function (figure 72), as outlined above.

The second hypothesis is derived from the fact that carbon starvation limits ammonium assimilation (Stitt & Krapp, 1999; Osuna *et al*., 2007) amino acid biosynthesis (Stitt & Krapp, 1999; Thimm *et al*., 2004; Osuna *et al*., 2007) induces several genes assigned to amino acid breakdown (Thimm *et al*., 2004; Osuna *et al*., 2007) and induces expression and activity of *ASN1* (Lam *et al*., 1994; 1998; Thimm *et al*., 2004; Osuna *et al*., 2007). Under these conditions, *ASN1* is supposed to redirect the flow of nitrogen from Gln into Asn for nitrogen transport (Lam *et al*., 1994, 1995) supporting the idea that under carbon limitation *GDH1* and *GDH2* could be implicated in ammonia recycling from glutamate for its incorporation into the amino acid Asn by the concerted action of *ASN1* and cytosolic *GS* (Lam *et al.,* 1998; see figure 72).

A third hypothesis is related to the energy requirements within the cell. During the light period, plants convert the light energy to chemical energy in the form of ATP and NADH that is used to fix carbon dioxide into carbohydrates used for synthesis of other organic compounds such as starch, cellulose, precursors for lipids, nucleotides and amino acid biosynthesis. Part of the photosynthates accumulated during the light period, usually starch, are remobilised to support sucrose synthesis and export at night (Stitt *et al*., 1987; Geiger and Servaites, 1994; Scheible *et al*., 1994; Stitt, 1996; Geiger *et al*., 2000). Carbon starvation or extended night conditions lead to decreased expression of genes assigned to TCA cycle, mitochondrial electron transport and ATP synthesis (Thimm *et al*., 2004; Osuna *et al*., 2007) consistent with a general slowing down of respiration energy metabolism. Hence, deaminating GDH could help the electron chain supplying redox groups in the form of NADH in order to support energy metabolism in response of carbon starvation (see figure 72). This notion is supported by the induction of several genes encoding NADH dehydrogenases in the mitochondrial electron transport chain (Thimm *et al*., 2004). In that case, the oxidation of glutamate could be considered as a key

anapleurotic process linking amino acids metabolism with TCA cycle activity (Miflin & Habash, 2002).

Double transformant plants (*gdh1*KO-*gdh2*RNAi) displayed a 2 fold reduction in total GDH activity during a normal diurnal cycle and the total activity did not increase in the transformant plants compared to the wild type during the extended night period (carbon depletion situation). The composition of soluble sugars (glucose, fructose and sucrose) showed a similar pattern between transformant and wild type plants, suggesting that the reduction of GDH activity should not have an effect in the accumulation of sugars during a normal diurnal cycle. The only difference was that the timing of the degradation of starch during the night was apparently altered in *gdh1*KO-*gdh2*RNAi. Starch breakdown is linear throughout the night in wild type *Arabidopsis*, as in other plants (Fondy & Geiger, 1985; Geiger & Servaites, 1994; Matt *et al*., 1998; Stitt *et al*., 1987; Zeeman *et al*., 1998; Gibon *et al*., 2004a). This pattern was seen in the controls wild type and wild type with the empty vector in the present experiments. Strikingly, in *gdh1*KO-*gdh2*RNAi starch breakdown was inhibited in the first 6 hours of the night, and starch breakdown was accelerated in the second half of the night. However, more independent experiments are needed to confirm this observation. In the single *gdh1*KO mutant and in the *gdh1* RNAi lines, such delay in starch breakdown was not observed.

Similarly, no significant changes were observed in the pool of free amino acids measured, suggesting that *GDH1* and *GDH2* may not be involved in the assimilation of amino acids during the day and in response to a prolonged period of night. Considering our previous hypothesis, another alternative could involve GDH in the recycling of ammonium from glutamate for its assimilation into Gln and Asn in response to carbon limitation (e.g. extended night period), but based in our experiments no significant changes were observed in the pool of or derivatives such as Gln, Asn, or Asp. This could be explained by the fact that the GS/GOGAT cycle is present and able to fulfil its function under those conditions. Moreover, it could also be possible that the oxidation of glutamate could produce 2-oxoglutarate for its use in the TCA cycle in response to low carbon, but no convincing evidences supported this notion. Other experiments should be needed to help to understand the role of GDH in *Arabidopsis thaliana* in such conditions.

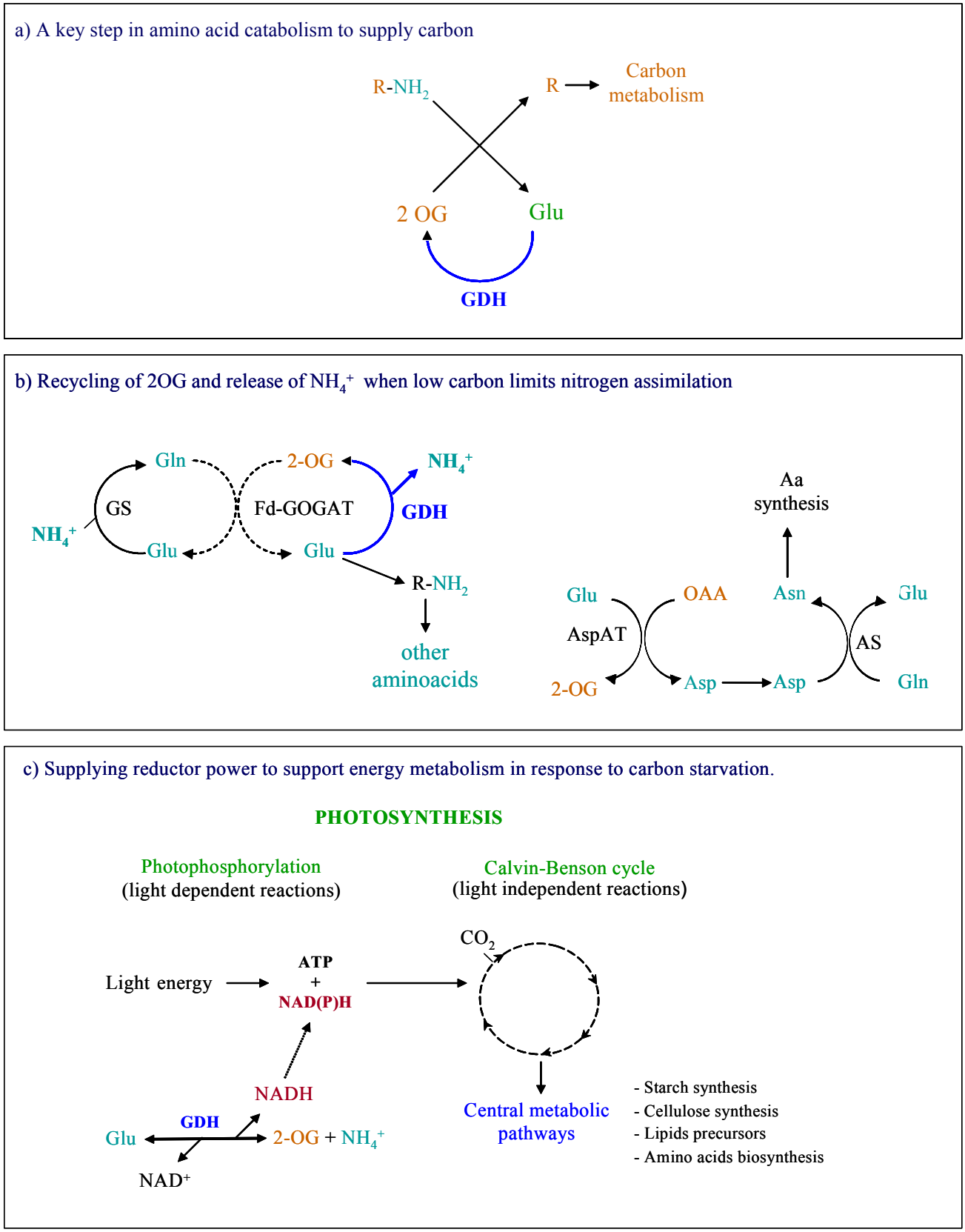

Figure 72. Hypothesis of the role of GDH in response to low sugars. a) GDH plays a key step in the catabolism of amino acids supplying carbon in terms of 2-oxoglutarate. b) GDH plays an important role in 2-oxoglutarate recycling and in the ammonium release for synthesis of other amino acids via amino transferases when the assimilation of ammonium is inhibited in response to low sugars. c) GDH deaminating reaction supports energy metabolism by supplying redactor power in form of NADH. In blue, the reaction catalysed by GDH in the given situation.

Nitrogen assimilation is not a simple process and it can be influenced by a large range of substrates and metabolites at multiple levels under different environmental conditions. So far it is known that the rate of photorespiration influences significantly the content of amino acids exported in leaves under light conditions in C3 species (Madore & Grodzinski, 1984). Thus, it is possible that in the dark, the activity of glycine decarboxylase confers an alternative route for ammonium release as a result of high photorespiratory activity occurring during the day. Therefore, during the analyses, a further set of experiments were carried out in which seedling were grown for 11 days in a 12h light/ 12h dark light regime on vertical agar plates in the absence of added sugar and the roots were separated from shoots in order to avoid such factors like photorespiration.

The analysis of plants with reduced total GDH activity (*gdh1*KO-*gdh2*RNAi) in these conditions revealed an unexpected accumulation of soluble sugars (glucose, fructose and sucrose) compared to wild type at the end of the light period and after 11 days growing in the sugar free medium (see section 3.5.1). Thus, there was a higher internal content of sugars and higher levels of starch in the mutants compared to wild type. Towards the end of the night the increase in soluble sugars and starch content was less marked, and there were similar levels to wild type after 24h of extended night. These results differ from the analyses in rosettes in older plants on soil, where carbohydrates were unaltered or even slightly lower in *gdh1*KO-*gdh2*RNAi and it is contradictory to previous hypothesis involving GDH in the recycling of ammonia for its incorporation into other amino acids or in the supplying of C-skeletons for the TCA cycle to work in conditions of limiting carbon. According to that hypothesis, a reduction of GDH activity could lead to lower amounts of 2-oxoglutarate and furthermore to lower levels of sugars instead of their accumulation. Accumulation of sugars could be triggered by the inhibition of their utilization for transport during the day in response to carbon limiting conditions, however, plants did not reveal any visible growth phenotype (data not shown) as it has been suggested by some authors (Thimm *et al*., 2004; Gibon *et al*., 2004a). Another possible explanation could be that the synthesis of sugars and therefore their accumulation is stimulated towards the production of starch for storage, however, this suggestion is contradictory to results shown by Thimm and co workers indicating the induction of genes involved in nutrients breakdown in response to low carbon (Thimm *et al.,* 2004) and thus, there should not be a need for synthesise glucose in carbon limiting conditions. The increase in starch content during the day could be directly a consequence of extreme limitation of carbon sources during the night in a sugar free medium. Higher starch would provide a larger store to

support metabolism and carbon export during the night in carbon limiting conditions. These results contrast to those of plants grown in soil and differences could be explained by the different experimental system.

Regarding the nitrogen metabolism compounds, no changes were observed in the pool of free amino acids or in the total content of proteins suggesting the enzyme is not involved in the synthesis of glutamate under such conditions of sugar limitation.

However, as there is still remaining GDH activity, the simplest explanation could be that the transgenic approach did not success in decreasing the total GDH activity enough to see a phenotype and thus, the remaining activity should be able to compensate that decrease in total activity.

These experiments do not yet define the role of GDH. The decrease in activity in *gdh1* (2-fold decrease in *gdh1KO* and 1.8-fold in *gdh1*RNAi), in *gdh2*RNAi (1.7-fold decrease), and in *gdh1*KO-*gdh2*RNAi genotypes (around 1.5-2-fold decrease), during the diurnal cycle did not lead to major or reproducible changes in growth or the levels of carbohydrates or amino acids. *GDH* transcripts are induced and GDH activity rises around 1.5-fold in wild type plants during carbon starvation in an extended night. Genotypes with lower activity during the extended nigh (2-fold decrease in *gdh1KO* and 1.5-fold in *gdh1*RNAi; a decrease of 2.2-fold in *gdh2*RNAi; and around 1.5-2-fold decrease in *gdh1*KO-*gdh2*RNAi), did not show any major changes in the levels of carbohydrates or amino acid, and did not show any of the specific responses predicted by the existing hypotheses about the role of GDH. Two obvious possibilities remain. One is that GDH activity has not been decreased enough in the *gdh1*KO-*gdh2*RNAi lines to lead a metabolic phenotype. The other is that GDH is completely redundant.
To elucidate the accumulation of sugars in plants with decreased GDH expression and activity, other measurements may also be needed including determination of enzymes involved in TCA cycle (malate dehydrogenase) glucose synthesis (PEPCK) or degradation (pyruvate kinase), starch synthesis (AGPase) and enzymes involved in assimilation of ammonia and amino acids production (GS/GOGAT, AspAT, AS).

5.4. Expression pattern of the putative GDH (*GDH3*) reveals different role compared to *GDH1* and *GDH2.*

A third gene encoding for NAD(H)-GDH is termed *GDH3* or putative NAD(H)-GDH. The putative NAD(H)-GDH encodes a protein of around 44,53 KD with high similarity to GDH1 protein sequence (92% protein identity). So far, nothing is known about its possible function in plants.

The expression pattern of the putative NAD(H)-GDH analysed by real time RT-PCR, promoter GUS fusion and AtGenExpress gave an indication about its tissular localization and metabolic regulation. On a whole plant level, the *GDH3* gene was found to be poorly expressed in vegetative tissues of young plants grown in soil. Transcript increased with aging of the plant. Furthermore, the gene was higher expressed in vascular tissue of old leaves, also localised in the main part of the root and in petals of old flowers. Accordingly, RT-PCR expression analysis and promoter-*GUS* fusion data were confirmed by AtGenExpress data from Affymetrix ATH1 microarrays that in addition showed a marked expression of *GDH3* in hypocotyls of young seedlings. The expression pattern displayed by *GDH3* suggests that it may be involved in the recycling of ammonium in senescing tissues in order to support the growth of young parts of the plant. Consistent with that idea, Miflin & Habash (2002) proposed that the up regulation of GDH in senescing leaves should lead to glutamate production for translocation. The proposed function of *GDH3* in sensing C:N metabolites of phloem stream is consistent with the localisation of the enzyme in vascular tissue, specifically in phloem companion cells (Laforgue *et al*., 2004). Additionally, the high expression of *GDH3* detected in hypocotyls could involve the enzyme in the recycling of ammonium from glutamate for its assimilation and transport to developing tissues suchlike stem and cotyledons, since hypocotyls is the primary organ of extension of the young plant that develops into the stem.

Regarding the metabolic regulation of the gene, it has been shown that the putative NAD(H)-GDH is induced in conditions of nitrate starvation (Scheible *et al*., 2004) and repressed with the nitrate re-addition (Scheible *et al*., 2004). This again could implicate the gene in the recycling of ammonium during amino acid catabolism. In contrast to *GDH1* and *GDH2*, the putative *GDH3* is not up-regulated in response to sugar starvation, which induces the other two members of the GDH family (Thimm *et al*., 2004; Osuna *et al*., 2007) supporting the distant role of *GDH3* compared to the others. These results were confirmed by promoter-*GUS* fusion analyses of the gene in response to various concentrations of nitrate (0,150mM, 1mM, 3mM

and 35mM KNO_3), without additional source of glutamine. Under nitrate starvation conditions (0,150mM KNO_3), GUS activity was localised mainly in veins of cotyledons, slightly present in hypocotyl and markedly expressed along the root, especially at the upper part, secondary roots and root tip. In response to low nitrate (1mM KNO_3), *GDH3* appeared to be weakly present in cotyledons, markedly expressed in hypocotyl and specifically localised in the upper part of the root. In response to 3mM KNO_3, the expression of *GDH3* was similar to that shown for 1mM KNO_3 treatment. In response to high nitrate (35mM KNO_3), *GDH3* expression appeared to be weakly localised to main vascular veins and hypocotyl and absent in root tissue. The gradual decrease of *GDH3* expression shown in parallel to the increasing external nitrate is consistent with the previous hypothesis that involves *GDH3* in the catabolism of amino acids in response to nitrate limitation. In such conditions, *GDH3* would provide an additional form of nitrate scavenging to supply a nitrogen source to GS/GOGAT cycle for its assimilation and transport into other amino acids (Gln, Asp, Asn).

On a whole plant level, considering the non overlapping expression patterns observed for *GDH3* and its closely related *GDH1*, it is likely that *GDH3* and *GDH1*/*GDH2* are not functionally redundant in conditions of nitrate starvation. This is supported by the fact that *GDH3* is not up regulated in low sugar conditions (Thimm *et al*., 2004; Osuna *et al*., 2007), it does not display diurnal regulation, and it shows poor expression in vegetative tissues compared to the other NAD(H)-GDHs.

5.5. Decreasing *GDH3* expression led to lower amino acids and protein content under high nitrate conditions.

Down regulation of *GDH3* gene expression resulted in changes regarding the pool of nitrogen compounds under different concentrations of nitrate. Plants with reduced expression of *GDH3* (*GDH3* RNAi) showed slightly lower content of total amino acids and lower amounts of total proteins in response to high nitrate. This could in principle be due to decreased amino acid synthesis, increased amino acid degradation or increased use of amino acids for protein synthesis in such conditions. When compared to their respective control lines, differences among transformant and wild type plants were more evident in root tissue than in shoots.

Under high nitrate conditions, the putative GDH seems to be involved in the synthesis of glutamate for further synthesis of other amino acids rather than in the ammonia recycling from glutamate. This is supported by the notion that a decrease on *GDH3* expression led to a reduction in glutamate content and its derivatives amino acids Gln, Asp and Asn. The organic acid 2-oxoglutarate would therefore be accumulated and used by the TCA cycle for glucose

synthesis and energy production. Also, 2-oxoglutarate could be used as acceptor for ammonia upon synthesis of amino acids. Taken together, all this data propose that *GDH3* could be playing an alternative role to GS/GOGAT in glutamate synthesis, although there are many evidences against this suggestion (see section 5.2).

A reduction in *GDH3* expression could have an influence in the level of sugars in the plant, however, no alterations in the carbohydrates content were observed suggesting that *GDH3* may not be involved in the accumulation of carbohydrates in the plant at least in response to the different nitrate concentrations used in the analysis.

5.6. GDH3 RNAi plants displayed improved growth

The effect of *GDH* gene on plant growth and development has been studied in transgenic tobacco plants expressing a bacterial NADP-GDH gene from *E.coli*. Tobacco plants expressing ectopic GDH displayed significant increased biomass compared to control lines (Ameziane *et al*., 2000). Similar results were previously observed in transgenic Lotus plants over-expressing GS in which the changes in plant biomass were explained by improved ammonium assimilation in the transgenic plants correlated by a large increase in amino acids content (Hirel *et al*., 1997). However, the direct involvement of GDH in the increased biomass needs to be proven.

Considering that the putative GDH could be involved in the recycling of ammonium from glutamate in response to low nitrogen and based on previous experiments shown by Melo-Oliveira and co workers, it would be expected that genotypes with reduced *GDH3* expression display impaired growth phenotype under such conditions. However, contrary to earlier observations, plants with decreased *GDH3* expression showed improved root and shoot growth compared to control lines (see section 3.6.2.6). A possible explanation for the unexpected phenotype could be that *GDH3* forms part of a futile cycle, in which proteins and amino acids breakdown are induced during the response to low nitrogen (Scheible *et al*., 2004). The additional ammonium recycled from glutamate by *GDH3* would be re-assimilated into glutamate by GS/GOGAT, a reaction that is energetically expensive consuming 1 ATP for the production of 1 mol of glutamate. According to that, those plants with a reduction in *GDH3* expression could have less amount of free toxic ammonium to be assimilated into amino acids and therefore less energy should be dissipated for its assimilation into amino acids. In addition, the possibility that the RNAi construct could have secondary effects may be excluded since the control line with empty vector showed similar growth to the normal wild type.

Plants over expressing *GDH3* could give an indication about the unexpected phenotype in response to low nitrogen.

5.7. Influence of nitrate in the transition to flowering time in *Arabidopsis thaliana.*

As already mentioned, the transition to flowering is regulated by several environmental stimuli including day length, temperature, light quality and nutrient availability (Bernier *et al.*, 2003; Simpson *et al*., 1999; Reeves & Coupland, 2000). For almost a century the plant nutritional status was believed to be an essential factor in the control of flowering time. Klebs (1913) suggested that a high endogenous ratio of carbohydrates to nitrogen promotes flowering whereas a high nitrogen availability, resulting in a low C:N, promotes vegetative growth. This idea was inferred from the facts that favourable photosynthetic CO_2 fixation generally accelerates flowering whereas a high nitrogen supply (fertilizer) delays or reduces reproductive development in some plants (reviewed in Bernier *et al*., 1981). On the other hand, Sach & Hackett (1977) proposed that floral induction consists of modification of source:sink relationships in the way that the shoot apical meristem (SAM) receives a better supply of assimilates (mainly carbohydrates). However, Raper *et al*., (1988) and Rideout *et al*., (1992) hypothesized that floral transition is induced by an imbalance in the relative availability of carbohydrates and nitrogen in the SAM. The importance of an appropriate C:N ratio for the promotion of flowering has been also observed in vitro, as for example in *Torenia fournieri* (Tanimoto & Harada, 1981), *Pharbitis nil* (Ishioka *et al*., 1991) and tomato (Dielen *et al*., 2001). Also, the delay in flowering time caused by high concentrations of nitrogen in the medium was previously reported (reviewed in Bernier *et al*., 1981; Dickens & van Staden, 1988; Bernier, G. *et al*., 1993).

Nitrate emerges as a metabolite that triggers widespread and coordinated changes in metabolism and development (Stitt, 1999). Studies of rapid changes in gene expression (Wang *et al*., 2000) and studies of changes in genes expression, metabolism, whole plant allocation and root architecture in mutants with decreased expression of nitrate reductase (Stitt, 1999; Stitt & Scheible, 1999) show that nitrate, rather than metabolites further downstream in nitrogen metabolism, is the parameter sensed by the plant.

The effects of nitrogen on flowering time could be due to nitrogen acting as a resource, affecting growth directly, or serving as a signal molecule that influences the transition of flowering time in the plant. Hence, one of the main aims of this work is to add novel findings on the effects of different nitrate concentrations in the regulation of the transition to the floral

stage and to elucidate if nitrate is serving as a signal molecule involved in the regulation of the transition to flowering time in *Arabidopsis thaliana.*

5.8. Nitrate as signal molecule.

A role for nitrate as a signalling molecule comes from physiological studies in the 1950s showing that a treatment with nitrate was able to induce nitrate reductase activity (NR) and nitrate transport. Twenty years later, antibodies against NR indicated that NR was induced by nitrate and furthermore it was demonstrated that nitrate applications induced the expression of NR and other genes involved in C and N metabolisms (Crawford, 1995; Forde, *et al*., 1999). Tobacco plants with low NR activity indicated the ability of nitrate to regulate gene expression even thought it could not be reduced and further metabolized (Scheible *et al*., 1997a).

To dissect the response of flowering to nitrogen sensing and signalling, it is therefore necessary to develop an experimental system that allows separating the impact of nitrogen on growth from the action of nitrate as a signal molecule. The approach taken differs from that used in earlier studies of the role of nitrate in the regulation of metabolism of shoot/root ratios, where genotypes with decreased NR activity were used. In this method plants were grown with 4mM glutamine as a constitutive nitrogen source that prevents nitrogen deficiency in low nitrogen conditions, and to prevent large changes in the rate of plant growth ensuring rapid growth to the plants.

Previous work by Dr. Irene Loef showed that high nitrate delayed flowering, in time (enlarged vegetative phase) and related to leaf number and plant biomass. Also, results from her work revealed that the level of metabolites such as amino acids, protein, or sugars were similar in plants grown in high nitrate or in low nitrate, indicating that the effect of nitrate was not related to changes in the level of key metabolites in the leaf. The root:shoot ratio decreased as the nitrate level in the medium increased showing that the experimental system captures growth and responded to nitrate.

Nevertheless, the role of nitrate as signalling molecule involved in the induction or repression of flowering is too simple and other factors and signals must be taken into account. It is already known that nitrate signal can interact with signals generated further downstream in nitrogen metabolism and that those downstream products (ammonium or Gln/Glu) might act as signalling molecules (Scheible *et al.,* 1997b; Stitt, 1999). This is confirmed by the molecular evidence of Gln acting as signalling molecule that regulates the expression of the ammonium

transporter AMT1 in *Arabidopsis* roots (Rawat *et al*., 1999). Also, the concentration of the amino acid glutamine increased when *Arabidopsis* plants are exposed to long days that induce flowering in *Arabidopsis* (Corbesier *et al*., 2000).

5.9. Regulation of flowering time by nitrate in response to different photoperiods.

Photoperiodism is one of the most important factors affecting the timing of flowering.

The effect of different concentrations of nitrate (1mM, 10mM and 35mM KNO_3) in the transition to flowering time in Col-0 under different photoperiods (16h, 12h and 8h light) was investigated by Dr. Irene Loef. Results from her work, indicated that under short day conditions, high nitrate led to a strong delay in flowering time whereas low nitrate caused earlier floral initiation. Moreover, the delay in flowering time by high nitrate was slightly reduced in neutral day conditions, and completely absent in long days (condition in which all plants flowered at the same time in response to all nitrate concentrations). These results indicate that the day length signal abolishes the influence of nitrate signal in the transition to flowering.

Leaf number (considered as an indication of the physiological age of the plants) confirmed that the delay in flowering time under short day photoperiod was due to a prolonged vegetative phase probably caused by the influence of high nitrate in the medium. Plants grown under neutral day exhibited slight differences in leaves number among the different nitrate treatments. By contrast, under long day photoperiod plants flowered at the same time independently of other factors and presented similar number of leaves in response to all the nitrate treatments. In addition, differences in the shoot:root ratio were visible in response to short days, with an increase of shoot:root ratio according to the increasing external nitrate. This observation is in agreement with Scheible *et al.,* 1997a, suggesting that high nitrate leads to a stimulation of shoot growth and inhibition of root growth. Variations in the shoot:root ratio were less marked in response to neutral days and practically unchanged under long day between the different nitrate conditions.

The content of nitrate in the plant was influenced by external concentration of nitrate, so that higher external nitrate led to higher internal concentration. By contrast, the day-length did not affect the internal nitrate concentration, which presented similar values under all photoperiods. Regarding the total amino acids pool, the reduction in the light period resulted in a general decrease in the total amino acids content, which was independent of the external nitrate

concentration. This is consistent with studies from Matt *et al.,* 1998 indicating that tobacco plants grown under short day conditions contained lower amounts of *NIA* transcript and lower NR activity, leading to high levels of nitrate and low levels of amino acids, indicating that nitrogen assimilation was inhibited as a consequence of a low carbon fixation during the short light period. Similarly, individual nitrogen-containing amino acids (Gln, Glu, Asp and Asn) showed independence of the external nitrate concentration and presented slightly decrease in response to short photoperiods. These results suggest that nitrogen-containing amino acids may not be involved in the regulation of flowering time by nitrate arguing against the idea that proposed amino acids (especially Gln and Asn) as controlling factors of the floral transition in some plants (Corbesier *et al*., 1998; Corbesier *et al*., 2000; Suárez-López, 2002).
The content of glucose and fructose decreased in short day conditions. Similarly, sucrose level decreased in short day regime. The starch content was highest in low nitrate under short day light period and markedly reduced with the additional external nitrate, supporting the notion that high nitrate inhibits the synthesis of starch (Scheible *et al*., 1997b; Stitt, 1999).

5.10. Flowering time mutants respond to external nitrate concentration.

The use of flowering mutants has been of crucial importance for the study of mechanisms that control flowering time in *Arabidopsis thaliana*. The behaviour of mutants exhibiting a severe delay in flowering was first described in detail by Redei in 1962 and later broadened and extended by Koornneef (Koornneef, Hanhart & Van Der Veen, 1991; Koornneef *et al*., 1998). More recently a large number of mutants and natural accessions showing either earlier or later flowering have been described by Mouradov *et al*., (2002) and the genes identified by mutagenesis were placed in pathways based on genetic criteria and their effect on the response of flowering time to different environmental cues (Koornneef *et al*., 1998).

In order to gain insights into the influence of nitrate on floral initiation, different mutants affected in flowering pathways were used and studied in response to three different concentrations of nitrate (1mM, 10mM and 35m $MKNO_3$). Of particular interest will be whether the delay of flowering caused by the mutation and that associated with the nitrate concentration are additive or whether the mutants are not affected by nitrate. Additive interactions would suggest that the mutation and the effect of nitrate act independent of one another, or that nitrate is acting further downstream of the pathway affected by the mutation , whereas no effect of nitrate on flowering time would suggest that nitrate acts through pathway affected in the mutant.

Previous results from Dr Irene Loef, indicated that the response to nitrate was retained in mutants defective in photoperiod (*fd-1)* and autonomous *(fwa-1*, *fve-1, fy)* pathways which accordingly displayed shifted flowering curves depending on the external nitrate concentration when compared to wild type. These results led to propose that nitrate should be interacting further downstream of the photoperiod, vernalization and autonomous, flowering pathways.
Plants over-expressing *CO* displayed similar effect to those found in plants growing under long days showing early flowering independently of the external nitrate. This indicates that constitutive expression of CO is overriding the effect induced by nitrate. On the other hand, plants lacking a functional CO protein (*co2tt4* mutant) exhibited a dramatic delay in floral initiation and total dependency from nitrate, resembling the situation of plants grown in short day conditions. All these results together suggest that nitrate signal acts downstream of the day length pathway.

The finding that *ga1-3*, a mutant deficient in GA biosynthesis, is not able to flower under short day conditions even after vernalization, suggested that GA may be required for an alternative pathway that promotes flowering under non-inductive photoperiods and that GA may not have a direct role in the vernalization response (Michaels & Amasino, 1999). Under neutral day length (12h light), the g*a1-3* mutant displayed earlier flowering time in response to low nitrate and compared to wild type. Similar response was seen in *gai,* a mutant affected in GA reception and signalling, that showed a slight displaced flowering curve in response to high nitrate. These results led us to conclude that GA mutants are still influenced by nitrate and thus, nitrate signal acts downstream of the GA signalling pathway.

The GA pathway regulates positively the expression of *SOC1* which together with *FT* promote the transition to flowering by activating the floral meristem identity genes. Mutants defective in *SOC1* and *FT* flowered later than wild type and displayed early flowering in response to low nitrate. High nitrate led to retardation in the floral initiation in both mutants being more drastic the effect in *ft-7* mutant plants. The double mutant *soc1-1-ft7* showed a strong delay in flowering time, and flowering was strongly dependent on the external nitrate concentration.

So far, it is known that both floral integrators are negatively regulated by the floral repressor *FLC*. Analyses of plants over-expressing *FLC* showed that its constitutive over-expression suppress the effect of nitrate triggering a strong delay in response to all conditions. This result together with the fact that the double mutant *soc1-1-ft-7* appeared to be affected by nitrate, led

to propose that the nitrate signal may enter downstream of *FLC* and, also acts independently or further downstream of *SOC1* and *FT*.

Further strong evidence that nitrate is involved in the regulation of the transition to flowering came from analysis of the triple mutant *fcaco2ga1-3* in response to nitrate. Previous studies showed that this genotype never flowers under long- or short-day conditions, indicating that the three pathways impaired by the mutations are absolutely required for flowering (Reeves & Coupland 2001). Analyses of *fcaco2ga1-3* plants in response to different concentrations of nitrate revealed the ability of low nitrate to promote flowering even when these major flowering pathways are not functioning. In contrast, high nitrate was not able to promote flowering in the triple mutant, and the plants entered senescence without flowering. These results indicate that nitrate could act as a possible alternative signalling pathway able to promote the transition to flowering independently of the other known pathways. Results from this part indicate that the nitrate signal should not require the function of genes in the autonomous and gibberellic acid pathways to promote flowering, however, should require the absence of *CO* function and/or lower FLC activity to induce the floral stage.

Taken together, analyses of mutants defective in flowering pathways in response to nitrate lead to the proposal that nitrate is affecting the promotion of *Arabidopsis* plants to the floral stage. A tentative model is placing nitrate signal further down stream or independently of the main pathways that promote the transition to flowering in *Arabidopsis* (figure 73).

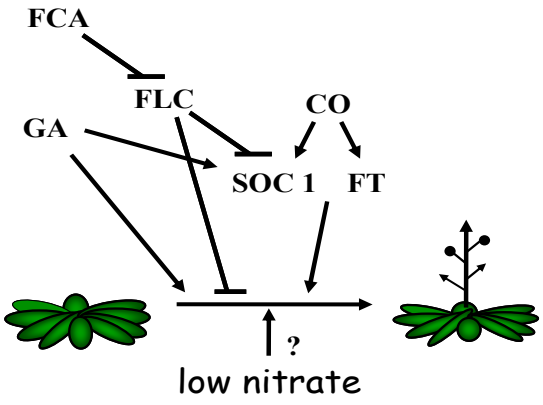

Figure 73. Schematic model of flowering pathways in *Arabidopsis*. The long-day, autonomous, and GA pathways promote flowering of *Arabidopsis* under standard long-day conditions. The autonomous pathway acts by repressing the expression of the floral inhibitor FLC and accelerates flowering by facilitating the activity of the long-day and GA pathways. The nitrate signal is interacting with the other pathways in the promotion of flowering.

5.11. The triple mutant flowers in response to low phosphate but not in response to other stresses.

Plant development is very sensitive to changing environmental conditions and the fine tuned regulation of the floral promotion pathways in an interactive network ensures the onset of flowering at the proper time of the year. It has been postulated that plants exposed to stressing environmental conditions activate the flowering program prematurely in order to enhance the chance of a plant population to survive a transient period of threatening environmental conditions (Martinez *et al*., 2004; Balasubramanian *et al*., 2006). However, so far, the mechanism by which stress functions is not yet well understood.

In order to gain more insights into the regulation of flowering by stress, wild type *Arabidopsis* plants and the triple mutant blocked in the major pathways controlling flowering (*fcaco2ga1-3)* was grown in response to various abiotic stresses and the transition to flowering was studied.

As already mentioned, several authors have postulated about the role of nutritional status in the control of flowering time. Phosphate is an essential macronutrient that plays a central role in virtually all processes in plant and its deprivation elicits a complex array of morphological, physiological and biochemical adaptations (Abel *et al*., 2002; Raghothama, 1999; Rausch C & Bucher M, 2002; Vance *et al.*, 2003). Studies of wild type *Arabidopsis* plants in response to nutritional phosphate deprivation revealed that flowering was accelerated in the plants and this response was similar to that shown when plants are grown in low nitrate conditions (see figure 59, section 4.4.1). Interestingly, the triple mutant flowered in response to low phosphate and showed similar flowering pattern of plants grown in nitrate starvation. The cross talk between nitrate and phosphate responses has been previously suggested and plants have developed similar adaptations to low phosphate and low nitrate.

Water availability imposes another strong influence in almost all aspects of plant biology; however, neither drought nor flooding experiments seemed to cause significant effect on flowering time in different wild type of *Arabidopsis* (Pigliucci *et al*., 1995; Pigliuci & Kolodynska, 2002).

Several authors support the idea that chilling and high irradiances induce flowering in plants (Shubhangi, *et al*., 2003; Hirai *et al.*, 1995) more specifically through the synthesis of salicylic acid (SA; Martinez. *et al*., 2004).

Exposure to excess light irradiance causes earlier flowering in wild type *Arabidopsis* plants compared to those grown under normal light conditions (see 4.4.2.1). This treatment did not induce flowering in the triple mutant *fcaco2ga1-3*.
Wild type *Arabidopsis* plants in response to photo-chilling stress (high light intensities and low temperatures) showed similar flowering curves compared to the control, indicating that photo chilling is not promoting flowering in *Arabidopsis*.

Temperature has a great effect on plant growth and flowering time of *Arabidopsis thaliana* ecotypes (Shubhangi, *et al*., 2003). High temperature causes protein denaturation, alters membrane fluidity, disrupts the balance of metabolic processes and leads to oxidative stress (Dewey, 1989; Larkindale & Knight, 2002). Oxidative stress arises from an imbalance in the generation and removal of reactive oxygen species (ROS) such as superoxide molecules and hydrogen peroxide (H_2O_2). ROS are required for many developmental processes (Krekule & Machackova, 1986; Fontaine *et al*., 1995; Henmi *et al*., 2001; Ogawa & Iwabuchi 2001; Ogawa *et al*., 2001) and it has been shown that the level of antioxidants increases during the transition from vegetative phase to reproductive stage, speculating that plants undergo stressful conditions during the flowering process (Hirai *et al*., 1995; Badiani *et al*., 1996; Gielis *et al*., 1999). To gain more insights into the influence of high temperatures in the transition to flowering, analyses of flowering time of *Arabidopsis* plants exposed to high t^a (26ºC/day, 22ºC/night) versus control conditions (20ºC day/night), were investigated.
Flowering was slightly accelerated in wild type La*er* grown in high t^a (see section 4.4.2.2). This result agrees to the work of Balasubramanian *et al*., (2006), who showed that growth temperatures above a threshold rapidly triggered flowering by alterations in RNA processing. This effect was abolished in the triple mutant that was unable to flower in such conditions.

According to our results, the transition to the floral stage in wild type *Arabidopsis* plants is influenced by a given stress (for example, high light or high t^a). The triple mutant is unable to flower in response to those specific abiotic stresses (high light, high temperature, photo-chilling) and only flowers in response to phosphate or nitrate limitation. Interestingly, the triple mutant remains vegetative and dies without producing flowers in response to high nitrate treatment.
Taken together, the fact that low nitrate is enough to induce flowering in the triple mutant (unable to flower in response to all conditions used) allowed to propose that flowering time in *Arabidopsis thaliana* is affected by nitrate, indeed, it may be induced by low nitrate.

Moreover, the "nitrate-signal" must be operating independently of the photoperiod, gibberellic acid and autonomous flowering signalling pathways to promote the transition to the floral onset in *Arabidopsis thaliana.*

5.12. Transcripts changes in response to nitrate towards the floral initiation.

In order to study the global response of plants to nitrate and to study processes underlying the floral transition at transcriptional level, two different genotypes were used.

Transgenic plants defective in CO gene (*co2* mutant), were used to strengthen the response to nitrate; in this genotype the photoperiod signalling pathway is blocked, and flowering is strongly inhibited in the presence of nitrate in intermediate photoperiods.

Transgenic plants over-expressing the floral repressor *FLC* were studied because in them the floral response to nitrate is totally blocked and therefore they could serve as a control for the transcriptional changes occurring in *co2* plants.

In the analyses, low nitrate (1mM KNO_3) was used as inducing treatment, and high nitrate (35mM KNO_3) used as repressive treatment. Analyses of flowering time of *co2* genotype revealed differences in response to nitrate, that means, plants were induced to flower in response to low nitrate concentration and displayed delayed flowering under high nitrate. (*co2* mutant and 35S::*FLC*). According to previous analyses, these responses were blocked in FLC over-expressing plants as result of the constitutive expression of the floral repressor *FLC.* Expression analyses of some nitrate markers (RT-PCR and Affymetrix; data not shown) confirmed that the conditions used in the experiment were appropriate. In addition, a global comparison of these results with published data on nitrate responses (Scheible *et al*., 2004) showed that most of genes shared responses; genes that were repressed in N-starvation and induced after nitrate readdition tended to show lower transcript levels in 1 as compared to 35mM nitrate in my experiments, while genes that were induced in N-starvation and repressed after nitrate readdition tended to show higher transcript levels in 1 as compared to 35m nitrate. This confirmed once again the experimental conditions (low and high nitrate). However, due to the fact that both systems are different, including differences in plant age and organs studied but especially the inclusion of glutamine in the growth medium (different experimental conditions), a large number of genes showed opposite responses.

A first criteria including the comparison between plants defective in CO protein (*co2* mutant) under low nitrate and those plants grown under high nitrate, revealed at first glance a set of genes with a trend to increase in time towards the floral onset. The expression of those genes did not vary in plants over expressing FLC (35S::*FLC*) in low nitrate versus high nitrate

conditions, leading to suggest that they could be involved in the "low nitrate" signalling pathway that should be promoting flowering in the mutant *co2*.

A main focus was set on the expression of genes encoding for transcription factors since a substantial number of them emerge as having crucial roles in controlling the complex regulatory network that underpin the transition to flowering. Some AP2 DNA-binding domain proteins and several transcription factors containing zinc finger regions and CCT motifs displayed a tendency to increase in expression in *co2* plants versus control lines involving them as possible candidate genes. Many of these AP2-EREBP and zinc-finger containing transcription factors have been implicated in the regulation of important biological processes unique to plants, like flower development, light-regulated morphogenesis and pathogen responses (Riechmann, J & Meyerowitz, EM., 1998; Takatsuyi, 1998). Further up-regulated genes belonged to WRKY, MYB and NAC families of transcription factors shown to play regulatory roles in developmental processes and defence responses in plants and also have been involved in some aspects of flowering plants. Given the implication of several MADS Box proteins in floral initiation and flower morphogenesis, special attention was taken on their regulation, however, no significant expression changes were visible upon the floral initiation in *co2* transgenic plants. Additionally, genes involved in calcium signalling displayed a trend to increase in expression upon flowering without changing in the control *FLC* over expressing plants. Two of these genes are termed "touch responsive proteins" *TCH2* and *TCH3* that encode for two calcium-binding proteins shown to be induced in plants subjected to touch and darkness and expressed at sites of predicted mechanical stress like regions undergoing growth, vascular tissues and floral organs.

In order to obtain insights into the behaviour of flowering genes, the expression of around 44 flowering specific genes was investigated according to the first criteria (genes changing between 1mM nitrate and 35mM nitrate in *co2* mutant but not in 35S::*FLC*). However, in general, the expression was not significant considering a threshold of 1, and only two genes showed 2 fold changes in one or more of the time points. A NAC domain protein NAM- like (At1g69490) appeared to be induced between day19 and 25 in *co2*. It is a direct target gene of the floral homeotic protein heterodimer APETALA3/PISTILLATA and it is required for meristem establishment and separation of floral organs. A flavin-binding kelch domain F box protein (FKF1/ADO3, At1g68050) was slightly induced at 19d tending to decrease thereafter. *FKF* is clock-controlled and is also implicated in the regulation of the transition to flowering. The rest of central flowering time genes did not show any major changes.

A second criteria was followed to look for candidate genes putatively involved in the transition to flowering in response to nitrate. It would consist in looking for genes induced or repressed strongly (≥ 2 fold) in *co2* plants under low nitrate compared with plants over expressing the floral repressor *FLC*. If these genes are involved in the transition to flowering in response to low nitrate they should therefore show opposite response to high nitrate. That expression pattern would therefore become the basis for the identification of genes involved in the promotion of flowering in response to low nitrate.

According to this second filter (different as the one in the previous paragraph as described in the text), several transcripts increased significantly their expression in *co2* mutant plants grown under low nitrate compared to high nitrate. Among them, two CAAT binding transcription factors (At5g06510 and At1g72830) were induced upon flowering. Interestingly, both of them contain potential target sites for different microRNAs. Micro RNA-guided degradation of specific mRNAs has been shown to be important in plant development, including the regulation of flowering time and floral organ identity (Palatnik *et al.*, 2003; Aukerman & Sakai, 2003; Chen, 2004). Three zinc finger proteins showed similar expression pattern, and of notable interest was the detection of At1g51700, a dof-type zinc finger domain containing protein previously mentioned for its induced expression in *co2* plants in low nitrate versus *co2* under high nitrate. Dof 1 transcription factors have been related with an improved nitrogen assimilation and growth under low nitrogen conditions (Yanagisawa *et al*., 2004).

Regarding specific flowering time genes, two positive regulators, *CO* and *SOC1/AGL20* showed a significant induction in *co2* plants versus 35S::*FLC* in response to low nitrate. However, as already discussed, mutations in these genes does not prevent flowering in low nitrate.

Two positive floral regulators, a NAC domain protein and the transcription factor *SPL3* were down-regulated in one of the time points. Regarding the negative regulators of flowering, *SVP* (short vegetative phase), a putative AP2 domain protein and *ELF3* showed slight induction in one of the conditions.The over expression of *FLC* quantitatively should block the floral transition in 35S::*FLC* plants in part by repressing expression of floral integrators *FT* and *SOC1*, however, only *SOC1* showed significant induction in *co2* (or repression in 35S::*FLC*) transgenic plants. It is possible that the putative pathway promoted by nitrate signal should be mediated by target genes of the MADS-box transcription factor *FLC*. *FLC* expression is negatively regulated by the autonomous and vernalization pathways. Therefore, of notable interest should be an analysis of the expression pattern of those genes in response to nitrate in

plants with reduced expression of *FLC*, for example, plants subjected to vernalization or plants over-expressing any genes belonging to the autonomous signalling pathway.

This kind of experiments is somehow risky due to complications that could lead to contradictory interpretations. First, it is difficult to guess "when" and "where" the nitrate signal is entering into the system to regulate flowering, it could act at the very beginning in growth or closer in time to the floral onset. Also, it is possible to estimate approximately the "flowering day" (day when 50% of plants, at least, have been induced to flower) but it is difficult to reproduces it even when the conditions between separated experiments are rigorously maintained. Second, each sample must contain a combination of 15-20 plants to avoid phenotypic variations, but every single plant must be at similar developmental step in order to avoid physiological variations among the plants. This is important to assume a general response, that is, to assume that all the plants are "induced" or "repressed" to flower. Therefore, all the plants collected into the same sample must contain similar number of leaves and similar phenotypic appearance. Third, in our experiments, plants were germinated and grown in the same nutritional media till they were induced to flower, therefore, it is complicated to find out "how fast" plants consume the nutrients (especially nitrate) of the medium and "when" plants become really nutrients limited. This is particularly important because we must be sure that the induction of flowering occurs as a result of external low nitrate or high nitrate and not as consequence of the nutritional status of the plants.
Another important point is that analyses in the whole shoot may not be sensitive enough to detect the changes in the meristem, which are linked very directly to signalling and floral initiation (Huang *et al*., 2005; Wigge *et al*., 2005; Abe *et al.*, 2005).

In any case, it must be remembered that the floral initiation is a complex process subjected to a tight regulation, and therefore every single variation in flowering time can be triggered by multiple factors within the plant.

5.13. Conclusion

The functional characterization of GDH is highly relevant for some reasons. Firstly, it is ubiquitous to all organisms and GDH enzyme activity exists in plant tissues at high levels. Secondly, because even though several lines of research have been focused in the study of the enzyme GDH, its biological role in vivo remains largely obscure and controversial. Also, the enzyme exhibits marked and interesting responses of expression in response to carbon and

nitrogen. Two members of the GDH family are modulated by sugars (*GDH1* and *GDH2*) and show diurnal rhythm regulation. The third member of the family, *GDH3* is regulated by nitrogen and does not show diurnal regulation. For one of these genes, *GDH1*, T-DNA lines could be obtained. The transcription of each member of the GDH family was down-regulated using an RNAi approach. Also, a double mutant *GDH1-GDH2* was created using the same method. However, change in transcript level of GDH family members achieved by T-DNA insertion (*gdh1*) or RNAi approach (*gdh1*, *gdh2*, *gdh3* and *gdh1-gdh2*) did not reveal robust changes in development or at metabolic level under the experimental conditions used in this work. This lack of visual phenotype could be due to pathway redundancy (GS/GOGAT; photorespiration) or to the fact that remaining glutamate dehydrogenase activity is still able to function.

In a second part of this thesis, the influence of nitrate in the initiation of flowering was analysed in some known flowering time mutants. Based on the current state of knowledge, nitrate addition has been shown to delay flowering. However, the regulation of the process at molecular level is largely unknown. The analyses of flowering time mutants in response to nitrate revealed that a signal initiated by nitrate or a closely related metabolite has an effect in the transition from vegetative stage to flowering in *Arabidopsis*. Furthermore, conclusive results in the triple mutant blocked in three of the major pathways involved in floral initiation led to suggest that low nitrate promotes flowering in the plants while high nitrate concentration delays the initiation of flowers, and that the nitrate signalling pathway acts further downstream or independently of all known flowering pathways (autonomous, vernalization, gibberellic and photoperiodism).

CHAPTER 6 REFERENCES

Abe, M., Kobayashi, Y. et al. (2005). FD, a bZIP protein mediating signals from the floral pathway integrator FT at the shoot apex. *Science*. **309**: 1052-1056.

Abel, S., Ticconi C.A, et al. (2002). Phosphate sensing in higher plants. *Physiologia Plantarum* **115:** 1-8.

Alexandrow, V. (1994). Functional aspects of cell response to heat shock. *Int Rev Cytol.* **148**: 171-227.

Ameziane, R., Bernhard, K. et al. (2000). Expression of the bacterial *gdhA* gene encoding glutamate dehydrogenase in tobacco affects plant growth and development. *Plant and Soil*, **221**: 47-57.

Araki, T. (2001). Transition from vegetative to reproductive phase. *Curr. Opin. Plant Biol*. **4:** 63-68.

Aubert, S., Bligny, R. et al. (2001). Contribution of glutamate dehydrogenase to mitochondrial metabolism studied by ^{13}C and ^{31}P nuclear magnetic resonance. *Journal of Experimental Botany* **52**: 37-45.

Aukerman, M. J., Lee, I. et al. (1999). The *Arabidopsis* flowering-time gene *LUMINIDEPENDENS* is expressed primarily in regions of cell proliferation and encodes a nuclear protein that regulates *LEAFY* expression. *The Plant Journal*. **18(2)**:195-203.

Aukerman, M. J. and Sakai, H. (2003). Regulation of flowering time and floral organ identity by a microRNA and its *APETALA2*-like target genes. *Plant Cell 15*:2730-2741.

Ausin, I., Alonso-Blanco, C. et al. **(2005).** Environmental regulation of flowering. *Int. J. Dev. Biol*. **(49)**: 689-705.

Ausin, I., Alonso-Blanco, C. et al. (2004). Regulation of flowering by *FVE*, a retinoblastome-associated protein. *Nat. Genet*. **36**: 162-166.

Avendano, A., Deluna, A. et al. (1997). *GDH3* encodes a glutamate dehydrogenase isoenzyme, a previously unrecognized route for glutamate biosynthesis in *Saccharomyces cecevisiae. J. Bacteriol* **179**: 5594- 5597.

Avila, C., Márquez, A. J. et al. (1993). Cloning and sequence analysis of a cDNA for Barley ferredoxin-dependent glutamate synthase and molecular analysis of photorespiratory mutants deficient in the enzyme. *Planta* **189**: 475-483.

Badianai, M., Paolacci, AR. et al. (1996). Seasonal variations of antioxidants in wheat (*Triticum aestivum*) leaves grown under field conditions. *Aust J Plant Physiol*. **23**: 687-698.

Balasubramanian, S., Sureshkumar, S. et al. (2006). Potent induction of *Arabidopsis thaliana* flowering by elevated growth temperature. *PLos Genetics* **2(7)**: e106.

Bastow, R. et al. (2004). Vernalization requires epigenetic silencing of *FLC* by histone methylation. Nature, **427**:164-167.

Bernier, G., Kinet, JM. et al. (1981). The Physiology of Flowering. *Volume I. CRC Press, Boca Raton.*

Bernier, G. (1988). The control of floral evocation and morphogenesis. *Annu Rev Plant Physiol Plant Mol Biol* **39**: 175-219.

Bernier, G., Havelange, A. et al. (1993). Physiological signals that induce flowering. *Plant cell* **5**:1147-1155.

Bernier, G. and Périlleux, C. (2005). A physiological overview of the genetics of flowering time control. *Plant Biotechnology Journal*. **3**: 3-16.

Bläsing, O. E., Gibon, Y. et al. (2005). Sugars and circadian regulation make major contributions to the global regulation of diurnal gene expression in *Arabidopsis*. *The Plant Cell* **17**: 3257-3281.

Blázquez, M., Soowal, L.N. et al. (1997). *LEAFY* expression and flower initiation in *Arabidopsis. Development*, **124**: 3835- 3844.

Blázquez, M. and Weigel, D. (2000). Integration of floral inductive signals in *Arabidopsis*. *Nature* **404**: 889-892.

Blázquez, M. (2005). The right time and place for making flowers. *Science*. **309**: 1024-1025.

Bradley, D., Ratcliffe, O. et al. (1997). Inflorescence commitment and architecture in *Arabidopsis. Science* **275**: 80-83.

Britton, K.L., Baker, P.J. et al. (1992). Structural relationship between the hexameric and tetrameric family of glutamate dehydrogenase . *Eur. J. Biochem* **209**: 851-859.

Boss, P.K., Bastow, R.M. et al. (2004). Multiple pathways in the decision to flower: enabling, promoting, and resetting. *Plant Cell* **16**: S18-S31.

Botrel, A. and Kaiser, KM. (1997). Nitrate reductase activation state in barley roots in relation to the energy and carbohydrate status. *Planta*. **201**(4):496-501.

Bowman, J.L., Smyth, D.R. et al. (1991). Genetic interactions among floral homeotic genes of *Arabidopsis. Development*. **112**: 1-20.

Cammaerts, D. and Jacobs, M. (1985). A study of the role of glutamate dehydrogenase in the nitrogen metabolism of *Arabidopsis thaliana*. *Planta* **163**: 517-526.

Carvalho, H., Pereira, S. et al. (1992). Detection of cytosolic glutamine synthetase in leaves of *Nicotiana tabacum* L. by inmunocytochemical methods. *Plant Physiology* **100**: 1591-1594.

Caspar, T., Huber, SC. et al. (1985). Alterations in growth, photosynthesis, and respiration in a starchless mutant of *Arabidopsis thaliana* L. deficient in a chloroplast phosphoglucomutase activity. *Plant Physiol* **79**: 11-17.

Chandler, J., Wilson, A. et al. (1996). *Arabidopsis* mutants showing an altered response to vernalization. *Plant J*. **10**: 637-644.

Chen, X. (2004). A microRNA as a translational repressor of *APETALA2*. *Arabidopsis* flower development. *Science* **303**: 2022-2025.

Cheng, C. L., Acedo, G. N. et al. (1992). Sucrose mimics the light induction of *Arabidopsis* nitrate reductase gene transcription. *Proceedings of the national Academy of Science of the USA* **89**: 1861-1864.

Clough, S. J. and Bent A. F. (1998). Floral dip: a simplified method for *Agrobacterium* mediated transformation of *Arabidopsis thaliana*. *Plant Journal* **16**: 735-743.

Cock, J. M., I. W. Brock. et al. (1991). Regulation of glutamine synthetase genes in leaves of *Phaseolus vulgaris. Plant Molecular Biology* **17**: 761-771.

Coen, E.S and Meyerowitz, E.M. (1991). The war of the whorls: genetic interactions controlling flower development. *Nature* **353**:31-37.

Corbesier, L., Lejeune, P. et al. (1998). The role of carbohydrates in the induction of flowering in *Arabidopsis thaliana*: comparison between the wild type and a starchless mutant. *Planta* **206**: 131-137.

Corbesier, L., Havelange, A. et al. (2001). N content of phloem and xylem exudates during the transition to flowering in *sinapis alba* and *Arabidopsis thaliana*. *Plant Cell and Environment.* **24**: 365-375.

Coruzzi, G. M. and Zhou L. (2001). Carbon and nitrogen sensing and signaling in plants: emerging matrix effects. *Curr Opin Plant Biol.* **4**: 247-253.

Coschigano, K. T., Melo-Oliveira, R. et al. (1998). Arabidopsis *gls* mutants and dinstinct Fd-GOGAT genes: implications for photorespiration and primary nitrogen assimilation. *The Plant Cell* **10**: 741-752.

Crawford, N. M. and Forde, B. G. (1995). Nitrate: nutrient and signal for plant growth. *Plant Cell* **7**: 859–868.

Crawford, N. M. and Forde, B. G. (2001). Molecular and developmental biology of inorganic nitrogen nutrition. *The Arabidopsis Book, eds. C.R. Somerville and E.M. Meyerowitz, American Society of Plant Biologist* **doi/10.1199/tab.0011**.

Daniel-Vedele, Filleur, F., S. et al. (1998). Nitrate transport: a key step in nitrate assimilation. *Current Opinion in Plant Biology* **1**: 235–239.

Day, D. A., Salom, C. L. et al. (1988). Glutamate oxidation by soybean cotyledon and leaf mitochondria. *Plant Cell Phisiol*. **29**: 1193-1200.

Dewey, WC. (1989). The search for critical cellular targets damaged by heat. *Radiat Res*. **120:** 91-204.

Dielen, V., Lecouvet, V. et al. (2001). In vitro control of floral transition in tomato (*Lycopersicum esculentum* Mill.), the model for autonomously flowering plants, using the late flowering *uniflora* mutant. *J. Exp.Bot*. **52**:715-723.

Ding, B. Itaya, A. et al. (2003). Symplasmic protein and RNA traffic: regulatory points and regulatory factors. *Curr Opin Plants Biol.* **6(**6): 596-602.

Edwards, J. W. and Coruzzi G. (1989). Photorespiration and light act in concert to regulate the expression of the nuclear gene for chloroplast glutamine synthetase. *Plant Cell* **1**: 241-248.

Evans, L. T. (1971). Flower induction and the florigen concept *Annu Rev Plant Physiol. Plant Mol. Biol.* **22**: 365-394.

Faure, J. D., Jullien, M. et al. (1994). *Zea3*: a pleiotropic mutation affecting cotyledon developmetn, cytokinin, resistance and carbon-nitrogen metabolism. *Plant Journal* **5**: 481-491.

Fichtner, K. and Schulze E. D. (1992). The effect of nitrogen nutrition on annuals originating from habitats of different nitrogen availability. *Oecologia* **92**: 236-241.

Fondy, BR., and Geiger, DR. (1985). Diurnal changes of allocation of newly fixed carbon in exporting sugar beet leaves. *Plant Physiol.* **78**: 753- 757.

Fontaine, O., Billard, JP. et al. (1995). Effect of glutathione on dormancy breakage in barley seeds. *Plant growth regul*. **16***:* 55-58.

Forde, B. and Clarkson, D. (1999). Nitrate and ammonium nutrition of plants: physiological and molecular perspectives. *Advances in Botanical Research* **30:** 1–90.

Forde, B. (2002). Local and long-range signalling pathways regulating plant responses to nitrate. *Annu. Rev Plant Biol* **53**:203-224.

Fox, G. G., Ratcliffe, R. G. et al. (1995). Evidence for deamination by glutamate dehydrogenase in higher plants. *Can. J.Bot.* **73**: 1112-1115.

Foyer, C. H., Parry, M. et al. (2003). Markers and signals associated with nitrogen assimilation in higher plants. *J Exp Bot.* **54**: 585-593.

Fritz, C., Matt, P. et al. (2006). Impact of the C-N status on the amino acid profile in tobacco source leaves. *Plant Cell Environ.* **11**: 2055-76.

Galangau, F., F. Daniel-Vedele, et al. (1988). Expression of leaf nitrate reductase gene form tomato and tobacco in realtion to light dark regimes and nitrate supply. *Plant Physiology* **88,**: 383-388.

Galvan, A. and Fernandez, E. (2001). Eukaryotic nitrate and nitrite transporters. *Cellular and Molecular Life Sciences* **58**: 225–233.

Geiger, D. R. and Servaites, J. C. (1994). Diurnal regulation of photosynthetic carbon metabolism in C3 plants. *Annu Rev Plant Physiol Plant Mol Biol* **45**: 235-256.

Geiger, D. R. and Servaites, J. C. (2000). Role of starch in carbon translocation and partitioning at the plant level. *Aust. J. Plant Physiology*. **27**:571-582.

Geiger, M., Walch-Liu, P. et al. (1998). Enhanced carbon dioxide leads to a modified diurnal rhythm of nitrate reductase activity in older plants, and a large stimulation of nitrate reductase activity and higher levels of aminoacids in higher plants. *Plant, Cell and Environment.* **21**: 253-268.

Gibon, Y., Bläsing, O. et al. (2004a).Adjustment of diurnal starch turnover to short days: A transient depletion of sugars towards the end of the night triggers a temporary inhibition of carbohydrate utilisation, leading to an accumulation of sugars and post-translational activation of ADP glucose pyrophosphorylase in the following light period. *Plant J*. **39**: 847-862.

Gibon, Y., Bläsing, O. et al. (2004b). A robot-based platform to measure multiple enzyme activities in Arabidopsis using a set of cycling assays: comparison of changes of enzyme activities and transcript levels during diurnal cycles and in prolonged darkness. *The Plant Cell* **16**: 3304-3325.

Gielis, J., Goetghebeur,P. et al. (1999). Physiological aspects and experimental reversion of flowering in *Fagesia murieliae* (Poaceae, Bambusoideae). *Syst Georg Pl***. 68**: 147-258.

Glass, A., Brito, D. et al. (2001). Nitrogen transport in plants, with an emphasis on the regulaiton of fluxes to match plant demand. *Journal of Plant Nutrition and Soil Sciences* **164**: 199-207.

Gojón, A., Dapoigny, L. et al. (1998). Effects of genetic modification of nitrate reductase expression on $^{15}NO_3^-$ uptake and reduction in *Nicotiana* plants. *Plant, Cell and Environment*. **21**,: 43-53.

Guo, LP., Zhang, FS. et al. (2001). Effect of long-term fertilization on soil nitrate distribution. *J. Environ. Sci. (China*) **13**: 58-63.

Gutiérrez, RA., Lejay, L. et al. (2007). Qualitative network models and genome-wide expression data define carbon/nitrogen-responsive molecular machines in *Arabidopsis*. *Genome Biology,* **8:** R7.

He, Y., Michaels, S.D. et al. (2003). Regulation of flowering time by histone acetylation in *Arabidopsis*. *Science* **302**: 1751-1754.

Heliwell, C., Waterhouse, P. (2003). Constructs and methods for high-throughput gene silencing in plants. *Methods* **30**: 289-295.

Hempel, FD and Feldman, LJ. (1995). Specification of chimeric flowering shoots in wild type *Arabidopsis*. *The Plant Journal* **8** (5): 725-731.

Henmi, K., Tsubci, S. et al. (2001). A possible role of glutathione disulfide in tracheary element differentiation in the culture mesophyll cells of *Zinnia elegans*. *Plant Cell Physiol*. **42**: 673-676.

Hilhorst, H.W. M and Karssen, C. M. (1989). Nitrate reductase independent stimulation of seed germination in *Sysimbrium officinale* L (hedge mustard) by light and nitrate. *Annals of Botany (Lond.)* **63**: 131-137.

Hirai N, Kojima, Y. et al. (1995). Accumulation of ascorbic acid in the cotyledons of morning glory (*Pharbitis nil*) seedlings during the induction of flowering by low temperature treatment and the effect of prior exposure to high intensity light. *Plant Cell Physiol*. **36**: 1265-1271.

Hirel, B., Phillipson B. et al. (1997). Manipulating the pathway of ammonia assimilation in transgenic non-legumes and legumes. *J. Plant Nut*. **160,** 283-290.

Hirel, B. and Lea, P. J. (2001). Ammonia Assimilation. *Plant Nitrogen* (Lea, P.J and Gaudry, J.F.-M., eds). Berlin, Heidelberg, Springer-Verlag: 79-99.

Hoff, T., Truong, H.-N. et al. (1994). The use of mutants and transgenic plants to study nitrate metabolism. *Plant, Cell and Environment.* **17**: 486-506.

Huang, T., Böhlenius, H. et al. (2005). The mRNA of the *Arabidopsis* gene *FT* moves from leaf to shoot apex and induces flowering. *Science,* **309**: 1694- 1696.

Imsande, J. and Touraine, B. (1994). N Demand and the Regulation of Nitrate uptake. *Plant Physiology*, **105:** 3-7.

Ireland, R. J. and Joy, K. W. (1988). Plant transaminases. In *Transaminases*. ed. P. Christen and D.E. Metzler.: 376-384.

Ireland, R. J. and Lea, P. J. (1999). The enzymes of glutamine, glutamate, asparagine and aspartate metabolism. In BK Singh, ed, *Plant amino acids.* Biochemistry and Biotechnology. Inc, American Cyanamid Company, Dekker, M., New York, Basel, Hong Kong.: 49-10.

Irizarri, R.A., Bolstad, B. M. et al. (2003). Summaries of Affymetrix GeneChip probe level data. *Nucleic Acids Res*. **31**, e 15.

Ishioka, N. Tanimoto, S. et al. (1991). Roles of nitrogen and carbohydrate in floral bud formation in *Pharbitis* apex cultures. *J. Plant Physiol*.. **138**: 573-576.

James D. Mauseth (2003). In *Botany: an introduction to plant biology.* Science, p: 47.

Kaiser, W. M. and Brendle-Behnish, E. (1991). Rapid Modulation of Spinach Leaf Nitrate Reductase Activity by Photosynthesis: I. Modulation in Vivo by CO(2) Availability. *Plant Physiol* **96**(2):363-367.

Kaiser, W. M. and Föster (1989). Low CO(2) Prevents Nitrate Reduction in Leaves. *Plant Physiol*.; **91**(3):970-974.

Kaiser, W. M. and Huber, S. C. (1994). Post-translational regulation of nitrate reductase in higher plants. *Plant Physiology* **106**: 817-821.

Kamachi, K., T. Yamaya. et al. (1992). Changes in cytosolic glutamine synthetase polypeptide and its mRNA in a leaf blade of rice plants during natural senescence. *Plant Physiology* **98**: 1323- 1329.

Kar, M. and Feierabend, J. (1984). Metabolism of activated oxygen in detached wheat and rye leaves and its relevance to the inititation of senescence. *Planta* **160**: 385-391.

Kardailsky, I., Shukla, V.K. et al. (1999). Activation tagging of the floral inducer *FT*. *Science* **286**: 1962-1965.

Karimi, M., Inze, D. et al. (2002). GATEWAY vectors for Agrobacterium mediated plant transformation. *Trends Plant Science.* **7**: 193-195.

Kempin, S.A. et al. (1995). Molecular basis of *cauliflower* phenotype in *Arabidopsis. Science* **267**: 522- 525.

Kendall, A. C., Wallsgrove, R. M. et al. (1986). Carbon and nitrogen metabolism in barley (*Hordeum vulgare* L.) mutants lacking ferredoxin-dependent glutamate synthase. *Planta* **168**: 316-323.

Kim, M., Canio, W. et al (2001). Developmental changes due to long-distance movement o a homeobox fusion transcript in tomato. *Science*. **293**: 287-289.

Kisaka, H. and Kida, T. (2003). Transgenic tomato plant carrying a gene for NADP-dependent glutamate (*gdhA*) from *Aspergillus nidulans*. *Plant Science* **164**: 35-42.

Klebs, G. (1913). Über das Verhältnis der Aubenwelt zur Entwincklung der Pflanze. *Sitz - Ber.Akad.Wiss.Heidelberg Ser.B* **5**:3-47.

Klimyuk, V. I., Carroll, B. J. et al. (1993). Alkali treatment for rapid preparation of plant material for reliable PCR analysis:technical advance. *Plant Journal* **3**: 493-494.

Kobayashi, Y., Kaya, H. et al. (1999). A pair of related genes with antagonistic roles in mediating flowering signals. *Science* **286:** 1960-1962.

Koch, KE. (1996). Carbohydrate modulated gene expression in plants. *Annual Reviews of Plant Physiology and Plant Molecular Biology* **47**: 509-540.

Koncz, C., Nemeth, K. et al. (1992). T-DNA insertional mutagenesis in *Arabidopsis. Plant Molecular Biology* **20:** 963-976.

Koornneef, M., Hanhart, C.J. et al (1991). A genetic and physiological, analysis of late flowering mutants in *Arabidopsis thaliana*. *Mol. Gen. Genet.* **229**: 57-66.

Koornneef, M., Alonso-Blanco, C. et al. (1998b). Genetic control of flowering time in Arabidopsis. *Annu Rev Plant Physiol Plant Mol Biol* **49**: 345-370.

Korves, TM., Bergelson, J. et al. (2003). A developmental response to pathogen infection in *Arabidopsis. Plant Physiol.* **133**: 339-347.

Krapp, A., Hofmann, B. et al (1993). Regulation of the expression of *rbc*S and other photosynthetic genes by carbohydrates: a mechanism for the "sink" regulation of photosynthesis? *Plant Journal* **3**: 817-828.

Krapp, A., Fraisier, V. et al. (1998). Expression studies of Nrt2:1 Np, a putative high affinity transporter: evidence for its role in nitrate uptake. *Plant Journal*. **6**: 723-732.

Krekule, J and Machackova, I. (1986). The possible role of auxin and of its metabolic changes in the photoperiodic control of flowering. In *Molecular and physiological aspects of plant peroxidases*. Universite of Geneve, Switzerland.

Kruger, N. J. (1997). Carbohydrates synthesis and degradation. *Plant metabolism. D.T. Dennis, D.H. Turpin, D.D. Lefebvre and D.B. Layzell. Harlow, UK, Longman* **83-104**.

Lam, HM., Hsieh, MH. et al. (1998). Reciprocal regulation of distinct asparagine synthetase genes by light and metabolites in *Arabidopsis thaliana. Plan J* **16**:345-353.

Lam, HM, Coschigano, C. et al. (1995). Use of Arabidopsis mutants and genes to study amide amino acid Biosynthesis. *The Plant Cell* **7:** 887- 898.

Lam, H. M., Peng, S. Y. et al. (1994). Metabolic regulation of the gene encoding glutamine-dependent asparagine synthetase in *Arabidopsis thaliana*. *Plant Physiology* **106**: 1347-1357.

Lam, HM., Wong, P. et al. (2003). Overexpression of the ASN1 gene enhances nitrogen status in seeds of *Arabidopsis. Plant Physiology* **132**: 926-935.

Lang, A. (1952). Physiology of flowering. *Annu Rev Plant Physiol* **3**: 265-306.

Langridge, J. (1957). Effect of day-length and gibberellic acid on the flowering of *Arabidopsis*. *Nature* **180**:36-37.

Larkindale, J. and Knight, MR. (2002). Protection against heat stress-induced oxidative damage in Arabidopsis involves calcium, abscisic acid, ethylene, and salicylic acid. *Plant Physiol* **128**: 682-695.

Lea, P. J., Blackwell, R. D. et al. (1989). The use of mutants lacking glutamine synthetase and glutamate synthase to study their role in plant nitrogen metabolism. *In Recent Advances in Phytochemistry*, J.E. (New York: Plenum Press). 157-189.

Lea, P. J. and Ireland, R. J. (1999). Nitrogen metabolism in higher plants. In BK Singh, ed, *Plant amino acids.* Biochemistry and Biotechnology. Inc, American Cyanamid Company, Dekker, M., New York, Basel, Hong Kong.: 1-47.

Lea, P. J., Robinson, S. A. et al. (1990). The enzymology and metabolism of glutamine, glutamate, and asparagine. In *The Biochemistry of Plants*, ed. BJ Miflin, PJ Lea. New York: Academic **16**: 121–59.

Lea, P. J. and Thurman, D. A. (1972). Intracellular localization and properties of plant L-glutamate dehydrogenases.*J Exp Bot.* **23**: 440-449.

Lee, H., Suh, S. et al. (2000). The AGAMOUS-LIKE 20 MADS domain protein integrates floral inductive pathways in *Arabidopsis*. *Genes Dev*. **14**: 2366- 2376.

Lee, S., Cheng, H. et al. (2002). Gibberellin regulates *Arabidopsis* seed germination via *RGL2*, a *GAI/RGA-like* gene whose expression is up-regulated following imbibition. *Genes Dev*. **16**: 646-658.

Lejay, L., Tillard, P. et al. (1999). Molecular and functional regulation of two NO_3^- uptake systems by N- and C- status of *Arabidopsis* plants. *Plant Journal* **18**: 509-519.

Levy, Y.Y. et al. (2002). Multiple roles of *Arabidopsis VRN1* in vernalization and flowering time control. *Science*, **297:**243-246.

Lin, TP., Caspar, T. et al. (1988). Isolation and characterization of a starchless mutant of *Arabidopsis thaliana* L. Heynh lacking ADP glucose pyrophosphorylase. *Plant Physiol*. **86**: 1131-1135.

Lin, Y., Hwang, C. F. et al. (1994). 5´proximal regions of Arabidopsis nitrate reductase genes indirect nitrate induced transcription in transgenic tobacco. *Plant Physiology*, **106,**: 477-484.

Loef, I. (2002). Auswirkungen von Nitrat auf die Blühinduktion von *Arabidopsis thaliana* (L.) Heyn. Dissertation, Ruprecht-Karls-Universität, Heidelberg.

Lokhande, SD., Ogawa, K. et al. (2003). Effect of temperature on ascorbate peroxidase activity and flowering of *Arabidopsis thaliana* ecotypes under different light conditions. *J. Plant Physiol.* **160**: 57-64.

Loulakakis, C. A. and Roubelakis-Angelakis, K. A. (1990b). Intracellular localization and properties of NADH-glutamate dehydrogenase from *Vitis vinifera* L.: purification and characterization of the major leaf isoenzyme. *J Exp Bot.* **41**: 1223-1230.

Loulakakis, C. A. and Roubelakis-Angelakis, K. A. (1991). Plant NAD(H) glutamate dehydrogenase consists of two subunit polypeptides and their participation in the seven isoenzymes occurs in an ordered ratio. *Plant Physiol.* **97**: 104-111.

Loulakakis, C. A., Roubelakis-Angelakis, K. A. et al. (1994). Regulation of glutamate dehydrogenase and glutamine synthetase in avocado fruit during development and ripening. *Plant Physiology* **106**: 217-222.

Loulakakis, C. A. and Roubelakis-Angelakis, K. A. (1996). The seven NAD(H)-glutamate dehydrogenase isoenzymes exhibit similar anabolic and catabolic activities. *Physiol Plant*. **96**: 29-35.

Maarten J. Chrispeels and David E. Sadava. (2003). In *Plants, Genes and Crop Biotechnology*. Science, p: 241.

Macknight, R., Bancroft, I. et al. (1997). *FCA*, a gene controlling flowering time in *Arabidopsis*, encodes a protein containing RNA –binding domains. *Cell* **89**: 737-745.

Madore, M., Grodzinski, B. (1984). Effect of oxygen concentration on ^{14}C-photoassimilate transport from leaves of *Salvia splendens* L. *Plant Physiology* **76**: 782-786.

Magalhaes, J. R., Ju, G. C. et al. (1990). Kinetics of nitrogen-15-labelled ammonium ion assimilation in *Zea mays* : preliminary studies with a glutamate dehydrogenase (GDH1) null mutant. *Plant Physiol*. **94**: 647-656.

Marschner, M. (1995). Mineral nutrition of higher plants. ed. 2. London: Academic press L

Martin, T., Oswald, O. et al. (2002). *Arabidopsis* seedling growth, storage lipid mobilization, and photosynthetic gene expression are regulated by carbon:nitrogen availability. *Plant Physiology*, **128:** 472-481.

Martinez, C., Pons, E. et al. (2004). Salicylic acid regulates flowering time and links defence responses and reproductive development. *The Plant Journal* **37**: 209-217.

Martinez-Zapater, J., Coupland, G. et al. (1994). The transition to flowering in *Arabidopsis*. In *Arabidopsis, Cold Spring Harbor, NY: Cold Spring Harbor* Laboratory Press. 403-433.

Masclaux, C., Valadier, MH. et al. (2000). Characterization of the sink/source transition in tobacco (*Nicotiana tabacum* L.) shoots in relation to nitrogen management and leaf senescence. *Planta* **211**: 510-518.

Masclaux-Daubresse, C, Reisdorf-Cren, M. et al. (2006). Glutamine synthetase/glutamate synthase pathway and glutamate dehydrogenase play distinct roles for sink/source nitrogen cycle in tobacco (*Nicotiana tabacum* L.) *Plant Physiology* **140**: 444-456.

Matt, P., Schurr, U. et al. (1998). Growth of tobacco in short days conditions leads to high starch, low sugars, altered diurnal changes of the Nia transcript and low nitrate reductase activity, and an inhibition of amino acid synthesis. *Planta* **207**: 27-41.

Matt, P., Geiger, M. et al. (2001a). The diurnal changes of nitrogen metabolism in leaves of nitrate-replete tobacco are driven by an imbalance between nitrate reductase activity and the rate of nitrate uptake and ammonium and glutamine metabolism during the first part of the light period. *Plant Cell Environ*. **24**: 177-190.

Matt, P., Geiger, M. et al. (2001b). Elevated carbon dioxide increases nitrate uptake and nitrate reductase activity when tobacco is growing on nitrate, but increases ammonium uptake and inhibits nitrate reductase activity when tobacco is growing on ammonium nitrate. *Plant Cell Environ.* **24**: 1119-1137.

Melo-Oliveira, R., Cunha-Oliveira, I. et al. (1996). Arabidopsis mutant analysis and gene regulation define a non-redundant role for glutamate dehydrogenase in nitrogen assimilation. *Proc. Natl. Acad. Sci. USA* **93**: 4718-4723.

Michaels, S.D. and Amasino, R.M. (1999a). The gibberellic acid biosynthesis mutant *ga1-3* of *Arabidopsis thaliana* is responsive to vernalization. *Developmental genetics* **25** (3): 194-198.

Michaels, S.D. and Amasino, R.M. (1999b). FLOWERING LOCUS C encodes a novel MADS domain protein that acts as a repressor of flowering. *Plant Cell* **11**: 949-956.

Michaels, S.D., Bezerra, I.C. et al. (2004). *FRIGIDA*-related genes are required for the winter-annual habit in *Arabidopsis*. *Proc. Natl. Acad. Sci. USA*. **101**: 3281-3285.

Miesak, B.H. and Coruzzi, G.M. (2002). Molecular and physiological analysis of *Arabidopsis* mutants defective in cytosolic or chloroplastic Aspartate aminotransferase. *Plant Physiology*. **129:** 650-660.

Miflin, B. J. (1974). The location of nitrite reductase and other enzymes related to amino acids biosynthesis in the plastids of root and leaves. *Plant Physiology* **54**: 550-555.

Miflin, B. J. and Habash, D. Z. (2002). The role of glutamine synthetase and glutamate dehydrogenase in nitrogen assimilation and possibilitites for improvement in the nitrogen utilization of crops. *J Exp Bot.* **53**: 979-987.

Miflin, B. J. and Lea, P. J. (1980). Ammonia assimilation. *The Biochemistry of Plants: Aminoacids and Derivatives. Academic Press, New York.* **5**: 329-357.

Moon, J., Suh, S-S. et al. (2003). The SOC1 MADS-box gene integrates vernalization and gibberellin signals for flowering in *Arabidopsis. The Plant Journal*. **35**: 613-623.

Morcuende, R., Krapp, A. et al. (1998). Sucrose feeding leads to increased rate of nitrate assimilation, increased rates of 2-oxoglutarate synthesis, and increased synthesis of a wide spectrum of aminoacids in tobacco leaves. *Planta* **206,**: 394-409.

Mouradov, A., Cremer, F. et al. (2002). Control of flowering time: Interacting pathways as a basis for diversity. *Plant Cell* **Suppl. 2002**: S111-S130.

Nilsson, O., Lee, I. et al. (1998). Flowering-time genes modulate the response to *LEAFY* activity. *Genetics* **150**: 403-410.

Nussaume, L., Vincentz, M. et al. (1995). Post-transcriptional regualiton of nitrate reductase by light is abolished by a N-terminal deletion. *Plant Cell* **7**: 611-621.

Oaks, A., Stulen, I. et al. (1980). Enzymes of nitrogen assimilation in maize roots. *Planta* **148**: 477-484.

Oaks, A. and Ross, D. W. (1984). Asparagine synthetase in *Zea mays*. *Can. J.Bot.* **62**: 68-

Ogawa, K. and Iwabuchi, M. (2001). A mechanism for promoting the germination of *Zinnia elegans* seeds by hydrogen peroxide. *Plant Cell Physiol* **42:** 286-291.

Ogawa, K., Tasaka, Y (2001). Association of glutathione with flowering in *Arabidopsis thaliana. Plant Cell Physiol*. **42**: 524-530.

Ohto, M., Onai, K. et al. (2001). Effects of sugars on vegetative development and floral transition in *Arabidopsis. Plant Physiol.* **127**: 252-261.

Oliveira, I. C. and Coruzzi, G. M. (1999). Carbon and Amino acids reciprocally modulate the expression of glutamine synthetase in Arabidopsis. *Plant Physiology* **121**: 301-309.

Onouchi, H., Igeno, M.I. et al. (2000). *Mutagenesis* of plants overexpressing *CONSTANS* demostrates novel interactions among *Arabidopsis* flowering-time genes. *Plant Cell* **12**: 885-900.

Orsel. M., Filleur. S. et al. (2001). Nitrate transport in plants: which gene and which control? *Journal of Experimental Botany*, **Vol. 53, No. 370**: 825-833.

Osuna, D., Usadel, B. et al. (2007). Temporal responses of transcripts, enzyme activities and metabolites after adding sucrose to carbon-deprived *Arabidopsis* seedlings. *The Plant Journal* **49** (3): 463-491.

Palatnik,J., Allen, F. et al. (2003). Control of leaf morphogenesis by microRNAs. *Nature* **425**: 257-263.

Parcy, F., Nilsson, O. et al. (1998). A genetic framework for floral patterning. *Nature* **395:** 561- 566.

Parcy, F. (2005). Flowering: a time for integration. *Int J Dev Biol*. **49**: 585- 593.

Pavesi, A., Ficarelli, A. et al. (2000). Cloning of two glutamate dehydrogenase cDNAs from *Asparagus officinalis*: sequence analysis and evolutionary implications. *Genome* **4**: 306-316.

Peng, J., Carol, P., et al. (1997). The Arabidopsis GAI defines a signaling pathway that negatively regulates gibberellins responses. *Genes Dev*. **11** (23): 3194-3204.

Peterman, TK. and Goodman, HM. (1991). The glutamine synthetase gene family of *Arabidopsis thaliana*: light regulation and differential expression in leaves, roots and seeds. *Mol Gen Genet.* **230:** 145-154.

Pidkowich, M. S., Klenz, E. et al. (1999). The making of a flower: control of floral meristem identity in *Arabidopsis*. *Trends in Plant Science* **4** (2): 64-70.

Pigliucci, M., and Kolodynska, A. (2002). Phenotypic plasticity and integration in response to flooded conditions in natural accessions of *Arabidopsis thaliana* (L.) Heynh (Brassicaceae). *Ann. Bot. (Lond).* **90**: 199-207.

Pigliucci, M., Whitton, J. et al. (1995). Reaction norms of *Arabidopsis*. I. Plasticity of characters and correlations across water, nutrients and light gradients. *J. Evol. Biol*. **8**: 421-438.

Pouteau, S., Cherel, I. et al. (1989). Nitrate reductase mRNA regulation in Nicotiana plumbaginifolia nitrate-reductase- deficient mutants. *Plant Cell* **1,**: 1111-1120.

Price, J., Laxmi, A. et al (2004). Global transcription profiling reveals multiple sugar signal transduction mechanism in *Arabidopsis*. *Plant Cell* **16**:2128-2150.

Pryor, A. J. (1990). A maize glutamic dehydrogenase null mutant is cold temperature sensitive. *Maydica* **35**: 367-372.

Putterill, J., Robson, F. et al. (1995). The CONSTANS gene of *Arabidopsis* promotes flowering and encodes a protein showing similarities to zinc finger transcription factors. *Cell* **80**: 847-857.

Purnell, M. P., Skopellitis, D. S. et al. (2005). Modulation of higher-plant NAD(H)-dependent glutamate dehydrogenase activity in transgenic tobacco via alteration of beta subunit levels. *Planta* **222**: 167-180.

Quesada, V., Macknight, R. et al. (2003). Autoregulation of FCA pre-mRNA processing controls *Arabidopsis* flowering time. *EMBO J*. **22**: 3142-3152.

Ratcliffe, O., Bradley, D.J. et al. (1999). Separation of shoot and floral identity in *Arabidopsis*. *Development.* **126** (6): 1109-1120.

Raghothama KG. (1999). Phosphate acquisition. *Annual Review of Plant Physiology* **50:** 665-693.

Raper CDJ., Thomas JF. et al. (1988). Assessment of an apparent relationship between availability of soluble carbohydrates and reduced nitrogen during floral initiation in tobacco. *Bot. Gaz.* **149**: 289-294.

Rausch C, Bucher M. (2002). Molecular mechanisms of phosphate transport in plants. *Planta* **216:** 23-37.

Rawat, SR., Salim, N. et al. (1999). *AtAMT1* gene expression and NH_4^+ uptake in roots of *Arabidopsis thaliana*: evidence for regulation by root glutamine levels. *The Plant Journal.* **19** (2): 143-152.

Reeves, RH & Coupland, G. (2001). Analysis of flowering time control in *Arabidopsis* by comparison of double and triple mutants. *Plant Physiology*. **126** (3): 1085-91.

Restivo, F. M. (2004). Molecular cloning of glutamate dehydrogenase genes of *Nicotiana plumbaginifolia*: structure and regulation of their expression by physiological and stress conditions. *Plant Science* **166**: 971-982.

Richards, N. G. J. and Schuster, S. M. (1992). An alternative mechanism for the nitrogen transfer reaction in asparagine synthetase. *FEBS lett.* **313**: 98-102.

Rideout, JW., Raper, CD. et al. (1992). Changes in ratio of soluble sugars and free amino nitrogen in the apical meristem during floral transition of tobacco. *Int. J. Plant Sci*. **153**: 78-88.

Riechmann, J & Meyerowitz, EM. (1998). The AP2/EREBP family of transcription factors. *Biol Chem*. **379** (6):633-646.

Robinson, S. A., Slade, A. P. et al. (1991). The role of glutamate dehydrogenase in plant nitrogen metabolism. *Plant Physiology* **95**: 509-516.

Robinson, S. A., Stewart, G. R. et al. (1992). Regulation of glutamate dehydrogenase activity in relation to carbon limitation and protein catabolism in carrot cell suspension cultures. *Plant Physiology* **98**: 1190-1195.

Robson, F., Costa, MM. et al. (2001). Functional importance of conserved domains in the flowering-time gene CONSTANS demonstrated by analysis of mutant alleles and transgenic plants. *Plant Journal* **28**: 619-631.

Roldán, M., Gómez-Mena, C. et al. (1997). Effect of darkness and sugar availability to the apex on morphogenesis and flowering time of *Arabidopsis*. *Flowering Newsl*. **24**:18-24.

Ross, J.J., Murfet, I.C. et al. (1993). Distribution of Gibberellins in *Lathyrus odoratus L.* and Their Role in Leaf Growth. *Physiol. Plant* **100**: 550-560.

Ruiz-García, L., Madueño, F. et al. (1997). Different roles of flowering-time genes in the activation of floral initiation genes in *Arabidopsis. Plant Cell* **9**: 1921-1934.

Sachs, R. M. and Hackett, W. P. (1983). Source-sink relationships and flowering. In *Beltsville symposia in Agricultural research*. **6**: 263-272.

Sahulka, J. and Lisa, L (1980). Effect of some dissacharides, hexoses and pentoses on nitrate reductase, glutamine synthetase and glutamate dehydrogenase in excised pea roots. *Physiol Plant* **50**: 32-36.

Sakakibara,H., Hawabata, S. et al. (1992). Molecular cloning of the family of glutamine synthetase genes from maize: expression of genes for glutamine synthetase and ferredoxin dependent-glutamate synthase in photosynthetic and non-photosynthetic tissues. *Plant Cell Physiol*. **33**: 49-58.

Samach, A., Onouchi, H. et al. (2000). Distinct roles of CONSTANS target genes in reproductive development of *Arabidopsis*. *Science* **288**: 1613-1616.

Sambrook, J. and Russell, D. W. (2001). Molecular cloning: A laboratory manual. *Cold Spring Harbor, Laboratory press, New York.*

Scheible, W. R., Lauerer, M. et al. (1997a). Accumulation of nitrate in the shoot acts as signal to regulate shoot-root allocation in tobacco. *Plant Journal* **11**: 671-691.

Scheible, W. R., Gonzalez-Fuentes, A. et al. (1997b). Nitrate acts as a signal to induce organic acid metabolism and repress starch metabolism in tobacco. *The Plant Cell* **9**: 783-79.

Scheible, W. R., Gonzalez-Fuentes, A. et al. (1997c). Tobacco mutants with a decreased number of functional *nia* genes compensate by modifying the diurnal regulation of transcription, post-translational modification and turnover of nitrate reductase. *Planta* **203,**: 304-319.

Scheible, W. R., Morcuende, R. et al. (2004). Genome-Wide Reprogramming of Primary and Secondary Metabolism, Protein Synthesis, Cellular Growth Processes, and the Regulatory Infrastructure of Arabidopsis in Response to Nitrogen. *Plant Physiology,* **136,**: 2483–2499.

Schultz, C. J. and Coruzzi, G. M. (1995). The aspartate aminotransferase gene family of Arabidopsis encodes isoenzymes localized to three distinct subcellular compartments. *Plant Journal* **7**: 61-75.

Sechley, K. A., Yamaya, T. et al. (1992). Compartmentation of nitrogen assimilation in higher plants. *Int. Rev. Cytol.* **134**: 85–163.

Shannon, S. and Meeks-Wagner, D. (1991). A mutat in the *Arabidopsis TFL1* gene affects inflorescence meristem development. *The Plant Cell* **3**: 877-8892.

Sheldon, C.C., Burn, J.E. et al. (1999). The FLF MADS box gene: a repressor of flowering in Arabidopsis regulated by vernalization and methylation**.** *Plant Cell*, **11**: 445- 458.

Sheldon, C.C., Rouse, D.T. et al. (2000). The molecular basis of vernalization: The central role of FLOWERING LOCUS C (FLC). *Proc. Natl. Acad. Sci*.USA, **97**: 3753- 3758.

Singla, S.L., Pareek A. et al. (1997). In *Plant Ecophysiology* (ed. Prasad, M.N.V.), John Wiley, New York, pp. 101-127.

Simon, R. Igeno, M. I. et al. (1996). Activation of floral meristem identity genes in *Arabidopsis*. *Nature* **384**: 59-62.

Simpson, G. G., Gendall, A. R. et al. (1999). When to switch to flowering. *Annu Rev Cell. Dev. Biol.* **15**: 519-550.

Simpson, G. G., Dean, C. (2002). *Arabidopsis*, the Rosetta stone of flowering time? *Science* **296**: 285-289.

Sivasankar, S., Rothstein, S. et al. (1997). Regulation of the accumulation and reduction of nitrate by nitrogen and carbon metabolite in maize seedlings. *Plant Physiology,* **114**: 583-589.

Snape, J.W., Quarrie, S.A. et al. (1996). Comparative mapping and its use for the genetic analysis of agronomic characters in wheat. *Euphytica,* **89:** 27-31**.**

Somerville, C. R. and Ogren, W. L. (1980). Inhibition of photosynthesis in Arabidopsis mutants lacking leaf glutamate synthase activity. *Nature* **286**: 257-259.

Srivastava, H. S. and Singh, R. P. (1987). Role of regulation of $_{L}$-glutamate dehydrogenase activity in higher plants. *Phytochemistry* **26**: 597-610.

Stewart, G. R., Mann, A. F. et al. (1980). Enzymes of glutamate formation: glutamate dehydrogenase, glutamine synthetase, glutamate synthase. *The Biochemistry of Plants: Amino Acids and Derivatives*, ed. BJ Miflin, New York: Academic **5**: 271–327.

Stewart, G. R., Shatilov, V. R. et al. (1995). Evidence that glutamate dehydrogenase plays a role in oxidative deamination of glutamate in seedlings of *Zea mays*. *Plant Physiology* **22**: 805-809.

Stitt, M. (1996). Metabolic regulation of photosynthesis. In *Advances in Photosynthesis*. Environmental Stress and Photosynthesis, N. Baker, ed. (Dordrecht, The Netherlands: Kluwer academic publishers), **3**: 151-190.

Stitt, M. (1999). Nitrate regulation of metabolism and growth. *Curr Opin Plant Biol.* **2**: 178-86.

Stitt, M., Huber, S. et al. (1987). Control of photosynthetic sucrose synthesis. *In The Biochemistry of Plants*. M.D. Hatch and N.K. Boardman, eds (San Diego, CA: Ac ademic Press) **10**: 327-409.

Stitt, M. and Feil, R. (1999). Lateral root frequency decreases when nitrate accumulates in tobacco transformant with low nitrate reductase activity: consequences for the regulation of biomass partioning between shoots and roots. *Plant Soil* **215**: 143-153.

Stitt, M., Cseke, C. et al. (1984). Regulation of fructose 2,6-bisphosphate concentration in spinach leaves. *Eur J Biochem* **143(1)**: 89-93.

Stitt, M. and Krapp, A. (1999). The molecular physiological basis for the interaction between elevated carbon dioxide and nutrients. *Plant, Cell & Environment* **22**: 583- 622.

Stitt, M., Müller, C. et al. (2002). Step towards an integrated view of nitrogen metabolism. *Journal of Experimental Botany* **53**: 959-970.

Suárez-López, P., Wheatley, K. et al. (2001). CONSTANS mediates between the circadian clock and the control of flowering in *Arabidopsis*. *Nature*. **410**: 1116-1120.

Suárez-López, P., (2005). Long-range signalling in plant reproductive development. *Int. J. Dev. Biol*. **49**: 761-771.

Sun, T.P., Goodman, H.M., et al. (1992). Cloning the *Arabidopsis GA1* locus by genomic subtraction . *Plant Cell* **4**: 119-128.

Sung, S. and Amasino, R.M. (2004). Vernalization in *Arabidopsis thaliana* is mediated by the PHD finger protein VIN3. *Nature* **427**:159-164.

Suzuki, A. and Gadal, P. 1984). Glutamate synthase: physicochemical and functional properties of different forms in higher plants and other organisms. *Physiol.Veg.* **22**: 471–86.

Suzuki, A., Vidal, J. et al. (1982). Glutamate synthase isoforms in rice: immunological studies of enzymes in green leaf, etiolated leaf, and root tissues. *Plant Physiology* **70**: 827–32.

Takatsuyi, H., (1998). Zinc finger transcription factors in plants. *Cell Mol Life Sci*. **54** (6): 582-596.

Tanimoto, S., and Harada, H (1981). Chemical factors controlling floral bud formation of *Torenia* stem segments cultured in vitro. I. Effect of mineral nutrients and sugars. *Plant Cell Physiol.* **22**: 533-541.

Tempest, DW., Meers, JL. et al. (1970). Synthesis of glutamate in *Aerobacter aerogenes* by a hitherto unknown route. *Biochem. J* **117**: 405-407.

Tercé-Laforgue, T., Dubois, F. et al. (2004). Glutamate dehydrogenase of tobacco is mainly induced in the cytosol of phloem companion cell when ammonia is provided Esther externally or released during photorespiration. *Plant Physiology* **136**: 4308-4317.

Thimm, O., Bläsing, O. et al. (2004). MAPMAN: a user-driven tool to display genomics data sets onto diagrams of metabolic pathways and other biological processes. *Plant J* **37**:914-939.

Thomas, B. and Vince-Prue, D. (1997). Photoperiodism in plants. *2nd ed. San Diego CA: Academic Press*.

Tsai, F. Y. and Coruzzi, G. M. (1990). Dark-induced and organ-specific expression of two asparagine synthetase genes in *Pisum sativum*. *EMBO Journal* **9**: 323-332.

Tsai, F. Y. and Coruzzi, G. M. (1991). Light represses the transcription of asparagine synthetase genes in photosynthetic and non-photosynthetic organs of plants. *Mol. Cell. Biol.* **11**: 4966-4972.

Turano, F. J., Dashner, R. et al. (1996). Purification of mitochondrial glutamate dehydrogenase from dark-grown Soybean seedlings. *Plant Physiology* **112**: 1357-1364.

Turano, F. J., Thakkar, S. S. et al. (1997). Characterization and expression of NAD(H)-dependent glutamate dehydrogenase genes in Arabidopsis. *Plant Physiology* **113**: 1329-1341.

Ullrich, W. R., Larsson, M. et al. (1984). Ammonium uptake in Lemna gibba G-1, related membrane potential changes and inhibition of anion uptake. *Physiologia Plantarum* **61**: 369-376.

Ueki, S. and Citovsky, V. (2001). RNA commutes to work: regulation of plant gene expression by systematically transported RNA molecules. *Bioessays.* **23** (12): 1087-1090.

Valverde, F., Mouradov, A. et al. (2004). Photoreceptor regulation of CONSTANS protein in photoperiodic flowering. *Science*, **303:**1003-1006.

Vance, CP., Uhde-Stone C, et al. (2003). Phosphorus acquisition and use: critical adaptations by plants for securing a nonrenewable resource. *New Phytologist* **157:** 423-447.

Vincentz, M. and Caboche, M. (1991). Constitutive expression of nitrate reductase allows normal growth and development of *Nicotiana plumbaginifolia* plants. *EMBO Journal* **10**: 1027-1035.

Vincentz, M., Moureaux, T. et al. (1993). Regulation of nitrate and nitrite reductase expression in *Nicotiana plumbaginifolia* leaves by nitrogen and carbon metabolites. *Plant Journal* **3,**: 313-324.

Wagner, D., Wellmer, F. et al. (2004). Floral induction in tissue culture: a system for the analysis of *LEAFY*-dependent gene regulation. *Plant Journal*. **39**: 273- 282.

Wallsgrove, R. M., Turner, J. C. et al. (1987). Barley mutants lacking chloroplast glutamine synthetase- biochemical and genetic analysis. *Plant Physiology* **83**: 155-158.

Wang, M. Y., Siddiqi, M. et al. (1993). Ammonium uptake by rice roots. *Plant Physiology* **103**: 1259-1267.

Weller, J.L., Reid, J.B. et al. (1997). The genetic control of flowering in pea. *Trends Plant. Sci*. **2**: 412-418.

Wigge, P.A., Kim, M.C. et al. (2005). Integration of spatial and temporal information during floral induction in *Arabidopsis*. *Science* **309**: 1056-1059.

Wilkie, S. E., Roper, J. et al. (1995). Isolation, characterization and expression of a cDNA clone encodin aspartate aminoransferase from *Arabidopsis thaliana*. *Plant Molecular Biology* **6**: 1227-1233.

Wilson, R.N., Heckman, J.W. et al. (1992). Gibberellin is required for flowering in *Arabidopsis thaliana* under short days. *Plant Physiol*. **100**:403-408.

Wray, J. L. (1993). Molecular biology, genetics and regulation of nitrite reduction in higher plants. *Physiol. Plant* **89**: 607-612.

Wu, P., Ma, L. et al. (2003). Phosphate starvation triggers distinct alterations of genome expression in Arabidopsis roots and leaves. *Plant Physiology* **132**: 1260-1271.

Xoconostle-Cazarés, B., Xiang, Y. et al. (1999). Plant paralog to viral movement protein that potentiates transport of mRNA into the phloem. *Science.* **283** (5398): 12-13.

Yamaya, T. and Oaks, A. (1987). Synthesis of glutamate by mitochondria-n anaplerotic function of glutamate dehydrogenase. *Physiol. Plant* **70**: 749-756.

Yanagisawa, S., Akiyama, A., et al. (2004). Metabolic engineering with Dof1 transcription factor in plants: improved nitrogen assimilation and growth under low- nitrogen conditions. *PNAS*. **101**(20): 7833-7838.

Yanhui, C., Xiaoyuan, Y. et al. (2006). The MYB transcription factor superfamily of Arabidopsis: expression analysis and phylogenetic comparison with the rice MYB family. *Plant Mol Biol*. **60**: 107-124.

Yoo, B.C., Klager, F, et al. (2004) A systemic small RNA signaling system in plants. *The Plant Cell*. **16:** 1979-2000.

Yu, T., Kofler, H. et al. (2001). The Arabidopsis *sex1* mutant is defective in the R1 protein, a general regulator of starch degradation in plants, and not in the chloroplast hexose trnasporter. *The Plant Cell*. **13**: 1907- 1918.

Zeeman, SC, Northrop, F et al. (1998). A starch-accumulating mutant of *Arabidopsis thaliana* deficient in a chloroplastic starch-hydrolysing enzyme. *Plant J.* **15**:357- 365.

Zhang, H. and Forde, B. G. (1998). An *Arabidopsis* MADS-box gene controlling nutrient-induced changes in root architecture. *Science* **279**: 407-409.

Zhang, H., Jennins, A. et al. (1999). Dual pathways for regulation of root branching by nitrate. *Proceedings of the national Academy of Science of the USA* **96**: 6529-6534.

Zhou, L., Jang, JC. et al. (1998) Glucose an ethylene signal transduction crosstalk revealed by an *Arabidopsis* glucose insensitive mutant. *Proc Natl Acad Sci* USA. **95**: 10294-10299.

CHAPTER 7 APPENDIX

7.1. Sugars and starch content in plants with decreased GDH1 compared to wild type in Diurnal rhythm experiments.

line	timepoint	Glucose	SD	Fructose	SD	Sucrose	SD	Starch	SD
Col-0	0h	0,35	± 0,07	0,55	± 0,02	2,32	± 0,72	3,09	± 0,75
gdh1 11-7 KO	0h	0,36	± 0,10	0,65	± 0,17	2,48	± 0,25	3,38	± 0,25
gdh1-2 RNAi	0h	0,21	± 0,06	0,28	± 0,10	1,59	± 0,20	2,37	± 0,73
Col-0	12h	0,74	± 0,30	0,60	± 0,11	4,06	± 0,60	34,67	± 5,77
gdh1 11-7 KO	12h	0,63	± 0,13	0,56	± 0,21	3,25	± 0,36	28,77	± 2,40
gdh1-2 RNAi	12h	0,59	± 0,11	0,36	± 0,08	3,31	± 0,33	34,94	± 4,80
Col-0	18h	0,42	± 0,19	0,48	± 0,17	2,99	± 0,72	18,77	± 3,15
gdh1 11-7 KO	18h	0,43	± 0,10	0,58	± 0,18	3,60	± 0,59	18,43	± 4,15
gdh1-2 RNAi	18h	0,43	± 0,09	0,23	± 0,07	2,29	± 0,39	19,28	± 3,38
Col-0	24h	0,41	± 0,03	0,40	± 0,25	2,02	± 0,81	2,97	± 0,73
gdh1 11-7 KO	24h	0,35	± 0,05	0,65	± 0,04	2,17	± 0,32	3,63	± 1,53
gdh1-2 RNAi	24h	0,38	± 0,14	0,17	± 0,09	1,31	± 0,27	2,82	± 0,92

Table 1. Plants were harvested throughout a day/night cycle of 12h light/12h dark photoperiod: (0h) at the beginning of the day; (12h) at the end of the day; (18h) middle of the night; and (24h) end of the night. Sugar and starch content were assayed in rosette leaves of 6 weeks old plants. Values are means ± SD (n=5) in WT and *gdh1*KO plants and ± SD (n=10-15) in the RNAi lines. Sugars are given in µmol_g FW.

7.2. Sugar and starch content in plants with decreased GDH1 compared to wild type in extended night experiment.

line	timepoint	Glucose	SD	Fructose	SD	Sucrose	SD	Starch	SD
Col-0	0h	0,41	± 0,03	0,40	± 0,25	2,02	± 0,81	2,97	± 0,73
gdh1 11-7 KO	0h	0,35	± 0,05	0,65	± 0,04	2,17	± 0,32	3,63	± 1,53
gdh1-2 RNAi	0h	0,38	± 0,14	0,17	± 0,09	1,31	± 0,27	2,82	± 0,92
Col-0	24h ext.night	0,32	± 0,10	0,34	± 0,12	0,98	± 0,34	0,45	± 0,26
gdh1 11-7 KO	24h ext.night	0,28	± 0,06	0,42	± 0,13	0,80	± 0,09	0,84	± 0,22
gdh1-2 RNAi	24h ext.night	0,17	± 0,07	0,18	± 0,07	0,45	± 0,24	0,60	± 0,25
Col-0	48h ext.night	0,27	± 0,12	0,24	± 0,06	0,79	± 0,49	0,46	± 0,15
gdh1 11-7 KO	48h ext.night	0,27	± 0,09	0,25	± 0,11	0,55	± 0,11	0,68	± 0,17
gdh1-2 RNAi	48h ext.night	0,13	± 0,04	0,12	± 0,06	0,22	± 0,09	0,70	± 0,22
Col-0	72h ext.night	0,26	± 0,08	0,34	± 0,20	0,71	± 0,42	0,45	± 0,06
gdh1 11-7 KO	72h ext.night	0,21	± 0,08	0,18	± 0,02	0,57	± 0,10	0,36	± 0,10
gdh1-2 RNAi	72h ext.night	0,13	± 0,06	0,23	± 0,05	0,16	± 0,08	1,35	± 0,34

Table 2. Extended night experiment. Plants were harvested after transferring to continuous darkness: 24h, 48h and 72h extended night. Sugar and starch content were assayed in rosette leaves of 6 weeks old plants. Values are means ± SD (n=5) in WT and in the GDH1KO lines; ± SD (n=10-15) in transgenic lines. Sugars (glucose, fructose and sucrose) and starch are given in µmol_g FW.

7.3. Sugars and starch content in plants with decreased GDH2 compared to wild type in Diurnal rhythm experiments.

line	timepoint	Glucose	±	SD	Fructose	±	SD	Sucrose	±	SD	Starch	±	SD
Col-0	0h	0,32	±	0,08	0,43	±	0,19	1,73	±	0,33	2,82	±	0,82
gdh2-39 RNAi	0h	0,57	±	0,17	0,18	±	0,13	1,29	±	0,16	3,26	±	1,00
gdh2-46 RNAi	0h	0,23	±	0,08	0,35	±	0,08	1,30	±	0,25	1,21	±	0,18
Col-0	12h	0,44	±	0,05	0,39	±	0,12	3,11	±	0,66	38,21	±	6,69
gdh2-39 RNAi	12h	0,47	±	0,18	0,32	±	0,11	3,00	±	0,38	40,22	±	4,44
gdh2-46 RNAi	12h	0,46	±	0,08	0,39	±	0,07	3,04	±	0,49	38,15	±	5,12
Col-0	18h	0,29	±	0,02	0,22	±	0,06	2,17	±	0,12	19,65	±	0,04
gdh2-39 RNAi	18h	0,39	±	0,21	0,22	±	0,13	2,17	±	0,59	19,93	±	3,63
gdh2-46 RNAi	18h	0,38	±	0,15	0,19	±	0,05	2,13	±	0,37	19,75	±	1,97
Col-0	24h	0,38	±	0,00	0,19	±	0,03	1,53	±	0,61	2,82	±	0,14
gdh2-39 RNAi	24h	0,57	±	0,17	0,15	±	0,08	1,29	±	0,16	3,26	±	1,00
gdh2-46 RNAi	24h	0,27	±	0,08	0,18	±	0,06	1,36	±	0,25	3,36	±	0,71

Table 3. Plants were harvested as described for GDH1 (see table 1).

7.4. Sugar and starch content in plants with decreased GDH2 compared to wild type in extended night experiments.

line	timepoint	Glucose	±	SD	Fructose	±	SD	Sucrose	±	SD	Starch	±	SD
Col-0	0h	0,38	±	0,00	0,19	±	0,03	1,53	±	0,61	2,82	±	0,14
gdh2-39 RNAi	0h	0,57	±	0,17	0,15	±	0,08	1,29	±	0,16	3,26	±	1,00
gdh2-46 RNAi	0h	0,27	±	0,08	0,18	±	0,06	1,36	±	0,25	3,36	±	0,71
Col-0	24h ext.night	0,23	±	0,01	0,17	±	0,09	0,34	±	0,08	0,91	±	0,18
gdh2-39 RNAi	24h ext.night	0,21	±	0,16	0,31	±	0,13	0,52	±	0,15	1,02	±	0,22
gdh2-46 RNAi	24h ext.night	0,18	±	0,07	0,12	±	0,05	0,28	±	0,12	0,65	±	0,20
Col-0	48h ext.night	0,14	±	0,00	0,29	±	0,12	0,40	±	0,09	0,51	±	0,03
gdh2-39 RNAi	48h ext.night	0,08	±	0,10	0,17	±	0,08	0,61	±	0,29	1,09	±	0,23
gdh2-46 RNAi	48h ext.night	0,15	±	0,05	0,11	±	0,08	0,23	±	0,05	0,83	±	0,37
Col-0	72h ext.night	0,12	±	0,07	0,17	±	0,09	0,35	±	0,11	0,79	±	0,44
gdh2-39 RNAi	72h ext.night	0,03	±	0,04	0,12	±	0,09	0,75	±	0,27	1,46	±	0,34
gdh2-46 RNAi	72h ext.night	0,15	±	0,06	0,18	±	0,08	0,24	±	0,08	0,48	±	0,17

Table 4. Plants were harvested as described for GDH1 (see table 2).

7.5. Major amino acids determined by HPLC in *GDH1*KO and transgenic *GDH1* lines and WT in Diurnal rhythm experiments.

line	timepoint	Aspartate	SD	Glutamate	SD	Asparagine	SD	Glutamine	SD
Col-0	0h	1,53	±0,17	2,65	±0,55	0,79	±0,20	1,32	±0,30
gdh1 11-7 KO	0h	1,21	±0,05	2,94	±0,23	0,55	±0,24	1,34	±0,22
gdh1-2 RNAi	0h	1,29	±0,48	2,73	±0,36	0,71	±0,15	1,46	±0,39
Col-0	12h	1,74	±0,04	3,19	±0,51	0,66	±0,07	2,56	±0,20
gdh1 11-7 KO	12h	1,92	±0,21	3,47	±0,46	0,80	±0,10	3,17	±0,47
gdh1-2 RNAi	12h	1,44	±0,08	3,26	±0,20	0,74	±0,07	2,75	±0,21
Col-0	18h	1,52	±0,17	3,03	±0,09	0,77	±0,18	2,05	±0,16
gdh1 11-7 KO	18h	1,89	±0,50	3,39	±0,81	0,85	±0,26	2,08	±0,57
gdh1-2 RNAi	18h	1,92	±0,20	3,79	±0,50	0,83	±0,19	2,09	±0,50
Col-0	24h	1,84	±0,26	2,88	±0,91	0,85	±0,38	1,53	±0,62
gdh1 11-7 KO	24h	1,81	±0,46	3,32	±0,86	1,01	±0,16	1,62	±0,49
gdh1-2 RNAi	24h	1,69	±0,24	3,30	±0,35	0,85	±0,17	1,71	±0,40

Table 5. Composition of the major amino acids of rosette leaves of plants harvested at four times trough the diurnal cycle, (0h) at the beginning of the day; (12h) at the end of the day; (18h) middle of night and (24h) end of the night. Free amino acids content were assayed in rosette leaves of 6 weeks old plants. Values are means ± SD (n=5) in WT and *gdh1*KO and and ± SD (n=10-15) in the RNAi lines. Amino acids content are given in µmol_g FW.

7.6. Major amino acids determined by HPLC in *GDH1*KO and transgenic *GDH1* lines and WT in extended night experiments.

line	timepoint	Aspartate	SD	Glutamate	SD	Asparagine	SD	Glutamine	SD
Col-0	0h	1,84	± 0,26	2,88	± 0,91	0,85	± 0,38	1,53	± 0,62
gdh1 11-7 KO	0h	1,81	± 0,46	3,32	± 0,86	1,01	± 0,16	1,62	± 0,49
gdh1-2 RNAi	0h	1,69	± 0,24	3,30	± 0,35	0,85	± 0,17	1,71	± 0,40
Col-0	24h ext.night	1,58	± 0,27	3,95	± 0,83	5,56	± 1,06	1,01	± 0,30
gdh1 11-7 KO	24h ext.night	1,42	± 0,24	3,98	± 0,70	5,42	± 1,01	1,16	± 0,19
gdh1-2 RNAi	24h ext.night	1,18	± 0,27	3,69	± 0,75	4,60	± 1,17	0,98	± 0,26
Col-0	48h ext.night	1,35	± 0,46	3,39	± 0,45	8,59	± 0,30	1,02	± 0,30
gdh1 11-7 KO	48h ext.night	0,68	± 0,13	3,19	± 0,19	8,39	± 1,21	0,82	± 0,15
gdh1-2 RNAi	48h ext.night	1,00	± 0,12	3,79	± 0,16	10,58	± 1,10	1,02	± 0,23
Col-0	72h ext.night	1,04	± 0,24	3,07	± 0,44	10,13	± 0,74	0,78	± 0,18
gdh1 11-7 KO	72h ext.night	0,46	± 0,08	3,19	± 0,64	11,46	± 1,57	0,93	± 0,24
gdh1-2 RNAi	72h ext.night	0,75	± 0,09	3,50	± 0,35	12,33	± 1,41	1,14	± 0,28

Table 6. A) Composition of the major amino acids of rosette leaves of plants harvested after transferring to continuous darkness: 24h, 48h and 72h extended night. Free amino acids were assayed in rosette leaves of 6 weeks old plants. Values are means ± SD (n=5) in WT and ± SD (n=10-15) in transgenic lines. Values are given in µmol_g FW.

7.7. Major amino acids determined by HPLC in transgenic *GDH2*RNAi lines and WT in Diurnal rhythm experiments.

line	timepoint	Aspartate	SD	Glutamate	SD	Asparagine	SD	Glutamine	SD
Col-0	0h	1,58	±0,15	2,67	±0,33	0,71	±0,10	1,32	± 0,30
gdh2-39 RNAi	0h	1,58	±0,40	2,81	±0,56	0,31	±0,20	-	± -
gdh2-46 RNAi	0h	1,55	±0,30	2,70	±0,52	0,71	±0,16	1,25	± 0,29
Col-0	12h	1,57	±0,36	3,24	±0,58	0,66	±0,07	2,56	± 0,20
gdh2-39 RNAi	12h	2,20	±0,29	3,19	±0,52	0,72	±0,10	-	± -
gdh2-46 RNAi	12h	1,40	±0,24	3,42	±0,53	0,76	±0,09	2,69	± 0,34
Col-0	18h	1,73	±0,47	3,08	±0,01	0,71	±0,16	2,05	± 0,16
gdh2-39 RNAi	18h	2,02	±0,29	2,89	±0,42	0,65	±0,14	-	± -
gdh2-46 RNAi	18h	1,81	±0,15	3,17	±0,38	0,80	±0,15	1,96	± 0,35
Col-0	24h	1,51	±0,06	2,82	±0,12	0,81	±0,05	1,53	± 0,62
gdh2-39 RNAi	24h	1,58	±0,40	2,81	±0,56	0,31	±0,20	-	± -
gdh2-46 RNAi	24h	1,19	±0,19	2,91	±0,34	0,80	±0,15	1,55	± 0,28

Table 7. Composition of the major amino acids of rosette leaves of plants harvested at four times trough the diurnal cycle, (0h) at the beginning of the day; (12h) at the end of the day; (18h) middle of night and (24h) end of the night. Free amino acids content were assayed in rosette leaves of 6 weeks old plants. Values are means ± SD (n=5) in WT and ± SD (n=10-15) in the RNAi lines. Amino acids content are given in µmol_g FW.

7.8. Major amino acids determined by HPLC in transgenic *GDH2*RNAi lines and WT in extended night experiments.

line	timepoint	Aspartate	SD	Glutamate	SD	Asparagine	SD	Glutamine	SD
Col-0	0h	1,51	± 0,06	2,82	± 0,12	0,81	± 0,05	1,53	± 0,62
gdh2-39 RNAi	0h	1,58	± 0,40	2,81	± 0,56	0,31	± 0,20	-	± -
gdh2-46 RNAi	0h	1,19	± 0,19	2,91	± 0,34	0,80	± 0,15	1,55	± 0,28
Col-0	24h ext.night	1,49	± 0,13	3,84	± 0,64	5,97	± 0,95	1,01	± 0,30
gdh2-39 RNAi	24h ext.night	1,46	± 0,44	3,33	± 0,35	4,02	± 0,77	-	± -
gdh2-46 RNAi	24h ext.night	1,81	± 0,10	3,80	± 0,17	6,18	± 0,90	1,12	± 0,10
Col-0	48h ext.night	1,66	± 0,30	3,67	± 0,08	8,27	± 0,56	1,02	± 0,30
gdh2-39 RNAi	48h ext.night	1,50	± 0,20	3,35	± 0,35	7,09	± 0,75	-	± -
gdh2-46 RNAi	48h ext.night	1,04	± 0,27	2,98	± 0,32	9,30	± 1,58	1,02	± 0,26
Col-0	72h ext.night	1,15	± 0,23	3,26	± 0,12	10,66	± 0,22	0,78	± 0,18
gdh2-39 RNAi	72h ext.night	1,58	± 0,30	2,66	± 0,53	9,14	± 0,70	-	± -
gdh2-46 RNAi	72h ext.night	1,25	± 0,38	3,12	± 0,32	13,22	± 1,31	0,71	± 0,18

Table 8. Composition of the major amino acids of rosette leaves of plants harvested after transferring to continuous darkness: 24h, 48h and 72h extended night. Free amino acids were assayed in rosette leaves of 6 weeks old plants. Values are means ± SD (n=5) in WT and ± SD (n=10-15) in transgenic lines. Values are given in µmol_g FW.

7.9. Starch content of in leaves and roots of the double transformant *gdh1*KO-*gdh2*RNAi in response to low sugars.

(A) Roots

line	timepoint	Starch		SD
Col-0	End day	0,416	±	0,588
WT ev	End day	0,347	±	0,323
# 5	End day	0,455	±	0,247
# 6	End day	0,265	±	0,375
# 9	End day	0,331	±	0,468
# 16	End day	0,729	±	0,636
Col-0	End night	0,513	±	0,388
WT ev	End night	0,259	±	0,233
#5	End night	0,433	±	0,506
#6	End night	0,157	±	0,118
#9	End night	0,372	±	0,406
#16	End night	0,696	±	0,757
Col-0	24h	0,172	±	0,244
WT ev	24h	0,110	±	0,155
#5	24h	0,119	±	0,168
#6	24h	0,752	±	1,064
#9	24h	0,895	±	0,181
#16	24h	2,382	±	1,962

(B) Leaves

line	timepoint	Starch		SD
Col-0	End day	19,783	±	1,664
WT ev	End day	13,423	±	3,863
#5	End day	21,760	±	1,295
#6	End day	23,982	±	4,253
#9	End day	27,699	±	3,503
#16	End day	24,034	±	4,495
Col-0	End night	3,149	±	1,085
WT ev	End night	3,392	±	0,197
#5	End night	3,362	±	0,941
#6	End night	3,963	±	1,687
#9	End night	3,329	±	0,281
#16	End night	3,368	±	0,518
Col-0	24h	0,076	±	0,107
WT ev	24h	0,673	±	0,479
#5	24h	0,373	±	0,254
#6	24h	0,358	±	0,347
#9	24h	0,496	±	0,375
#16	24h	0,453	±	0,573

Table 9. Starch content from roots and leaves of 11 days old seedlings in wild type and four independent *gdh1*KO-*gdh2*RNAi transgenic plants harvested at the end of the day, end of the night and after 24h in darkness. Seedlings were grown on vertical agarose plates containing AMOZ medium without additional sucrose. Each datapoint is the aritmetric mean of two independent biological replicates, each consisting of the leaves or roots pooled from 30-40 seedlings.

7.10. Amino acids content in leaves and roots of the double transformant *gdh1*KO-*gdh2*RNAi in response to low sugars.

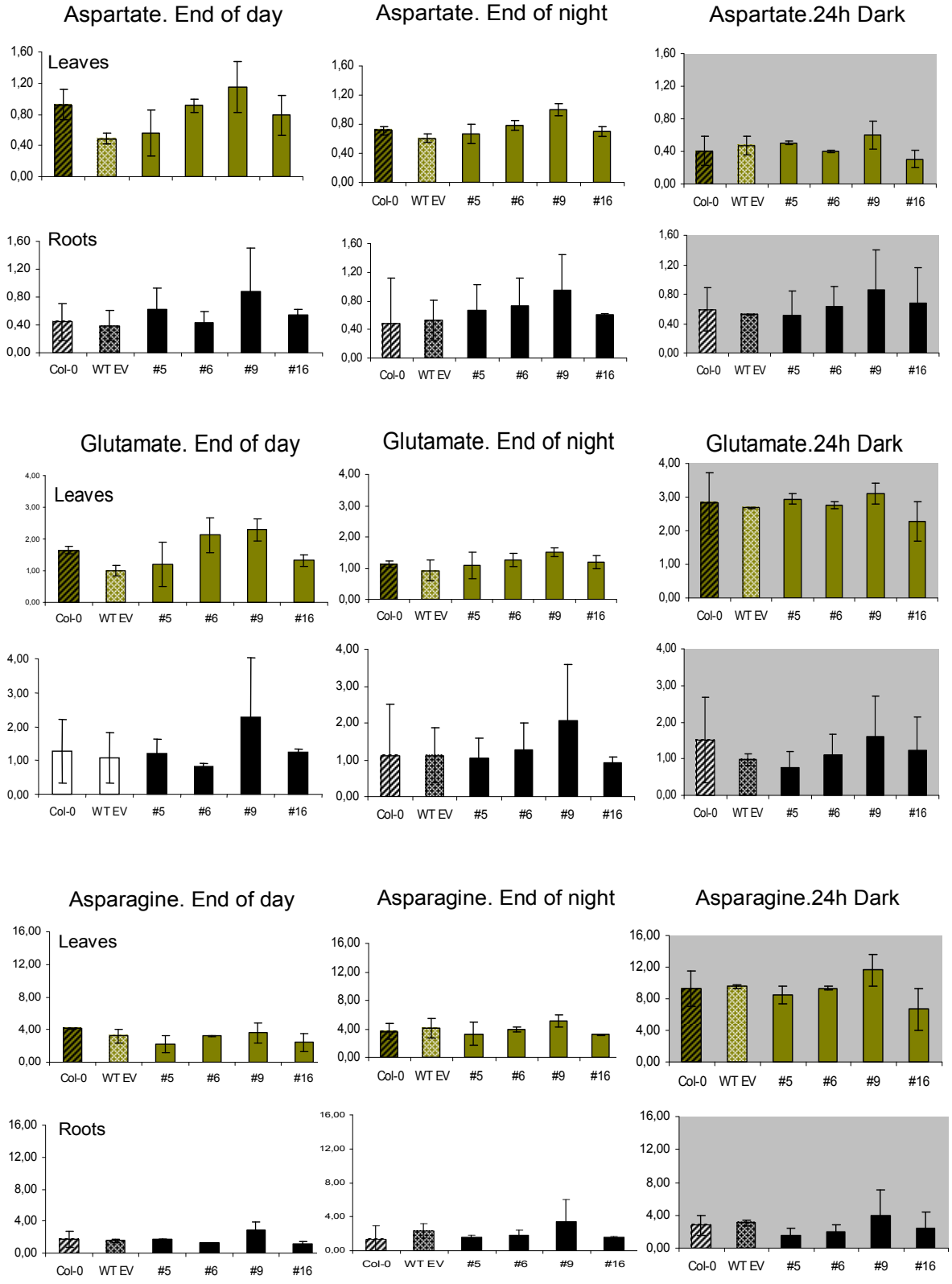

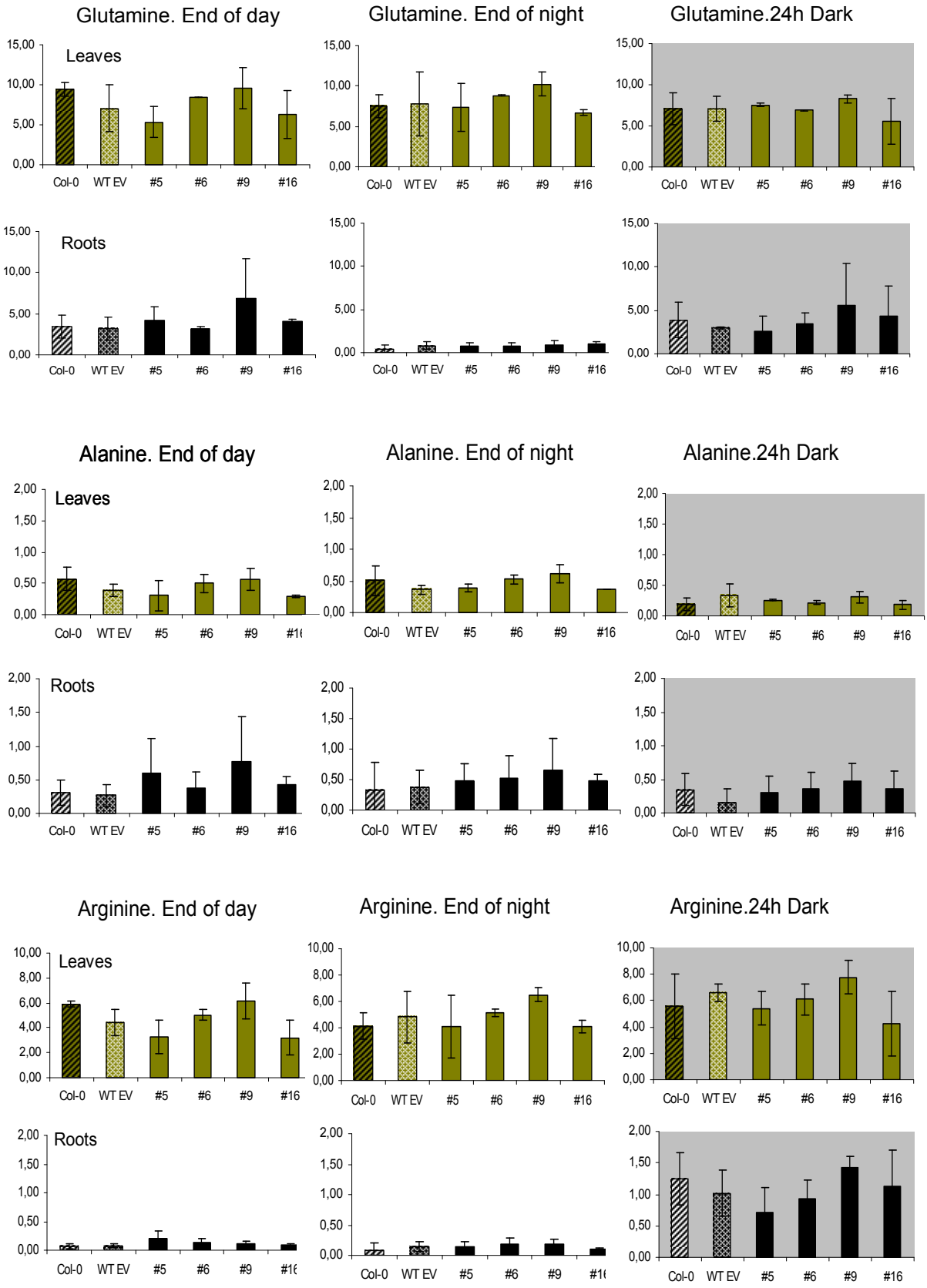
Glutamine. End of day
Glutamine. End of night
Glutamine.24h Dark
Leaves
Roots
Alanine. End of day
Alanine. End of night
Alanine.24h Dark
Leaves
Roots
Arginine. End of day
Arginine. End of night
Arginine.24h Dark
Leaves
Roots
Col-0
WT EV
#5
#6
#9
#16

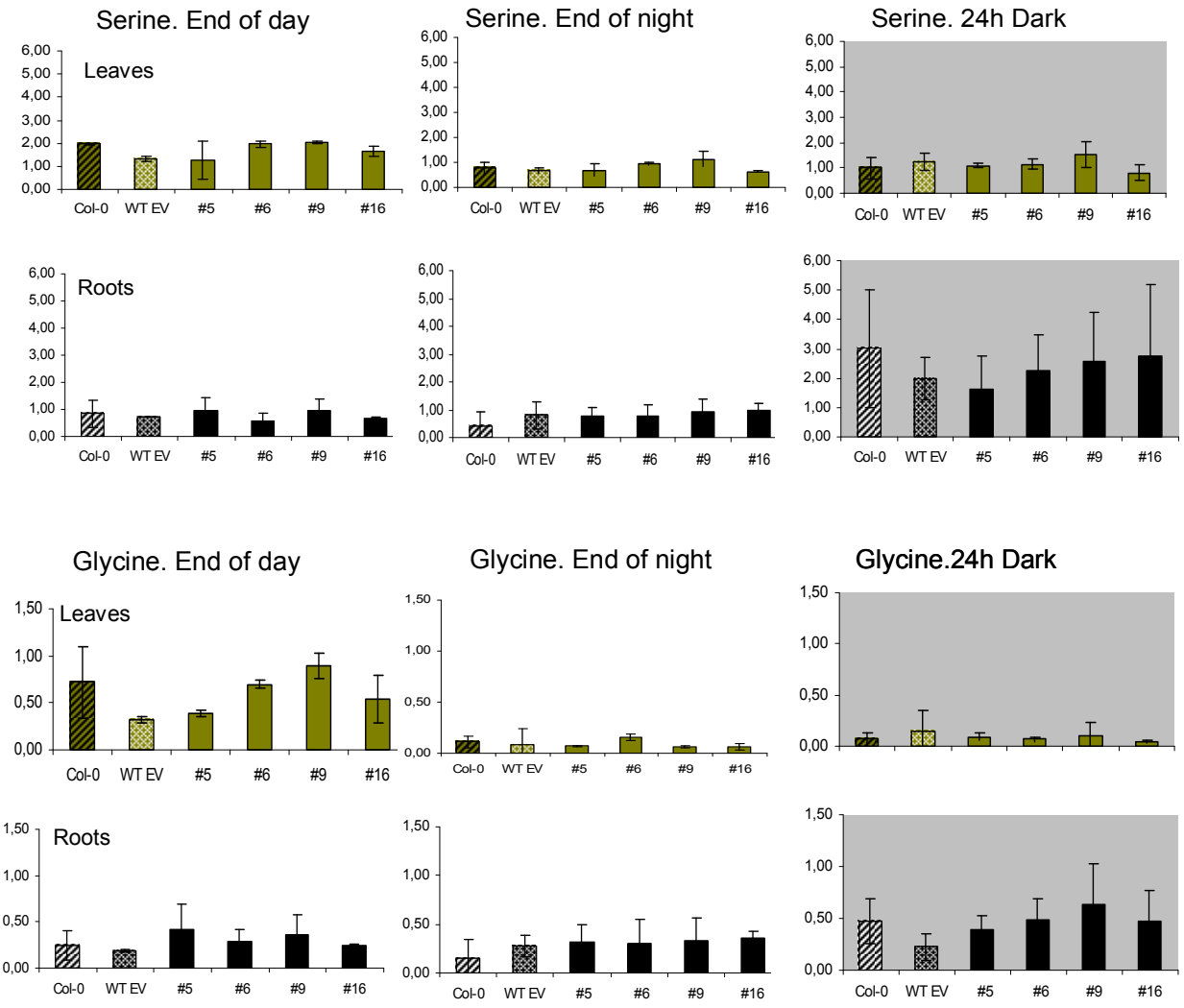

Figure 1. HPLC content from roots and leaves of 11 days old seedlings in wild type and four independent *gdh1*KO-*gdh2*RNAi transgenic plants. Plants were harvested as described in table 9.

7.11. Soluble sugars determination in *GDH3*RNAi plants and wild type.

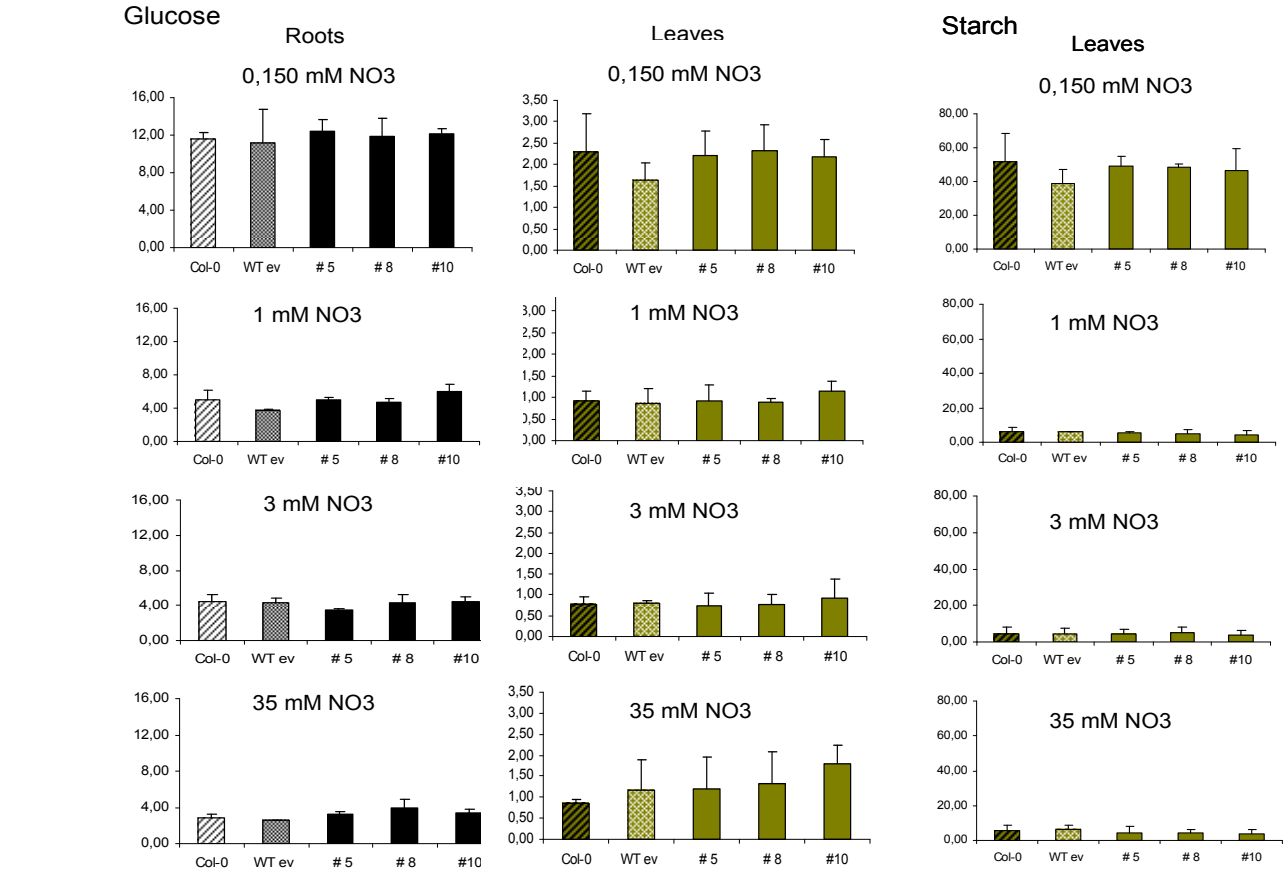

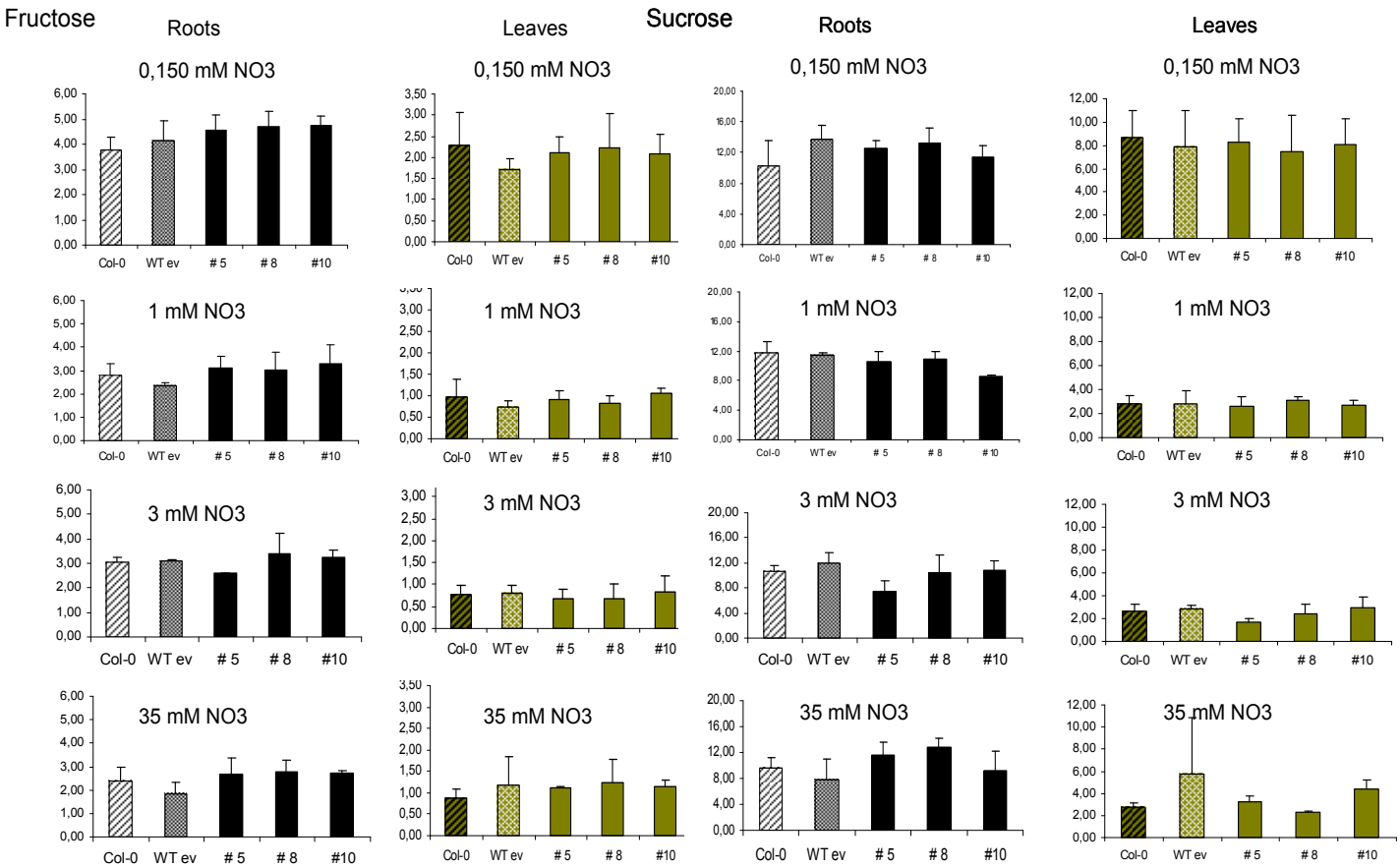

Figure 2. *GDH3*RNAi plants were grown in vertical agar plates containing different concentrations of nitrate (0,150mM, 1mM, 3mM and 35mM) in a normal 12h light/12h dark photoperiod. Shoots and roots were separated and harvested 14 days after the sowing date. Soluble sugars (glucose, fructose and sucrose) were determined in leaves and roots material. Starch could only be measured in leaves. Values are mean of three independent biological replicates each consisting of the leaves or roots pooled from 30 seedlings. Values are given in µmol_g FW.

7.12. α-ketoglutarate content in leaves of *GDH3*RNAi and wild type plants grown under different nitrate concentrations.

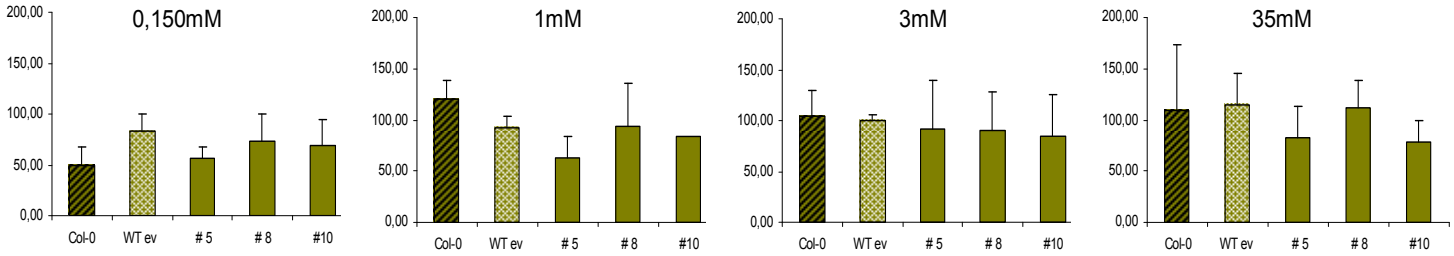

Figure 3. Plants were grown and harvested as described in figure 2. Values are given in µmol_g FW.

7.13. Nitrate and total amino acids in plants growing under different nitrate concentrations. (Results from the work of Dr. Irene Loef).

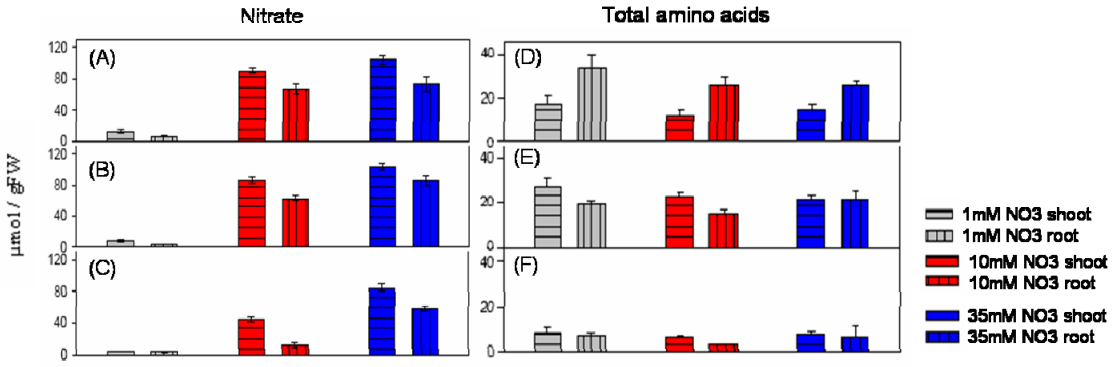

Figure 4. Nitrate and total amino acids content in Col-0 plants under different nitrate concentrations and light conditions at flowering time. A, B, and C, nitrate content in plants grown under long, neutral and short photoperiods, respectively. D, E and F, total amino acids content in plants grown under long, neutral and short photoperiods, respectively. Results obtained from the work of Dr. Irene Loef.

7.14. Soluble sugars and starch content in plants growing under different nitrate concentrations. (Results from the work of Dr. Irene Loef).

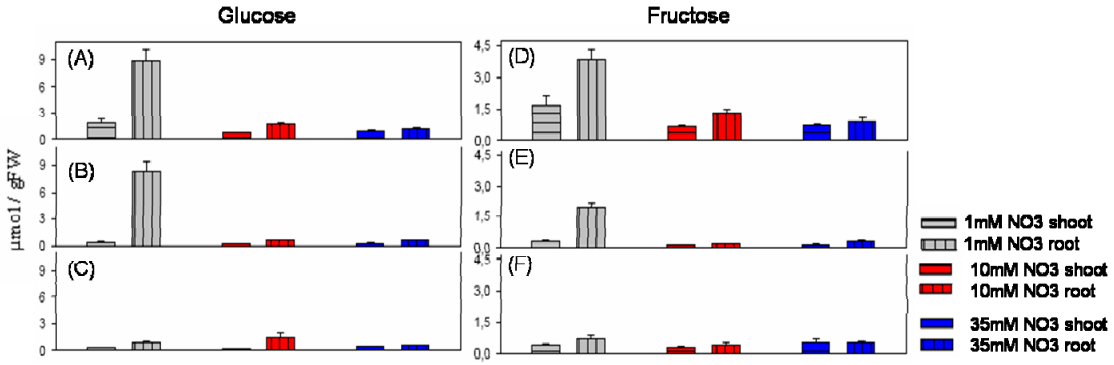

Figure 5. Glucose and fructose content in Col-0 plants under different nitrate concentrations and light conditions at flowering time. A, B, and C, glucose content in plants grown under long, neutral and short photoperiods, respectively. D, E and F, fructose content in plants grown under long, neutral and short photoperiods, respectively. Results obtained from the work of Dr. Irene Loef.

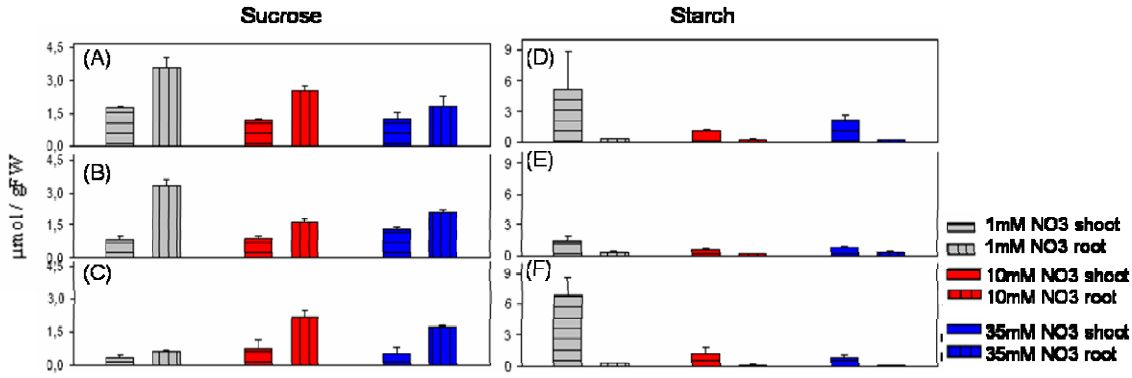

Figure 6. Sucrose and starch content in Col-0 plants under different nitrate concentrations and light conditions at flowering time. A, B, and C, sucrose content in plants grown under long, neutral and short

photoperiods, respectively. D, E and F, starch content in plants grown under long, neutral and short photoperiods, respectively. Results obtained from the work of Dr. Irene Loef.

7.15. Flowering responses in all flowering mutants used during this work.

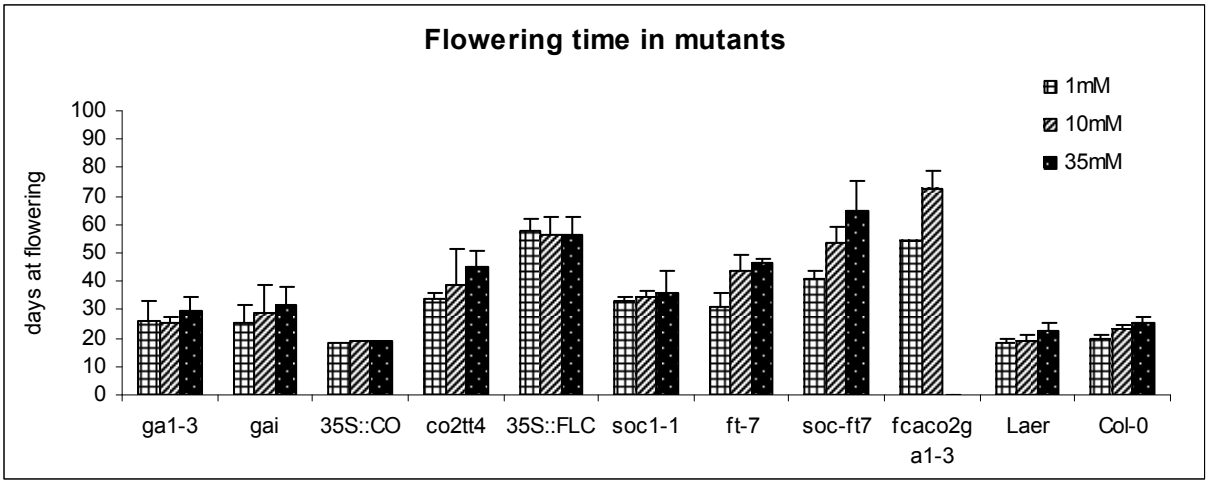

Figure 7. Transition to flowering in all flowering mutants used during this work. Values represent the flowering time of 30% of the plants induced to flower. Error bars indicate the standard deviation of two independent experiments.

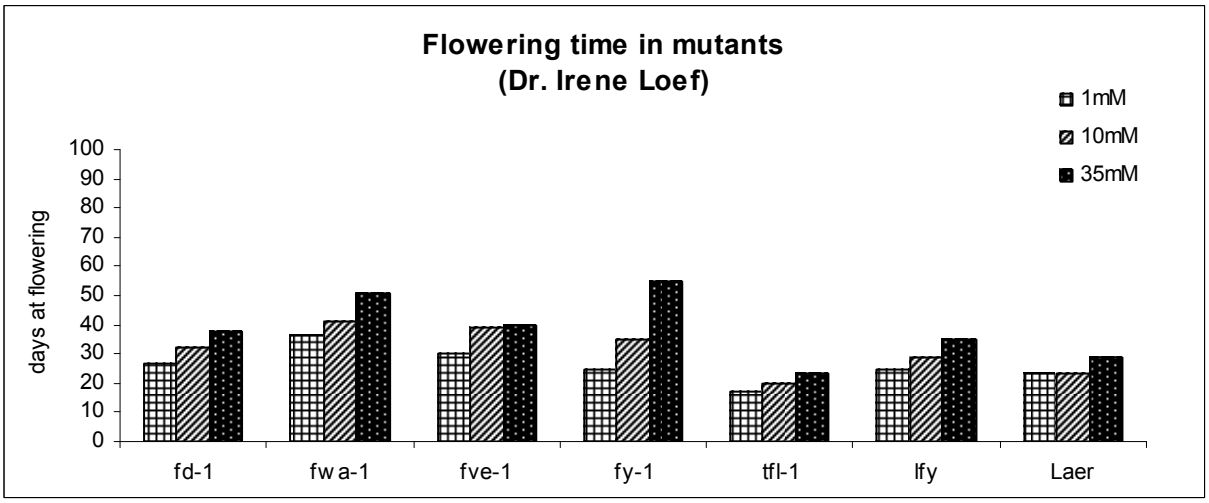

Figure 8. Transition to flowering in all flowering mutants from the work of Irene loef (Dissertation, 2002). Values represent the flowering time of 30% of the plants induced to flower.

7. 16. Genes induced between day 19 and 25 in *co2* 1mM vs 35mM and compared to the control 35S::*FLC*.

Gene code	co 1/35mM 19days	co 1/35mM 23days	co 1/35mM 25days	FLC oe 1/35mM 23days	FLC oe 1/35mM 28days	Shared response with N	T0/3h	T0/FN	Descriptions
At1g80840	-0,910	3,060	4,213	-0,292	0,737	0	0,163	-0,398	transcription factor similar to WRKY transcription factor
At2g40000	-1,285	1,766	3,855	0,233	0,264	0	-0,412	-0,689	putative nematode-resistance protein
At3g55980	-0,637	1,620	3,809	-0,227	0,361	0	-0,356	0,176	putative protein zinc finger transcription factor (PEI1)
At3g04640	-1,153	1,798	3,631	0,465	0,232	0	-0,166	0,394	hypothetical protein
At1g68840	0,018	1,488	3,613	0,517	0,782	0	0,393	-0,226	putative DNA-binding protein (RAV2-like)
At4g23810	-0,573	1,762	3,390	-0,794	-0,328	0	-0,160	-1,447	putative protein AR411
At2g21650	2,473	3,072	3,289	-0,239	0,092	0	-0,635	1,519	unknown protein
At2g25735	-0,736	1,381	3,080	0,475	0,877	0	-0,431	-2,062	Expressed protein
At1g05575	-0,645	1,793	3,028	0,456	0,756	0	-0,262	-1,149	Expressed protein
At1g57990	-1,385	1,221	3,014	0,986	0,406	1	1,248	0,820	unknown protein
At2g41640	-0,530	2,221	2,967	0,513	0,940	0	0,191	1,110	unknown protein
At3g44260	-0,787	1,555	2,895	-0,915	0,687	0	0,282	-0,405	CCR4-associated factor 1-like protein ribonuclease activity
At1g28370	-0,628	1,747	2,859	0,298	0,115	0	0,763	-0,567	ethylene-responsive element binding factor
At3g10930	-1,440	2,530	2,841	-0,848	0,896	0	-0,800	0,279	hypothetical protein
At2g38470	-0,317	1,566	2,775	-0,205	0,470	0	0,441	0,640	putative WRKY-type DNA binding protein
At1g24140	-0,567	1,172	2,696	-0,673	0,466	0	0,900	0,820	putative metalloproteinase
At1g19380	-1,203	1,307	2,636	0,930	0,648	0	-0,103	-2,008	hypothetical protein
At1g76650	-0,914	2,091	2,595	0,423	0,123	0	0,754	0,567	putative calmodulin
At5g37770	-0,806	1,056	2,541	0,850	0,704	0	-0,332	0,127	Calmodulin related protein, (TCH2)
At5g54490	-0,091	1,070	2,441	-0,734	0,338	0	0,466	-0,307	putative protein
At4g37610	-2,300	0,585	2,438	0,046	-0,180	1	-2,830	-1,651	putative protein SPOP
At5g57220	-0,204	1,464	2,424	0,300	0,455	0	-1,315	-2,738	cytochrome P450
At3g52400	-1,447	1,160	2,420	0,329	-0,249	0	0,128	0,143	syntaxin-like protein synt4
At5g10695	-1,701	0,895	2,399	0,662	-0,056	0	0,680	0,009	Expressed protein
At4g11280	-0,251	1,136	2,396	-0,443	0,748	0	0,665	1,951	ACC synthase (AtACS-6)
At1g66160	-0,418	1,396	2,396	0,668	0,963	0	-0,387	-0,891	unknown protein
At2g24600	-1,593	1,375	2,385	0,489	0,157	0	0,848	-0,323	hypothetical protein predicted by genscan
At3g57530	-0,342	1,375	2,356	0,782	0,840	0	0,547	1,010	calcium-dependent protein kinase
At3g50060	-1,022	0,037	2,307	0,177	0,480	0	-0,211	-0,217	R2R3-MYB transcription factor
At5g27420	-0,345	1,428	2,271	-0,432	0,278	0	0,834	0,604	RING-H2 zinc finger protein-like
At4g25490	-0,334	1,249	2,262	0,129	-0,177	0	-0,228	-0,123	transcriptional activator CBF1 CRT CRE binding factor
At1g32920	-0,304	0,942	2,252	-0,238	0,970	0	-1,785	0,129	unknown protein
At1g80440	-1,112	-0,362	2,222	0,612	0,111	1	-2,214	-1,632	unknown protein contains two Kelch motifs
At2g40140	-0,406	1,351	2,222	-0,672	0,574	0	-0,225	0,368	putative CCCH-type zinc finger protein
At3g56880	-0,498	1,197	2,176	0,399	0,682	0	0,427	-0,015	putative protein
At1g23710	-0,205	1,741	2,149	-0,572	0,500	0	0,497	0,804	unknown protein
At5g66210	-0,645	1,220	2,145	0,978	0,494	0	0,525	0,374	calcium-dependent protein kinase
At1g76600	-0,354	1,250	2,141	-0,504	0,631	0	-0,332	0,569	unknown protein
At1g69890	-0,367	1,024	2,111	0,321	0,483	0	0,019	0,467	hypothetical protein
At2g24550	-2,202	-0,017	2,061	0,336	-0,218	1	-1,370	-0,249	unknown protein
At5g41740	-1,261	1,144	2,036	0,404	0,048	0	0,714	0,841	disease resistance protein-like
At1g09070	-0,667	1,266	2,026	0,958	0,391	0	0,441	0,289	unknown protein Similar to Glycine SRC2
At5g59450	0,123	1,310	2,009	0,196	0,355	0	0,793	1,473	scarecrow-like 11 - like
At5g67450	-1,116	0,823	2,003	-0,598	-0,159	0	0,720	0,502	Cys2/His2-type zinc finger protein 1
At1g18570	-0,195	1,387	1,989	-0,188	0,295	0	0,465	-0,512	myb factor
At5g04340	0,148	1,905	1,982	-0,603	0,626	0	0,902	0,986	putative c2h2 zinc finger transcription factor

At5g59820	-1,295	1,410	1,976	-0,659	0,746	0	-0,508	-0,246	zinc finger protein Zat12
At4g18880	-0,253	1,674	1,954	-0,218	0,114	0	0,028	0,929	heat shock transcription factor
At2g01180	-0,978	1,021	1,944	0,787	0,441	0	0,346	0,437	putative phosphatidic acid phosphatase
At1g19770	-0,658	1,030	1,905	0,564	0,795	0	0,580	0,473	unknown protein
At2g35930	-0,629	1,339	1,904	-0,003	0,401	0	0,718	-0,018	unknown protein
At4g34150	-1,139	0,842	1,881	0,441	0,257	0	0,104	-0,044	putative protein hydroxyproline-rich glycoprotein precursor
At5g16570	1,668	1,723	1,857	0,775	0,449	1	3,436	5,412	Expressed protein
At2g41100	-1,031	0,725	1,839	0,324	0,036	1	1,110	0,286	calmodulin-like protein (TCH3)
At5g05410	-1,116	2,103	1,823	0,470	-0,028	0	0,060	-0,370	DREB2A
At5g06320	-1,130	0,732	1,821	0,250	0,123	0	0,430	-0,193	harpin-induced protein-like
At1g72900	-0,649	1,157	1,820	0,829	0,737	1	1,164	1,301	virus resistance protein
At2g44500	-1,104	0,654	1,819	0,767	0,886	0	0,410	0,935	similar to axi 1 protein from Nicotiana tabacum
At5g47220	1,126	1,213	1,812	-0,028	0,277	1	1,327	-0,409	ethylene responsive element binding factor 2 (ATERF2)
At2g44080	0,594	1,014	1,785	0,381	0,584	0	0,779	-0,457	unknown protein
At1g19180	-0,094	1,082	1,777	0,529	0,796	0	0,756	0,007	unknown protein
At3g14440	-0,070	1,019	1,772	0,648	0,914	0	0,080	0,093	9-cis-epoxycarotenoid dioxygenase
At5g16200	-0,525	1,076	1,760	0,219	-0,289	0	0,747	-0,084	putative protein
At5g16200	-0,525	1,076	1,760	0,219	-0,289	0	0,747	-0,084	putative protein
At1g07135	-0,151	1,178	1,723	-0,053	0,670	0	0,232	-0,357	unknown protein
At3g02550	-1,188	0,004	1,716	0,955	-0,078	0	-0,269	-0,044	unknown protein
At2g39650	-0,665	1,108	1,710	0,389	0,416	0	-1,289	-0,270	unknown protein
At3g48650	-1,777	1,583	1,708	-0,220	0,052	0	0,621	0,120	hypothetical protein
At3g02800	-0,364	1,330	1,694	-0,035	0,209	0	0,566	0,707	unknown protein
At4g02330	-1,240	-0,016	1,684	0,690	0,000	0	-0,252	-3,518	hypothetical protein similar to pectinesterase
At3g19580	-1,022	0,363	1,673	0,090	0,505	0	0,111	0,910	zinc finger protein
At1g02660	-1,065	0,450	1,662	0,827	0,463	0	0,730	0,411	hypothetical protein similar
At3g15530	-0,104	1,096	1,651	0,083	0,361	0	-0,071	-0,070	unknown protein
At5g47070	-0,942	1,033	1,649	0,175	0,118	0	0,434	0,410	protein serine threonine kinase-like
At4g36500	-0,036	1,131	1,636	-0,126	0,358	0	0,713	0,412	putative protein
At5g66070	-0,468	1,000	1,619	0,013	0,117	0	0,065	-0,053	putative protein
At1g01560	-1,942	0,825	1,610	0,156	-0,418	0	0,478	0,887	MAP kinase
At4g02410	0,167	1,290	1,603	-0,226	-0,051	0	0,396	0,883	contains similarity to a protein kinase domain
At1g42990	-0,289	1,093	1,597	0,299	0,381	0	-0,147	0,402	bZIP transcription factor
At1g22190	-1,107	0,790	1,596	-0,043	0,117	0	-0,529	-0,283	AP2 domain containing protein RAP2
At5g19120	-2,934	-1,366	1,569	0,631	0,024	1	-3,523	-4,243	conglutin gamma
At1g74450	-0,469	1,174	1,551	0,149	0,236	0	0,356	0,544	unknown protein
At1g78410	0,083	1,042	1,542	-0,801	-0,007	0	0,632	0,181	hypothetical protein
At5g35735	-0,271	1,155	1,515	0,564	0,414	0	-0,154	-0,621	Expressed protein
At5g20230	-1,310	1,141	1,500	0,762	0,105	0	-0,383	-2,229	blue copper binding protein
At4g39830	-1,665	0,390	1,495	-0,245	-0,913	0	-0,064	-0,945	putative L-ascorbate oxidase
At5g63130	0,055	1,282	1,470	0,177	0,361	0	0,879	0,751	unknown protein
At1g70290	-2,349	-0,806	1,459	0,787	-0,462	1	-1,690	-2,318	trehalose-6-phosphate synthase
At3g08720	-0,490	1,310	1,448	0,417	-0,019	0	0,588	0,798	putative ribosomal-protein S6 kinase (ATPK19)
At3g50260	0,037	1,075	1,444	0,732	0,305	1	1,458	0,685	putative protein EREBP-3 homolog
At2g46400	-1,001	1,139	1,443	0,289	-0,137	1	1,206	1,750	putative WRKY-type DNA binding protein
At3g44350	-1,477	0,500	1,437	0,048	-0,860	0	-0,072	0,064	NAC domain -like protein
At4g33920	-0,082	1,119	1,437	0,638	0,215	0	0,341	0,531	putative protein protein phosphatase Wip1
At3g01290	-1,049	0,313	1,429	0,045	-0,364	1	2,141	0,017	unknown protein
At3g50930	-1,174	1,375	1,429	-0,467	0,103	0	-0,231	1,301	BCS1 protein-like protein
At2g44840	-1,275	0,457	1,416	-0,390	0,229	0	0,325	-0,393	putative ethylene response element binding protein (EREBP)

At4g33050	-0,235	1,056	1,414	-0,169	-0,048	1	1,401	0,594	putative protein
At5g65300	0,373	1,299	1,412	-0,145	0,616	0	0,206	1,233	unknown protein
At2g32030	-0,541	1,100	1,408	-0,322	0,739	0	-0,062	0,377	putative alanine acetyl transferase
At3g46620	-0,150	1,065	1,382	-0,972	0,206	0	0,571	0,911	putative protein
At5g26920	-1,127	1,117	1,359	-0,586	-0,484	1	2,227	1,139	calmodulin-binding
At5g55050	0,177	1,229	1,344	0,488	0,196	1	1,352	0,245	GDSL-motif lipase/hydrolase-like protein
At1g51700	-0,066	1,118	1,314	-0,667	0,093	0	0,553	0,224	dof zinc finger protein
At2g20670	-2,687	-1,753	1,311	0,093	-0,082	1	-1,031	-1,122	unknown protein
At1g63840	0,213	1,239	1,292	0,542	0,526	1	1,071	1,304	putative RING zinc finger protein
At2g37940	-0,387	1,242	1,289	0,884	0,204	0	0,588	0,703	unknown protein
At5g07100	-0,050	1,079	1,228	0,782	0,715	1	1,321	-0,852	SPF1-like protein
At4g14365	-1,569	0,232	1,218	-0,114	-0,630	1	1,626	0,236	Expressed protein
At5g52760	-1,703	0,400	1,203	-0,240	-0,371	0	0,935	2,796	putative protein
At5g05300	-1,278	0,513	1,197	0,467	-0,720	0	0,476	0,520	putative protein
At1g07000	-1,184	0,640	1,155	0,229	-0,322	0	0,761	0,986	leucine zipper protein
At1g22890	-2,273	0,412	1,146	0,726	-0,350	0	-0,681	-3,487	unknown protein
At2g33580	-1,035	0,760	1,143	0,271	0,175	0	0,271	0,704	putative protein kinase
At3g48640	-1,443	0,431	1,137	-0,234	-0,351	1	2,537	3,020	hypothetical protein
At1g80920	-1,157	-0,336	1,076	0,413	0,087	1	-0,971	-1,769	J8-like protein similar to DnaJ homologueJ8
At4g17245	-1,005	-0,347	1,069	0,552	-0,092	0	-0,621	-1,971	Expressed protein
At1g26800	-1,477	-0,200	1,067	0,996	-0,172	0	0,147	-0,661	hypothetical protein
At3g10720	-1,422	0,201	1,044	0,696	0,388	0	-0,533	-1,075	putative pectinesterase
At2g18700	-2,686	-1,049	0,753	0,789	-0,782	0	-0,634	-1,130	putative trehalose-6-phosphate synthase
At3g07350	-1,210	-1,050	0,079	0,124	0,032	1	-1,745	-1,535	unknown protein
At5g49360	-2,163	-1,052	-0,110	0,088	-0,252	0	-0,931	-2,597	xylosidase
At2g26980	-1,208	-1,001	-0,714	0,027	-0,218	1	-3,002	-1,156	putative protein kinase
At4g28270	-1,132	-1,170	-1,001	-0,639	-0,928	0	0,343	-0,576	putative protein
At5g40890	-1,596	-1,245	-1,136	-0,673	-0,474	1	-1,916	-2,085	anion channel protein
At4g15660	-3,146	-2,602	-2,420	-0,770	-0,825	1	-2,582	-3,143	glutaredoxin
At5g61600	-0,524	0,626	2,729	-0,876	0,677	0	-0,155	0,380	DNA binding protein EREBP-4
At4g27280	-0,865	0,425	2,725	-0,598	0,574	0	0,677	1,069	putative protein centrin
At1g32920	-0,304	0,942	2,252	-0,238	0,970	0	-1,785	0,129	unknown protein
At1g13260	0,438	0,463	2,168	-0,204	0,066	0	-0,279	-0,280	DNA-binding protein RAV1
At1g58420	-0,646	0,877	2,065	0,135	-0,200	0	0,063	0,361	hypothetical protein
At3g59080	-0,941	0,539	2,058	0,850	0,109	0	-0,531	-0,646	putative protein CND41
At3g46600	-0,827	0,631	2,055	0,364	0,312	0	0,559	0,841	scarecrow-like protein
At2g23810	-0,928	0,649	1,834	0,278	0,208	0	0,318	0,315	hypothetical protein
At2g27500	-0,342	0,628	1,842	0,882	0,676	0	-0,053	0,404	putative beta-1,3-glucanase
At1g11050	0,099	0,836	1,727	0,476	0,543	0	0,854	0,967	Ser/Thr protein kinase isolog
At5g46710	-0,168	0,881	1,721	-0,375	0,350	0	-1,325	-0,201	putative protein similar to unknown protein
At3g16720	-0,301	0,833	1,720	-0,632	0,226	1	1,120	0,858	putative RING zinc finger protein similar to RING-H2 zinc finger protein
At2g43290	-0,745	0,681	1,717	0,777	0,209	0	0,619	1,422	putative calcium binding protein
At4g17500	0,374	0,729	1,716	0,073	0,477	0	0,466	-0,412	ethylene responsive element binding factor1
At2g17040	-0,945	0,482	1,710	-0,225	-0,548	1	1,917	2,083	NAM (no apical meristem)-like protein
At1g21130	-0,210	0,211	1,703	0,046	0,224	0	0,373	-0,223	O-methyltransferase
At4g11370	0,333	0,793	1,682	0,054	-0,171	0	0,423	0,857	RING-H2 finger protein RHA1a
At4g37260	-0,636	-0,143	1,668	0,713	0,394	0	0,230	0,402	myb-related protein
At1g72920	0,285	0,967	1,664	-0,382	0,979	0	0,942	-0,165	virus resistance protein
At3g10980	-0,738	0,372	1,660	0,862	0,025	0	0,207	-0,540	unknown protein
At1g59910	-0,813	0,867	1,654	0,735	0,321	0	0,148	0,254	hypothetical protein
At1g66180	-0,712	0,752	1,649	0,611	0,484	0	0,243	0,277	unknown protein
At4g00970	-0,709	0,853	1,637	0,441	-0,504	0	0,021	0,056	Similar to receptor kinase
At2g41010	-0,677	0,915	1,634	0,779	0,584	0	0,054	-0,687	unknown protein

At1g29690	-0,635	0,923	1,631	0,475	0,524	0	0,049	0,071	unknown protein
At1g21110	0,636	0,785	1,627	-0,151	0,761	0	-0,525	0,690	O-methyltransferase
At3g43430	-0,170	0,584	1,618	0,330	0,129	0	-0,659	-0,548	putative protein RING-H2 zinc finger protein ATL4
At1g25560	0,341	0,243	1,612	-0,363	-0,074	0	0,260	-0,177	DNA-binding protein RAV2
At1g25400	-0,724	0,803	1,599	0,026	0,024	0	0,833	0,541	unknown protein
At3g05200	-0,303	0,601	1,561	0,182	0,338	0	-0,182	0,491	putative RING-H2 zinc finger
At1g35350	-0,138	0,586	1,545	0,680	-0,066	0	0,032	0,227	unknown protein
At3g49530	-0,806	0,905	1,527	0,191	0,308	0	0,793	0,526	NAC2-like protein NAC2
At4g24380	-0,081	0,446	1,520	0,643	0,879	0	0,435	-0,075	putative protein dihydrofolate reductase
At5g13190	-0,700	0,682	1,491	0,621	0,203	0	0,275	0,530	putative protein
At2g18680	-0,435	0,926	1,487	0,200	-0,531	0	0,132	0,668	unknown protein
At5g26030	-0,382	0,922	1,479	0,465	0,174	0	-0,076	-0,083	ferrochelatase-I
At5g58430	-0,372	0,859	1,472	0,379	0,390	0	0,722	0,695	leucine zipper-containing protein
At2g41410	0,117	0,375	1,466	0,192	0,260	1	1,263	0,454	calmodulin-like protein
At1g17990	-0,571	0,383	1,464	0,514	-0,045	1	1,591	1,638	12-oxophytodienoate reductase
At5g52750	-0,415	0,962	1,463	-0,344	-0,411	0	0,215	1,077	putative protein
At1g18740	-0,696	0,815	1,454	0,639	0,302	0	0,236	0,581	unknown protein
At2g47060	-0,878	0,658	1,443	0,913	0,301	0	0,483	0,729	putative protein kinase
At3g09020	-0,504	0,213	1,441	-0,639	-0,296	0	0,670	0,389	unknown protein
At5g25930	-0,511	0,710	1,431	0,700	-0,053	0	0,980	0,574	receptor-like protein kinase
At3g25600	-0,341	0,857	1,426	-0,150	-0,141	0	0,194	-0,103	calmodulin
At2g18210	0,430	0,845	1,392	0,272	0,489	0	0,960	0,748	unknown protein
At3g45640	0,013	0,686	1,390	0,250	0,367	1	1,437	0,796	mitogen-activated protein kinase 3
At2g26190	-0,466	0,693	1,369	-0,291	-0,128	0	0,209	0,131	unknown protein
At1g70740	-0,565	0,646	1,367	0,537	0,235	0	0,269	1,118	putative protein kinase
At2g38390	-0,305	0,140	1,365	0,876	0,298	0	-0,239	0,438	peroxidase
At1g08930	-0,651	0,602	1,365	0,577	0,255	0	0,532	0,242	zinc finger protein ATZF1
At2g15390	0,291	0,979	1,363	0,665	0,518	1	1,184	0,394	unknown protein
At3g15770	-0,931	0,154	1,362	0,654	-0,156	0	-0,148	-0,367	hypothetical protein
At5g46780	-0,589	0,794	1,355	0,408	0,493	0	-0,482	-0,178	putative protein
At1g27770	-0,821	0,864	1,352	0,425	0,248	0	0,929	0,540	envelope Ca2+-ATPase
At2g22500	-0,877	0,859	1,342	-0,400	-0,157	0	-0,735	0,197	putative mitochondrial dicarboxylate carrier protein
At3g28180	-0,274	0,408	1,324	0,416	0,295	0	-0,646	-0,338	unknown protein
At5g62570	-0,775	0,991	1,316	0,446	0,045	0	0,710	0,263	putative protein
At2g27830	-0,464	-0,030	1,305	0,395	0,538	0	-0,089	1,053	unknown protein
At2g37970	-0,312	0,797	1,299	0,728	0,029	0	-0,241	-0,146	unknown protein
At1g51800	0,737	0,903	1,295	0,148	0,070	1	1,378	-1,525	receptor protein kinase
At4g17230	-0,920	0,610	1,289	0,534	0,240	0	0,644	0,653	scarecrow-like 13 (SCL13)
At1g06160	0,883	0,847	1,279	0,361	0,457	0	0,064	-0,636	ethylene response factor
At4g22710	0,192	0,701	1,267	0,634	0,496	0	0,515	-0,564	cytochrome P450
At1g52200	0,524	0,836	1,264	0,739	0,208	0	0,645	-0,676	unknown protein
At3g44720	-0,275	0,556	1,263	0,080	0,454	0	0,837	0,349	putative chloroplast prephenate dehydratase
At1g59590	-0,954	0,609	1,256	-0,292	-0,096	0	-0,137	0,629	hypothetical protein
At3g57450	-0,798	0,677	1,255	0,166	0,771	0	-0,421	-0,842	putative protein
At1g27100	-0,503	0,687	1,232	0,295	0,329	0	0,403	0,556	unknown protein
At3g28340	-0,489	0,790	1,223	-0,097	0,481	0	-0,222	0,460	unknown protein
At4g37240	-0,937	-0,060	1,218	0,550	-0,008	0	0,060	-0,536	putative protein
At4g39670	-0,763	0,583	1,213	-0,492	0,460	0	0,014	0,374	putative protein
At3g52800	-0,479	0,787	1,212	0,551	0,628	0	0,413	0,643	zinc finger
At3g09260	-0,235	-0,317	1,208	0,977	0,715	0	0,007	-0,105	thioglucosidase 3D precursor
At1g63720	-0,104	0,956	1,206	-0,098	0,314	0	0,852	0,941	hypothetical protein
At1g20823	0,015	0,824	1,204	-0,222	0,393	1	0,914	1,036	predicted protein

At5g61440	-0,891	-0,030	1,202	0,868	0,501	0	-1,165	-0,364	thioredoxin-like 3
At4g33985	-0,138	0,474	1,195	0,043	0,076	0	0,357	0,015	Expressed protein
At5g24590	-0,601	0,506	1,194	0,604	0,315	0	0,324	0,417	NAC2-like protein
At4g20830	-0,563	0,670	1,193	0,606	-0,294	0	-0,204	0,065	reticuline oxidase
At2g31880	-0,855	0,520	1,183	-0,201	-0,347	1	1,392	0,892	putative receptor-like protein kinase
At4g25470	-0,166	0,590	1,178	-0,070	0,198	0	-0,119	-0,032	DRE CRT-binding protein DREB1C
At1g76360	0,633	0,694	1,173	0,034	-0,053	0	0,844	0,740	putative protein kinase similar to protein kinase (APK1A)
At1g27200	-0,014	0,561	1,165	0,518	-0,023	1	0,986	1,121	unknown protein
At5g01540	-0,232	0,754	1,159	0,209	0,275	0	-0,178	-1,492	receptor like protein kinase
At4g15975	-0,099	0,555	1,156	-0,329	0,339	0	0,098	-0,415	Expressed protein
At5g08240	-0,832	0,619	1,155	-0,152	-0,837	0	-0,055	0,261	putative protein
At4g23180	-0,474	0,737	1,151	0,632	0,150	0	0,634	0,285	serine/threonine kinase
At2g46600	0,179	0,512	1,148	0,013	0,098	1	2,581	1,608	putative caltractin
At1g07520	-0,396	0,704	1,138	0,140	0,148	0	0,229	0,743	transcription factor scarecrow-like 14
At2g30930	-0,865	-0,024	1,137	0,934	0,320	0	0,120	1,335	unknown protein
At3g54810	-0,652	0,282	1,133	0,320	0,429	0	0,084	0,647	putative protein GATA transcription factor 3
At4g36550	-0,005	0,943	1,132	-0,118	0,090	0	-0,089	0,418	putative protein
At1g55450	-0,790	0,587	1,132	0,250	0,002	0	0,473	-0,948	hypothetical protein similar
At1g61340	-0,566	0,873	1,125	-0,023	0,847	0	0,020	0,240	late embryogenesis abundant protein
At1g14370	-0,353	0,766	1,116	-0,081	-0,352	0	0,424	0,227	protein kinase
At1g72430	-0,737	-0,270	1,113	0,900	0,363	0	0,012	-0,090	hypothetical protein
At4g14450	-0,387	0,349	1,109	0,129	0,375	0	-0,111	-0,161	hypothetical protein
At2g38790	-0,089	0,846	1,107	-0,024	0,448	0	0,404	0,328	unknown protein
At2g23320	-0,518	0,471	1,099	0,137	0,327	0	-0,065	0,337	putative WRKY-type DNA-binding protein
At3g54000	-0,187	0,430	1,099	0,608	0,675	0	-0,001	0,382	hypothetical protein
At1g49780	0,037	0,336	1,097	-0,072	0,328	0	0,121	0,203	hypothetical protein
At4g31550	0,051	0,733	1,087	0,059	0,808	0	0,010	-0,180	putative DNA-binding protein DNA-binding protein WRKY3
At1g33600	-0,074	0,719	1,080	0,566	0,447	0	-1,143	-3,194	putative disease resistance protein
At3g11650	-0,792	0,090	1,078	0,409	-0,253	0	-0,415	-0,231	unknown protein
At5g52050	-0,793	0,683	1,073	-0,380	0,434	0	-2,370	-0,214	integral membrane protein-like
At4g02200	-0,258	0,566	1,071	0,165	-0,055	0	0,572	0,206	drought-induced-19-like 1
At5g42050	-0,288	0,688	1,067	0,347	0,050	1	1,090	1,127	putative protein
At5g28630	-0,503	0,673	1,061	0,788	0,988	0	0,004	-0,785	putative protein retinal glutamic acid-rich protein
At4g01950	-0,902	-0,088	1,053	0,720	0,675	0	0,014	0,971	predicted protein of unknown function
At3g23920	-0,698	0,801	1,048	1,141	0,261	0	0,686	0,939	beta-amylase
At1g09970	0,057	0,480	1,047	0,673	0,354	0	0,578	0,700	unknown protein
At4g28400	-0,495	0,605	1,047	0,452	-0,039	1	0,925	1,360	protein phosphatase 2C-like protein
At4g01250	-0,473	0,536	1,045	0,191	1,097	0	-0,040	-1,048	putative DNA-binding protein
At4g24160	-0,002	0,644	1,038	0,785	0,517	0	0,772	0,942	putative protein CGI-58 protein
At1g20510	0,170	0,955	1,034	0,561	0,489	1	1,014	0,320	hypothetical protein
At3g05320	-0,082	0,879	1,024	0,364	0,007	0	0,808	0,679	unknown protein
At3g26510	-0,873	-0,532	1,022	0,900	-0,143	0	0,526	-1,455	unknown protein
At5g04720	-0,365	0,429	1,018	0,061	0,041	1	1,146	1,042	disease resistance - like protein rpp8
At1g73830	0,064	-0,105	1,017	-0,180	-0,270	0	0,326	-0,434	putative helix-loop-helix DNA-binding protein
At4g27300	0,633	0,710	1,011	0,494	0,197	0	0,159	-0,335	putative receptor protein kinase
At4g08780	0,391	0,108	1,005	0,595	0,679	0	-0,074	0,075	peroxidase C2 precursor like
At4g35180	0,550	0,674	1,004	-0,267	-0,170	1	1,878	2,124	amino acid permease
At5g25190	-0,254	-0,164	1,003	0,052	-0,237	0	-0,656	-0,642	ethylene-responsive element

Table 10. Values represent the log 2 scaled ratio of each day in 1mM vs 35mM nitrate. The list includes genes with significant expression (≥ 2 fold changes) or unchanged expression (1≥ log2 ≥ -1). Expression data from Scheible´s group (starvation/re-addition experiment) was included for comparison with expression changes of *co2*.

Shared response with nitrate "0" means non shared response with nitrate experiment and "1" means shared response with nitrate experiment at least in one of the time points.

7.17. Genes gradually down regulated between day 19 and 25 in *co2* 1mM vs 35mM and compared to the control 35S::*FLC*.

Gene code	*co* 1/35mM 19days	*co* 1/35mM 23days	*co* 1/35mM 25days	FLC oe 1/35mM 23days	FLC oe 1/35mM 28days	Shared response with N	T0/3h	T0/FN	Descriptions
At2g47880	1,584	1,457	1,398	0,521	0,264	1	1,031	2,753	putative glutaredoxin
At4g34135	1,752	1,211	1,176	0,702	0,536	0	0,534	2,387	glucosyltransferase
At2g26020	1,991	1,860	1,019	0,902	-0,504	0	-0,209	-1,788	putative antifungal protein
At1g66690	1,375	1,220	0,777	-0,078	0,350	1	1,141	2,171	unknown protein
At5g45820	1,782	1,253	0,764	-0,172	0,509	0	-0,177	-1,449	serine threonine protein kinase
At5g63790	1,330	1,003	0,749	-0,088	0,602	1	0,758	1,620	putative NAC-domain protein
At5g49480	1,823	1,520	0,729	0,655	1,079	0	-1,221	0,221	NaCl-inducible Ca2+-binding protein-like
At3g22840	2,384	1,067	0,574	0,772	0,614	1	2,199	2,427	early light-induced protein
At4g33040	1,507	1,222	0,421	0,215	0,334	1	3,355	3,739	putative protein
At1g61800	2,884	1,255	0,395	0,437	0,793	1	1,662	2,973	glucose-6-phosphate/phosphate-translocator precursor
At1g77760	-1,045	-1,920	-0,240	0,517	0,321	1	-3,370	0,757	nitrate reductase 1 (NR1) identical to nitrate reductase 1 (NR1)
At2g39030	0,016	-1,213	-1,264	0,794	0,645	0	0,046	-5,714	unknown protein
At5g04950	-0,231	-1,197	-1,605	-0,274	0,109	1	-5,327	-1,791	nicotianamine synthase
At2g14610	-1,077	-1,294	-1,900	-0,790	-0,461	1	0,632	-1,639	pathogenesis-related PR-1-like protein

Table 11. Values represent the log 2 scaled ratio of each day in 1mM vs 35mM nitrate. The list includes genes with significant expression (≥ 2 fold changes) or unchanged expression (1≥ log2 ≥ -1). Expression data from Scheible´s group (starvation/re-addition experiment) was included for comparison with expression changes in *co2* 1mM. Shared response with nitrate "0" means non shared response with nitrate experiment and "1" means shared response with nitrate response at least in of the time points.

7.18. Expression of known flowering time genes in *co2* induced plants in low nitrate versus *co2* in high nitrate, compared to control 35S::*FLC* plants.

Gene code	co 1/35mM 19days	co 1/35mM 23days	co 1/35mM 25days	floral regulator	FLC 1/35mM 23days	FLC 1/35mM 28days	T0/3h	T0/FN	Descriptions
At5g15840	0,276	0,080	0,235	+	-0,274	0,090	0,199	-0,049	CONSTANS
At2g45660	0,254	0,285	-0,202	+	-0,331	-0,168	0,578	0,477	MADS-box protein (SOC1, AGL20)
At1g65480	-0,149	-0,228	-0,115	+	-0,121	-0,045	-0,285	-0,204	flowering signal FLOWERING LOCUS T, FT
At2g46830	0,179	-0,081	0,348	+	0,002	0,448	0,488	-0,221	MYB-related transcription factor (CCA1)
At4g02560	0,137	-0,096	0,097	+	0,192	0,189	-0,253	0,008	LUMINIDEPENDENS protein, LD
At2g17770	0,013	-0,085	0,047	+	-0,112	0,097	-0,182	0,327	putative bZIP transcription factor. FD
At4g35900	-0,147	0,071	0,461	+	-0,114	-0,077	0,064	0,281	FD,putative bZIP transcription factor Dc3 promoter-binding factor-2
At4g16280	0,232	0,079	0,365	+	0,392	0,078	0,050	0,499	FCA gamma protein.Autonomous pathway.
At2g19520	0,186	0,058	-0,342	+	-0,265	-0,096	-0,463	-0,019	FVE, ACG1. Autonomous pathway
At4g25530	0,156	-0,173	0,408	+	-0,165	-0,143	-0,114	-0,322	homeodomain-protein. FWA. Autonomous pathway.
At3g04610	0,239	-0,065	-0,127	+	-0,112	0,109	-0,347	0,115	putative RNA-binding protein. FLK Autonomous pathway
At3g10390	-0,051	-0,024	0,213	+	-0,200	-0,091	-0,040	0,010	FLD, Flowering locus D. Autonomous pathway
At2g01570	0,037	0,043	-0,262	+	0,046	0,154	-0,315	0,375	GA1-3, RGA1 member of SCARECROW family
At5g61850	-0,240	-0,049	-0,040	+	-0,066	-0,105	0,048	-0,022	LFY floral meristem identity control protein
At1g68050	1,042	0,486	-0,258	+	-0,514	0,003	0,678	0,780	F-box protein FKF1/ADO3

At4g18960	-0,073	0,088	0,114	+	0,113	-0,027	0,015	-0,144	floral homeotic protein agamous (AGAMOUS)
At3g02310	0,023	0,114	0,239	+	0,093	0,196	0,068	-0,062	floral homeotic protein AGL4, SEP4
At1g69120	-0,105	0,009	0,171	+	-0,002	0,100	-0,136	-0,212	APETALA 1, AP1, floral homeotic protein
At4g36920	0,406	0,256	-0,034	+	-0,100	-0,037	0,401	0,727	APETALA2 protein, AP2
At1g69490	0,177	1,048	1,929	+	1,004	-0,336	2,761	0,439	NAC domain protein NAM. NAC-LIKE, activated by AP3
At1g26310	0,097	-0,120	0,299	+	-0,081	-0,076	-0,259	-0,463	CAULIFLOWER, CAL1, AGL10
At2g27250	-0,256	-0,111	-0,136	+	-0,025	-0,135	-0,033	-0,126	CLAVATA3 CLE family of proteins; ligand for CLV1
At4g15880	0,163	0,031	0,042	+	-0,197	-0,024	-0,070	0,371	ESD4, EARLY IN SHORT DAYS 4
At5g24860	-0,058	-0,006	-0,005	+	0,114	0,348	0,329	1,246	FPF1 protein
At2g33810	-0,162	0,311	0,128	+	0,036	0,199	0,258	-0,455	SPL3, squamosa-promoter binding protein like 3
At2g22540	0,358	0,080	-0,048	-	-0,144	-0,053	0,505	0,072	MADS-box protein. SVP, SHORT VEGETATIVE PHASE (AGL22)
At2g39250	0,114	-0,314	-0,430	-	-0,330	-0,159	-1,449	-0,646	putative AP2 domain transcription factor
At2g25930	-0,237	-0,008	-0,127	-	-0,159	-0,050	-0,302	-0,073	unknown protein
At4g00650	0,000	-0,284	-0,053	-	-0,127	-0,095	-0,178	0,046	FRIGIDA (FRI) FLOWERING LOCUS A
At1g14920	0,155	-0,075	-0,447	-	-0,279	-0,228	0,412	0,614	RGA2, GAI
At1g12610	-0,189	-0,108	-0,026	-	-0,207	-0,119	0,024	-0,067	transcriptional activator CBF1
At5g16320	-0,067	-0,117	-0,215	-	0,292	-0,273	0,025	-0,093	FRL1, FRIGIDA LIKE1
At4g16845	0,369	-0,063	0,061	-	0,033	-0,106	0,021	0,282	VRN2
At5g03840	-0,119	-0,273	-0,281	-	-0,154	-0,194	0,067	-0,440	Terminal flower1 (TFL1)
At3g12810	0,088	-0,090	0,060	-	0,092	-0,060	-0,008	0,008	Snf2-related CBP activator protein. PIE1, Phtotoperiod independent early flowering
At5g51230	0,114	-0,099	0,047	-	-0,050	0,017	-0,060	-0,513	EMF2, EMBRYONIC FLOWER 2
At1g77080	0,184	-0,047	-0,419	-	0,157	-0,133	0,196	0,203	MADS box transcription factor MADS AFFECTING FLOWERING (MAF1, FLM)
At5g11530	0,193	0,043	0,334	-	0,254	0,213	0,397	0,242	EMBRYONIC FLOWER, EMF1
At3g54990	0,117	-0,049	0,014	-	-0,113	0,257	-0,199	-0,382	APETALA2 - like protein APETALA2
At5g65080	0,167	-0,161	0,054	-	0,229	-0,223	0,099	-0,191	MADS box transcription factor-like protein MADS AFFECTING FLOWERING 5 (MAF5)
At1g31814	-0,078	0,046	-0,170	-	0,063	0,130	0,302	0,025	FRL2, FRIGIDA LIKE 2
At3g18990	0,130	-0,053	0,121	-	0,191	0,009	-0,026	0,853	VRN1
At5g61150	0,256	0,015	0,186	-	0,226	0,212	-0,030	-0,083	VERNALIZATION INDEPENDENCE 4, VIP4
At4g20830	-0,563	0,670	1,193	-	0,606	-0,294	-0,204	0,065	VERNALIZATION INDEPENDENCE3, VIP3
At5g10140	-0,003	-0,036	0,058	-	0,108	0,091	0,343	-0,019	MADS box protein FLOWERING LOCUS C (FLC, FLF)

Table 12. Values represent the log 2 scaled ratios of *co2* vs 35S::*FLC*. Significant expression was considered at a threshold of 0.5 (1 fold- change). "+" means positive regulator of flowering and "-" negative regulator of flowering.

7.19. Expression of known flowering time genes in *co2* induced plants versus the control 35S::*FLC* in response to low and high nitrate.

Gene code	co19d 1mM vs FLC 1mM	co23d 1mM vs FLC 1mM	co25d 1mM vs FLC 1mM	co19d 35mM vs FLC 35mM	co 23d 35mM vs FLC 35mM	co 25d 35mM vs FLC 35mM	floral regulator	Descriptions
At5g15840	0,722	0,652	1,120	0,354	0,480	0,794	+	CONSTANS
At2g45660	2,845	3,117	2,745	2,342	2,582	2,697	+	MADS-box protein (SOC1, AGL20)
At1g65480	0,169	0,113	0,002	0,235	0,258	0,033	+	flowering signal FLOWERING LOCUS T, FT
At2g46830	0,148	-0,013	0,112	0,194	0,293	-0,010	+	MYB-related transcription factor (CCA1)
At4g02560	0,029	-0,017	0,201	0,083	0,269	0,294	+	LUMINIDEPENDENS protein, LD
At4g35900	0,345	0,574	0,781	0,396	0,407	0,224	+	FD,putative bZIP transcription factor Dc3 promoter-binding factor-2
At4g16280	0,003	-0,058	0,330	0,006	0,098	0,200	+	FCA gamma protein.Autonomous pathway.
At2g19520	0,177	0,062	0,081	-0,190	-0,177	0,242	+	FVE, ACG1. Autonomous pathway
At4g25530	0,373	0,061	0,157	0,064	0,080	-0,405	+	homeodomain-protein. FWA. Autonomous pathway.
At3g04610	0,145	0,116	0,173	-0,096	0,179	0,299	+	putative RNA-binding protein. FLK Autonomous pathway
At3g10390	0,142	0,161	0,332	0,048	0,040	-0,027	+	FLD, Flowering locus D. Autonomous pathway
At2g01570	0,028	0,088	0,070	0,091	0,144	0,431	+	GA1-3, RGA1 member of SCARECROW family
At5g61850	0,026	0,166	0,154	0,181	0,129	0,108	+	LFY floral meristem identity control protein
At1g68050	0,609	0,210	0,290	-0,688	-0,531	0,293	+	F-box protein FKF1/ADO3
At4g18960	0,078	0,185	0,158	0,194	0,139	0,088	+	floral homeotic protein agamous (AGAMOUS)
At3g02310	-0,074	0,108	-0,001	0,047	0,138	-0,095	+	floral homeotic protein AGL4, SEP4
At1g69120	0,191	0,359	0,254	0,345	0,399	0,131	+	APETALA 1, AP1, floral homeotic protein
At4g36920	0,075	0,117	0,089	-0,400	-0,207	0,055	+	APETALA2 protein, AP2
At1g69490	-0,751	-0,224	0,047	-0,595	-0,938	-1,548	+	NAC domain protein NAM. NAC-LIKE, activated by AP3
At1g26310	0,457	0,232	0,201	0,282	0,273	-0,176	+	CAULIFLOWER, CAL1, AGL10
At2g27250	0,102	0,135	-0,211	0,278	0,166	-0,155	+	CLAVATA3 CLE family of proteins
At4g15880	0,029	0,025	0,209	-0,245	-0,117	0,057	+	ESD4, EARLY IN SHORT DAYS 4
At5g24860	-0,203	-0,202	-0,296	0,086	0,034	-0,061	+	FPF1 protein
At2g33810	-1,255	-0,232	-0,145	-0,976	-0,425	-0,155	+	SPL3, squamosa-promoter binding protein like 3
At2g22540	1,071	1,080	1,039	0,615	0,901	0,989	-	MADS-box protein. SVP, SHORT VEGETATIVE PHASE (AGL22)
At2g39250	0,846	0,467	0,689	0,487	0,536	0,874	-	putative AP2 domain transcription factor
At2g25930	0,304	0,605	0,686	0,437	0,509	0,708	-	ELF3, Early flowering 3
At4g00650	0,264	-0,116	-0,146	0,153	0,058	-0,205	-	FRIGIDA (FRI) FLOWERING LOCUS A
At1g14920	0,254	0,132	0,282	-0,155	-0,046	0,475	-	RGA2, GAI
At1g12610	0,236	0,138	0,116	0,262	0,083	-0,021	-	transcriptional activator CBF1. DDF1, Dwarf and Delayed flowering1.
At5g16320	0,168	0,146	0,016	0,244	0,272	0,240	-	FRL1, FRIGIDA LIKE1
At4g16845	0,160	0,118	0,290	-0,245	0,145	0,192	-	VRN2
At5g03840	0,090	0,006	-0,075	0,035	0,105	0,033	-	Terminal flower1 (TFL1)
At3g12810	0,046	0,024	-0,006	-0,025	0,129	-0,050	-	Snf2-related CBP activator protein. PIE1, Photoperiod independent early flowering
At5g51230	0,031	0,089	-0,101	-0,099	0,172	-0,164	-	EMF2, EMBRYONIC FLOWER 2

At1g77080	0,024	0,053	-0,099	-0,148	0,112	0,332	-	MADS box transcription factor MADS AFFECTING FLOWERING (MAF1, FLM)
At5g11530	-0,053	-0,062	0,096	-0,013	0,128	-0,005	-	EMBRYONIC FLOWER, EMF1
At3g54990	-0,055	-0,284	-0,409	-0,100	-0,163	-0,350	-	APETALA2 - like protein APETALA2
At5g65080	-0,070	-0,189	-0,183	-0,234	-0,026	-0,234	-	MADS box transcription factor-like protein MADS AFFECTING FLOWERING 5 (MAF5)
At1g31814	-0,149	-0,095	-0,125	0,025	-0,045	0,141	-	FRL2, FRIGIDA LIKE 2
At3g18990	-0,182	-0,113	0,002	-0,212	0,040	-0,019	-	VRN1
At5g61150	-0,205	-0,302	-0,058	-0,241	-0,099	-0,025	-	VERNALIZATION INDEPENDENCE 4, VIP4
At4g20830	-1,238	-0,446	-0,692	-0,519	-0,960	-1,729	-	VERNALIZATION INDEPENDENCE3, VIP3
At5g10140	-8,813	-9,039	-8,289	-8,712	-8,905	-8,248	-	MADS box protein FLOWERING LOCUS C (FLC, FLF)

Table 13. Values represent the log 2 scaled ratios of *co2* vs 35S::*FLC*. Significant expression was considered at a threshold of 0.5 (1 fold- change). "+" means positive regulator of flowering and "-" negative regulator of flowering.